SEDIMENT TRANSPORT IN IRRIGATION CANALS

NN08201, 2526

Sediment Transport in Irrigation Canals

DISSERTATION
Submitted in fulfilment of the requirements of
the Board of Deans of the Wageningen Agricultural University
and the Academic Board of the International Institute for Infrastructural,
Hydraulic and Environmental Engineering for the Degree of DOCTOR
to be defended in public
on Tuesday, 19 May 1998 at 11:00 h

by

NESTOR J. MENDEZ V.
Master of Science in Land and Water Development, CIDIAT Venezuela
Master of Science in Hydraulic Engineering, IHE Delft
born in Lagunillas, Edo. Zulia, Venezuela

ISN 955022

This dissertation has been approved by the promoters:
Dr ir E. Schultz, professor in Land and Water Development
Dr ir L.C. van Rijn, professor in Fluid Mechanics

Authorization to photocopy items for internal or personal use, or the internal or personal use of specific clients, is granted by A.A. Balkema, Rotterdam, provided that the base fee of US$1.50 per copy, plus US$0.10 per page is paid directly to Copyright Clearance Center, 222 Rosewood Drive, Danvers, MA 01923, USA. For those organizations that have been granted a photocopy license by CCC, a separate system of payment has been arranged. The fee code for users of the Transactional Reporting Service is: 90 5410 413 9/98 US$1.50 + US$0.10.

Published by
A.A. Balkema, P.O. Box 1675, 3000 BR Rotterdam, Netherlands
Fax: +31.10.4135947; E-mail: balkema@balkema.nl; Internet site: http://www.balkema.nl

A.A. Balkema Publishers, Old Post Road, Brookfield, VT 05036-9704, USA
Fax: 802.276.3837; E-mail: info@ashgate.com

ISBN 90 5410 413 9

© 1998 A.A. Balkema, Rotterdam
Printed in the Netherlands

BIBLIOTHEEK
LANDBOUWUNIVERSITEIT
WAGENINGEN

NN08201,2526

THESES

belonging to the dissertation:

Sediment transport in irrigation canals

Néstor J. Méndez V.

May 19, 1998
Delft, The Netherlands

1. Sediment problems in irrigation canals should be analyzed in a wider context than that of sediment transport only. This analysis should also include different scenarios of water flow and sediment characteristics.

2. Any relationship that involves water velocity as a variable for describing the related physical processes should consider the distribution of that velocity over the considered cross section.

3. The accuracy of sediment transport predictions is substantially lower than that of water flow predictions. Sediment transport calculations should therefore be as accurate as possible to minimize an accumulation of inevitable errors and the effects of uncertainties.

4. An irrigation system should also be considered as a man-operated sediment transport system.

5. The magnitude of existing sedimentation problems in irrigation systems is comparable to those encountered in rivers, reservoirs and along coasts. Therefore it is strongly recommended that in the field of irrigation, an internationally recognized organization should systematically pay due attention to these problems.

6. Sediment deposition in agricultural areas mainly originates from erosion caused by use of land and associated practices in agriculture itself. This can be seen as the erosion paradox of agriculture.

7. Sediment transport predictions are generally comparable to weather predictions in the Netherlands.

8. Good maintenance also gives problems.

9. Considering the available water resources of the world as a single global system, irrigation efficiency at field level is often misused to generalize the overall use of water for irrigation purposes. In practice, the efficiency at a global scale is much higher.

10. The self-perception of being a "practical engineer" is often used as an excuse for reluctance to analyze the concepts underlying the physical processes. It is unlikely that these engineers will be able to provide sound practical solutions if they are not sufficiently acquainted with those concepts.

11. The development of mentality is the key to the development of human society, but how to achieve this is the biggest challenge.

12. Development of hardware, software and upgrading of their users should advance at a comparable rate.

TABLE OF CONTENTS

ACKNOWLEDGMENTS IX

SUMMARY XI

1 INTRODUCTION 1
1.1 General 1
1.2 Problem description 2
1.3 Objectives 4
1.4 Outlines of the study 4

2 BACKGROUND 7
2.1 General 7
2.2 Design criteria for irrigation canals 13
2.2.1 Regime method 15
2.2.2 Tractive force method 16
2.2.3 Permissible velocity method 17
2.2.4 Rational method 17
2.3 Mathematical modelling of sediment transport in irrigation systems 18
2.3.1 Friction factor predictors 20
2.3.2 Sediment transport in equilibrium conditions 21
2.3.2.1 Initiation of motion 22
2.3.2.2 Initiation of suspension 23
2.3.2.3 Sediment transport capacity 24
2.3.3 Sediment transport in non-equilibrium condition 27
2.3.3.1 2-D or 3-D Convection-diffusion equations 28
2.3.3.2 Depth integrated models 29
2.3.4 Simulation of sediment transport in irrigation systems 30
2.4 Conclusions 32

3 WATER FLOW AND SEDIMENT TRANSPORT EQUATIONS 35
3.1 General 35
3.2 Governing equations for water flow 35
3.3 Governing equations for sediment transport 39
3.3.1 Friction factor predictors 43
3.3.1.1 Bed form development 43
3.3.1.2 Effect of bed form on the flow resistance 44
3.3.1.3 Determination of friction factor 47
3.3.1.4 Composite roughness 50
3.3.2 Sediment transport equations 56

3.3.2.1 Sediment transport predictors 56
3.3.2.2 Suspended sediment transport in non-equilibrium condition 58
3.3.2.3 Sediment transport computations for non-wide canals 63
3.3.3 Mass balance equation for sediment transport 68
3.4 Conclusions 69

4 APPLICATION OF SEDIMENT TRANSPORT CONCEPTS IN IRRIGATION CANALS 71
4.1 General 71
4.2 Prediction of friction factors in irrigation canals 72
4.2.1 Prediction of bed forms in irrigation canals 72
4.2.2 Prediction of friction factor 77
4.2.3 Prediction of composite roughness for non-wide irrigation canals 81
4.2.3.1 Schematization of a new predictor method of composite roughness for a trapezoidal cross section 82
4.2.3.2 Correction for the distribution of velocities 88
4.2.3.3 Experimental set-up 91
4.2.3.4 Comparison of the composite roughness predictors in trapezoidal canal 97
4.2.3.5 Prediction of composite roughness in a rectangular cross section 103
4.3 Methods to estimate sediment transport in irrigation canals 109
4.3.1 Laboratory and field data 109
4.3.2 Evaluation of the methods to predict the sediment transport 110
4.3.3 Sediment transport computation in non-wide canals 117
4.3.3.1 Velocity distribution in lateral direction 120
4.3.3.2 Determination of exponent N 121
4.3.3.3 Determination of correction factor α for the sediment transport computation in non-wide canals 125
4.3.4 Comparison of procedures to compute sediment transport in non-wide canals 131
4.4 Conclusions 138

5 MATHEMATICAL MODEL FOR SEDIMENT TRANSPORT IN IRRIGATION CANALS 139
5.1 General 139
5.2 Numerical solution for water flow equations 139
5.3 Morphological changes of the bottom level 145
5.4 General description of the mathematical model 156
5.4.1 Functional description 157
5.4.2 Input data 162

5.4.3 Output data 163
5.5 Conclusions 163

6 APPLICATIONS OF THE MATHEMATICAL MODEL FOR SEDIMENT TRANSPORT IN IRRIGATION CANALS 165
6.1 General 165
6.2 Changes of the discharge 168
6.3 Changes in the incoming sediment load 172
6.4 Controlled sediment deposition 176
6.5 Sediment transport predictors 181
6.6 Flow control structures 186
6.7 Maintenance activities 190
6.8 Operation activities 197

7 EVALUATION 209
7.1 General 209
7.2 Simulation of sediment transport in irrigation canals 210

REFERENCES 219

APPENDICES 233
Appendix A Description of the selected methods to estimate the total sediment transport in irrigation canals 233
Appendix B Description of the methods to estimate friction factor 245
Appendix C Data collected on single and composite roughness at the hydraulics laboratory of Wageningen Agricultural University (WAU) 257
Appendix D Depth averaged velocity distribution in the cross section of a trapezoidal canal 263
Appendix E Determination of the exponent N in the sediment transport predictors 267

LIST OF SYMBOLS 273

SAMENVATTING 277

CURRICULUM VITAE 285

ACKNOWLEDGMENTS

The research work for this thesis was carried out at the International Institute for Infrastructural, Hydraulic and Environmental Engineering (IHE), Delft, the Netherlands.

I would like to thank all those who supported me during the study. In the first place I would like to thank my promoters Prof. dr. ir. E. Schultz and Prof. dr. ir. L. C. van Rijn for their guidance, academic advices and support for carrying out this research. Also my thanks to my mentor Ir. H. W. Th. Depeweg for his assistance, guidance and discussions on items related to my research but also related with the daily life in this country.

Also I would like to thank the staff members of the core Land and Water Development who supported me during my study.

Ir. A. Verwey, Ir. G. J. Klaassen, Dr. ir. E. Mosselman and Dr. ir. E. Valentine provided me assistance during my study. Ir. W. Boiten and Mr. A. Dommerholt from Wageningen Agricultural University (WAU) provided me support and guidance during my experiments.

I am grateful for the friendly working atmosphere that surrounded my stay at IHE specially with my colleagues F. X. Suryadi, R. Gupta and A. Mehdi. This gratitude should also be extended to my other colleagues and friends from IHE.

I remain very thankful to my employer in Venezuela, Universidad Centro Occidental "Lisandro Alvarado", Consejo Nacional de Investigaciones Cientificas y Tecnologicas (CONICIT) and FUNDAYACUCHO for the financial support.

Last but not least my thanks go to my family and friends, whose support and affection encouraged me to complete this research. Finally most of all to my wife Aidee and our daughters Maria Julietta and Maria Veronica for their continuous support, endless patience and understanding they gave me during all these years.

SUMMARY

The world population is rapidly increasing and is expected to double to about 10 billion by the year 2050. To support an increasing population in terms of food sufficiency, more and more water will be required. Irrigation is the most critical component of the modern package of inputs to effect high crop production. Irrigation has been the largest recipient of public agricultural investment in the developing world. Hence, continued investment in irrigation along with reforms in institutional arrangements for management of water are very much necessary to ensure adequate supply of food. Simultaneously, water requirements for other purposes, domestic, industrial and hydropower will steadily increase as well. Under this competing situation irrigation will have to become increasingly more efficient in the future. Improved management and operation activities must be implemented to prevent recurring degradation of irrigation projects. Clogging of turnouts and reduction of the conveyance capacity of canals by siltation are problems frequently met in irrigation systems. Annually, high investments are required for rehabilitation of irrigation systems in order to keep them suitable for their purposes. New development of irrigation projects or upgrading of existing schemes will require a better understanding of the sediment transport process under the prevailing flow conditions in irrigation canals. Applicability of the existing sediment transport relationships on irrigation canals has to be better understood. In this way predictions on sediment deposition in irrigation canals will be more reliable.

The present study is focused on sediment transport in irrigation canals which may have a serious impact on the operation and maintenance activities. The design of the canal system either should be based on the transport of all the in the water present sediment to the fields or to places in the canal system, where the deposition can be removed with least costs. Sedimentation should be prevented in canals and near structures, as it will hamper and endanger a proper irrigation management. In the design and operation of irrigation canals with sediment-laden water several aspects related to irrigation criteria and sediment transport must be taken into consideration. The need for conveying different discharges at a required water level to meet the irrigation requirement and at the same time to convey the sediment load with a minimum deposition and/or erosion in the canal system should be the main criteria for the canal design. Irrigation canals are generally designed upon the assumption of uniform and steady flow. It is also assumed that there exists an equilibrium situation where the sediments entering into the irrigation canals will be transported without settling or erosion. However, uniform and steady flow are seldom found in reality. In the operation of an irrigation system the flow is predominantly non-uniform. While the sediment transport is highly dependent on the flow conditions it is obvious that the sediment transport capacity of the canals varies as well.

Development on sediment transport in open channels have been mainly focused on river engineering. Even though certain similarities between rivers and irrigation canals are present, these concepts are not fully applicable to irrigation canals. A description and analysis of the

sediment transport concepts under the specific conditions of irrigation canals will contribute to improve the understanding of these concepts and will help to decide on the applicability of them on simulation of the sediment transport processes for particular conditions of water flow and sediment inputs. A mathematical model which includes sediment transport concepts for the specific conditions of irrigation canals will become an important and timely tool for designers and managers of those systems.

The aim of this research is to present a detailed analysis of the sediment transport processes, a physical and mathematical description of the behaviour of sediment transport under flow conditions encountered in irrigation canals and to develop a model to predict sediment transport and the deposition or entrainment rate for various flow conditions and sediment inputs.

Sediment transport processes

Sediment transport and water flow are interrelated and cannot be separated. From a mathematical point of view the interrelation can be described for a one-dimensional phenomenon without changes in the shape of the cross section by the following equations:

- *governing water flow equations*: continuity and dynamic equations;
- *governing sediment equations*: resistance to flow, sediment transport equations, continuity equation for sediment mass.

Water flow equations: although one-dimensional flow hardly can be found in nature, water flow in an irrigation canal will be considered to be one-dimensional. Under this assumption, the general equations for one dimensional flow can be described by the Saint Venant equations. The amount of water flowing into irrigation canals during the irrigation season and moreover during the life time of irrigation canals is not constant. For the time depending changes in the bottom of the canal the water flow can be easily schematized as quasi-steady which means that the time depending factors in the Saint Venant equations can be neglected.

Resistance to flow: the resistance to flow in open channels is affected by several factors, among which the development of bed forms play an important role. Determination of the friction factor of a movable bed is a complex problem that requires knowledge of an implicit process of flow conditions and bed form development. In order to predict the type of bed forms in irrigation canals the theories developed by Liu, Simons and Richardsons, Bogardi and van Rijn were compared to a selected set of laboratory and field data. Also a comparison of the most widely used methods to predict the resistance to flow with field and flume data has contributed to select an appropriate method for similar situations. The selected methods for predicting the resistance to flow were: White, Bettes and Paris (1979), Brownlie (1983) and van Rijn (1984c).The objective was to find the appropriate theories to describe the bed form and to estimate the resistance to flow (friction factor) in irrigation canals.

From the performance of each predictor of bed form type and friction factor method when compared with selected field and laboratory data some conclusions can be drawn:

- the theories of van Rijn and Simons and Richardson behave as the best to predict the bed form in irrigation canals;
- all the bed forms described for the lower regime (ripples, mega-ripples and dunes) can be expected in irrigation canals;
- the prediction of the friction factor by using the previously described methods takes only into account the bottom friction;
- the van Rijn method for predicting the friction factor shows the best results when compared with the selected data.

Another important feature related to the resistance of water flow in irrigation canals is the estimation of the friction factor of a irrigation canal with composite hydraulic roughness. The development of bed forms on the bottom, different material on the bottom and side of the canal or vegetated side banks are typical situations for the composite roughness conditions in irrigation canals. The most common cross sections in irrigation canals are the trapezoidal and rectangular cross section with a relatively small value for the bottom width-water depth ratio. In these cross-sections the velocity distribution is strongly affected by the varying water depth on the side slope and the boundary condition imposed to the velocity at the side wall. A method to estimate the effective roughness in a trapezoidal canal with composite roughness along the wetted perimeter which uses the theoretical velocity distribution in the cross section, is proposed.

In order to predict the effective roughness in irrigation canals with composite roughness, the existing methods for predicting the effective roughness and the proposed method in this study have been compared with a selected set of laboratory data, which has been collected in the hydraulic laboratory of the Wageningen Agricultural University. The aim of the experiments has been to investigate the friction factor in a trapezoidal canal having varying roughness on side and bottom and to find an appropriate method to estimate the friction factor in a non-wide canal with different roughness along the wetted perimeter. From the comparison the main conclusion can be drawn that the proposed method gives better results than the other methods.

For rectangular cross sections with composite roughness the existing methods for estimating the effective roughness can not explicitly be used. Therefor it is proposed to estimate the composite roughness in rectangular cross sections by the same principle as used for the side wall correction. The procedure to estimate the effective roughness in rectangular cross sections has been tested with a selected set of laboratory data used by Krüger. The proposed method predicts more than 95% of the measured values of the composite roughness within a range of error of 15%.

Sediment transport equations: sediment transport equations are related to the way in which the sediment is transported: namely in equilibrium and non-equilibrium condition.

Sediment transport predictors for equilibrium conditions have been established for different conditions. The use of those equations should be restricted to the conditions for which they were developed. However a comparison of the different equations under similar flow and sediment characteristics, both in irrigation canals and from field and laboratory data will be a useful tool to evaluate the suitability of each equation under these particular flow conditions. In this study, five of the most widely used equations to compute sediment transport have been compared, namely the Ackers and White, Brownlie, Engelund and Hansen, van Rijn and Yang equations. These equations have been compared with field and laboratory data. The objective was to find more reliable predictors of the sediment transport capacity under the flow conditions prevailing in irrigation canals. From that evaluation some remarks can be drawn:

- prediction of the sediment transport in irrigation canals within an error factor less than 2 is hardly possible;
- based on an overall evaluation of all performance criteria for each equation, the Ackers and White and Brownlie equations seem to be the best to predict the sediment transport rate in irrigation canals.

Sediment transport theories have been developed for wide, open channels. Most of the man-made irrigation canals are not considered as wide canals. Recommended values for the ratio of bottom width and water depth (B/h) in those canals are smaller than 8. Existing methods for calculating the total sediment transport capacity for the entire cross section of a non-wide canal do not take into account the velocity distribution over the cross section. A new method to compute the total sediment transport by using a cross section integrated method is proposed, which is based on the assumption of a quasi two-dimensional model. The objective is to consider the effect of the side banks on the distribution of velocities and to adapt the sediment transport predictors for computing the sediment transport for the entire cross section of a non-wide canal. The existing methods and the proposed method to compute the total sediment transport in non-wide canals were compared with a selected set of laboratory data. Based on the overall comparison the proposed method gives better results than the existing methods for computing the sediment transport capacity for the whole cross section.

An interesting phenomenon of the non-equilibrium sediment transport in irrigation canals is the adjustment of the actual sediment transport to the sediment transport capacity of the irrigation canal. To simulate the sediment transport under non-equilibrium conditions, the Gallapatti's depth integrated model for adaptation of the suspended load has been used. It has been assumed that the adaptation length for bed load is the same adaptation length for suspended load. Therefore the Gallapatti's depth integrated model can be used to describe the approach of the total sediment concentration to the transport capacity of the irrigation canal.

Application of mathematical modelling of sediment transport in irrigation canals

In order to simulate the sediment transport in irrigation canals, a computer program (SETRIC) has been developed. The computer program can simulate water flow, sediment transport and changes of bottom level in a network composed by a main canal and several laterals with/without tertiary outlets. Also some hydraulics structures are included in the program: overflow and undershot type, submerged culverts and inverted siphons, flumes and drops.

The computer program is based on a sub-critical, quasi-steady, uniform or non-uniform flow (gradually varied flow). The water flow can be simulated in open channels, with a rectangular or trapezoidal cross section with single or composite roughness. Only friction losses are considered. No local losses due to changes in the bottom level, cross section or discharges are taken into account. However, changes in the bottom level are included.

Sediment characteristics are defined by the sediment concentration at the head of the canal and sediment size is characterized by the mean diameter d_{50}. The range of values is 0.05 mm $\leq d_{50} \leq$ 0.5 mm. A uniform sediment size distribution has been assumed.

The simulation periods take into account the variation of the irrigation water requirement during the growing season. The growing season is divided into four stages depending on the crop development and climate conditions. The program assumes a maximum of four different periods in which the discharges along the system can be varied.

Maintenance activities can also be included into the program. Those maintenance activities are referred to the obstruction degree due to weed growth on the banks and by its effect on the roughness condition of the canal. From that point of view three types of maintenance are included in the program: ideal maintenance, well maintained and poor maintained.

Some applications of the model to simulate sediment transport in irrigation canals are shown. The results can not be generalized so that they can only be applied for the local flow conditions and sediment characteristics of each application. The applications are meant to show the applicability of the model and to improve the understanding of the sediment transport process for situations usually encountered in irrigation systems. The sediment deposition in an irrigation canal during a certain period will be simulated for each of the different applications. The sediment transport capacity of the irrigation canal is computed according to the Ackers and White's predictor method. The adjustment towards the sediment transport capacity is according to the Gallapatti's depth integrated model. A sediment mass balance in each reach of the canal will give either the net deposition or net entrainment between the two boundaries of a specific canal reach. From the application cases some conclusions are drawn:

Changes of discharges: during the simulations for reductions of discharge to 80% of the design value (equilibrium condition), more than 40% of the incoming sediment load was deposited.

Changes in the incoming sediment load: the effect of changes in the incoming sediment load on the sediment transport include the effect of variations in the incoming sediment concentration and in the median sediment size during the irrigation season and/or the lifetime of an irrigation canal. For 100% of variation in the incoming sediment concentration about 30% of the incoming sediment load is expected to settle into the canal. A similar behaviour is observed for the case of changes in the design value of the median size of the incoming sediment. For instance a total of about 45% of the incoming sediment during the simulation period is deposited when the sediment size deviates 100% from the equilibrium size.

Controlled sediment deposition: two scenarios to concentrate the sediment deposition at the head reach of a canal were simulated. They can be described as: widening (scenario 1) and deepening (scenario 2). No additional considerations for optimizing economical cost and sediment deposition were done. For the specific flow and sediment transport conditions scenario 2 trapped 4 times more sediment than an irrigation canal without control and 1.3 times more than scenario 1.

Sediment transport predictor: large differences in the computed sediment deposition were observed among the sediment transport predictors. The hydraulic conditions during the simulation period gave a low sediment transport capacity for the Engelund and Hansen predictor and larger for Brownlie and Ackers and White predictors. By using the Engelund and Hansen's predictor the sediment deposition was 2 and 3 times more that the Brownlie and Ackers and White's predictors respectively.

Flow control structures: two types of flow control structures were compared: overflow type and undershot type. The observed total deposition in both cases is rather similar. A larger difference was observed in the distribution of the sediment deposition along the canal. That difference was mainly concentrated in the upstream part of the structure.

Maintenance activities: maintenance was related to weed infestation and it was simulated by assuming optimal maintenance and no maintenance at all during the irrigation season. No direct effect of the growth of the weed on the sediment transport is considered. More sediment deposition was observed in the ideally maintained canal than the non-maintained canal. Due to the constant water level at the downstream side of the irrigation canal the flow condition within the canal behaved as: in the ideally maintained canal a gradually varied flow (backwater curve) remained constant during the simulation period. A continuous deposition was observed during all the time along the irrigation canal. In the non-maintained canal the initial flow condition changed in time from a backwater curve to a drawdown curve due to the constant water level at the downstream end and due to the variation of the water level within the canal imposed by the variation of the roughness condition. A sediment deposition period followed by an entrainment period was observed during the irrigation season.

Operation activities: for simulating the effect of the operation procedures on the sediment deposition in the main canal four scenarios were investigated. The four scenarios are: scenario 1 (continuous flow); scenario 2 (rotational flow by hour); scenario 3 (rotational flow by day); scenario 4 (rotational flow by week). From the comparison the following conclusions can be drawn:

- the largest total sediment deposition was observed in scenario 1. Total sediment deposition in scenarios 2, 3 and 4 was rather similar;
- large differences were observed in the distribution of the sediment deposition within the reaches of the main canal.

By considering the results of the applications of the mathematical modelling, it can be concluded that model is a useful tool for assessing the sediment deposition within irrigation canals under different flow conditions and sediment characteristics. Nevertheless, the mathematical model's performance can most probably be improved when it is applied in more situations. Monitoring of the sediment deposition in irrigation networks is required to evaluate the model under specific conditions and to investigate the response in time and space of the bottom level to determined water flows and sediment characteristics. Influences of the type and operation of flow control structures, geometrical characteristics of the canals, water flow and incoming sediment characteristics on the deposition, which the mathematical model predicts, will contribute to a better understanding of the sediment transport processes in irrigation canals.

1 INTRODUCTION

1.1 General

Irrigation is a primary method for realising a sustainable agricultural production through the supply of the deficit of crop water requirements in areas where precipitation is not enough to meet the needs. Therefore, design, installation and management of an irrigation system play an important role in the performance and aim of those systems. An irrigation system enables the supply of the required amount of water at the proper time and at the correct water level to the fields and it comprises all the structures and the organization which manages the water flow to the fields trough the irrigation network. A main feature of irrigation is that the infrastructure (irrigation facilities) is man-made, man-managed and man-used.

Sediment transport in irrigation canals is an important aspect in the design and operation of an irrigation system. The need for more efficient irrigation systems increases every day. A minimum of capital investments in design, construction and operation linked to the optimal use of the available water are, among others, important factors in the development of an irrigation project. Clogging of turnouts and reduction of the conveyance capacity of canals by siltation are problems frequently met in irrigation systems. They cause reduction in the amount of water available for the areas to be irrigated. Annually, high investments are required for rehabilitation of irrigation systems in order to keep them suitable for their purpose. The sediments are coming in most cases from rivers. They enter into the irrigation network when the water is taken directly from the river, either without sediment diverters or with diverters, which are not able to eliminate the sediment at the diversion points in an adequate way. Once, the sediment load enters into the canal system, it can be disposed in different ways. Depending on the transport capacity in the canal network and the capacity of the irrigated land to absorb sediments, the sediments can either be distributed over the farmlands or be accumulated in the canals, where they periodically have to be removed.

To convey the sediment load with the water supply to the fields, irrigation canals must be designed and operated in such a way that any sediment that enters the system is transported through the canals with a minimum of deposition. The transport capacity of the sediments along the canals must be maintained at or above the required one to avoid sedimentation, but it should not be too high to prevent scouring of the bed. Operation conditions and poor maintenance do not permit a consistent transport capacity of the canals during all time. Changes in water supply, reduction in flow velocity will produce variations in the transport capacity of the canals and deposition and/or scouring along the canal system will occur.

The aim of this study is to present a detailed analysis of the main processes, a physical and mathematical description of the behaviour of sediment transport under the flow conditions prevailing in irrigation canals and to develop a model to predict sediment transport and the

deposition or entrainment rate for various flow conditions and sediment inputs. The model will offer the possibility to simulate the behaviour of the water flow, sediment transport and changes in bottom level for the changing flow conditions of the irrigation canals which are usually caused by the operation and/or maintenance activities in those canals.

1.2 Problem description

The study of sediment transport in irrigation canals is focused on the sediment and erosion processes in a canal network. In view of maintenance activities the head work should be designed to prevent or to limit the entrance of sediment into canals, the design of the canal system either should be based upon the transport of all the in the sediment present in the water to the fields or to a place in the canal system, where they can be removed at a minimum cost. Sedimentation should be prevented in the canals and near structures, as it will hamper and endanger a proper irrigation management, which main objectives are to deliver the water in an adequate, reliable, fair and efficient way to the farmers. Improper management will result in a low efficiency and needless waste of the already scarce water resources.

Irrigation canals are generally designed based upon the assumption of uniform and steady flow of water and sediments in such a way that they are able to carry water and sediments to the fields. It is assumed that there exists an equilibrium situation where the sediments and water entering into the irrigation canals will be transported without settling or erosion. However, uniform and steady flow is seldom found in reality. In the operation of an irrigation system the flow is predominantly non-uniform, with a time dependent discharge and with a constant water level at regulation points supplying offtakes. While the sediment transport is highly dependent on flow conditions, obviously the sediment transport capacity of the canals varies as well. Although water flow can be modelled with a high degree of accuracy, sediment transport is only understood to a limited extent. The predictive ability of sediment transport equations and models on the quantity of sediment that needs to be removed is still rather poor. Computations of the effects of these non-equilibrium conditions on sediment transport are required to determine whether deposition and/or entrainment occurs and the amount and distribution along the canals. Numerical mathematical modelling of sediment transport offers the possibility of predicting for a particular flow and a particular situation the distribution of sediment deposition or entrainment rates.

Developments in the area of sediment transport in open canals have mainly been focused on natural channels. Sediment transport theories, development of bed forms, resistance factors, etc. have been developed under assumptions applicable to those particular conditions encountered in rivers and even though certain similarities between rivers and irrigation canals exist, these concepts are not fully applicable to irrigation canals. Irrigation canals are rather different. Mostly these are man-made canals and the irrigation environment presents several unique problems generally hardly encountered in river modelling. The need for controlling the level (in upstream and downstream direction) and discharge of the water flow and for finding

an optimization of the cross section of the canals, the high influence of the side banks on the velocity distribution across the section, presence of large number of flow control structures, gate submergence, flow in inverted siphons, multiple flow paths create some differences in both kinds of canals. Table 1.1 shows some of the main differences between rivers and irrigation canals.

Table 1.1 General characteristics of water flow and sediment transport in rivers and irrigation canals

WATER FLOW AND SEDIMENT TRANSPORT		
	RIVERS	**IRRIGATION CANALS**
- Water profiles	generally without water level control: nearly uniform flow	water level control: gradually varied flow
- Froude number	wide range	restricted by operation of flow control structures (Fr <0.4)
- Discharge	not controlled; increasing in downstream direction	controlled by operation rules; decreasing in downstream direction
- Flow control	almost no control structures	several flow control structures: water level and discharge
- Width (B)/depth (h)	$B/h > 15$ (wide canals)	$B/h < 7 - 8$
- Velocity distribution	nearly uniform velocity distribution in lateral direction	velocity distribution strongly affected by side wall and by side slope
- Alignment	hardly straight, meandered and braided	straight
- Topology	convergent	divergent
- Lining	alluvial river bed	man-made canals: lined or no lined
- Main function	conveyance of water and sediment	conveyance and distribution of water
- Sediment size	wide range of sediment size	fine sediment
- Size distribution	graded sediment	nearly uniform distribution
- Sediment material	river bed	external sources
- Sediment transportation	suspended and bed loads	mainly suspended load
- Bed forms	mostly dunes	mostly ripples and mega-ripples
- Roughness	skin and form friction	form friction
- Sediment concentration	wide range	controlled at headwork

A description and analysis of the sediment transport concepts under the specific conditions of irrigation canals, will contribute to an improved understanding on these concepts and will help to decide on the applicability for the simulation of the sediment transport processes under particular conditions of water flow and sediment inputs.

1.3 Objectives

The objective of this research is to improve the understanding of sediment transport in irrigation canals. Based on this improved understanding a mathematical model to simulate this process will be developed. The model will have to provide for particular combinations of water flow and sediment characteristics, the distribution of sediment concentration and the associated sediment load as well as the deposition rate and/or entrainment rate in time and place.

To realise the objectives several specific activities have been carried out:

- investigation of the characteristics of bed forms in irrigation canals;
- testing of several friction factor predictors for flow conditions prevailing in irrigation canals;
- laboratory investigation on composite roughness in non-wide canals with trapezoidal or rectangular cross sections;
- testing of several sediment transport theories for flow conditions prevailing in irrigation canals;
- investigation of the effect of side banks on sediment transport capacity;
- adaptation of the sediment transport theories to compute sediment transport in non-wide canals;
- development of a mathematical model for water flow and sediment transport in irrigation systems;
- application of the mathematical model to an irrigation system;
- simulation and comparison of the sediment transport for: changes in discharge, changes in the incoming sediment load characteristics, controlled deposition, several sediment transport predictors, different types of flow control structures, several operation strategies and different types of maintenance activities.

1.4 Outline of the study

To report on the work done, the thesis consists of seven chapters, which can be summarized as:

- *Chapter 1*: this work is started with an introduction to the topic to be dealt with. A description of the problem and the objectives of this study are presented;
- *Chapter 2*: a review of selected references dealing with sediment transport and particularly its influence on irrigation canals is presented. Identification of the more relevant advances in previous works and using their results in this study. Among the aspects reviewed are:

* design criteria for irrigation canals;
* description and application of sediment transport theories in irrigation canals;
* review of existing mathematical models to compute sediment transport;
* development of bed form and its influence on friction factor;
* influence of flow control structures on the sediment transport;
* solutions of the equations governing sediment transport and water flow;
* simulation of sediment transport in irrigation canals;

- *Chapter 3*: a general description of the governing processes in the sediment transport in open channels is presented. Assumptions, equations, range of applications, data requirements for the mathematical formulation of the sediment transport computation in open channels are described.;
- *Chapter 4*: the previously described theories related to sediment transport are tested and adapted for computing the sediment transport in irrigation canals. These tests will give some ideas about the applicability of each formula for a specific condition and may reduce inevitable errors and inaccuracies;
- *Chapter 5*: once the sediment transport has been determined for the specific conditions of irrigation canals it will be the basis of a mathematical model for simulating sediment transport processes in those types of open canals. A description of the mathematical model is given in this chapter;
- *Chapter 6*: in this chapter some applications of the sediment transport modelling in irrigation canals will be described. The mathematical model is applied to an irrigation system to evaluate the sediment transport under different situations of:
  * changes in discharge;
  * changes in the incoming sediment load;
  * controlled deposition;
  * sediment transport predictors;
  * flow control structures;
  * maintenance activities;
  * operation strategies.
- *Chapter 7*: an evaluation of the applicability of the processes of the sediment transport under the prevailing flow conditions in irrigation canals is presented. At the end, an evaluation of the simulation of the sediment transport for several application cases related to the irrigation practice is given.

2. BACKGROUND

2.1 General

The expected growth of world population and rise in the standard of living will produce an enormous increase of water requirements. The world population is still increasing and is expected to double to about 10 billion by the year 2050. To support an increasing population in terms of food sufficiency, more and more water will be required (Biswas, 1995). Demand for irrigation water can be regarded as derived for food. As demand for agricultural products increases driven by population growth, the preponderance of increased production will have to come from irrigated lands. Irrigated lands have a higher yield and higher yield potential than rainfed land. They account for only 16 per cent of the world's crop land, but provide 40 per cent of the world's food (Chitale, 1996). Contribution of irrigation to global food production are in the range of 25% to 50%, a share that is set to rise as the new biotechnology input come on stream (Carruthers et al, 1997). Irrigation is the most critical component of the modern package of inputs to effect high crop production. It has enabled farmers to use fertilizers and high yielding seeds systematically in a confident manner. It also made possible two or three harvest per year from the same piece of land.

The 20th century can be considered the age of irrigation. In the first half of this century the irrigated area worldwide nearly doubled to 94 million ha. In the second half expanded further tb about 240 million ha (Schultz, 1997). Irrigation has been the largest recipient of public agricultural investment in the developing world. From 1950 through 1993 seven percent of the World Bank (US$ 31 billion) lending has been for irrigation. Irrigation investment will continue to be needed, to meet the demands for food of an ever-growing population. Hence, continued investment in irrigation along with reforms in institutional arrangements for management of water is very much necessary to ensure adequate supply of food at all time. Emphasis of the irrigation investment has shifted away from new facilities towards rehabilitating and upgrading existing ones (World Bank, 1995).

Many projects do not meet the efficiencies as designed for, due to mismanagement, misoperation and inequities in distribution. With agriculture claiming two thirds of all the water removed from rivers, lakes, streams and aquifers, making more efficient use is a top priority in moving toward more sustainable water use. Simultaneously, water requirements for other purposes, domestic, industrial and hydropower will steadily increase as well. New sources of water are increasingly expensive to exploit, limiting the potential for expansion in new water supply systems. It is indicated that the cost of development of each cubic metre of water for the next generation of water projects is often two to three times higher than that for the present generation. Under this competing situation irrigation will have to become increasingly more efficient in the future.

Operation and maintenance are very important aspects of irrigation because they affect the cost recovery of the project and therefore the irrigation project sustainability (World Bank, 1995). Improved management and operation practices must be implemented to prevent recurring degradation of those irrigation projects. Siltation of the canal systems is one of the main preoccupations in irrigation practice. Siltation in canals produces clogging of turn-outs, reduction of conveyance capacity of irrigation canals, overtopping, changes in the water distribution if outlets are left unchanged, less reliable operation of flow control structures etc. Annually high investments are required for rehabilitation of those irrigation systems. As an example each year the Provincial Irrigation Department in Pakistan's Punjab spend the sum of US$35 million for the maintenance of irrigation canals which a large part of this is allocated to desiltation works in those canals (Van Waijjen et al, 1997). New development of irrigation projects or upgrading of existing schemes will require a better understanding of the sediment transport process under the prevailing flow conditions in irrigation canals. Theories related to sediment transport are generally based on statistical correlations which invariably reflect typical characteristics of the data and the conditions of its origin. Understanding of the sediment transport phenomena is inadequate and this makes it very difficult indeed to predict (Sanmuganathan, 1990). Applicability of the existing sediment transport relationship on irrigation canals has to be better understood. In that way predictions on the sediment deposition in irrigation canals will be more reliable.

Irrigation comprises the artificial supply of water for agriculture, the controlled distribution of this water and the removal of water to natural or man-made drains after it has been put to optimum use. To do that an irrigation system has to be planned, constructed, operated and managed in such a way that all the fields in the commanded area can receive water in an appropriate, conveniently arranged and adjustable manner (Dahmen, 1994).

Van Hofwegen (1993) defined an irrigation system as the system that enables water to be acquired, transported and supplied to the farming field. It consists of two components: hydraulic infrastructure and the organization in charge of managing the water through the network. The management component is responsible for operation and maintenance of the hydraulic infrastructure. Two management levels can generally be distinguished in an irrigation system, namely the main level, which is managed by the irrigation authority and the tertiary unit level, which is managed by the farmers or by a water user's organization. The hydraulic infrastructure of the irrigation system includes facilities for acquisition, conveyance, regulation and measurement of water: headworks and irrigation network. Headworks are the facilities at the head of the irrigation system which diverts water from the source and supplies it to the irrigation network. Headworks can be weirs, dams or pumping stations. Diversion can be from surface water (rivers, lakes and reservoirs) or from groundwater. Irrigation networks are the hydraulic systems of canals or pipes and flow structures which are required for conveying, dividing, regulating, measuring, supplying and protecting the water from the source to the individual fields. The drainage system, which forms an important component of any irrigation

system in order either to dispose irrigation water after it has been used or to drain off any excess water, will not be further discussed in this thesis.

Most irrigated areas have very specific land features and characteristics. Among these specific differences are: topography, water availability, soil types and the specific aims of the irrigation system. From an evaluation of those characteristics the method for conveying and distributing the water through the main and tertiary levels of the irrigation system is determined. In a broad sense, there are two methods to convey and to distribute water by an irrigation system (FAO, 1971): by pressure or by gravity. In pressurized irrigation (sprinkler and trickle irrigation) the water is carried through a pipe system to the point where it will be consumed. By gravity irrigation the water is conveyed in open canals. Also a combination of these methods can be found at main and tertiary level. A gravity irrigation system comprises the hydraulic structures to transport water and to deliver water at a certain point at the required time in the right amount and at the right elevation to the command area. For a gravity irrigation system these irrigation structures can be divided in:

- *irrigation canals*: primary, secondary (lateral), tertiary (sub-lateral) and field canals. Often the primary and secondary canals are referred to as the main canal system. All those canals transport and distribute the water over the irrigated area;
- *flow structures*: weirs, culverts, gates, diversion boxes, etc. These structures are required for conveying, regulating, dividing, measuring, supplying and protecting the water flow.

In this study emphasis will be given to gravity irrigation systems, which receive water from surface water sources. Figure 2.1 shows a schematization of irrigation canals and structures in an irrigation network.

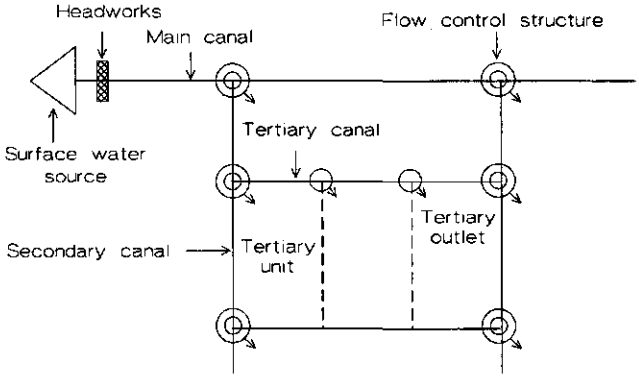

Figure 2.1 Schematization of irrigation canals and flow structures in an irrigation network

Irrigation canals should be designed to meet the varying irrigation requirements at farm level. The design of irrigation canals is based on the following criteria:

- *capacity*: the capacity of irrigation canals is determined by the water delivery method which describes how the irrigation requirements are delivered in time and place in the irrigation system. Delivery methods differ from each other with the scheduling of the water demands. Nowadays several classifications for water delivery schedules are available (Ankum, 1995). The World Bank (1986) classifies the water delivery schedules as:
  * *on demand*: water delivery reacts instantaneously to the water demand;
  * *continuous*: the irrigation canals supply a varying or constant continuous flow during the whole irrigation season;
  * *fixed rotation:* water delivery is scheduled with a constant flow and periods of rotation;
  * *variable rotation*: water delivery is programmed with a variable supply, with fixed /flows with variables periods (rotation) or variable supply and variable periods;

  An example of the water scheduling based on the rotational method is shown in figure 2.2. That figure also indicates the main variables involved in the water delivery scheduling.

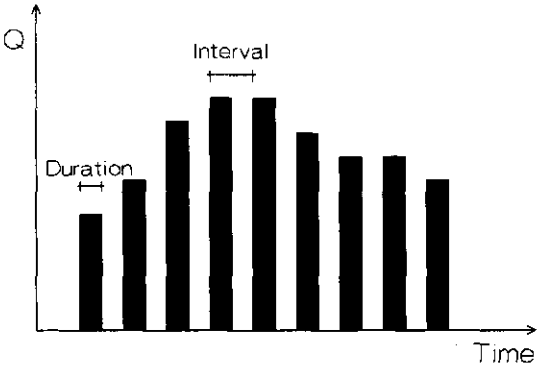

Figure 2.2 Variables in a water delivery schedule based on a variable rotational delivery method

The canal capacity is also determined by the flow control method (van Hofwegen, 1992). For instance, a downstream flow control method requires a "level top" canal to facilitate the zero flow condition, because the water level for zero discharge is above the full discharge level (Ankum, 1995).

- *command*: the command criteria are determined by the fact that the water has to command most of the area. The water level in the irrigation canals must be above the ground surface at any point of delivery. Due to the presence of flow structures and the

need to meet the varying irrigation requirements during the whole irrigation season the water flow in irrigation canals varies in time and space. Water flow and sediment transport in irrigation canals should be viewed in this context of operation of the system. The flow of water can be simulated with a high degree of accuracy, however, the description of sediment transport still lies on gross simplifications;

- *sedimentation and/or erosion*: irrigation canals must be designed based on the criteria that no sedimentation and no erosion occur during a certain period. A design of a stable cross section will be the end result of this criterion;
- *cost*: the application of the presented criteria for the design of irrigation canals will result in the determination of the alignment, longitudinal slope and cross section of the canals. It should result in balanced earthwork as far as possible. So, the irrigation canals have to give the best effect at minimum cost.

Ankum (1995) defined flow control structures as the structures required to keep the irrigation system in the desired state. Disturbances, such as a change in water supply, may transfer the system to an unwanted state. But it is also possible that the desired state has to be changed and that a new steady state of the system is required. The function of flow control structures is to distribute and to deliver the flows to the end-users in accordance with the system delivery schedules. Mostly flow control structures are designed at bifurcations for water level regulation, discharge regulation and discharge measurement. Figure 2.3 shows some basic configurations of flow control at bifurcations. Often the regulation and measurement of discharges is combined in one structure. Also other additional structures may be required for the crossing of roads or drains (culvert, siphons, aqueducts) and for dissipating energy (drops, chutes).

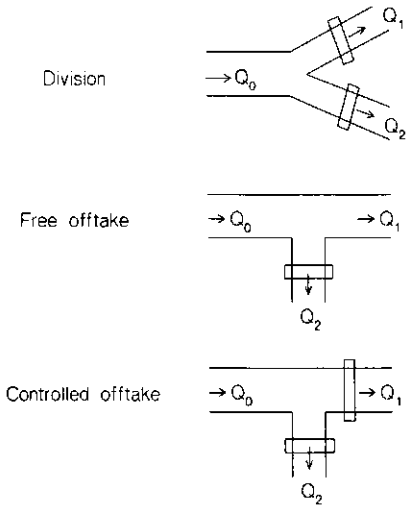

Figure 2.3 Basic configurations of flow control structures (after Hofwegen, 1993)

The purpose of water level regulators is to maintain the water level at a certain target at every discharge and to divide the flow over the outlets (Dahmen, 1994). Division of flow can also be done without water level control. In this case the water flow is only controlled by dividing the flow proportionally. Main reasons for water level control are to keep command of the service area through gravity, canal protection against deterioration, canal safety and flow control at offtakes (World Bank, 1989). Water level regulators can be divided in constant volume control, upstream control and downstream control. When the control point is located approximately in the middle of the canal the control is called constant volume control. Upstream control is designed to maintain a constant and predetermined water level upstream of the structure by either a fixed crest (weirs) or by manual or automatic operated devices, such as stop-logs, slide gates and radial gates. Upstream control is still the most common method for the operation of irrigation systems (Dahmen, 1994). In downstream control, both water level and flow are controlled downstream of the structure; changes are gradually passed on in upstream direction till the headworks. The selection of the most appropriate flow control method in irrigation systems appears to be quite complex and depends on the operational objectives of the irrigation systems. Selection of flow control structures is based on the following criteria (Ankum, 1995): hydrodynamic performance, hydrological and geographical setting, design and construction, operation and maintenance, economy, political and social aspects. Figure 2.4 shows a schematization of the main types of water level control.

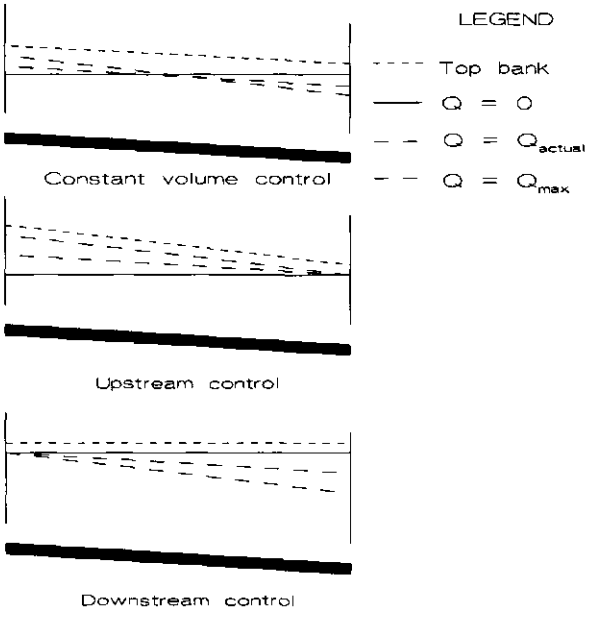

Figure 2.4 Constant volume control, upstream and downstream water level control

Regulating structures are used to control the discharge from one canal to another. They can be located at different places as at headworks, head-end of secondary and tertiary canals and at offtakes of the tertiary units (Ankum, 1995). Flap-, slide, roller and radial gates are several types of flow regulating equipment. Generally they are not equipped with measuring devices. In many irrigation systems the discharge is regulated and measured by two structures (Bos, 1989). Additional measuring discharge structures (broad-crested and sharp-crested weirs, Cipoletti weir, Parshall flume and Ballofet flume) have to be placed in series with the regulating structure to determine the flow rate from the parent canal to another canal (figure 2.5). Due to the large head losses, the time consuming and complicated procedure to operate both structures they often are replaced by one structure only. Both regulating and measurement functions can be combined in one structure (Romijn weir, single and double baffle distributor, Crump-de Gruyter gate and Constant Head Orifice).

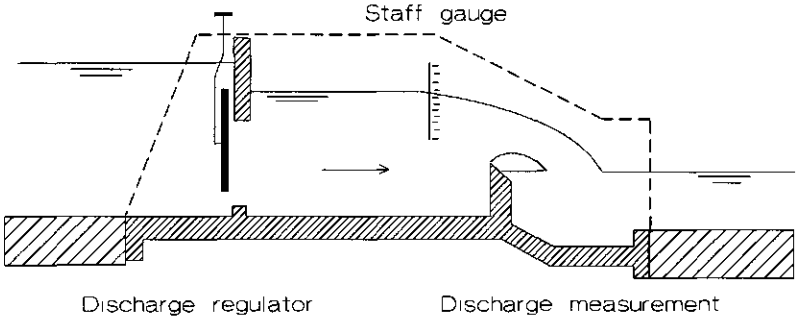

Figure 2.5 Discharge regulator and discharge measurement

2.2 Design criteria for irrigation canals

In the design of irrigation canals for sediment laden water aspects related to irrigation criteria as well as to the sediment transport must be taken into consideration. The need of conveying different amounts of water to meet the irrigation requirements for a required water level is the main criterion for canal design. Furthermore, the design must be compatible with a particular local sediment load in order to avoid silting and/or scouring. The diverted discharge should meet the irrigation requirements and at the same time the least deposition and/or erosion should occur in the canal system.

Vanoni (1975) mentioned that the canal design must be based on an operation study to determine the pattern of water demand. In that way the sediment transport characteristics in time can be established. Sediment may be deposited during one phase of operation and eroded during another phase with a balanced or stabilized condition.

According to FAO (1981), the objective of a canal design is to select such a bottom slope and geometric dimensions of the cross section that during a certain period the sediment flowing into an irrigation canal is equal to the sediment flowing out of the canal. Changes in equilibrium conditions for sediment transport result in periods of deposition or erosion.

Chang (1985) mentioned that because of the sediment problems, the geometry and the slope of the canal must be interrelated in order to maintain sediment equilibrium. The sediment problem in the design of canals can be controlled by conserving the continuity in sediment transport.

Dahmen (1994) pointed out that the irrigation network should be designed and operated in such a way that:

- the needed flow passes at the design water level;
- no erosion of the canal bottom and banks occurs;
- no deposition of sediment in the canal takes place.

The design of a canal that has to convey a certain sediment load, requires a set of equations related to the water-sediment flow to provide the unknown variables of slope and cross section (bottom width and water depth). The geometry of a sediment carrying irrigation canal will be the end product of a process in which the flow of water and sediment transport interacts.

For the design phase irrigation canals can be divided into three categories (Ranga Raju, 1981) which can be described as follows:

- *canals with a rigid boundary*: the canal design is based on the determination of the velocity at which any sediment entering into the canal will not settle on the boundary. High velocities are allowed, but they should not produce damage to the lining or create large disturbance in the water surface. A simulation of the changes of the flow conditions during the irrigation season becomes an important tool to ensure that the sediment does not deposit, even due to low velocities;
- *canals with erodible boundary and carrying clean water*: the canal design is based on the determination of the cross section for which the bed material does not move. The smallest cross section with a velocity as large as possible and without scouring of the bed should be the result of the canal design;
- *canals with erodible boundary and carrying water with sediment*: the design principle is that the canal should transport the water as well as the sediment. The cross section must ensure flow conditions for which the velocity is as large as possible to convey the sediment and at the same time not too large to prevent scouring of the bed. For the whole irrigation season both restrictions are difficult to meet simultaneously. Therefore, the canal design must look for a stable canal during a long period. Thus, these irrigation canals require that the total sediment inflow during a certain time period is equal to the total sediment outflow.

A conclusion to be drawn from the previous paragraphs is the need for the design of stable irrigation canals during the full operating life of the irrigation system. Sediments may be deposited during one phase of the irrigation season and be eroded during another phase, but with an overall balanced erosion and deposition for the total operation period.

To design stable canals four methods are mentioned by Chow (1983), Raudkivi (1990), HR Wallingford (1992) and Simons and Sentürk (1992):

- regime method;
- tractive force method;
- permissible velocity;
- rational methods.

2.2.1 Regime method

For the regime theory sets of simple empirical equations are available. The equations are derived from observations of alluvial canal systems that are relatively stable or in regime (HR Wallingford, 1992). The regime method considers the periphery of the open canal, the water and sediment flowing in it as a single whole and attempts to lay down the attributes for a stable (non silting/non scouring) canal primarily on the basis of empirical studies of the interaction of the above mentioned factors (Naimed, 1990). The regime theory is entirely empirical and is based on data observed in canals in regime. The regime method originates from India and Pakistan and most of the canal designs in these countries apply this method, specifically to the Lacey regime theory. The so-called regime equations are based on on-going observation and experience. The regime concept represents a long term average rather than some instantaneously variable state. It therefore expresses the natural tendency for channels that convey sediment within alluvial boundaries to seek a dynamic stability. Some of the equations given by Lacey are (Ackers, 1992):

$$P = 4.84\ Q^{0.5} \tag{2.1}$$

$$V = 0.625\ (f\ R)^{0.5} \tag{2.2}$$

$$S_0 = 0.0003\ \frac{f^{5/3}}{Q^{1/6}} \tag{2.3}$$

$$f = \sqrt{2500\ d} \tag{2.4}$$

where:

P = wetted perimeter (m)
R = hydraulic radius (m)
d = sediment size (m)
V = mean velocity (m/s)
S_0 = bottom slope
f = Lacey's silt factor for a sediment size d
Q = discharge (m^3/s)

The applicability of this method can be challenged in the case of a highly time dependent operational regime as practised in many irrigation systems at present (Bruk, 1986).

2.2.2 *Tractive force method*

The concept of the tractive force method originates primarily from work done by the U.S. Bureau of Reclamation under the direction of Lane (Raudkivi, 1990 and HR Wallingford, 1992). This method is based on a consideration of the balance of forces acting on sediment grains and it is used for evaluating the erosion limits only. No sediment transport is considered. The tractive force method is suited if the water flow transports very little or no sediment (Breusers, 1993). Since the method assumes no bed material transport, it is only relevant for canals with coarse bed material and zero (or very small) bed material sediment input (HR Wallingford, 1992). The tractive force depends on the shear stress at the bottom, which can be expressed as (Dahmen, 1994):

$$\tau = c\ \rho\ g\ h\ S_0 \qquad (2.5)$$

where:

τ = shear stress (N/m^2)
c = correction factor depending on the B/h ratio. For wide canal c = 1.
h = water depth (m)
ρ = density of water (kg/m^3)
S_0 = bottom slope
g = acceleration due to gravity (m/s^2)

The tractive force method is developed for the threshold condition of sediment transport. It assumes that the threshold condition, being the critical shear stress, exists along the canal and over the periphery. The allowable shear stress is given as function of the mean grain diameter and the quality of the water.

Dahmen (1994) mentioned as a "rule of thumb" for many irrigation engineers, that the maximum boundary shear stress in "normal" soil, for a "normal canal" and under "normal

conditions" could be between 3 and 5 N/m^2. Table 2.1 shows the recommended critical boundary shear stress (N/m^2) for fine non cohesive sediment material.

Table 2.1 Recommended critical boundary shear stress (N/m^2) for fine, non-cohesive sediment (from Dahmen, 1994)

d_{50} (mm)	clear water	light load	heavy load
0.1	1.20	2.40	3.60
0.2	1.25	2.49	3.74
0.5	1.44	2.64	3.98

To apply the tractive force method two other equations are required: one equation to compute the discharge (Manning, Strickler or Chézy) and one relationship between the bottom width and the water depth.

2.2.3 Permissible velocity method

Depending on whether there is a non-erodible or an erodible canal a permissible velocity can be used as criteria for the design of stable canals. A minimum permissible velocity is that which will not start sedimentation or induce the growth of aquatic plants. It is determined by the sediment transport capacity of the flow. A maximum permissible velocity is that which will not cause erosion of the canal. This velocity is very uncertain and variable and can be estimated only with experience and judgement (Chow, 1983). Maximum permissible velocities are given depending on the bed material (Simons and Sentürk, 1992).

2.2.4 Rational method

Four variables, namely the bottom width, water depth, bottom slope and side slope, are unknown for the design of irrigation canals. The side slope can be fixed depending on the mechanical soil properties. Therefore three equations are required to determine the other variables. They are an alluvial friction predictor, a sediment transport equation and the third can be obtained from a minimum stream power or maximum sediment transport efficiency. Sometimes a regime relationship is used to provide the width equation (HR Wallingford, 1992). Among the rational methods are mentioned: White, Bettess and Paris (1982) and Chang (1985).

The methods to design stable canals are useful in case of one specific flow condition. For large deviations in flow rate and sediment inputs these methods are inadequate to describe the sediment transport process, as they do not describe the conveyance of the sediment load through the whole canal system. The design criteria for conveying the sediment load through the canal system are based on energy dissipation considerations. By applying these energy

considerations de Vos (1926) and Vlugter (1962) described the relative sediment transport capacity. Based on those works, Dahmen (1994) describes that:

- for the conveyance of sediment in suspension, the hydraulic characteristics of the system should be such that:

  $\rho * g * V * S$ = constant or non-decreasing in downstream direction

- for the conveyance of non-suspended material, the hydraulic characteristics of the system should be such that:

  $h^{1/2} * S$ = constant or non-decreasing in downstream direction

where:

ρ = water density (kg/m^3)
g = gravity acceleration (m/s^2)
V = mean velocity (m/s)
S = energy line slope
h = water depth (m)

2.3 Mathematical modelling of sediment transport in irrigation systems

From a mathematical point of view the interrelation between water flow and sediment transport can be described for a one-dimensional phenomenon without changes in the shape of the cross section by the following equations (Cunge, 1980):

- *Continuity equation for water movement*:

$$\frac{\partial A}{\partial t} + \frac{\partial Q}{\partial x} = 0 \qquad (2.6)$$

- *Dynamic equation for water movement:*

$$\frac{\partial h}{\partial x} + \frac{V^2}{C^2 R} + \frac{\partial z}{\partial x} + \frac{V}{g}\frac{\partial V}{\partial x} + \frac{1}{g}\frac{\partial V}{\partial t} = 0 \qquad (2.7)$$

- *Friction factor predictor* which be given as a function of:

$$C = f(d_{50}, V, h, S_0) \qquad (2.8)$$

- *Continuity equation for sediment transport:*

$$(1 - p)\, B \frac{\partial z}{\partial t} + \frac{\partial Q_s}{\partial x} = 0 \qquad (2.9)$$

- *Sediment transport equation* which is given as a function of:

$$Q_s = f(d_{50}, V, h, S_0) \qquad (2.10)$$

where:

A = area of cross section (m^2)
Q = water discharge (m^3/s)
V = mean velocity (m/s)
Q_s = sediment discharge (m^3/s)
B = bottom width (m)
h = water depth (m)
R = hydraulic radius (m)
C = Chézy coefficient ($m^{1/2}/s$)
S_0 = bottom slope
g = acceleration due to gravity (m/s^2)
x = length co-ordinate (m)
t = time co-ordinate (s)
d_{50} = mean diameter of sediment (m)
p = porosity
z = bottom level above datum (m)

These equations form a non-linear partial differential system, which can not be solved analytically, but by a numerical method (Cunge, 1980). They are not independent, but they are implicit equations depending on each other. For instance the water flow condition influences the roughness coefficient and vice versa the sediment transport depends strongly on the water flow.

Most existing mathematical models are based on the finite difference method in which the set of equations 2.6 to 2.10 is replaced by a system of numerical discrete equations. To solve that equation system two methods are used:

- *Uncoupled solution*: the solution of the set of equations is separated by solving first the equations related to the water movement. The results found from that first step are used to solve the sediment transport equation and the continuity equation for sediment flow. The uncoupled solution can be used for long term simulation without rapid changes (Chuang, 1989);
- *Coupled solution*: the equations for water movement and sediment transport are solved simultaneously. In this way numerical oscillation and instability are reduced. The solution of the set of equations requires a general boundary condition for the water flow and the sediment transport. This method is recommended for short term simulations with rapid changes (Chuang, 1989)

Equations 2.6 and 2.7 are related to the water movement. The resistance to flow is represented by equation 2.8. This friction factor is a function of the water motion, sediment properties and development of bed forms. Very often this term is assumed to be a constant. This would reduce the problem of five equations to four equations. The sediment transport equations (equation 2.9 and 2.10) are related to the way in which the sediment is transported: namely in equilibrium and non-equilibrium condition. Equilibrium condition refers to the amount of sediment for a certain flow condition that can be transported without deposition or erosion (sediment transport capacity). The non-equilibrium condition describes how the amount of sediment is conveyed by the water flow as well as the erosion and deposition processes.

2.3.1 Friction factor predictors

The hydraulic resistance of the water flow in open canals is affected by several factors among which the development of bed features such as ripples, mega-ripples and dunes play an important role. The hydraulic resistance is measured in terms of a friction factor. In this study the Chézy coefficient is used to describe the friction factor. Further description with the Darcy-Weisbach and Manning (Strickler) coefficients can be made by using the relationship between them.

Determination of the friction factor (Chézy coefficient) of a movable bed is a complex problem that requires knowledge of the implicit process of flow conditions and bed form development. Thus, the hydraulic roughness depends on the flow conditions (velocity, water depth and sediment transport rate), but these flow conditions also affect strongly the development of bed forms and the hydraulic roughness. In fact, the dynamics of the bed form development, the multiplicity of bed configurations that may simultaneously occur, make it almost impossible to find an equation to describe accurately the friction factor. Researchers, such as Engelund (1966), Simons and Richardson (1966), Alam and Kennedy (1969), White et al. (1979), Brownlie (1983) and van Rijn (1984c) have tried to explain the resistance to flow by assuming a single type of bed form developed on the bottom. However, no method is fully acceptable due to the tremendous inexactitudes involved. Nevertheless a comparison of the most widely used methods to predict the resistance to flow with field and flume data will contribute to select an appropriate method for situations prevailing in irrigation canals.

Another important feature of water flow in irrigation canals is the estimation of the composite hydraulic roughness. In those canals, the flow encounters frequently a varying roughness along the wetted perimeter. Different roughness occurs on the bottom and side banks of the canals. The development of bed forms on the bottom, different material on the bottom and the sides or vegetated side banks are typical situations for flow conditions in irrigation canals. For these different roughnesses along the perimeter a composite roughness should be calculated from weighed component roughness. In the past some methods have been developed to compute the composite roughness, which are based on several assumptions for the flow conditions in the cross section of the canal. Chow (1983), Vanoni (1975) and Raudkivi (1990) mentioned that

the composite roughness of the entire cross section could be found by considering the total cross section as an area composed by sub-sections. Each sub-section has the same mean velocity and same energy line slope as the whole cross section. Chow (1983), Krishnamurthy and Christensen (1972), Motayed and Krishnamurthy (1980), suggested that the total resistance to the flow in a cross section is equal to the summation of the resisting forces in each sub-section and the hydraulic radius of each sub-section equal to that of the whole cross section.

Those authors also described another method, which is based on the assumption that the total discharge of the whole cross section is equal to the summation of all the discharges in the sub-sections. Krishnamurthy and Christensen (1972) proposed that the summation of the discharges in the sub-sections with different roughness coefficient k_{si} is equal to the summation of the discharges in the sub-sections with a composite roughness k_{se}. The flow in each section is assumed to be rough turbulent and the velocity distribution is explained by the logarithmic law. This method is rather similar to the one described by Asano (1985), but it only differs in the description of the mean velocity in the sub-sections.

2.3.2 Sediment transport in equilibrium conditions

Many theories have been developed for sediment transport in alluvial channels (equation 2.10). All of them are based on the same basic hypothesis of uniform and steady flow, channel bed in equilibrium and negligible washload (Cunge, 1980).

The aim of sediment research is to predict the sediment transport in relation to known sediment input values. Three modes of motion can be distinguished in the sediment transport induced by flowing water: 'rolling and sliding', 'saltation' and 'suspension'. These modes of motion are related to the flow conditions, especially the hydrodynamic forces, which are expressed in terms of mean velocity or bottom shear stress acting on a bed of sediments. Firstly the hydrodynamic forces have to reach a critical or threshold value for the initiation of motion, before a small increase of the forces will put the grain or aggregate into motion by irregular jumps or by rolling of the particles. Secondly when the hydrodynamic forces reach a threshold value for initiation of suspension the sediment particles start to diffuse into the water flow. Yalin (1977) expressed that process by:

$\tau < \tau_{cr}$ no motion (2.11)

$\tau_{cr} \leq \tau \leq \tau'_{cr}$ bed load transport (2.12)

$\tau \geq \tau'_{cr}$ bed and suspended load transport (2.13)

where:

τ = bottom shear stress
τ_{cr} = critical shear stress for initiation of motion
τ'_{cr} = critical shear stress for initiation of suspension

Indeed there is not truly a critical condition at which the motion and suspension suddenly begins but it fluctuates around some average condition. The movement of the particles is highly unsteady and depending on the turbulence fluctuation. It is not possible to give a single value to represent the zero movement. For practical purposes it is better to define the condition for initiation of motion as the one below a certain value for which the sediment transport rate is of no useful importance (Paintal, 1971).

2.3.2.1 Initiation of motion: several authors have developed theories to explain the initiation of motion. Most of them are based on either a critical depth-averaged velocity or on a critical bed shear stress. Theories based on critical velocity require water depths to completely satisfy the flow condition at which the initiation of motion occurs whereas the theories based on critical shear stress describe the flow condition for initiation of motion by using a single critical value for the shear stress. ASCE (1966a) recommends that data on critical shear stress should be used wherever possible. Among the theories based on critical shear stress, the Shields' diagram is most widely accepted as criterion to describe the conditions for initiation of motion of uniform and non-cohesive sediment on a horizontal bed.

The Shields' diagram (figure 2.6) expresses a relation between the critical mobility Shields' parameter (θ_{cr}) and the hydraulic condition on the bed, which is represented by a dimensionless parameter, the particle Reynold's number (Re_*). This particle Reynold's number is based on grainsize and shear velocity. The initiation of motion will occur when the mobility Shields' parameter (θ) is greater than the critical mobility Shields' parameter (θ_{cr}). These parameters can be expressed by:

$$\theta_{cr} = \frac{u_{*cr}^2}{(s-1)\, g\, d_{50}} = \frac{\tau_{cr}}{(s-1)\, \rho\, g\, d_{50}} \qquad (2.14)$$

$$Re_* = \frac{u_{*cr}\, d_{50}}{\nu} \qquad (2.15)$$

$$\theta = \frac{u_*^2}{(s-1)\, g\, d_{50}} = \frac{\tau}{(s-1)\, \rho\, g\, d_{50}} \quad \text{with} \quad u_* = \sqrt{g\, h\, S_0} \qquad (2.16)$$

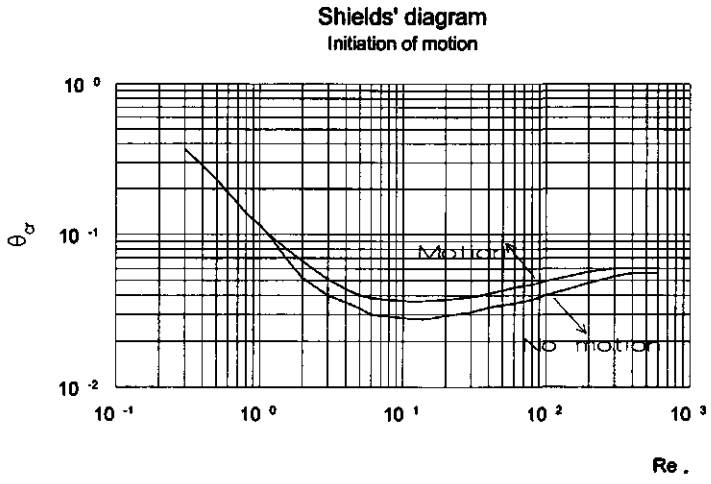

Figure 2.6 Shields' diagram for initiation of motion (after van Rijn, 1993)

The use of the Shields' diagram is not appropriate for practical purpose because the u_* value appears in both axes of the diagram and can be only solved by trial and error. This imperfection of the Shields' diagram can be eliminated by introducing the particle parameter D_* which is represented by (Yalin, 1977):

$$D_* = \frac{Re_*^2}{\theta} = \left[\frac{(s-1)\,g}{\nu^2}\right]^{1/3} d_{50} \qquad (2.17)$$

Next van Rijn (1993) presents the relationship between the critical mobility parameter θ_{cr} and D_* as:

$$\theta_{cr} = 0.24\, D_*^{-1} \quad \text{for} \quad 1 < D_* \leq 4 \qquad (2.18)$$

$$\theta_{cr} = 0.14\, D_*^{-0.64} \quad \text{for} \quad 4 < D_* \leq 10 \qquad (2.19)$$

$$\theta_{cr} = 0.04\, D_*^{-0.1} \quad \text{for} \quad 10 \leq D_* \leq 20 \qquad (2.20)$$

2.3.2.2 Initiation of suspension: van Rijn (1984b) describes the initiation of suspension by:

$$\theta'_{cr} = \frac{16}{D_*^2}\,\frac{w_s^2}{(s-1)\,g\,d_{50}} \quad \text{for} \quad 1 < D_* \leq 10 \qquad (2.21)$$

and for $D_* > 10$:

$$\theta'_{cr} = 16 \frac{w_s^2}{(s - 1)\, g\, d_{50}} \qquad \text{for} \quad D_* > 10 \tag{2.22}$$

where:

θ = dimensionless mobility Shields' parameter
θ_{cr} = dimensionless critical mobility Shields' parameter
Re_* = dimensionless particle Reynolds number
s = relative density (ρ_s/ρ)
u_* = local shear velocity (m/s)
w_s = fall velocity (m/s)
u_{*cr} = critical shear velocity (m/s)
τ = local shear stress (N/m^2)
τ_{cr} = critical shear stress (N/m^2)
D_* = dimensionless particle parameter
ν = kinematic viscosity (m/s^2)
d_{50} = median diameter (m)
g = acceleration due to gravity (m/s^2)
ρ = density (kg/m^3)

2.3.2.3 Sediment transport capacity: based on the three modes of motion as mentioned in section 2.3.2, two different types of sediment transport can be defined:

- bed load;
- suspended load.

Bed load is defined as that part of the sediment transport that is in contact with the bed during the transport and it includes the sliding, rolling and saltation modes.

Suspended load is defined as that part of the sediment transport that is moving with the water flow without contact with the bottom. It includes the suspension mode and a special mode of suspended load, the wash load. The wash load consists of cohesive and very fine sediments (smaller than 0.05 mm), which tends to be suspended by Brownian motion (Raudkivi, 1990).

Due to the fact that the sediments entering irrigation canals are from external sources (for instance rivers), the particle size of the sediment is most of the time different from the parent bed material. The sediment particle size depends on the operation of the sediment trap or intake at the head of the canal network. Normally the sediment entering into the irrigation canals are in the range of fine sand, silt and clay (Worapansopak, 1992). Bigger particles have preferably been excluded from entering the system by a judicious skimming of the water at the intake or have been allowed to settle in a sediment trap in the first reach of the canal system (Dahmen, 1994). For this study the sediment size is assumed to be in the range of 0.05 mm $< d_{50} <$ 0.5

mm. Also only non-cohesive material will be considered, despite some degree of cohesion that is present for the smaller sizes.

There is no universally accepted equation to determine the total sediment transport capacity of canals. Many methods have been proposed to predict the transport rate under a large range of flow conditions and sediment characteristics. The total sediment transport can be found either in an indirect way by summation of the bed load and the suspended load or by direct determination of the total sediment discharge. In the first group the theories of Einstein (1950), Bagnold (1966), Toffaletti (1969), van Rijn (1984a and 1984b) can be mentioned. By using the theories of Colby (1964), Bishop et al. (1965), Engelund and Hansen (1967), Ackers and White (1973), Yang (1973) and Brownlie (1981) the total sediment discharge can be directly determined. But, the predictability of all of them is still poor. van Rijn (1984a) stated that it is hardly possible to predict the sediment transport rate with an accuracy of less than 100%. A brief description of some of the most widely known sediment transport predictors will be presented.

The Einstein method is based on a logarithmic distribution of the velocity and a parabolic distribution of the fluid mixing coefficient. It uses a reference level (a) equal to $2*d_{65}$. The coefficients of the formula were determined by using a data set with sediment with a mean size larger than 0.785 mm (Vanoni, 1975). The sediment transport is computed for each size fraction and the computation requires the hydraulic radius (R), energy slope (S), mean velocity (V) and particle size (d_{65}) (Vanoni, 1975).

The Bagnold method is based on an energy balance concept, which relates the suspended load transport to the work done by the fluid (van Rijn, 1993). The method is considered to be a rational rather than an empirical theory, because the relationship was derived independently of any quantitative information drawn from experimental data (Worapansopak, 1992).

The Engelund and Hansen method is based on the energy method and it can be applied to dune beds and particle sizes greater than 0.15 mm (Yang and Molinas, 1982). According to Engelund and Hansen (1967) reservations must be taken, when the sediment size is smaller than about 0.15 mm. Although this formula is used to predict the total sediment transport, it can be used to predict suspended sediment specially when the bed load transport can be neglected (Engelund and Hansen, 1967).

The Toffaletti formula (1969) uses the same criteria as the Einstein formula. The sediment transport is divided in size fractions and the water depth is divided in four zones. The three upper zones correspond to the suspended sediment transport. The velocity distribution is represented by a power relation, which depends on the water temperature. The concentration distribution is given by a power relation for each of the three upper zones. The Toffaletti's formula is based on extensive data from rivers and flumes with sediments larger than 0.125 mm. The inputs required to compute the sediment transport are the temperature (T), energy

slope (S), mean velocity (V), hydraulic radius (R) and the sediment size expressed in terms of median diameter (d_{65}) (Vanoni, 1975).

The Ackers and White method considers separately the coarse and fine sediment. This method was developed by using a data set with grain sizes larger than 0.4 mm, Froude numbers lower than 0.8 and plain, ripple and dune bed configurations. The sediment transport is expressed in terms of the dimensionless parameters D_{gr} (size sediment), F_{cr} (mobility parameter) and G_r (transport parameter) (Ackers and White, 1973). Recent research has confirmed the Ackers and White method for assessing sediment transport. The method and its formulation have been reviewed recently against an even greater assemblage of open channel transport experiments, and have well confirmed. Additional data have permitted its recalibration to provide a better fit for both fine and coarse sediment (Ackers, 1993).

The method of Yang is based on the hypothesis that the rate of sediment transport should be related to the rate of energy dissipation of the flow. The rate of energy dissipation is defined as the unit stream power and it can be expressed by the product of the mean velocity and bottom slope (V * S). The theoretical basis for Yang's unit stream power is provided by the turbulence theory. Yang's method has been verified with laboratory and field data for sediment sizes between 0.15 mm and 1.7 mm and mean velocities in the range of 0.23 m/s and 1.97 m/s (Yang, 1973).

Brownlie (1981) defined a method to compute the sediment transport capacity based on a dimensional analysis and calibration of a wide range of field and laboratory data where uniform conditions were present. The graded sediment is represented by the D_{50} and the geometric standard deviation σ_s.

The van Rijn method (1984a and 1984b) computes the total sediment transport by summation of the bed and suspended load. The bed load is computed as the product of the saltation height, the particle velocity and bed load concentration. For the suspended load computation van Rijn uses a parabolic-constant distribution for the diffusion coefficient ϵ_s and a logarithmic distribution for the velocity. To verify this method a data set was used with flow depths larger than 0.1 m, mean flow velocities larger than 0.4 m/s, width/depth larger than 3, Froude number smaller than 0.9 and diameters smaller than 0.5 mm (van Rijn, 1984a and 1984b).

Woo (1988a) used a parameter-sensitivity analysis and some numerical experiments in an imaginary canal to asses the Einstein, Ackers and White, Yang, Toffaletti, Engelund and Hansen, Colby, Shen-Hung and van Rijn formula. Among the main conclusions are that the Einstein's, Toffaletti's and Colby's formula are very sensitive to the flow velocity, while the Engelund and Hansen's and Yang's formula are the least sensitive to that parameter. The Ackers and White formula is too sensitive to the particle size and it should not be used for fine sediments (Woo, 1988a). The formula of van Rijn and Engelund and Hansen predict larger

sediment transport than the other formulae, while Einstein's and Toffaletti's formulae predict smaller sediment transport.

Meadowcroft (1988) did a comparison of six sediment transport formulae (Ackers and White, Brownlie, Engelund and Hansen, Einstein, van Rijn and Yang) against data collected from field sites restricted to the range of discharges, sediment sizes and concentrations commonly encountered in irrigation canals. The main characteristics of the data used were discharges between 1 to 200 m^3/s, d_{50} between 0.1 mm and 1 mm, concentration less than 7200 ppm, Froude number between 0.1 and 0.99 and bottom shear stress between 0.65 and 10 N/m^2. The author concluded that the Engelund and Hansen sediment transport equation could be used in the absence of any local data. It is by a small margin the most accurate method and is the simplest one to use.

Nakato (1990) tested eleven sediment transport formulae against field data of the Sacramento river. The bed material size was classified ranging from fine sand to coarse sand. The formulae of Ackers and White, Einstein and Brown, Einstein and Fredsoe, Engelund and Hansen, Inglis and Lacey, Karim, Meyer-Peter and Mueller, van Rijn, Schoklitsch, Toffaletti, and Yang were tested. To evaluate the formulae for suspended transport (only eight), only suspended material larger than 0.062 mm was used. The Toffaletti formula proved to be the best among all formulae tested. Yang's predictions seem to be very close to the measured suspended load discharge at a higher range of sediment discharge.

Worapansopak (1992) evaluated five sediment transport formulae for the total suspended sediment. These were the formulae of Bagnold, Bruk, Celik, modified Celik, and Vlugter. Yang's formula was not included because it predicts the total sediment transport of bed material which was not included in his study. He used the Nakato (1990) data set to evaluate the suspended sediment transport formulae. Fine sediment flume data were also used for this evaluation. The main conclusion is that all the formulae overestimate the sediment transport. In some cases the formulae lead to unacceptable results. The modified Celik transport formula is recommended to be used in irrigation canals although the author suggests more research to verify the modified formula.

2.3.3 Sediment transport in non-equilibrium condition

Sediment transport in a long uniform stream with a steady uniform flow has an unique equilibrium transport rate, but the transport rate under variable conditions differs from the steady uniform and equilibrium one. Non-equilibrium conditions are more significant for suspended load because the excursion length of a suspended particle is in general much longer that the step length of bed load motion (Nagakawa, 1989). While it is possible to relate the bed load discharge to the local and instantaneous characteristics of water flow and bottom composition, no definitive relation of this kind can be found for the suspended load discharge

since this part of transport is substantially influenced by the upstream conditions (Armarini and Di Silvio, 1988).

Mathematical models for the simulation of non-equilibrium, suspended sediment transport in open canals are based on the solution of:

1) the 1-D, 2-D or 3-D convection-diffusion equation;
2) depth integrated models.

2.3.3.1 1-D, 2-D or 3-D convection-diffusion equations: they are based on the solution of the diffusion-convection equation which for two dimensional problems can be written as:

$$\frac{\partial c}{\partial t} + u\frac{\partial c}{\partial x} + w\frac{\partial c}{\partial z} = w_s\frac{\partial c}{\partial z} + \frac{\partial}{\partial z}(\epsilon_x\frac{\partial c}{\partial x}) + \frac{\partial}{\partial z}(\epsilon_z\frac{\partial c}{\partial z}) \qquad (2.23)$$

where:

c = sediment concentration
w_s = fall velocity (m/s)
t = time co-ordinate (s)
x, z = length co-ordinates (m)
u, w = velocity components in x and z direction (m/s)
ϵ_x, ϵ_z = sediment mixing coefficient in x and z direction (m^2/s)

The equation can be solved when the mean velocity components, the fall velocity and the mixing coefficients are known.

Singh and Scarlatos (1985), van Rijn (1987), Celik and Rodi (1985 and 1988) and Armanini and Di Silvio (1988) developed mathematical models to solve the equation (2.23).

Singh and Scarlatos (1985) investigated the effects of sediment motion in a vertical, two dimensional model, where both modes of sediment transport are present (suspended and bed load). In his study the suspended sediment transport is simulated by the convection-diffusion equation for a specific period, then the net influx or outflow from the bed is calculated as the difference between the eroded and deposited sediment mass. Here it is assumed that the suspended sediment distribution is uniform in vertical direction. Expressions for sedimentation and re-suspension rate are required for solving the suspended sediment transport.

van Rijn (1987) presented a vertical two dimensional model for suspended sediment transport based on the width integrated convection-diffusion equation, which is solved by a finite-element method. The vertical distribution of the velocity and mixing coefficient are represented by a simple model based on shape functions (profile model). The velocity profile is described by using a linear combination to represent the wall effect and the influence of the pressure gradient. The vertical distribution of the fluid mixing coefficient is described by a parabolic

constant profile. The sediment mixing coefficient is obtained from a relationship with the fluid mixing coefficient. The mentioned author recommended to do more verification by using field data in order to calibrate the profile model. It is suggested to apply the model for complicated flow conditions with strongly perturbed velocity profile.

Celik and Rodi (1988) presented a mathematical model to calculate the suspended sediment transport in canals under general non-equilibrium conditions. The model is applicable for both net deposition and net entrainment under non-equilibrium conditions and it is restricted to steady, two-dimensional flow (vertical plane). No assumptions are introduced concerning the velocity and the eddy-viscosity/diffusivity distribution. These are calculated by using a hydrodynamic model for a one-dimensional flow.

Armanini and Di Silvio (1988) derived a non-equilibrium, one-dimensional mathematical model based on the conservation equations for each sediment class at three different layers: in the water stream (suspended load), in the bottom layer (bed load) and in the mixing layer (bed material). Another model presented by those authors does not make difference between bed load and suspended load as both modes of transport are included in simplified equations.

2.3.3.2 Depth integrated models: based on the depth integrated approach, Galappatti (1983) developed a model for suspended sediment transport in unsteady and non-uniform flows based on the 2-D convection-diffusion equation. In his model the vertical dimensions are eliminated by means of an asymptotic solution in which the concentration c(x,z,t) is expressed in terms of the depth averaged concentration c(x,t). The latter concentration is represented by a series of previously determined profile functions. The model describes how the mean concentration adapts in time and space towards the local mean equilibrium concentration. The resulting model can be used together with the depth averaged hydrodynamic equations.

The validity of the Galappatti model was studied by Wang and Ribberink (1986). They concluded that for large deviations of the concentration profile compared with the equilibrium profile, the use of the model is not allowed. They recommend some specific requirements to be applied in the Galappatti model for the computation of suspended sediment transport. These requirements are:

- the Galappatti model is only valid for fine sediment. The factor w_s/u_* should be much smaller than unity. Recommended values of w_s/u_* are between 0.3 and 0.4;
- the time scale of the flow variations should be much larger than h/u_*;
- the length scale of the flow variations should be larger than Vh/u_*.

where:

u_* = local shear velocity (m/s)
w_s = fall velocity (m/s)
h = water depth (m)
V = mean velocity (m/s)

Armanini and Di Silvio (1988) considered the bed load and the suspended load as a whole by the summing up of the material conveyed by the flow. They expressed the longitudinal gradient of bed load transport by a non-equilibrium equation in which the characteristic length for bed load is substituted by the characteristic length for suspended load.

2.3.4 Simulation of sediment transport in irrigation systems

Although, it is difficult to predict the quantity of sediment that will be deposited in irrigation canals (Brabben, 1990), the numerical modelling of sediment transport offers the possibility to predict and to evaluate the sediment transport under very general flow conditions (Lyn, 1987).

Show-Shan (1989) reviewed twelve computer sedimentation models developed and implemented in the United States of America: HECG, TABS2, IALLUVIAL, STARS, GSTARS, CHARACTERISTICS, CHARIMA, SEDICOUP, FLUVIAL 12, HEC2SR, TWODSR and RESSED models. Among their conclusions are:

- computer modelling of sedimentation problems is still in the development stage. At present an exact representation is not possible, but at least an approximation of the problem for which it was designed;
- most models include the option of choosing a sediment transport function, but none of them provides the criteria needed to make a choice;
- few models have limited capabilities of modelling the effect of canal geometry and morphology changes;
- all models produce significantly different results even when they are run with the same set of inputs;
- most models have greatly simplified their unsteady flow problems to steady ones.

Also the Task Committee on Irrigation Canal System Hydraulic Modelling (ASCE, 1993) examined a number of the computer programs available for simulating open-channel flow (MODIS, DUFLOW, CANAL, CARIMA, USM). Irrigation canal modelling is based on the same unsteady flow conditions used for river modelling. However, the canal and irrigation environment present several unique simulation problems generally not encountered in river modelling (ASCE, 1993).The Committee identified current limitations of these models and the needs for improvements. At that time none of the models was able to compute morphological changes of the canal bottom.

Numerous other mathematical models to compute the water flow in open canals are available (among others SIC, PROFILE, FLOP, CID, MIKE 11, SOBEK, DORC, ODIRMO), but only a few of them are able to compute sediment transport. Among them Mike 11 (Danish Hydraulic Institute, 1995), DORC (HR Wallingford, 1992), SOBEK (Delft Hydraulics, 1994), ODIRMO (Delft University of Technology, DUT, 1985) can be mentioned. At the moment, CEMAGREF is exploring the possibilities to extend the Simulation of Irrigation Canal (SIC)

computer programme with a new module on sediment transport (personal communication). Also, at present the ODU is developing a model for routing sediment in irrigation canal networks (personal communication).

A brief description of some existing models to compute sediment transport will be given:
ODIRMO (DUT, 1985) is a one-dimensional model developed to study river morphology. This model is based upon the assumption that the total sediment transport depends only on the local flow conditions, meaning that the sediment transport is calculated by assuming an equilibrium conditions. The formula of Engelund and Hansen, Meyer-Peter and Mueller, Ackers and White and a power law equation can be used. Also a quasi steady flow, uniform sediment distribution and a rectangular cross section of the canal are assumed.

DORC (Design of Regime Canals) was developed by the Overseas Development Unit of Hydraulic Research Wallingford, to assist in the design of alluvial channels. The model provides a range of design methods together with procedures to predict alluvial friction and sediment transport. Alluvial canals can be designed by the regime, tractive force or rational method. The regime methods used in the model are the Lacey and Simons and Albertson method. Among the rational methods the White, Paris and Bettess (1982) and Chang (1985) method are included. Also the rational and regime methods can be combined in the model. The Manning equation is used when the width-depth ratio and the side slope of the canal are known. The model enables designers to compare the transport capacity with sediment inputs and to assess or to revise the canal slope and cross sections. The model is recommended for predicting the transport capacity of canals, but it is not possible to determine the sediment transport under non-equilibrium conditions (HR Wallingford, 1992).

MIKE 11 (DHI, 1993) is a 1-D hydrodynamic model developed by the Danish Hydraulic Institute, which permits the computation of the non-cohesive sediment transport capacity together with the corresponding accumulated erosion/sedimentation rate by using several transport and calculation models. The sediment transport is calculated in time and space as an explicit function of the hydraulic parameter previously calculated. There is no feedback from the sediment transport computation to the hydrodynamic computations. Five models to predict the sediment transport have been implemented, namely Engelund and Hansen, Ackers and White, Smart and Jaeggi, Engelund and Fredsoe and van Rijn. No guidelines for the preference of one model over another model is given (DHI, 1993).

DUFLOW is a micro-computer program for simulating one-dimensional unsteady flow in open canals. The Delft University of Technology, the International Institute for Infrastructural, Hydraulics and Environmental Engineering (IHE) and Rijkswaterstaat (Public Works Department) of The Netherlands contributed to the model development (IHE, 1998).The program was developed for simple canal networks with simple structures (Clemmens, 1993). Recently (1997) a module for calculating the suspended sediment transport in non-equilibrium conditions was incorporated. A depth integrated model based on the advection-diffusion

equation is used for the transport module. The model is driven by the deposition and re-suspension fluxes at the bed so that the morphological changes over small time intervals can be computed.

SOBEK (DHL, 1994) is capable of handling one-dimensional problems in open canal networks. Apart from steady or unsteady flow, the model can touch various other physical processes like salt intrusion and morphology, sediment transport and water quality. The model was developed by Delft Hydraulics and the Institute for Inland Water Management and Waste Water Treatment of the Netherlands (1994). Applications of SOBEK are mentioned for river training, dredging optimization, river bed cut-offs, water quality, water flow for industry, drinking water, cooling water and irrigation, regime changes of rivers, flood risk, low water, etc. Sediment transport and morphology modules are mainly used for indication of aggradation and degradation of river reaches due to river bend cut-offs, dredging, river training , water extraction, reservoir operation or flooding. The transport of sand in rivers and estuaries is estimated by using one of the following sediment transport formulae: Ackers and White, Engelund and Hansen, Meyer-Peter and Müller, van Rijn, Parker and Klingeman and a general user-adjustable formula.

Applications of simulations of sediment transport in rivers are frequently mentioned in the literature, only a very few works were found about sediment transport in irrigation canals.

Mahmood (1973b) considered the routing of sediment through an irrigation system with a goal of disposing the incoming sediment load with the water diversion. Also the distribution of bed material load over the irrigation diversions was studied. A numerical model to predict the water and sediment discharge through farm turnouts is presented. The bed material transport was computed by a method developed by the author. The analyses in his work were based on steady and equilibrium design flows.

Huang *et al.* (1993) simulated the sediment transport in an irrigation system along the lower reaches of the Yellow River in China. The research was based on a data analysis and the calculation of some operation schemes by a specially developed mathematical model. They showed that through adjustment of the distribution of the discharge in time, the water diversion conditions can be improved. The flow in the mathematical model was treated as a non-uniform and quasi-steady flow. The sediment transport for equilibrium conditions was calculated by a specific equation developed from the work of Celik and Rodi (1988) and from studies in some similar irrigation systems along the Yellow River. For the non-equilibrium conditions an equation describing the longitudinal variation of the sediment concentration was used.

2.4 Conclusions

From the previous paragraphs follows that the design of irrigation canals is based on engineering, agriculture, management and economic considerations. An optimal canal design

is difficult to be achieved. Final canal designs will have to poise all the criteria to find the best solution for the specific conditions of the irrigation system. In this study emphasis is given to the effect of the design and operation of irrigation canals on the sediment transport.

The existing methods for the design of irrigation canals are based on the interrelating equations of input variables for certain water flow and sediment transport conditions. They have been introduced in an attempt to design stable canals. However, the input variables will widely vary during the irrigation season and moreover during the lifetime of the irrigation canals. Most of the time, non-equilibrium conditions prevail in the irrigation systems and therefore the initial assumptions for the design of stable canals are not valid anymore. Also lined canals experience sedimentation problems. Although lined canals are designed for a high sediment transport capacity; variations in either flow condition or in the incoming sediment load will produce non-equilibrium conditions for the transport of the sediment. Therefore sediment problems in irrigation canals should be analysed in a more general context, including all the possible operation scenarios for water flow and sediment transport in time and space.

The existing concepts dealing with sediment transport mainly focus on river conditions and even though certain similarities exist between irrigation canals and rivers, these concepts are not fully applicable to irrigation canals. The concepts dealing with resistance to flow and sediment transport (equilibrium and non-equilibrium conditions) have been mainly developed to explain the sediment transport of alluvial channels. The problem is to decide which one to use, which forms one of the specific purpose of this research.

Determination of resistance to flow for a movable bed is a complex problem which depends on the implicit interaction between bed form development and flow conditions. Although all existing predictors take into account the bed form development on the resistance to flow some of them require explicitly to know the type and characteristics of the bed form. In other methods the effect of the bed form on resistance to flow is implicitly included. Those methods have been developed for a certain range of flow conditions in which the development of bed form were restricted to certain types and the flow conditions. So far, none of those can predict accurately the resistance to flow. Those predictors should be tested for further applications. They consider only the effect of the bottom on the resistance to flow. No effects of the side wall on the resistance to flow are considered.

It has been shown that a wide variety of methods to evaluate the capacity of certain flow for conveying sediment in equilibrium and non-equilibrium are presently available. Several researchers have assessed the sediment transport capacity by some performance tests and by comparison of each formula with the other ones. In fact it is quite difficult to make firm recommendations about which formula to use in practice. The predictability of all of them is still poor. These tests give some ideas about the applicability of each of the formulae for a specific condition. There are a few publications on the performance of the existing formulae in irrigation canals. Therefore it is still extremely difficult to select the appropriate one for this

specific topic. However, a comparison of the sediment transport methods under the typical flow conditions and sediment characteristics prevailing in irrigation canals could become a powerful tool to reduce inevitable errors and inaccuracies. They will be the basis of a mathematical model for simulating the sediment transport in irrigation canals.

It can be concluded that in the literature there is a surprisingly small number of mathematical models dealing with sediment transport in open canals and so far none has been found for the specific conditions of irrigation canals. The suitability of these models is not so high due to differences, among others, in the use of the appropriate sediment transport formula and friction factor predictor, effect of the side banks on the velocity distribution and sediment transport, neglecting the effect of composite roughness on the total friction factor, assumption of equilibrium condition, presence of flow control structures, operation rules, etc. A mathematical model for the specific conditions of irrigation canals may become an important tool for designers and managers of irrigation systems.

3 WATER FLOW AND SEDIMENT TRANSPORT EQUATIONS

3.1 General

Many irrigation systems acquire water from sediment carrying rivers. Some systems take directly water and sediment from the river; others control the sediment transport at the headwork, although a certain amount of sediment still enters into the canal system. Therefore, sediment transport is an important aspect in the design and operation of irrigation canals. The net deposition or net erosion in the canals are important processes to be taken into consideration during the design of the system, particularly when an irrigation system will be operated under highly variable discharges (Bruk, 1986). This chapter is limited to a revision of the governing processes for computing the sediment transport in open canal. Assumptions, equations, range of applications, data requirements for the mathematical formulation of the sediment transport computation in open canals are presented.

Sediment transport and water flow are interrelated and cannot be separated. From a mathematical point this interrelation can be described for a one-dimensional phenomenon without changes in the shape of the cross sections by the following equations (Cunge et al, 1980):

- *governing water flow equations:*
  - * continuity equation;
  - * dynamic equation;
- *governing sediment equations:*
  - * friction factor equation;
  - * sediment transport equation;
  - * continuity equation for the sediment mass.

3.2 Governing equations for water flow

Water flow in an irrigation canal can be considered to be one-dimensional. Although one-dimensional flow can hardly be found in nature, in this study the flow will be considered one-dimensional. The main direction of the flow will be assumed along the canal axis (x-direction), the velocity is assumed to be averaged over the cross section and the water level across the section is horizontal. Other assumptions are that the effect of the boundary friction and turbulence can be accounted for through resistance laws and that the curvature of the streamlines will be considered small with a negligible vertical acceleration. Under these assumptions, the general equations for one-dimensional flow can be described by the Saint Venant equations that read as (Cunge et al, 1980):

$$\frac{\partial A}{\partial t} + \frac{\partial Q}{\partial x} = 0 \qquad \text{Continuity equation} \qquad (3.1)$$

and,

$$\frac{\partial h}{\partial x} + \frac{V^2}{C^2 R} + \frac{\partial z}{\partial x} + \frac{V}{g}\frac{\partial V}{\partial x} + \frac{1}{g}\frac{\partial V}{\partial t} = 0 \qquad \text{Dynamic equation} \qquad (3.2)$$

where:

Q = flow rate (m^3/s)
V = mean velocity (m/s)
C = Chézy coefficient ($m^{1/2}/s$)
h = water depth (m)
R = hydraulic radius (m)
g = gravity acceleration (m/s^2)
A = cross section area (m^2)
x = length co-ordinates in x (m)
h = water level (m)
z = bottom level above datum (m)
t = time co-ordinate (s)

Equation 3.1 and 3.2 describe the mass and momentum conservation of the water flow. Equation 3.2 describes all the forces acting on the water flow in an open canal. In that equation represent:

- the terms $\partial h/\partial x$ and $\partial z/\partial x$ the gravity effect;
- the term $V^2\, g/C^2R$ the friction on the bottom;
- the term $(V/g)\partial V/\partial x$ the convection effect of the water flow;
- the term $(1/g)\partial V/\partial t$ the inertia of the water flow.

The amount of water flowing into an irrigation canal during the irrigation season and moreover during the life time of the irrigation canal is not constant. Seasonal changes in crop water requirement, water supply and variation in size and type of the planned cropping pattern are frequent during the life time of an irrigation canal. It must be designed and constructed to permit some flexibility for delivering different amounts of water. Irrigation canals are designed for a certain flow capacity, but most of the time they will convey different discharges and therefore it will be often necessary to have a certain control to maintain the desired flow rates and required water elevations.

From a computational point of view the importance of the unsteadiness of the flow in irrigation canals must be considered from two aspects.

First, the computation of water flow for programming the water delivery at any point of the system requires a good knowledge of the response time in order to deliver the right discharge at the right time and to avoid improper operation of water distribution. All the methods for delivering water to the conveyance system experience unsteady flow conditions due to the

initiation and termination of irrigation, changes in flow rate, stoppages of lateral flows, etc. The unsteady flow condition exists most of the time and should be taken into account as the unsteady flow may seriously affect the water distribution. It is important to know the response time of the system to various flow changes (Schuurmans, 1991). The response time of the system is a function of distance between the disturbance and the point of interest, the celerity of the propagation and the operation time of the structures.

Second, the computation of the water flow for determining morphological changes in the bottom of the canal can be done by assuming a quasi-steady flow. For the time depending changes in the canal bottom the water flow can be easily schematized as quasi-steady. Under these conditions the morphological changes in the bottom of the irrigation canal are so slow that for the computation of the water movement the bottom can be considered fixed for a single time step (de Vries, 1965).

For assuming whether the unsteady flow in the irrigation canal may properly be treated as a quasi-steady flow two facts are considered.

For one side, the need to avoid that the water surface becomes wavy, which would affect the canal operation. Therefor a reasonably low Froude number should be maintained and it is a safe practice to restrict the Froude number below 0.30-0.40 (Ranga-Raju, 1981). For $Fr < 0.4$ the celerities of the water level perturbations are not influenced by the mobility of the bed. Celerities of the water level perturbations are about 200 times faster than the celerities of the bed disturbances. In terms of a relative celerity which represents the ratio between the celerity of either the water level perturbations or the bed disturbances and the velocity of the water flow, the relative celerities of the water level perturbations are larger than 1, while the relative celerities of the bed disturbances are smaller than 0.005. When the celerity of the water level perturbations is much larger than the celerity of the bed movement it can be assumed that the disturbance of the bed will not influence the water movement (de Vries , 1987).

On the other hand, flow control structures are supposed to be operated slowly enough to avoid steep front surges. This means that changes of discharge in time are very gradual therefore unsteady flow can be approximated by a quasi-steady flow (Mahmood, 1975).

This study is focused on sediment transport processes in irrigation canals rather than on water delivery in irrigation canals therefore water flow will be schematized as quasi-steady flow. Hence the terms $\partial u/\partial t$ and $\partial A/\partial t$ in the continuity and dynamic equation (equations 3.1 and 3.2) can be neglected.

Figure 3.1 shows some hydrographs in an irrigation canal: (a) typical; (b) schematized in a quasi-steady state.

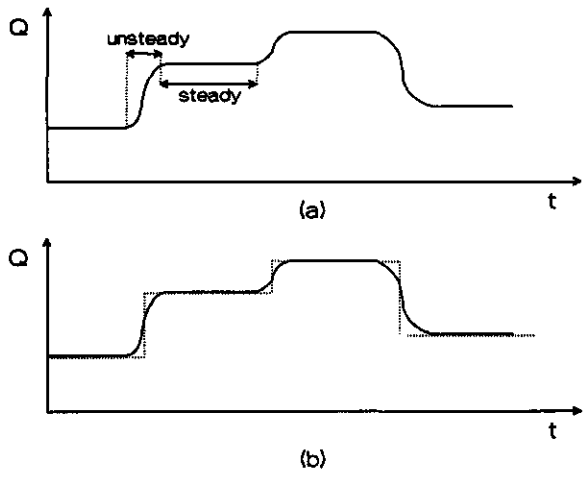

Figure 3.1 Hydrographs in an irrigation canal: (a) typical, (b) schematized

Based on these considerations the water flow equations can be simplified as:
- *Continuity equation:*

$$\frac{\partial Q}{\partial x} = 0 \qquad \therefore \qquad Q = \text{constant} \tag{3.3}$$

- *Dynamic equation:*

$$\frac{dh}{dx} = \frac{S_0 - S_f}{1 - Fr^2} \qquad \text{with} \qquad Fr = \frac{V}{\sqrt{g\ h}} \tag{3.4}$$

where:

Q	=	flow rate (m^3/s)
V	=	mean velocity (m/s)
h	=	water depth (m)
g	=	gravity acceleration (m/s^2)
S_0	=	bottom slope
S_f	=	energy slope
Fr	=	Froude number
x	=	length coordinates in x direction (m)
t	=	time co-ordinate (s)

The discharge may still vary during the irrigation season or any other period, but during a time step (Δt) of the computation of the morphological change in the canal bottom, the discharge

will be considered constant at any point of the irrigation canal. Equation 3.4 describes the variation of water depth in the x-direction. This equation cannot be explicitly solved, although particular solutions are available for prismatic canals. To solve the equation numerical methods are usually required.

The numerical solution of the one-dimensional flow equation requires certain flow conditions, which can be summarized as:

- condition describing the geometric variables of the canal: cross section (bottom width, bottom slope, length and side slope);
- condition related to the bed roughness (fixed or movable boundaries, single or composite roughness, obstruction degree due to vegetation on the side banks);
- boundary conditions related to the water flow;
- discharge at the inflow boundary;
- lateral discharge (q_l), if any;
- water level or discharge-water level relationship at the outflow boundary.

3.3 Governing equations for sediment transport

Irrigation canals are man-made canals, which are designed taking into account aspects related to the irrigation criteria and sediment transport. On the one side they should meet the irrigation requirements and on the other hand no deposition of the sediment entering into the system and no scouring of the parent material should occur. Suggested values for non-scouring bottom shear stress are available in the literature. Kinori (1970) and Chow (1983) give minimum values for the non-scouring shear stress for water containing fine sediments in the range between 1.5 N/m^2 (fine sand, sandy loam) and 15 N/m^2 (hard clay and gravel). Dahmen (1994) suggests a maximum value for the design of irrigation canals of 3-4 N/m^2. Even though the design values for the shear stress can be reduced due to changes in the operation strategies during the irrigation season, the value of the remaining shear stress is high enough to initiate motion and further suspension of the previously deposited sediment, but not so high to produce scouring of the parent material of the canal.

Figure 3.2 shows the Shields' curve for initiation of motion and the criteria used by van Rijn (1993) to initiate suspension. Also, figure 3.2 presents a range of shear stresses between 1 N/m^2 and 4 N/m^2, which is a range of shear stress commonly used for the design of irrigation canals.

It is clearly shown that typical flow conditions in irrigation canals are large enough to produce the suspension of the sediment particles. The sediment transport in irrigation canals is carried out in two modes: suspended load and bed load.

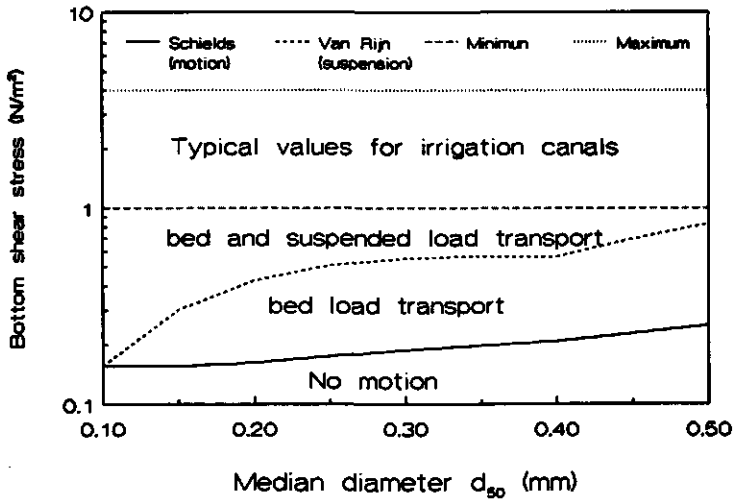

Figure 3.2 Initiation of motion, initiation of suspension and values of shear stress commonly used in irrigation canals as function of D.

To determine the distribution of the bed load and suspended load transport in a flow of an irrigation canal the procedure described by van Rijn (1984a and 1984 b) will be used. According to this procedure the sediment transport is divided into two components: bed and suspended load (details are described in appendix A). For doing that, both suspended load and bed load transport were computed for two different canals in which the flow conditions were characterized by:

- water depth = 1 m and 4 m;
- shear stress = 1 N/m^2 and 4 N/m^2;
- Chézy coefficient = 40 m$^{1/2}$/s.

Figure 3.3 shows the suspended load as a fraction of the total sediment load (bed and suspended load) for water flow and sediment characteristics prevailing in irrigation canals. For those conditions sediment smaller than 0.1 mm is almost only transported as suspended load. Sediment smaller than 0.35 mm is mainly transported as suspended load and sediment larger than 0.35 mm is transported as both bed and suspended load. For a given bottom shear stress and roughness characteristics the suspended load transport increases with the water depth (fig. 3.4).

Once the bottom shear stress for initiation of suspension has been reached the suspended load transport will increase till it reaches a certain value. From that point onward, further increase of the bottom shear stress does not produce important changes in the suspended load. Figure 3.5 shows the results of variation of the bottom shear stress between 1 and 7 N/m^2 and

suspended load for a canal with a depth of 4 m and a Chézy coefficient equal 40. Both bed load and suspended load will increase in the same proportion.
For a given water depth (h = 4 m) and bottom shear stress (τ = 4 N/m^2), variations of the Chézy coefficients between 25 and 60 do not produce important changes in the suspended load (fig. 3.6).

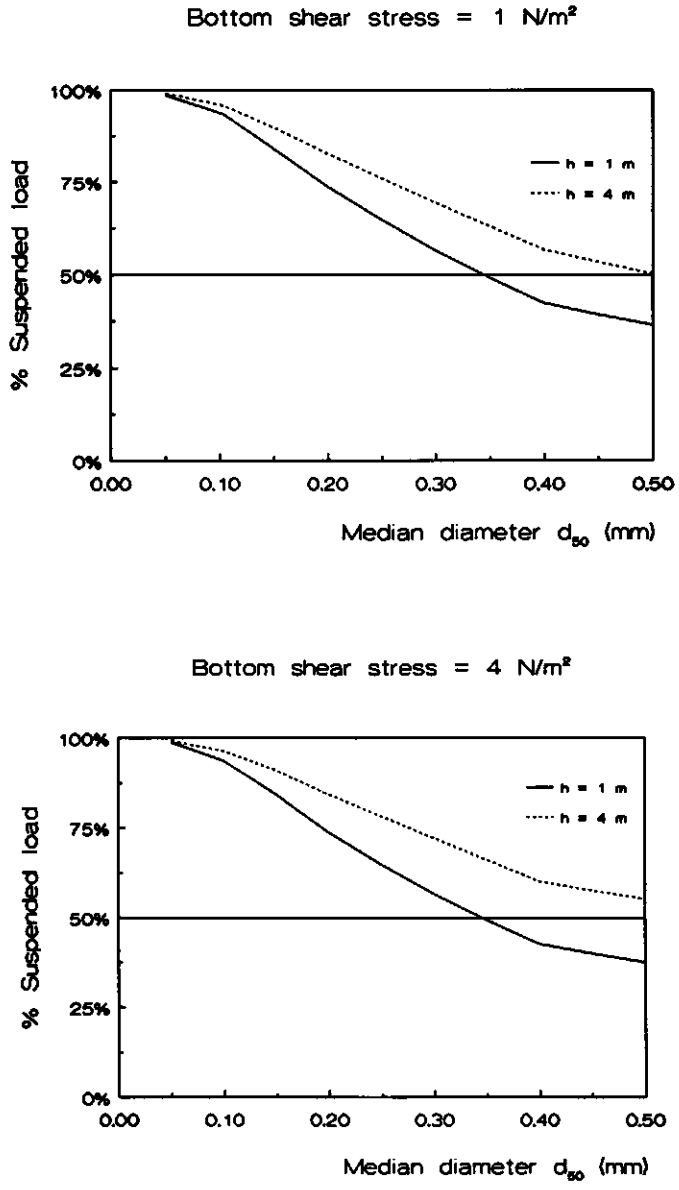

Figure 3.3 Suspended load transport in irrigation canals

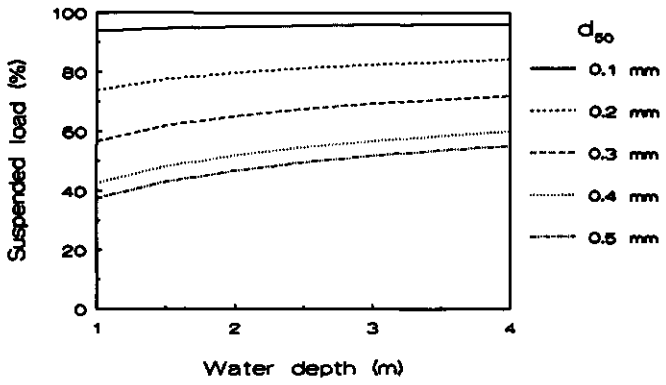

Figure 3.4 Variation of the suspended load as function of the water depth for a given roughness characteristic (C = 40 $m^{1/2}/s$) and bottom shear stress (τ = 4 N/m^2)

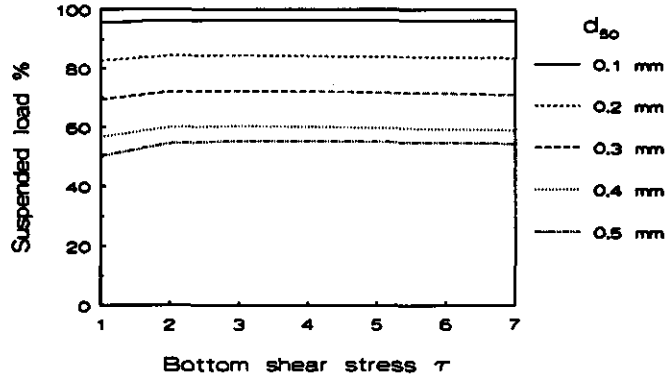

Figure 3.5 Variation of the suspended load as function of bottom shear stress for a given water depth (h = 4 m) and roughness characteristic (C = 40 $m^{1/2}/s$)

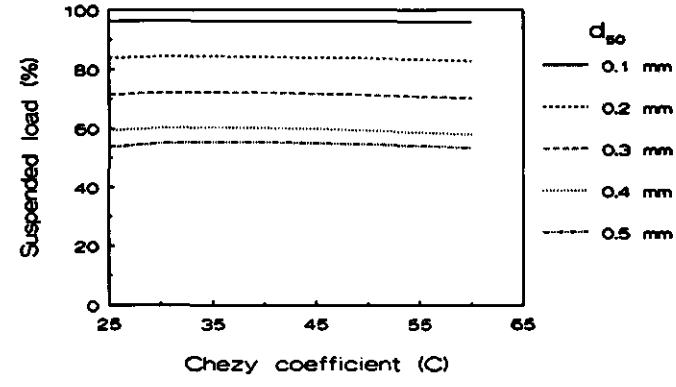

Figure 3.6 Variation of the suspended load as function of the Chézy coefficient for a given water depth (h = 4 m) and bottom shear stress (τ = 4 N/m^2)

The previous paragraphs clearly show that the sediment is transported both as bed load and suspended load for the flow conditions prevailing in irrigation canals. Therefore any predictor to estimate the sediment transport in irrigation canals should take this fact into account. Sediment transport predictors should be able to compute either the total transport load (bed load + suspended load) or the bed load and suspended load separately. Only for very fine sediment ($d_{50} < 0.1$ mm) a suspended sediment transport predictor can be used to estimate the sediment transport capacity of irrigation canals.

3.3.1 Friction factor equation

The resistance to flow in open canals is affected by several factors, among others by the development of bed features, such as ripples, mega-ripples and dunes. These bed forms play an important role in the hydraulic resistance of the water flow, which is measured in terms of a friction factor. In this study the Chézy coefficient will be used to describe the friction factor in irrigation canals. The Darcy-Weisbach and Manning (Strickler) coefficients can also be introduced by using the existing relationships between them.

3.3.1.1 Bed form development: water flow in irrigation canals is normally in the subcritical regime ($Fr < 1$) and more especially in the lower regime ($Fr < 0.7$). In general Froude numbers in irrigation canals are smaller than 0.4 (Ranga Raju, 1981). Bed features for the lower regimes are described as flat bed, ripples and dunes. The latter two are characterized by rough triangles in the longitudinal profile with a gentle sloping upstream face and an inclined downstream face (Figure 3.7).

Ripples and dunes show some subtle differences. However, no sharp distinction between ripples and dunes is possible. ASCE (1966b) described these bed forms as:

- *flat bed*: a bed surface devoid of any bed form. No motion of the bed sediment occurs;
- *ripples*: this bed form is said to be encountered in canals with bed material smaller than 0.6 mm, a wave length smaller than 30 cm and a height in the order of a few centimetres. When the velocity is slightly greater than the critical value ripples will be formed in the bed. The ripple geometry is practically independent of flow conditions;
- *dunes*: they occur in flows with a larger velocity, for all bed sediment sizes and with a length and height greater than the ripples. Sediment transport rates are larger than for ripples. The dunes geometry strongly depends on the flow depth.

Other authors have tried to explain the type of bed forms generated under certain flow conditions, based on the analysis of bed forms as observed under flume and field conditions. They have presented graphical solutions for the prediction of the bed forms by using dimensional and non-dimensional plots. Some of these authors are Liu (1957), Simons and Richardsons (1966), Bogardi (1974) and van Rijn (1993). Each theory is based on a particular classification parameter, which is summarized in table 3.1.

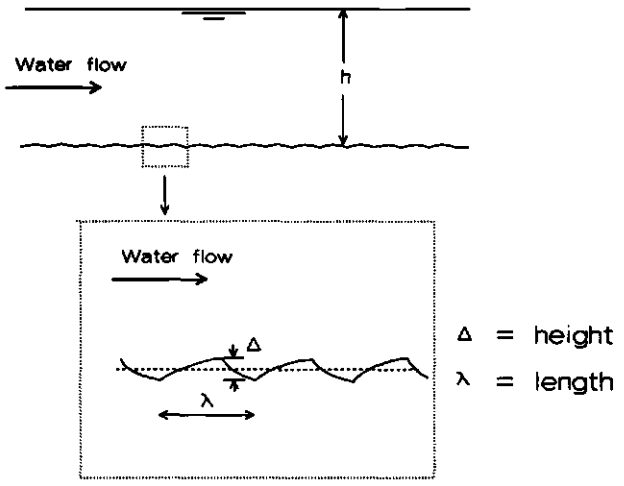

Figure 3.7 Schematic representation of bed forms

Table 3.1 Classification parameter used in bed form theories

Author	Classification parameter
Liu (1957)	u_*/w_s and u_*d_{50}/v
Simons & Richardsons (1966)	τ^*v and d_{50}
Bogardi (1974)	gd_{50}/u_*^2
van Rijn (1993)	T and D_*

3.3.1.2 Effect of bed forms on the flow resistance: the hydraulic resistance to water flow in open canal is affected by several factors. The development of bed features such as ripples, mega-ripples and dunes plays an important role in the hydraulic resistance of the flow. This study will be mainly focused on the hydraulic resistance due to the bed roughness.

This hydraulic resistance is measured in terms of a friction factor. Most common friction factors are described by:

- Darcy-Weisbach friction factor f represented by:

$$f = \frac{8\ g\ R\ S_f}{V^2} \tag{3.5}$$

- Chézy coefficient:

$$C = \frac{V}{\sqrt{S_f\ R}} \tag{3.6}$$

- Manning (Strickler) roughness coefficient:

$$n = \frac{R^{2/3} S_f^{1/2}}{V} \quad \text{with} \quad k = \frac{1}{n} \tag{3.7}$$

These coefficients are related each to another by:

$$C = \sqrt{\frac{8\,g}{f}} \tag{3.8}$$

and:

$$C = \frac{R^{1/6}}{n} \tag{3.9}$$

where:

f	= friction factor of Darcy-Weisbach
g	= acceleration due to gravity (m/s^2)
R	= hydraulic radius (m)
S_f	= energy gradient
V	= mean velocity (m/s)
C	= Chézy coefficient ($m^{1/2}/s$)
n	= Manning's roughness coefficient
k	= Strickler's roughness coefficient

Here, in this study the Chézy coefficient will be used to describe the friction factor in irrigation canals. Further descriptions with the Darcy-Weisbach and Manning (Strickler) coefficients can be found by using equations 3.8 and 3.9.

Bed features are also elements producing resistance to flow. It is accepted that the total drag under a movable bed condition is composed of two components:

- the surface drag due to the grain roughness; also called the skin resistance with a grain related shear stress τ'
- the form drag due to the hydrodynamic forces acting over the macro scale of the bed features. The form related shear stress is described by τ''

Figure 3.8 shows the behaviour of the shear stress for different flow conditions. For a low velocity the bed shear stress is smaller than the critical value and no motion occurs; the bed remains flat. The total bed shear stress is represented by the grain related shear stress. For increasing velocity, beyond the threshold, the sediment transport starts and the bed becomes unstable and configuration of the bed takes place. For small velocities, just exceeding the critical value, small disturbances, called ripples occur. Higher velocities will produce dunes.

For these conditions the total bed shear stress is produced by two effects, namely the skin and the form resistance. Thus, the total shear stress can be expressed as:

$$\tau = \tau' + \tau'' \tag{3.10}$$

from the definition of the Darcy-Weisbach friction factor:

$$\tau = \frac{f \rho V^2}{8} \tag{3.11}$$

in the same way the total friction factor can be expressed as composed of the two effects by combining equations 3.10 and 3.11 as:

$$f = f' + f'' \tag{3.12}$$

using:

$$f = \frac{8 g}{C^2} \tag{3.13}$$

results in:

$$\frac{1}{C^2} = \frac{1}{(C')^2} + \frac{1}{(C'')^2} \tag{3.14}$$

and using the same reasoning, it is possible to get

$$n = n' + n'' \tag{3.15}$$

where:

τ = total shear stress (N/m^2)
τ' = grain related shear stress (N/m^2)
τ'' = form related shear stress (N/m^2)
f = Total Darcy-Weisbach coefficient
f' = Darcy-Weisbach coefficient due to skin resistance
f'' = Darcy-Weisbach coefficient due to form resistance
C = total Chézy coefficient ($m^{1/2}/s$)
C' = Chézy coefficient due to skin resistance ($m^{1/2}/s$)
C'' = Chézy coefficient due to form resistance ($m^{1/2}/s$)
V = mean velocity (m/s)
ρ = density of water (kg/m^3)
g = acceleration of gravity (m/s^2)

n = total Manning coefficient
n' = Manning coefficient due to skin resistance
n'' = Manning coefficient due to form resistance

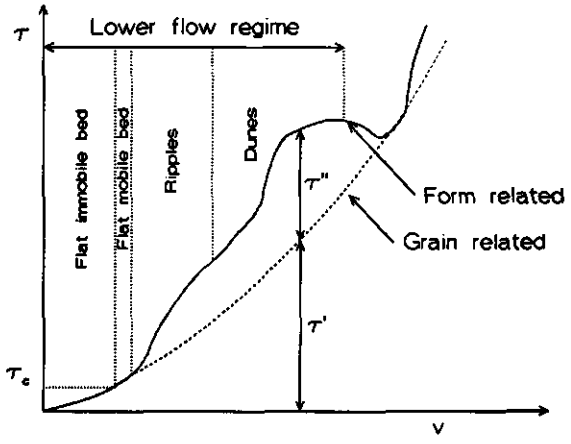

Figure 3.8 Schematization of the total shear stress due to bed form as a function of mean velocity (based on Jansen, 1994)

3.3.1.3 Determination of the friction factor: a revision of the most widely used methods to predict the resistance will be presented. A brief description of the selected methods is given in next paragraphs; they are:
- van Rijn (1984c);
- Brownlie (1983);
- White, Bettess and Paris (1979);
- Engelund (1966).

The methods of Engelund and Hansen, White et al and Brownlie to predict the friction factor are based on flow conditions and sediment sizes. No explicit determination of bed form characteristics is required. The van Rijn method is based on flow conditions and on bed form and grain related parameters as bed form length, height and sediment size. More details about the predictors for the friction factor can be found in appendix B.

van Rijn's method (1984 c): the Chézy coefficient can be calculated according to the flow regime type. Based on bed roughness conditions the hydraulic regime in open canals can be divided in a smooth, rough and transition regime. Roughness conditions on the bottom are simulated by using an equivalent height of the sand roughness k_s, which is equal to the roughness of a sand that gives a similar resistance as the bed form. The dimensionless value of $u_* k_s/\nu$ is used as classification parameter to distinguish the flow regime types. For a smooth

and transition flow regime type, the Chézy coefficient will be a function of the flow condition only and it can be calculated by (van Rijn, 1993):

$$C = 18 \log \left(\frac{12\ h}{3.3\ \frac{\nu}{u_*}} \right) \qquad \text{Smooth flow regime} \tag{3.16}$$

$$C = 18 \log \left(\frac{12\ h}{k_s + 3.3\ \frac{\nu}{u_*}} \right) \qquad \text{Transition flow regime} \tag{3.17}$$

The Chézy coefficient for the rough regime type will be calculated as (van Rijn, 1993):

$$C = 18 \log \frac{12\ h}{k_s} \tag{3.18}$$

where:

C = Chézy coefficient ($m^{1/2}/s$)
h = water depth (m)
ν = kinematic viscosity (m^2/s)
u_* = shear velocity (m/s)
k_s = total equivalent roughness height (m) as described in appendix B

Brownlie method (1983): Brownlie (1983) proposed a technique to predict the flow depth (and therefore the friction factor) when the discharge and slope value are known. No explicit calculation of the Chézy coefficient is proposed. The calculation of the coefficient is done by using equation B.15. The Brownlie method is based on a dimensional analysis, the basic principles of hydraulics and a verification with a large number of field and flume data. Step by step, the Chézy coefficient in the lower flow regime can be predicted by using the following relationships:

$$q_* = \frac{Q}{B\ g^{0.5}\ d_{50}^{1.5}} = \frac{q}{g^{0.5}\ d_{50}^{1.5}} \tag{3.19}$$

$$h = 0.372\ d_{50}\ q_*^{0.6539}\ S_f^{-0.2542}\ \sigma_s^{0.1050} \tag{3.20}$$

and

$$q = C\ h\ \sqrt{h\ S_f} \quad \therefore \quad C = \frac{q}{h^{1.5}\ S_f^{0.5}} \tag{3.21}$$

where:

Q = discharge (m^3/s)
q = unit discharge (m^2/s)
B = bottom width (m)
h = water depth (m)
S_f = energy slope
d_{50} = median diameter (m)
σ_s = gradation of sediment ($\sigma_s = \frac{1}{2}\ (d_{84}/d_{50} + d_{50}/d_{16})$)
q_* = dimensionless unit discharge

White, Paris and Bettess's method (1979): the flow resistance equation according to White et al is described in terms of dimensionless groups:

- dimensionless particle size D_*

$$D_* = \left[\frac{(s-1)\ g}{\nu^2}\right]^{1/3} d_{35} \tag{3.22}$$

- particle mobility

$$F_{fg} = \frac{u_*}{\sqrt{g\ d_{35}\ (s-1)}} \tag{3.23}$$

then:

$$n = 1 - 0.56 \log D_* \tag{3.24}$$

$$A = \frac{0.23}{\sqrt{D_*}} + 0.14 \tag{3.25}$$

$$F_{gr} = (F_{fg} - A)\left[1.0 - 0.76\left(1 - \frac{1}{\exp\ [(\log D_*)^{1.7}]}\right)\right] + A \tag{3.26}$$

$$V = \sqrt{32}\ \log\left(\frac{h}{d_{35}}\right)\left[\frac{F_{gr}\sqrt{g\ d_{35}\ (s-1)}}{u_*^{n}}\right]^{\frac{1}{1-n}} \tag{3.27}$$

$$C = \frac{g^{0.5}\ V}{u_*} \tag{3.28}$$

where:

D_* = dimensionless particle parameter
d_{35} = sediment size (mm)
s = relative density
v = kinematic viscosity (m^2/s)
u_* = shear velocity (m/s)
F_{fg} = mobility parameter related to the total shear stress
F_{gr} = mobility parameter related to the effective shear stress
A = initial motion parameter
n = exponent of the mobility parameter related to the effective shear stress
h = water depth (m)
V = mean velocity (m/s)
C = Chézy coefficient ($m^{1/2}/s$)

Engelund's method (1966): Engelund proposed to compute the Chézy coefficient by:

$$C = g^{0.5}\left(\frac{h'}{h}\right)^{0.5}\left[6 + 2.5\ \ln\left(\frac{h'}{2\ d_{65}}\right)\right] \tag{3.29}$$

where:

h = water depth (m)
h' = water depth related to the grain roughness (m)
g = gravity (m/s^2)
C = Chézy coefficient
d_{65} = median diameter (m)

3.3.1.4 Composite roughness: so far, in the previous sections, the prediction of the friction factor of a movable bottom has been discussed. No influence of the lateral roughness on the friction factor for the total cross section has been taken into account. In this section the effect of the different roughness on the effective roughness for the whole canal cross section will be considered. One of the most important features of the water flow in canals with composite roughness is the estimation of the effective roughness for the entire cross section of the canal. In irrigation canals the flow frequently encounters a different roughness on the bottom and

sides of the canal. Several cases of composite roughness along the wetted perimeter of an irrigation canal can be found.

Rigid boundaries: the flow resistance is only related to the roughness surface and not to the flow condition. The composite roughness is associated with different types of material on the side and bottom of the irrigation canal. Values of roughness coefficients for the side and bottom can be drawn from recommended values, depending on the type of material on bottom and side respectively. Chow (1983) gives a extensive list of roughness coefficients.

Movable bottom bed: the water flow conditions can change the roughness characteristics on the bed by developing bed forms, which are located on the bottom and not on the side slopes. The sediment particles on the side slope experience additional forces due to the gravity force besides the fluid force. The critical shear stress for the initiation of motion of particles on side slope becomes smaller due to the effect of the side slope. For angles of the side slopes larger than the angle of repose of the sediment material the critical shear stress for the initiation of motion is reduced to zero (Ikeda, 1982b). Recommended values of 'm' for side slopes in unlined irrigation canals are between 1 and 3. For most cases the angles of the side slopes (between 45^0 and 18.5^0) exceed the natural angle of repose of wet sand which is in the range between 15^0 and 25^0 (Kinori, 1970). Due to this fact deposition of sediment particles will be expected to occur on the bottom.

The two most frequently observed cases for the composite roughness of a movable bed are:

- bed form on the bed and a flat surface on the side banks: roughness on the bottom can be estimated from the bed form characteristics. Procedures to estimate the hydraulic roughness have been described before. Hydraulic roughness of the side slope can be estimated depending on the type of material.
- bed form on the bottom and a vegetated side slope: vegetation in a canal can be regarded as a type of roughness (Chow, 1983). Hydraulic roughness in vegetated canals is often given by a single value drawn from field measurements, but, indeed, the hydraulic roughness of those canals with a certain vegetation growth is a complex function of many variables related to the flow condition and vegetation characteristics and it can not be expressed by a single, fixed value. The determination of the flow resistance for a vegetated canal is a difficult problem, which requires considerable research before the phenomena involved are completely understood (Kouwen, 1969 and 1992). So far, it is impossible to make a proper estimate of the flow resistance based on analytical or theoretical considerations (Querner, 1993).

Some methods have been developed in the past to compute the composite roughness in open canals. They are based on several assumptions for the flow condition in the cross section of the canal. The assumptions on which each method is based will be described. The cross section of a trapezoidal canals is divided in a number N of sub-sections (figure 3.9). For this problem

the Manning coefficient will be used to describe the flow resistance. In sub-section 4.2.3.4 a comparison of these methods will be done.

Method 1: Vanoni (1975), Chow (1983), and Raudkivi (1990) mentioned that the composite roughness of the entire cross section can be calculated by considering the total cross section as an area composed by sub-sections. Each sub-section has the same mean velocity and the same energy gradient as the whole cross section. The composite roughness for the whole cross section is determined by:

$$A = \sum_{i=1}^{N} A_i \quad \therefore \quad \left(\frac{V\, P^{2/3}\, n_e}{S^{1/2}} \right)^{3/2} = \sum_{i=1}^{N} \left(\frac{V\, P_i^{2/3}\, n_i}{S^{1/2}} \right)^{3/2} \tag{3.30}$$

$$n_e = \left(\sum_{i=1}^{N} \frac{P_i\, n_i^{3/2}}{P} \right)^{2/3} \tag{3.31}$$

Method 2: As explained by Chow (1983), Krishnamurthy and Christensen (1972), Motayed and Krishnamurthy (1980), the total resistance to flow in a cross section is equal to the summation of the resisting forces in each sub-section and the hydraulic radius of each sub-section is equal to the radius of the whole cross section.

$$\tau\, P = \sum_{i=1}^{N} \tau_i\, P_i \quad \text{with} \quad \tau = \rho\, g\, R\, S \quad \text{and} \quad S = \frac{V^2\, n^2}{R^{4/3}} \tag{3.32}$$

replacing and rearranging:

$$n_e = \left(\sum_{i=1}^{N} \frac{P_i\, n_i^2}{P} \right)^{1/2} \tag{3.33}$$

Method 3a: The same authors also described another method which is based on the assumption that the total discharge of the whole cross section is equal to the summation of all the discharges in the subsections:

$$\frac{A R^{2/3}\, S^{1/2}}{n_e} = \sum_{i=1}^{N} \frac{A_i\, R_i^{2/3}\, S_i^{1/2}}{n_i} \tag{3.34}$$

$$n_e = \frac{P\, R^{5/3}}{\sum_{i=1}^{N} \frac{P_i\, R_i^{5/3}}{n_i}} \tag{3.35}$$

Method 3b: Asano et al (1985) modified the equation (3.35) by replacing the hydraulic radius R by a composite hydraulic radius R_e, which is given by:

$$R_e = \left(\sum_{i=1}^{N} \frac{P_i \, R_i^{5/3}}{P} \right)^{\frac{3}{5}} \tag{3.36}$$

and the composite roughness is expressed as:

$$n_e = \frac{\sum_{i=1}^{N} P_i \, R_i^{5/3}}{\sum_{i=1}^{N} \frac{P_i \, R_i^{5/3}}{n_i}} \tag{3.37}$$

Method 4: Krishnamurthy and Christensen (1972) proposed that the summation of the discharges in the sub-sections with roughness coefficient k_{si} is equal to the summation of the discharges in the sub-sections with an composite roughness k_{se}. The flow in each section is assumed to be rough turbulent and the velocity distribution is explained by the logarithmic law. This method is rather similar to the one described by Asano (1985) and differs only in the description of the mean velocity in the sub-sections. The composite roughness is computed by:

$$q_i = V_i \, h_i \, dy \tag{3.38}$$

$$\left(\frac{V_i}{u_{*_i}}\right) = 8.48 + 2.5 \ln \left(\frac{0.368 \, h_i}{k_{si}}\right) \tag{3.39}$$

expressed in terms of the composite equivalent roughness k_{se} gives:

$$\left(\frac{V_i}{u_{*_i}}\right) = 8.48 + 2.5 \ln \left(\frac{0.368 \, h_i}{k_{se}}\right) \tag{3.40}$$

The hydraulic roughness is related to the Manning's coefficient by (Henderson, 1966):

$$n = 0.034 \, k_s^{1/6} \tag{3.41}$$

Equating the discharges gives:

$$\ln n_e = \frac{\sum_{i=1}^{N} P_i R_i^{3/2} \ln n_i}{\sum_{i=1}^{n} P_i R_i^{3/2}} \qquad (3.42)$$

where:

n_e = composite Manning's roughness coefficient for the whole cross section;
n_i = Manning's roughness coefficient in sub-section i;
u_{*i} = shear velocity in sub-section i;
V_i = mean velocity in sub-section i;
A = cross section area;
A_i = area of sub-section i;
S = energy gradient;
q_i = discharge in sub-section i;
τ_e = shear stress for the whole cross section;
τ_i = shear stress in sub-section i;
P = wetted perimeter for the whole cross section;
P_i = wetted perimeter in sub-section i;
R = hydraulic radius for the whole cross section;
R_i = hydraulic radius for the sub-section i;
R_e = composite hydraulic radius;
h_i = water depth of sub-section i;
k_{si} = composite hydraulic roughness in each sub section i;
k_{se} = composite equivalent hydraulic roughness.
dy = width of sub-section i

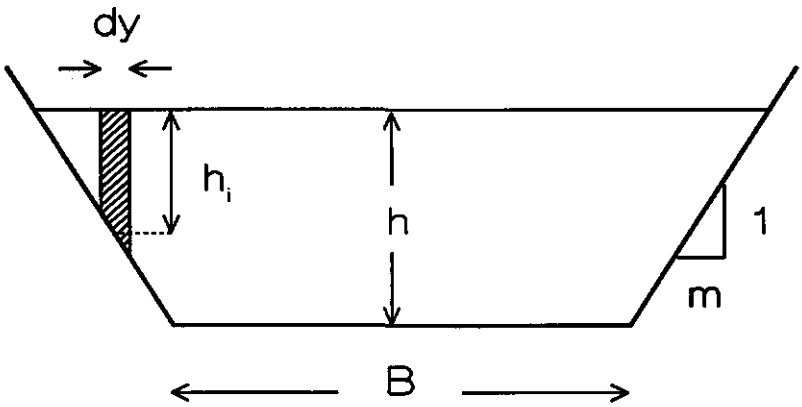

Figure 3.9 Trapezoidal cross-section composed by sub-sections

Comparison of methods: a comparison between the described methods is done. The aim is to present the differences between the methods when they are used to compute the effective roughness for a given canal composed of different roughness along the wetted perimeter. No comparison in terms of the ability to predict effective friction factor in field and/or laboratory condition is presented. The Manning coefficient is used for comparison of methods. The methods are applied in hypothetical trapezoidal canals which are characterized by:

cross section	= trapezoidal canal
side slope (m)	= 1
B/h ratio	= 1 to 8
Manning coefficient in bottom (n_b)	= 0.030
Manning coefficient in side slope (n_s)	= 0.017

The comparison is done in a relative terms by using the ratio between the effective Manning coefficient computed by each method (equations 3.31, 3.33, 3.35, 3.37 and 3.42) and the effective Manning coefficient computed by the method 1 (eq. 3.31) as:

$$\text{Ratio} = \frac{\text{effective Manning coefficient computed by each method}}{\text{effective Manning coefficient computed by method 1}}$$

Table 3.2 shows results of comparison of the described methods for computing effective roughness in a trapezoidal canal with different roughness along the wetted perimeter. From that comparison on this specific cases some conclusions can be draw:

- methods 1 and 2 behaved similars;
- large differences in computing the effective roughness in the specific case were found. Differences of 40% between the methods were found. Differences in computations are depending on B/h ratio, side slope, roughness conditions in bottom and side slopes of canal.
- these methods were developed for different conditions to those encountered in irrigation canals. A comparison of the ability for predicting the effective roughness with field and/or laboratory data is needed.

Table 3.2 Ratio of computation the effective Manning coefficient

	Methods				
B/h	1	2	3a	3b	4
1	1.00	1.01	0.64	0.74	0.79
2	1.00	1.02	0.65	0.74	0.78
3	1.00	1.02	0.68	0.76	0.80
4	1.00	1.02	0.71	0.78	0.81
5	1.00	1.02	0.73	0.80	0.83
6	1.00	1.02	0.75	0.81	0.84
7	1.00	1.02	0.77	0.83	0.85
8	1.00	1.02	0.79	0.84	0.86

3.3.2 Sediment transport equations

Sediment can be transported in equilibrium and non-equilibrium conditions. Equilibrium condition means that the amount of sediment for a certain flow condition can be transported without deposition or erosion. Sediment transport predictors are supposed to be in equilibrium conditions. The non-equilibrium condition describes how a certain amount of sediment is conveyed by the flow, as well as the erosion and deposition processes.

3.3.2.1 Sediment transport predictors: there is no universally accepted equation to determine the total sediment transport capacity of canals. But, the predictability of all of them is still poor. It would be not practical to describe in this study all the existing methods to predict sediment transport. Therefor only five of the most widely used methods to compute sediment transport will be briefly described. These methods are:

- Ackers and White;
- Brownlie;
- Engelund and Hansen;
- van Rijn;
- Yang.

Ackers and White method (1973): The Ackers and White (1973) method is based on flume experiments with an uniform or nearly uniform sediment size distribution, with an established movement including a range of bed forms, flow conditions for water depths smaller than 0.4 m and a lower flow regime ($Fr \leq 0.8$). The Ackers and White method describes the sediment transport in terms of three dimensionless parameters: D_* (grain size sediment parameter), F_{gr} (mobility) and G_{gr} (sediment transport parameter). Appendix A contains details of this method. The Ackers and White function to determine the total sediment transport reads as:

$$q_s = G_{gr}\, s\, d_{35} \left(\frac{V}{u_*}\right)^n \qquad (3.44)$$

here:

d_{35} = sediment diameter (m)
s = relative density
u_* = shear velocity (m/s)
V = mean velocity (m/s)
q_s = total sediment transport per unit width (m^2/s)
G_{gr} = sediment transport parameter
n = coefficient of the mobility parameter F_{gr}

Brownlie method (1981): Brownlie (1981) defined a method to compute the sediment transport rate, which is based on a dimensional analysis and calibration of a wide range of field and

laboratory data where uniform conditions were present. Appendix A contains details of this method. The transport rate (in ppm by weight) is calculated by:

$$q_s = 727.6\ c_f\ (F_g - F_{g_{cr}})^{1.978}\ S^{0.6601}\ (\frac{R}{d_{50}})^{-0.3301} \qquad (3.45)$$

where:

c_f = coefficient for the transport rate ($c_f = 1$ for laboratory conditions and $c_f = 1.268$ for field conditions
F_g = grain Froude number
F_{gcr} = critical grain Froude number
S = bottom slope
d_{50} = median diameter (mm)
R = hydraulic radius (m)
q_s = total sediment transport per unit width (m^2/s)

Engelund and Hansen method (1967): the method of Engelund and Hansen is based on an energy approach. They established a relationship between transport and mobility parameters. Appendix A contains details of this method. The Engelund and Hansen function for the total sediment transport is calculated by:

$$q_s = \frac{0.05\ V^5}{(s-1)^2\ g^{0.5}\ d_{50}\ C^3} \qquad (3.46)$$

where:

q_s = total sediment discharge (m^3/sm)
V = mean velocity (m/s)
C = Chézy coefficient ($m^{1/2}/s$)
s = relative density
d_{50} = mean diameter (m)
g = gravity (m/s^2)

van Rijn method (1984a and 1984b): the total sediment load transport by the van Rijn method can be computed by the summation of the bed and suspended load transport. The van Rijn method presents the computation of the bed load transport q_b as the product of the saltation height, the particle velocity and bed load concentration. It is assumed that the motion of the bed particles is dominated by gravity forces. Appendix A contains details of this method.

The bed load transport rate can be expressed as:

$$q_b = 0.053\ (s-1)^{0.5}\ g^{0.5}\ d_{50}^{1.5}\ D_*^{-0.3}\ T^{2.1} \qquad (3.47)$$

where:

q_b = bed load transport rate (m^2/s)
T = bed shear parameter
D_* = particle parameter
s = relative density
d_{50} = median diameter
g = gravity (m/s^2)

The suspended load transport q_{sus} is calculated by:

$$q_{sus} = F\ V\ h\ c_a \tag{3.48}$$

where:

F = shape factor
V = mean velocity (m/s)
h = water depth (m)
c_a = reference concentration

Yang method (1973): the Yang method is based on the hypothesis that the rate of sediment transport in a flow should be related to the rate of energy dissipation of the flow. The rate of energy dissipation is defined as the unit stream power and it can be expressed by the velocity times slope (V * S). The theoretical basis for the Yang's dimensionless unit stream power is provided by the turbulence theory. By integrating the rate of turbulence energy production over the depth of flow, the suspended sediment transport can be expressed as function of the unit stream power. Appendix A contains details of this method. The total sediment transport can also be expressed as a function of the unit stream power by:

$$\log c_t = I + J \log \left(\frac{V\ S - V_{cr}\ S}{w_s}\right) \tag{3.49}$$

where:

c_t = total sediment transport expressed in ppm by mass
I, J = coefficients in the total sediment transport of Yang's function
w_s = fall velocity (m/s)
V = mean velocity (m/s)
V_{cr} = critical velocity (m/s)
S = bottom slope

3.3.2.2 Sediment transport in non-equilibrium condition: an interesting phenomenon of the non-equilibrium sediment transport in an irrigation canal is the adjustment of the actual sediment transport to the sediment transport capacity of the irrigation canal. A continuous

deposition and/or entrainment process will be present in the canal due to the change in the local flow conditions. These processes will cause morphological changes in the bottom level.

Sediment transport in non-equilibrium condition is important for the suspended load. Bed load is assumed to react instantaneously to the flow condition. Nakagawa (1989) mentioned that the relaxation distances of the bed load motion over a flat bed is about 100 times the sand diameter and of course negligible in most engineering problems.

To simulate the suspended sediment transport under non-equilibrium conditions, various approaches are possible (van Rijn, 1987): (1) one dimensional, two dimensional models and three dimensional models and (2) depth integrated models.

The firsts are based on the solution of the diffusion-convection equation which for two-dimensional problems reads as:

$$\frac{\partial c}{\partial t} + u\frac{\partial c}{\partial x} + w\frac{\partial c}{\partial z} = w_s\frac{\partial c}{\partial z} + \frac{\partial}{\partial x}(\epsilon_x\frac{\partial c}{\partial x}) + \frac{\partial}{\partial z}(\epsilon_z\frac{\partial c}{\partial z}) \qquad (3.50)$$

where:

c = suspended sediment concentration
w_s = fall velocity (m/s)
t = time coordinate (s)
x, z = length coordinates (m)
ϵ_x, ϵ_z = sediment mixing coefficient in x and z direction (m^2/s)
u, w = velocity components in x and z direction (m/s)

The equation can be solved when the velocity components, the fall velocity and the mixing coefficients are known.

Galappatti (1983) developed a depth integrated model for suspended sediment transport in unsteady and non-uniform flow, is used. The model is based on the 2-D convection-diffusion equation.

The main concepts on which the depth integrated model of Galappatti is based on, include:
- the horizontal diffusive transport (ϵ_x) and the vertical component of the velocity (w) are neglected:

$$\frac{\partial c}{\partial t} + u\frac{\partial c}{\partial x} = w_s\frac{\partial c}{\partial z} + \frac{\partial}{\partial z}(\epsilon_z\frac{\partial c}{\partial z}) \qquad (3.51)$$

- the concentration $c_{x,z,t}$ (fig. 3.10) is expressed in terms of a depth averaged concentration $c_{x,t}$ (fig. 3.11).

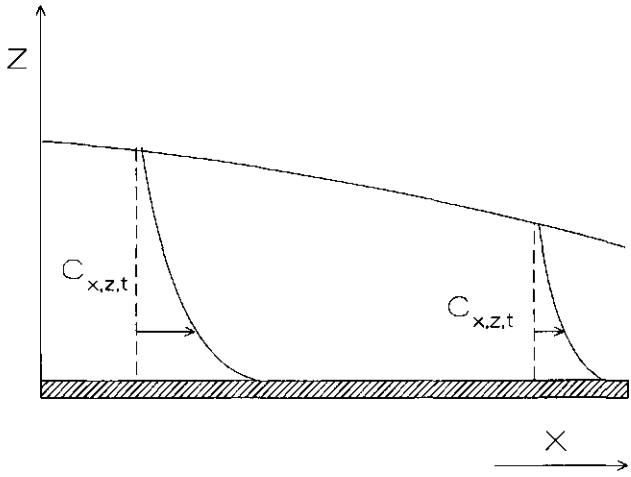

Figure 3.10 Schematization of 2-D suspended sediment transport model

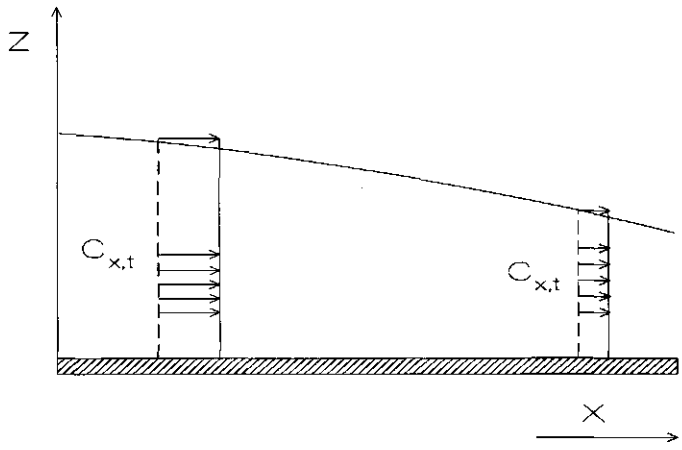

Figure 3.11 Schematization of a depth-integrated model

In an uniform flow, carrying sediments in non-equilibrium condition, the variation in concentration can be written according to the Galappatti's depth integrated model as:

$$c_e = c + T_A \frac{\partial c}{\partial t} + L_A \frac{\partial c}{\partial x} \qquad (3.52)$$

with

$$T_A = \frac{w_s}{u*} \frac{h}{w_s} \exp(f) \tag{3.53}$$

$$\frac{T_A u_*}{h} = \exp(f) \tag{3.54}$$

$$L_A = \frac{w_s}{u*} \frac{V h}{w_s} \exp(f) \tag{3.55}$$

$$\frac{L_A}{h} = \frac{w_s}{u_*} \frac{V}{w_s} \exp(f) \tag{3.56}$$

$$f = \sum_{i=1}^{4} \left(a_i + b_i \frac{u_*}{V} \right) \left(\frac{w_s}{u_*} \right)^{i-1} \tag{3.57}$$

where:

c_e = concentration of suspended load in equilibrium condition
c' = concentration of suspended load at distance x
T_A = adaptation time (s)
L_A = adaptation length (m)
w_s = fall velocity (m/s)
u_* = shear velocity (m/s)
V = mean velocity (m/s)
h = water depth (m)
a_i, b_i = constants

The adaptation length (L_A) and adaptation time (T_A) are constant for uniform flow. They are defined as the interval (both in length and time) required for the mean concentration to approach the mean equilibrium concentration. The adaptation length represents the length scale and the adaptation time the time scale (Ribberink, 1986). Characteristics values of adaptation length for irrigation canals will be given in sub-section 5.3 (see fig 5.7).

Values of a_i and b_i for $z_a/h = 0.01$ are given in table 3.3 (Gallapatti, 1983). For values of z_a/h less than 0.01, the same values of a_i and b_i will be used, as for smaller values the influence of z_a/h on the adaptation time and length is insignificant (Kerssens, 1979).

Table 3.3 a_i and b_i values for $z_a/h = 0.01$ (after Gallapatti, 1983)

	a_1	b_1	a_2	b_2	a_3	b_3	a_4	b_4
T_A	1.978	0.000	-6.321	0.000	3.256	0.000	0.193	0.000
L_A	1.978	0.543	-6.326	-3.331	3.272	0.400	0.181	1.790

For a steady sediment flow equation 3.51 can be written as:

$$c_e - c = L_A \frac{\partial c}{\partial x} \tag{3.58}$$

integration results in:

$$\int_0^x dx = L_A \int_{c_0}^{\bar{c}} \frac{dc}{c_e - c} \tag{3.59}$$

finally

$$c = c_e - (c_e - c_0) \exp -\frac{x}{L_A} \tag{3.60}$$

It was shown in figure 3.3 that the rates of suspended load and bed load transport of sediment larger than 0.3 mm are comparable and that the more reliable sediment transport predictor in irrigation canals (see paragraph 4.4.2) compute the total load (suspended and bed load). For that reason it will be unavoidable to consider the sediment transport in non-equilibrium condition as a whole. Although the bed load reacts instantaneously from non-equilibrium condition to equilibrium condition, it is assumed that the characteristic adaptation length for the bed load is the same characteristic adaptation length as for suspended load. Therefore equation 3.59 can be used to describe the total sediment transport under non-equilibrium conditions by using the total sediment concentration (bed and suspended load) in stead of suspended sediment concentration. This leads to:

$$C = C_e - (C_e - C_0) \exp -\frac{x}{L_A} \tag{3.61}$$

where:

C = total sediment concentration at distance x
C_e = total sediment concentration in equilibrium condition
C_0 = total sediment concentration at distance x = 0
L_A = adaptation length (m)

3.3.2.3 Sediment transport computations for non-wide canals: In paragraph 3.3.2.1 the sediment transport predictors were described. The sediment transport predictors have been developed for wide canals in an one-dimensional form in which the total flow is considered to be one large stream tube with an uniform velocity distribution and also an uniform distribution of the sediment transport in the whole cross section. Therefore the sediment transport capacity is expressed per unit width. In a simplified way, sediment transport equations per unit width can be written as:

$$q_s = M\ V^N \tag{3.62}$$

Therefore, the total sediment transport for the whole cross section in a wide canal can be expressed as:

$$Q_s = q_s * B \tag{3.63}$$

where:

Q_s = total sediment transport in the whole cross section
q_s = sediment transport per unit width
V = mean velocity
B = bottom width of the wide canal
M, N = coefficients depending on flow conditions and sediment characteristics

Procedures for computing sediment transport capacity in non-wide canals: in case of a non-wide canal the question is how to compute the total sediment transport for the whole cross section. Different computational procedures have been used for several available mathematical models to compute the total sediment discharge over the whole cross section in non-wide open channels. They are used without taking into account both the velocity distribution across the section and the type of non-linear relationship between the sediment transport and the flow velocity as shown in a simplified way by equation 3.61. They compute the sediment transport over the whole cross section in a similar way as described previously for wide canals as:

$$Q_s = q_s * B_{st} \tag{3.64}$$

where:

Q_s = total sediment transport in the whole cross section
q_s = sediment transport per unit width
B_{st} = sediment transport width

The existing procedures to compute the sediment transport in non-wide canals are:

A. - Procedure 1
B. - Procedure 2

A. - Procedure 1: the sediment discharge per unit width (q_s) is calculated by using the hydraulic radius as representative variable for the water flow as:

$$q_s = f(V) \quad \text{with} \quad V = f(R) \tag{3.65}$$

Using this procedure several cases to estimate the sediment transport over the whole cross section were found, they only differ in the way how to define the sediment transport width:

Case 1: the total sediment transport over the cross section is calculated by multiplying the sediment transport per unit width and the average width of the canal (HR Wallingford, 1992) as shown below:

$$Q_s = q_s * B_{av.} = q_s * \frac{(B + T)}{2} \tag{3.66}$$

where:

Q_s = total sediment transport in the whole cross section
q_s = sediment transport per unit width
$B_{av.}$ = averaged width
B = bottom width
T = water surface width

Case 2: the total sediment transport in a cross section is calculated by multiplying the sediment transport per unit width and the transport width W_s (Delft Hydraulics, 1994) as follows:

$$Q_s = q_s * W_s = q_s * \alpha_s * T \tag{3.67}$$

where:

Q_s = total sediment transport in the whole cross section
q_s = sediment transport per unit width
R = hydraulic radius
V = mean velocity
W_s = sediment transport width ($W_s = \alpha_s * T$)
T = water surface width
α_s = reduction factor with a value in the range $0 < \alpha_s \leq 1$.

Case 3: the total sediment transport over the whole cross section of the canal is compured in the following way (DHI, 1990):

$$Q_s = q_s * W \tag{3.68}$$

where:

Q_s = total sediment transport in the whole cross section
q_s = sediment transport per unit width
W = width which is defined as the wetted perimeter P

Comparison of cases 1, 2 and 3: those cases are rather similar, they only differ in the way in which the sediment transport width has been defined. Different values of the sediment transport width are found for each case; these differences are related to the geometrical characteristics of the canal: bottom width-water depth ratio (B/h) and side slope (m). Therefore, differences in the total sediment discharge are observed when they are compared with each other. A comparison between the computation of the total sediment transport over the whole cross section by the using the different cases was done. The comparison is based on the ratio of computation the total sediment transport capacity between the different cases. Figure 3.12 shows the results of the comparison of the total sediment discharge computation of each case compared with the results by using case 1 (average width) which is expressed by:

$$\text{Ratio} = \frac{\text{total sediment transport capacity according specific case (cases 2 or 3)}}{\text{total sediment transport capacity according case 1}} \qquad (3.69)$$

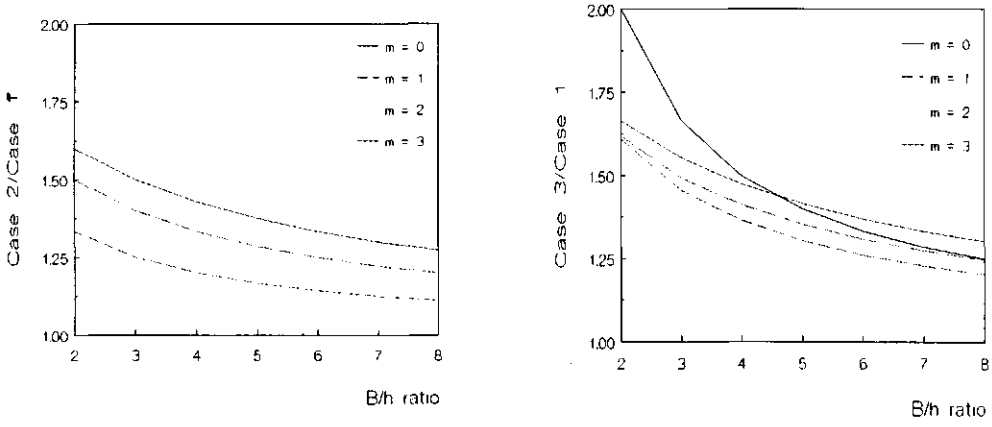

Figure 3.12 Ratio of computations of the total sediment transport for trapezoidal and rectangular cross sections

Comparison between case 1 and case 2 shows small differences which are in the range of 10% (m = 1) and 60% (m = 3) for trapezoidal cross sections and no differences are observed for rectangular cross section (m = 0). Larger differences were found for the comparison between case 1 and case 3. Differences in the range between 20% (m = 3) and 100% (m = 0) can be expected.

B. - Procedure 2: next to the procedure described before, the total sediment transport for the whole cross section can be computed by using another type of procedure. As described by DHI (1990), HR Wallingford (1992) and Delft Hydraulics et al (1994) it is possible to use predictor methods for estimating the alluvial friction as White, Paris and Bettess (1979), Engelund (1966) which use the water depth (h) in stead of hydraulic radius (R) as representative variable for the flow depth of the cross section (see equations B.26 and B.38 respectively) and therefore the flow velocity will also be a function of the water depth (h). The bottom width of the canal (B) is assumed as the sediment transport width (B_{st}). This procedure is fully suitable for very large canals where the influence of the side banks can be considered to be negligible. It can be described as:

$$q_s = f(V) \quad \text{with} \quad V = f(h) \tag{3.70}$$

and:

$$Q_s = q_s * B \tag{3.71}$$

where:

Q_s = total sediment transport in the whole cross section
q_s = sediment transport per unit width
V = mean velocity
B = bottom width of the wide canal
h = water depth

Comparison of procedures for computing sediment transport capacity in non-wide canals: Beside the comparison between the different cases of procedure 1 another comparison between the procedures (procedures 1 and 2) was done. Those comparisons were aimed to determine the suitability of the procedures to compute the sediment transport capacity in non-wide canals. In the comparison between procedures 1 and 2 the total sediment transport computation differ both in the representative variable for the flow depth and the representative width for the sediment transport. Only case 1 (equations 3.64 and 3.65) was used as representative of procedure 1 in which the sediment discharge per unit width (q_s) is calculated by using the hydraulic radius as representative variable for the water flow. The average width of the canal is assumed to be the representative canal width.

In procedure 2 the determination of the sediment transport per unit width (q_s) requires the water depth as representative variable of the water flow. Next the total sediment transport Q_s is calculated by multiplying the sediment transport per unit width (q_s) by the bottom width (B).

The differences between the procedures 1 and 2 are related to both the estimation of the sediment transport per unit width q_s and the sediment transport width B_{st} (eq.3.63). The

differences depend on the geometrical characteristics of the canal and the relationship between the sediment transport per unit width and the characteristic depth of the water flow.

In order to compare both procedures to compute sediment transport in non-wide channels, an application in some schematized canals was carried out. The Ackers-White (A-W), Brownlie (BRO) and Engelund-Hansen (E-H) sediment transport predictors were used to compute the total sediment transport for all canals. Comparison of both approaches was done in terms of the ratio of the computed total sediment transport which can be described as:

$$\text{Ratio} = \frac{\text{total sediment transport capacity according procedure 2}}{\text{total sediment transport capacity according procedure 1}} \qquad (3.72)$$

Computations have been performed for canals with the following characteristics:

- bottom width (B) = 6 m
- bottom slope (S_0) = 0.0003
- sediment diameter (d_{50}) = 0.2 mm
- side slope (m) = 0, 1 and 2
- Chézy coefficient (C) = 40 $m^{1/2}/s$
- B/h ratio = 3 to 8
- sediment transport predictors = A-W, BRO and E-H.

Figure 3.13 shows the results of the comparison of the procedures 1 and 2 used for computing sediment transport. The results describe the relative variation of the computed sediment transport for different values of B/h.

From that figure some conclusions can be drawn:

- the largest ratios of the calculated total sediment transport were observed for the rectangular cross section (m = 0). For that cross section the difference between water depth and hydraulic radius is larger than for other side slopes. Therefore the differences of the velocity calculated by using these representative depths will also be large;
- related to the sediment transport predictor, the Ackers and White predictor show the largest values for the ratio of computations than the Engelund and Hansen and Brownlie predictors. The non-linear relationship of the sediment transport and velocity are higher in Ackers and White than Engelund and Hansen and Brownlie predictors (see 4.3.3.2);
- for small values of B/h ratio, the ratio of computation of the total sediment transport was in a range between 60% and 375%. For larger values of the B/h ratio of 8 the difference was reduced to a range between 30% and 200%. It is expected that for the largest B/h ratio (wide channels) the differences in both procedures would be minimal;
- it is clear that for applying the available sediment transport formulae in the computation of total sediment transport capacity for non-wide channels a modification will be required.

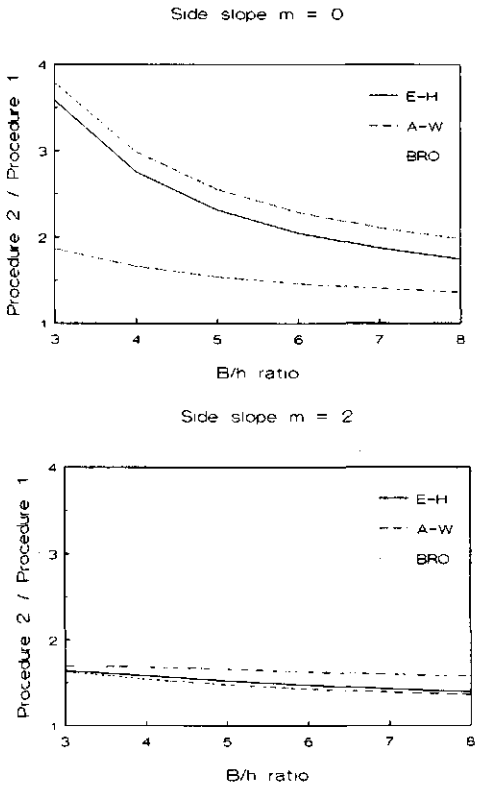

Figure 3.13 Ratio of the computation of the total sediment transport between the procedures 1 and 2

3.3.3 Mass balance equation for sediment transport

Derivations of the mass balance equations for the total sediment transport in an open canal are separately given for the suspended load layer and the bed load layer. A schematization of the mass balance in both regions is shown in figure 3.14.

From the mass balance in each control volume can be found that:

$$\frac{\partial h_s c_s}{\partial t} + \frac{\partial q_{sus}}{\partial x} = c_a (E - D) \qquad \text{Suspended load} \tag{3.73}$$

and

$$(1 - p) \frac{\partial z}{\partial t} + \frac{\partial a c_b}{\partial t} + \frac{\partial q_b}{\partial x} = - c_a (E - D) \qquad \text{Bed load} \tag{3.74}$$

By summation of both equations the mass balance equation for the total sediment transport load reads:

$$\frac{\partial h_s c_s}{\partial t} + (1 - p)\frac{\partial z}{\partial t} + \frac{\partial a c_b}{\partial t} + \frac{\partial (q_s + q_b)}{\partial x} = 0 \qquad \text{Total load} \qquad (3.75)$$

For steady condition of the sediment concentration and expressing for the total cross section the equation becomes:

$$B (1 - p)\frac{\partial z}{\partial t} + \frac{\partial Q_s}{\partial x} = 0 \qquad (3.76)$$

where:

a, h_S = depth of the bed load layer and depth of suspended layer respectively
c_s, c_b = suspended load and bed load concentration
c_a = reference concentration at the boundary of the bed load layer
q_b, q_{sus} = bed load and suspended load discharges per unit width
q_s = total sediment discharge per unit width
Q_s = total sediment discharge in the whole cross section
B = bottom width
p = porosity (sand porosity $p \approx 0.4$)
z = bottom level
x; t = length and time co-ordinates
E, D = upward flux and downward flux respectively

3.4 Conclusions

The theoretical aspects of the governing equations for sediment transport computations in open channels were described. First, a brief description of the water flow equation was given. Assuming an one-dimensional flow that can be described by the Saint Venants' equations. It was assumed that due to the fact that the celerities of the water level are much larger than the celerities of the bed movement there will be no influence of the disturbance of the bed on the water movement and the water flow can easily be schematized as a quasi-steady flow. Second, the description of the sediment equations has given emphasis to the sediment transport equations. The main conclusions derived from these concepts are:

- based on the characteristic flow conditions and the sediment sizes usually encountered in irrigation canals, the sediment could be transported as bed load and as suspended load. Therefore the sediment transport predictor should be able to compute both types of sediment transport;
- there are several theories to estimate friction factors and sediment transport rates (equilibrium and non-equilibrium conditions). These theories rely on field and laboratory observations but they are not able to explain with a very high degree of

accuracy, the phenomena concerned. Comparison of these theories for the same flow conditions as those encountered in irrigation canals will contribute to a reduction of the unreliability and unaccuracy of the prediction of the resistance to flow;

- computations of the friction factor for cross-sections with composite roughness along the wetted perimeter have been developed for river conditions in which the channel is divided in a main channel and two flood plains. Applicability of these computations for typical non-wide irrigation canals has to be investigated;
- there is no clear evidence for the selection of the most appropriate method to predict the sediment transport capacity for the flow conditions and sediment characteristics prevailing in irrigation canals;
- there are large differences between the existing procedures to compute the sediment transport capacity in non-wide canals;
- in order to be able to apply the available sediment transport formulae for the computation of the sediment transport capacity of non-wide channels a modification is required. The non-uniform distribution of the velocities over the cross section and the non-linear relationship between the sediment transport and the velocity do not allow for a full application of the sediment transport equations;
- most theories on sediment transport have been formulated by neglecting the influence of the geometry of the cross section. A wide channel concept has been assumed for these theories. Influences of the shape of the cross-section on the development of bed forms, friction factor predictors and sediment transport capacity should have been investigated.

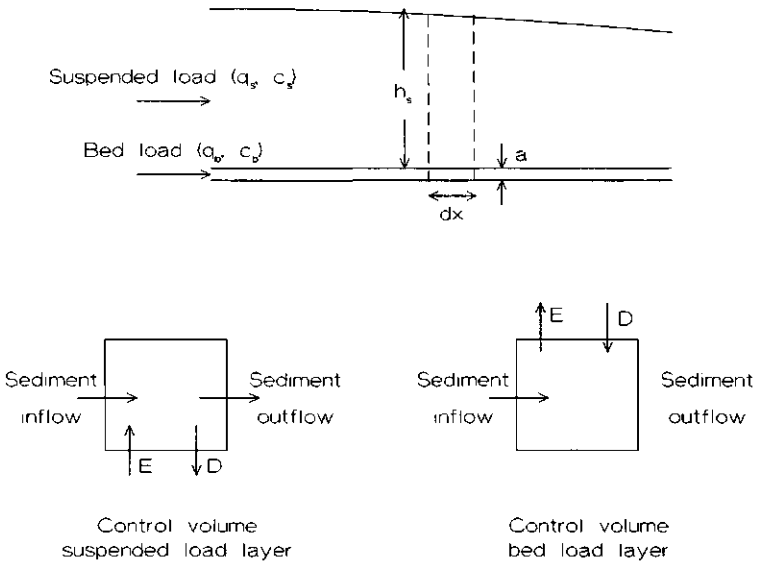

Figure 3.14 **Schematization of sediment transport modes and control sections for suspended and bed load layers**

4 APPLICATION OF SEDIMENT TRANSPORT CONCEPTS IN IRRIGATION CANALS

4.1 General

A wide variety of theories to explain the sediment transport phenomena is presently available. The problem for the specific purpose of this study is to decide which one is the most suitable one for irrigation networks. Several researchers have assessed the sediment transport by some performance tests and by comparison of each formula with the other ones. But in fact it is quite difficult to make firm recommendations about which formula to use in irrigation practice. Therefore it is still extremely difficult to select the appropriate one for this specific topic. First, they have focused on river conditions by assuming a wide alluvial channel. They consider an open canal with an infinite width without taking into account the geometry and its effect on the associated variables of a sediment laden water flow for the whole cross section (i.e friction factor, composite roughness, shear velocity, velocity distribution, sediment transport capacity, etc.). Second the use of those equations should be restricted to the conditions for which they were tested.

Most of the man-made irrigation canals have a trapezoidal or rectangular cross section and they can not be considered as wide canals. For those cross sectional shapes the imposed boundary condition for the velocity above the side bank and the varying water depth will affect the velocity and therefore the sediment transport capacity for the whole cross section. Also the flow conditions and the sediment characteristics frequently encountered in irrigation canals are restricted to the operation of the flow control structures and headworks of the irrigation system.

A comparison of the sediment transport concepts under the specific conditions of irrigation canals will help to improve the understanding of these concepts and to decide on the applicability of the concepts on the simulation of the sediment transport process for a given, particular condition of water flow and sediment inputs.

In the previous chapters the theoretical processes involved in sediment transport were described. In this chapter the applications of sediment transport concepts for the typical flow conditions and sediment characteristics of irrigation canals are presented. The various theoretical formulations of the processes will be tested on field and laboratory data, compared, adapted when necessary (non-wide canal specifically) and treated for the operational computation of sediment transport in irrigation canals. Also a new method for computing the effective friction factor in non-wide canals with different roughness along the wetted perimeter is proposed. The applications will give more details about the applicability of each of the formulae for a specific condition and may reduce inevitable errors and inaccuracies.

4.2 Prediction of the friction factor in irrigation canals

Applications of the theoretical concepts related to the determination of the friction factor under some specific flow conditions will help to select the most appropriate theories for those conditions as shown in the sequence.

4.2.1 Prediction of bed forms in irrigation canals

In order to predict the type of bed forms in irrigation canals the theories developed by Liu (1957), Simons and Richardsons (1966), Bogardi (1974) and van Rijn (1984c) will be compared with field and laboratory data. These theories have been developed to explain the bed forms in uni-directional currents for homogeneous flow conditions both in time and space (Jansen, 1994). The objective of the comparison is to find an appropriate theory to describe bed forms in irrigation canals. A selected set of laboratory and field data from the compilation by Brownlie (1981) has been used.

The criteria for selecting the data have been based on the flow conditions and sediment characteristics normally encountered in irrigation canals. The criteria are:

- the selected data should contain all the required quantities to compute the classification parameters of the theories to be compared, including description of bed forms;
- maximum sediment size d_{50} is 0.5 mm;
- Froude numbers is smaller than 0.5;
- shear stress on the bottom is less than 5 N/m^2;
- in order to avoid the influence of the side banks the value of the B/h ratio is larger than 10;
- description of the bed form.

A total of 102 records has been selected from the available data of Brownlie. Table 4.1 shows a summary of the selected data. Figure 4.1 shows the characteristics of the selected database.

The comparison among the selected theories will be based on a relative basis. It means the number of well-predicted bed forms according to each theory related to the total number of the observed bed forms from the laboratory and field data. Next the predictability of the theories will be compared each other. The predictability of the theory will be measured in terms of the number of well-predicted bed forms, which can be represented by:

$$\text{Accuracy (\%)} = \frac{\text{Number of well-predicted values}}{\text{total number of data}} \times 100 \qquad (4.1)$$

Figure 4.2 shows a graphical comparison of the different theories.

Table 4.1 Summary of selected data for predicting bed form from the compilation of Brownlie (1981)

Investigator and year	Data code	No. of records
Barton and Lin (1955)	BAL	4
Colby and Hembree (1955)	NIO	12
Guy, H.P. et al (1966)	GUY	48
Pratt, C.J. (1970)	PRA	7
Davies, T. R. (1971)	DAV	6
Mutter, D.G (1971)	MUT	18
Onishi, Y. et al (1972)	OJK	4
Culbertson et al (1976)	RGC	3

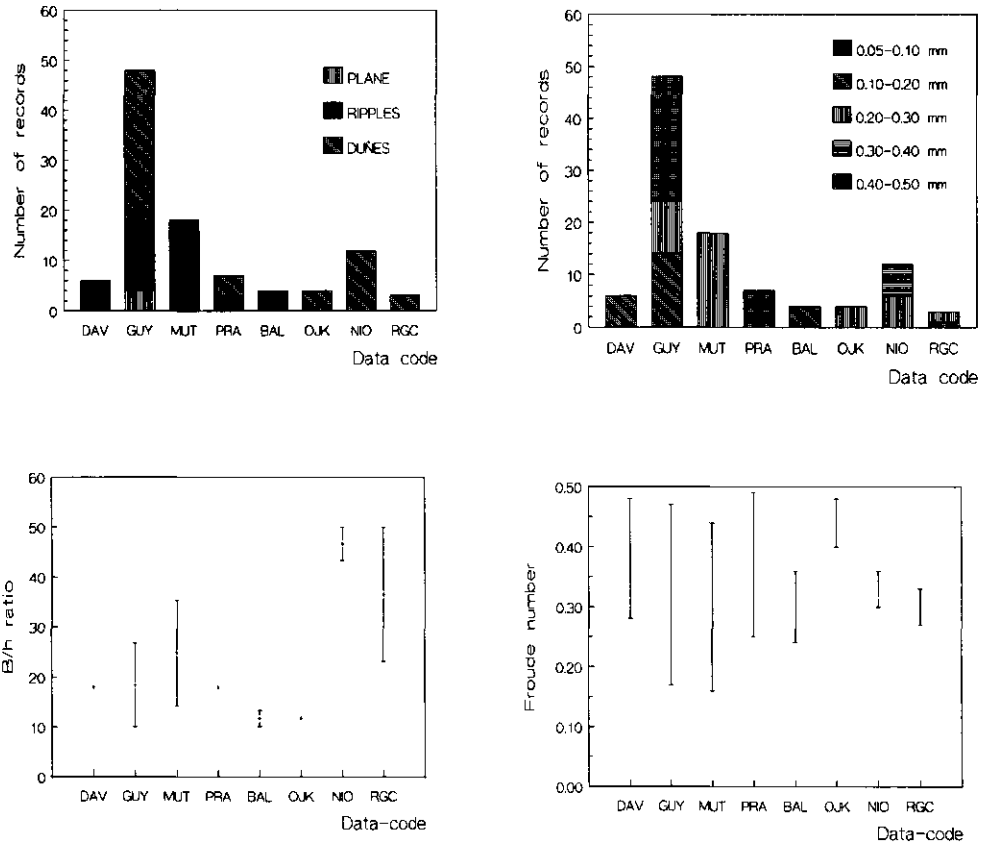

Figure 4.1 Characteristics of the selected data

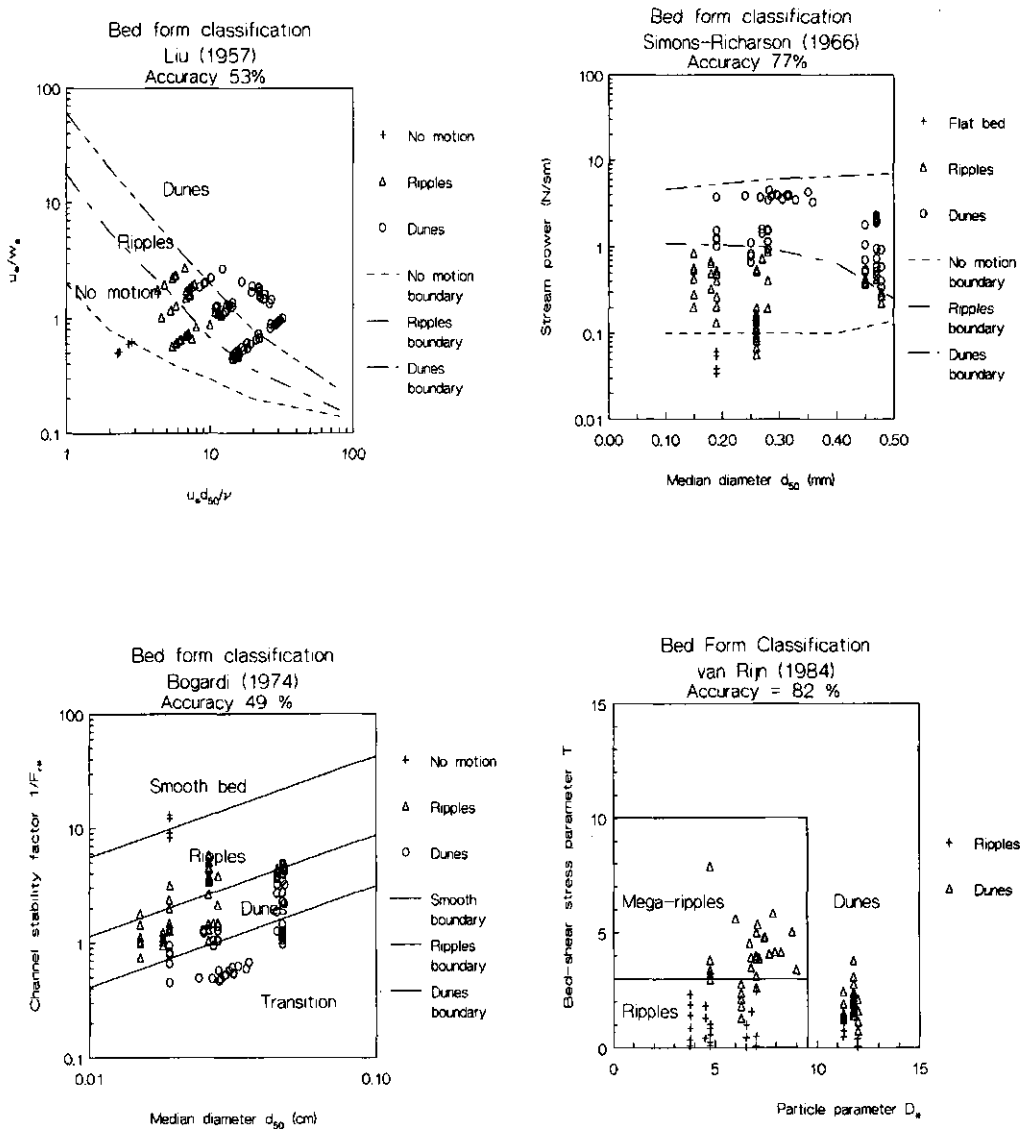

Figure 4.2 **Comparison of theories for predicting bed forms**

From the performance of each method to predict the type of bed form some conclusions can be drawn when the results of each method are compared with the selected field and laboratory data:

- the van Rijn (1984c) and Simons and Richardson (1966) behave as the best theories to predict the bed form in irrigation canals. 82% and 77% respectively of the observed bed forms from the selected data are well predicted by those theories;
- all the bed forms described for the lower regime (ripples, mega-ripples and dunes) can be expected in irrigation canals.

According to van Rijn (1993), bed forms can be classified based on the following classification parameters:

- particle parameter D_* which reflects the influence of gravity, density of the particle and viscosity:

$$D_* = \left[\frac{(s-1)\ g}{\nu^2}\right]^{1/3} d_{50} \qquad (4.2)$$

Characteristic values for the particle parameter D_* in irrigation canals are in the range of 1.5 to 7.3 (table 4.2).

Table 4.2 D_* parameter for sediment sizes encountered in irrigation canals

d_{50}	0.05	0.1	0.15	0.20	0.25	0.30	0.35	0.40	0.45	0.50
D_*	1.2	2.5	3.7	5.0	6.2	7.5	8.7	10.0	11.2	12.5

- Excess bed shear stress parameter T which is defined by:

$$T = \frac{\tau' - \tau_{cr}}{\tau_{cr}} \qquad (4.3)$$

with

$$\tau' = \rho\ g\ \left(\frac{V}{C'}\right)^2 \quad \text{and} \quad C' = 18\ \log\left(\frac{12\ h}{4.5\ d_{90}}\right) \qquad (4.4)$$

where:

D_* = particle parameter
V = mean velocity (m/s)
ρ = density of water (kg/m^3)
T = excess bed-shear stress parameter
τ_{cr} = critical shear stress according to Shields (N/m^2). It is computed according eq. 2.14
τ' = grain shear stress (N/m^2)
C' = Chézy coefficient due to grain resistance (m$^{1/2}$/s).
s = relative density of sediment
d_{50} = mean diameter (mm)

ν = kinematic viscosity (m^2/s)
g = acceleration due to gravity (m/s^2)

The ranges described by van Rijn (1993) are shown in table 4.3.

Table 4.3 Classification of bed forms according to van Rijn (1984c)

Bed forms	D_*	T
Ripples	$1 \leq D_* \leq 10$	$0 \leq T \leq 3$
Megaripples	$1 \leq D_* \leq 10$	$3 < T \leq 10$
Dunes	$D_* > 10$	$T > 0$

Figure 4.3 shows the ranges established by van Rijn (1984c) to distinguish ripples, mega-ripples and dunes. The curves of the maximum values of the classification parameter T encountered in small irrigation canals (hydraulic radius R = 0.5 m) are indicated for Froude numbers of 0.15, 0.25, 0.35 and 0.45. For large irrigation canals (hydraulic radius R = 4 m) the curves are given for Froude number equal to 0.08, 0.12 and 0.16. In large irrigation canals, higher values of Froude number will produce large values of the shear stress on the bottom beyond the normally allowed values (4-5 N/m^2).

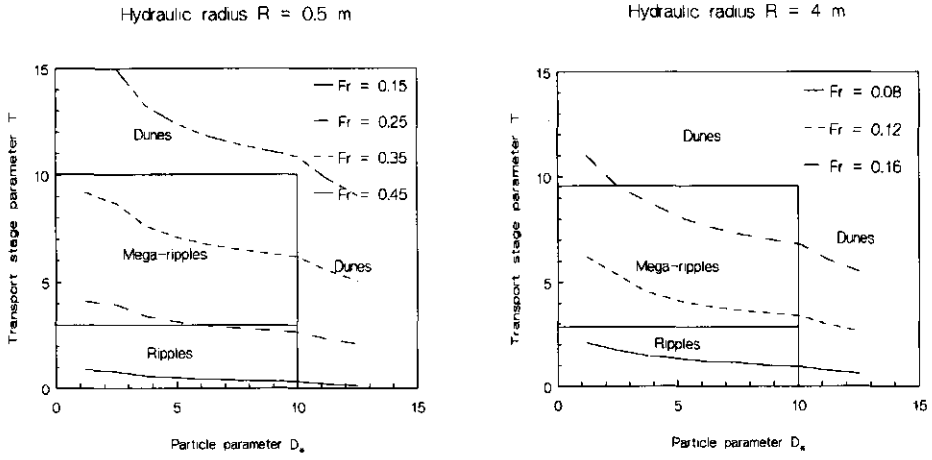

Figure 4.3 Classification of bed forms according to van Rijn (1984c) and expected bed forms in irrigation canals

The curves in the figure 4.3 were calculated in the following way:
Given are the dimensionless particle parameter (D_*), hydraulic radius (R) and Froude number (Fr) and compute the:

- median diameter d_{50} (eq. 4.2);

- critical mobility parameter θ_{cr} (equations 2.18 to 2.20);
- mean velocity V from $Fr = V/(gR)^{0.5}$
- critical shear stress τ_{cr} (eq. 2.14);
- grain shear stress τ' (eq. 4.4)
- excess bed shear stress parameter T (eq. 4.3)

4.2.2 Prediction of friction factor

A comparison of the most widely used methods to predict the resistance to flow with field and flume data will contribute to select an appropriate method for similar situations to those encountered in irrigation canals. The selected methods were previously described in subsection 3.3.1.3. They are:
- RIJ (van Rijn, 1984c);
- BRO (Brownlie, 1983);
- WBP (White, Bettess and Paris, 1979);
- ENG (Engelund, 1966).

The selected methods to estimate the friction factor, being the Chézy coefficient, have been verified with measured Chézy coefficients from flume and laboratory data. The same data as used for the comparison of bed form classification (table 4.1) has been selected for that purpose and only those data with well predicted bed forms have been used for the comparison with the van Rijn method. For the van Rijn method the type of bed form has to be explicitly determined, the other methods do not require the type of bed form for the determination of the friction factor.

The accuracy of the methods against field and flume data is based on the following:

$$\frac{C_{measured}}{f} \leq C_{predicted} \leq C_{measured} * f \qquad (4.5)$$

and:

$$\text{Accuracy} = \frac{\text{Number of well predicted values}}{\text{total values}} \qquad (4.6)$$

where:

$C_{measured}$ = measured Chézy coefficients from Brownlie (1981)
$C_{predicted}$ = predicted Chézy coefficients by the selected method
f = error factor

Also the mean values of the arithmetic and geometric values of the discrepancy ratios have been used to evaluate the accuracy of the selected methods. The discrepancy ratio dr is defined by:

$$\text{Discrepancy ratio (dr)} = \frac{\text{predicted values}}{\text{measured values}} \qquad (4.7)$$

with:

$$\text{Mean arithmetic} = \frac{\sum dr}{n} \quad \text{and} \quad \text{Mean Arithmetic} = \sqrt[n]{(dr_1 * dr_2 * \ldots\ldots * dr_n)}$$

From the performance of each method to predict the friction factor some conclusions can be drawn when the results of each method are compared with the selected field and laboratory data:

- the prediction of the friction factor by using the described methods takes only into account the bottom friction. The B/h ratio of the selected data is larger than 10. The side wall effect is considered negligible. For a non-wide canal the side banks will have an important effect on the friction factor. The varying water depth and the different roughness (no bed form) will require a weighed value of the friction factor;
- the van Rijn method (1984c) for predicting friction factors gives the best results when compared with the selected data. 41%, 71%, 88%, 97% and 98% of well predicted bed forms for error factors of 1.1, 1.2, 1.3, 1.4 and 1.5 respectively have been obtained (figure 4.4). The van Rijn method behaves well over the whole ranges of measured friction factors.

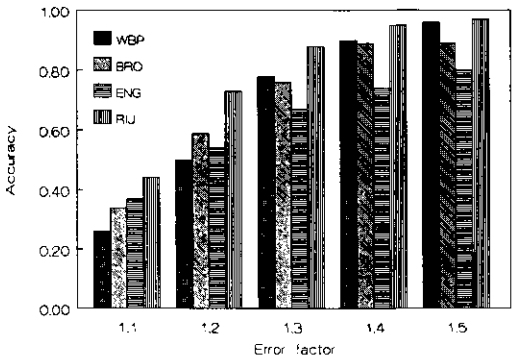

Figure 4.4 Accuracy of the methods to predict the friction factor for different values of error factor

- in terms of the arithmetic and geometric mean of the discrepancy ratios the Brownlie method gives the best result;

- the Brownlie and White et al methods overpredict the low measured C-values (C smaller than 30) and underpredict the high C-values (larger than 40), while in the Engelund method there is a tendency to overpredict the low measured values (C smaller than 35).

Figure 4.5 presents the results of the comparison of the proposed method and the selected data for a error factor f of 1.3.

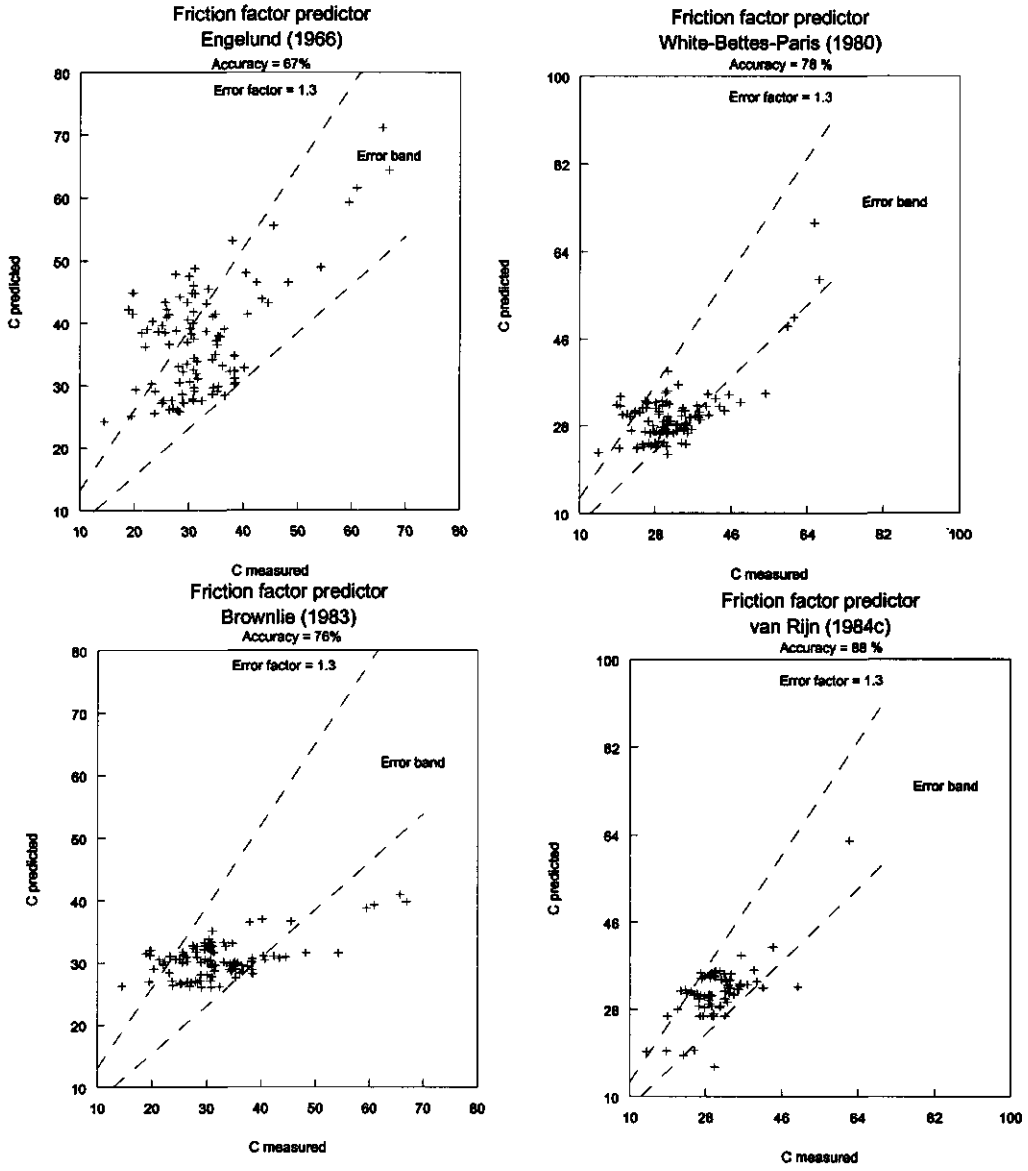

Figure 4.5 Accuracy of the friction factor predictors

Figure 4.6 shows the comparison of the friction factor predictors in terms of the arithmetic and geometric means.

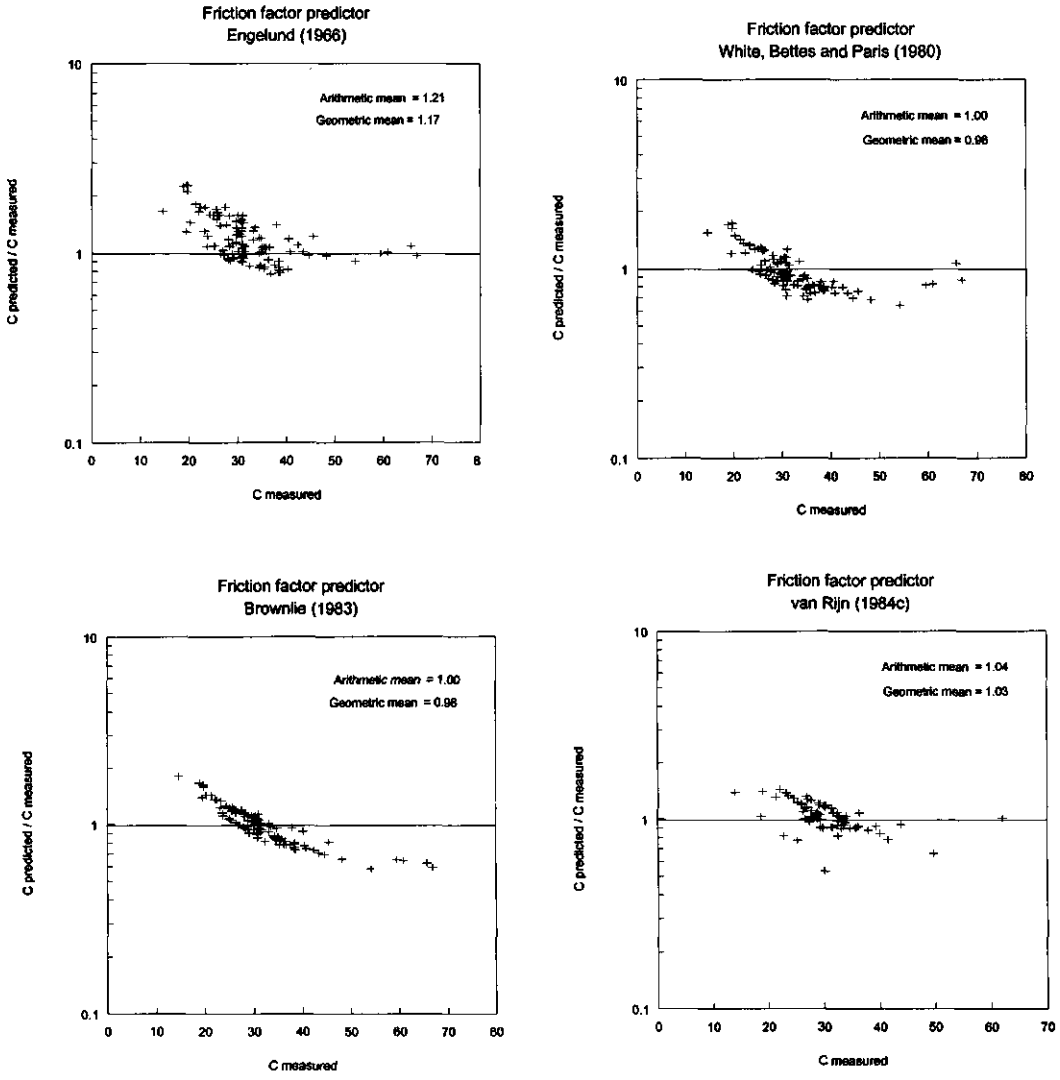

Figure 4.6 Accuracy of the factor predictors in terms of arithmetic and geometric means

4.2.3 Prediction of composite roughness for non-wide irrigation canals

The most common cross section in irrigation canals is the trapezoidal cross section with a relatively small value for the bottom width-water depth ratio. In such a cross section the velocity distribution is strongly affected by the varying water depth on the side slope and the boundary condition imposed to the velocity by the sidewall. An important interaction and transfer of momentum between the side part and the central part of the irrigation canal takes place. The existing methods for estimating composite roughness (see section 3.2.1.4) were developed for river conditions in which the cross section is divided in sub-sections: a main canal and two flood plains. Assumptions behind these existing methods are not valid for flow conditions in non-wide trapezoidal or rectangular canals. Main shortcomings in these methods are: neglecting the effect of the varying water depth on the friction factor, the assumption of equal mean velocity or equal hydraulic radius in all sub-sections.

Water flow conditions in irrigation canals are in a turbulent regime. Under that flow condition can be assumed that the lateral velocity distribution over the cross section in trapezoidal canals is more governed by the varying water depth on the side slope than the imposed boundary condition at the wall. Based on this assumption it is proposed to estimate the composite roughness by assuming that the cross section of the trapezoidal canal is composed by an infinite number of stream tubes (slices). The resistance to flow in each stream tube will be governed by the local water depth and by the local friction factor of the stream tube. No transfer of momentum between the stream tubes is considered. The Chézy coefficient will be used to evaluate the flow resistance in each tube (see figure 4.7). In order to be in line with the nomenclature described in section 3.3.1.4 this proposed method will be named method 5.

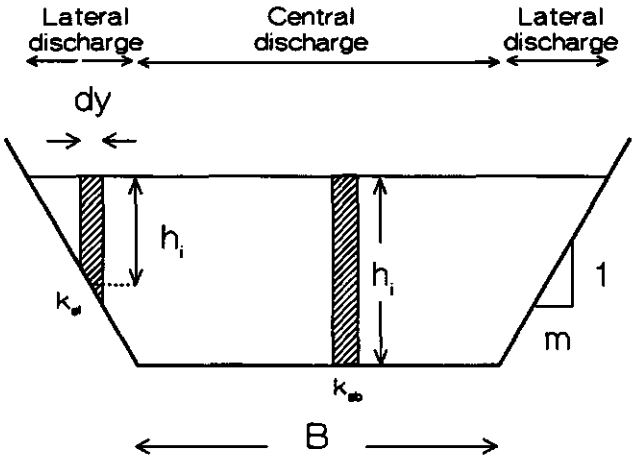

Figure 4.7 Composite roughness in a trapezoidal canal

4.2.3.1 Schematization of a new predictor method of composite roughness in trapezoidal cross section: the total discharge in an open canal with single roughness along the wetted perimeter is computed by the Chézy equation which is described by:

$$V = C\sqrt{R\,S_f} \quad \text{and} \quad Q = A\,V \tag{4.8}$$

with:

$$C = 18\log\left(\frac{12\,R}{k_s}\right) \tag{4.9}$$

where:

Q = total discharge
C = Chézy coefficient
V = mean velocity
A = cross section area
R = hydraulic radius
S_f = energy line slope
k_s = equivalent hydraulic roughness

In an open canal with composite roughness along the wetted perimeter the Chézy coefficient is described by:

$$C_e = 18\log\left(\frac{12\,R}{k_{se}}\right) \tag{4.10}$$

where:

C_e = effective Chézy coefficient for the entire cross section
k_{se} = effective hydraulic roughness for the entire cross section
R = hydraulic radius

A design problem for computing the discharge for a trapezoidal canal with different equivalent hydraulic roughnesses along the wetted perimeter is related to the estimation of an overall effective hydraulic roughness and the effective Chézy coefficient for the entire cross section (eq. 4.10). The effective hydraulic roughness for the whole cross section will be a function of the local equivalent hydraulic roughness in each subsection (k_{sl} and k_{sb} in figure 4.7).

The proposed method for estimating the effective hydraulic roughness and the effective Chézy coefficient in a trapezoidal canal with composite roughness along the wetted perimeter assumes

that the total discharge in the whole cross section can be computed as the summation of the local discharge of each stream tube as follows:

$$Q = Q_{lat} + Q_{cen} = 2 \int_0^{mh} C_i \, h_i \sqrt{h_i \, S_f} \, dy + \int_0^{B} C_i \, h_i \sqrt{h_i \, S_f} \, dy \qquad (4.11)$$

and

$$C_i = 18 \log \left(\frac{12 \, h_i}{k_{s_i}} \right) \qquad (4.12)$$

where:

Q = total discharge
Q_{lat} = discharge in the lateral part
Q_{cen} = discharge in the central part
h_i = local water depth in each stream tube
C_i = local Chézy coefficient in each stream tube
B = bottom width
m = side slope
k_{si} = hydraulic roughness in each stream tube
S_f = energy slope
dy = stream tube width

The described method does not take into account the transfer of momentum between the stream tubes. Therefore the total discharge computed by that method differs from the total discharge of the cross section based on the Chézy equation (eq.4.8). For an open channel composed of single roughness along the wetted perimeter the mean velocity computed by summation of the local discharge in each stream tube is larger than the mean velocity computed by the Chézy equation because lateral transfer of momentum is not taken into account. The difference between both velocities is measured in terms of the ratio of velocities (Rv), which is proposed to correct the mean velocity computed by equation 4.11. It will be expressed as:

$$Rv = \frac{\text{mean velocity computed by the Chézy equation (eq. 4.8)}}{\text{mean velocity computed by the proposed method (eq. 4.11)}} \qquad (4.13)$$

In the proposed method the local velocities in the central part of the canal are overweighted. All the stream tubes in the central part have the same local velocity, because no lateral transfer of momentum between them is considered. That assumption will have two effects in case of computing the composite roughness in trapezoidal canals. First the effect is related to the way of calculating the total discharge over the cross section (equation 4.8 and 4.11) and the second

is related to the way of calculating the effective hydraulic roughness for the entire cross section.

First, the effect related to the way of calculation of the discharge will be analyzed for a single roughness using eqs. 4.8 and 4.11. Equations 4.8 and 4.11 were solved for given values of energy slope (S_f), hydraulic roughness (k_s), bottom width (B), water depth (h) and side slope (m). Figure 4.8 shows the ratio (Rv) between the velocity computed by the Chézy equation given by equation 4.8 and the velocity computed by the proposed method (eq. 4.11). The relationship of the variables given in figure 4.8 was fitted by linear regression to the following equation:

$$Rv = a\ (B/h)^b \qquad (4.14)$$

where:

Rv = ratio between the mean velocity computed by the equation 4.8 and the mean velocity computed by using the summation of the local discharges (eq 4.10)

B/h = bottom width/water depth ratio of the trapezoidal canal

a, b = constants depending on the side slope.

Values of a and b are shown in table 4.4.

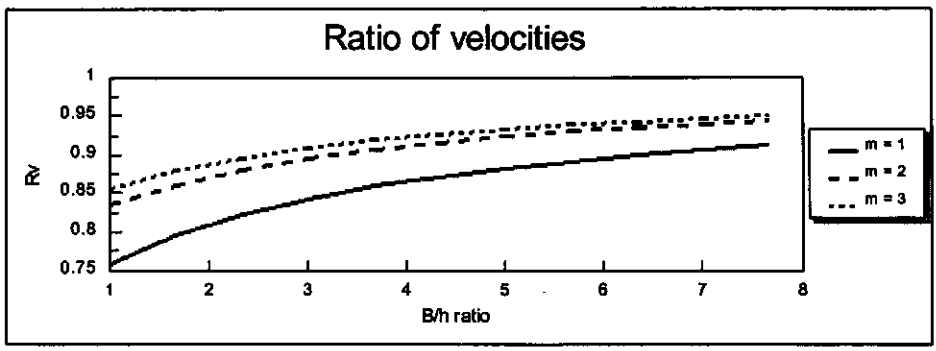

Figure 4.8 Ratio of velocities Rv (single roughness)

Table 4.4 Values of a and b for different values of side slope (single roughness)

Side slope (m)	a	b
1.0	0.76	0.078
1.5	0.81	0.060
2.0	0.84	0.052
2.5	0.85	0.047
3.0	0.86	0.044

Thus, the computation of the total discharge by the proposed method (eq. 4.11) has to be modified by the ratio of velocities in order to obtain the same value as given by equation 4.8. It is assumed that the Rv-value are also valid for composite roughness. Then the total discharge over the cross section can be written as:

$$Q = Rv\ (Q_{lat} + Q_{cen}) = Rv\ (2 \int_0^{mh} C_i\ h_i \sqrt{h_i\ S_f}\ dy \quad + \int_0^{B} C_i\ h_i \sqrt{h_i\ S_f}\ dy) \tag{4.15}$$

The lateral discharge is expressed by:

$$Q_{lat} = 2 \int_0^{mh} C_i \sqrt{h_i\ S_f}\ h_i\ dy \tag{4.16}$$

$$Q_{lat} = 2 \int_0^{mh} 18\ \log\frac{12\ h_i}{k_{sl}} \sqrt{h_i\ S_f}\ h_i\ dy \tag{4.17}$$

$$Q_{lat} = \frac{2\ 18\ \sqrt{S_f}\ m}{2.3} \int_0^{h} \ln\frac{12\ h_i}{k_{sl}}\ h_i^{3/2}\ dh \tag{4.18}$$

Solving this equation gives:

$$Q_{lat} = \frac{2*18*m*\sqrt{S_f}}{2.3} \left(\frac{2}{5}\ h_i^{5/2}\ \ln\ \frac{12\ h_i}{k_{sl}} - \int_0^{h} \frac{2}{5}\ h_i^{3/2}\ dh\right) \tag{4.19}$$

$$Q_{lat} = \frac{4}{5} * \frac{18*m*\sqrt{S_f}}{2.3}\ h^{5/2}\ \left(\ln\ \frac{12\ h}{k_{sl}} - \frac{2}{5}\right) \tag{4.20}$$

The central discharge is calculated by:

$$Q_{cen} = \int_0^{B} C_i \sqrt{h_i\ S_f}\ h_i\ dy \tag{4.21}$$

$$Q_{cen} = \int_0^{B} 18\ \log\frac{12\ h_i}{k_{sb}} \sqrt{h_i\ S_f}\ h_i\ dy \tag{4.22}$$

$$Q_{cen} = \frac{18\sqrt{S_f}}{2.3} \ln\frac{12\,h}{k_{sb}} h^{3/2} B \qquad (4.23)$$

From equation 4.15 the total discharge will be :

$$Q = \frac{18\,Rv\sqrt{S_f}\,h^{3/2}}{2.3}\left[\frac{4}{5} m h \left(\ln\frac{12\,h}{k_{sl}} - \frac{2}{5}\right) + B \ln\frac{12\,h}{k_{sb}}\right] \qquad (4.24)$$

Equation 4.24 can be used to estimate the discharge of a canal with composite roughness along the wetted perimeter. Here it is proposed to estimate the discharge by using the well-known Chézy equation (equations 4.8 and 4.10) therefore, an effective hydraulic roughness k_{se} is required.

The total discharge for the whole cross section can be calculated in the same way as described by equations 4.15 to 4.24, but by using an effective roughness k_{se} for the total cross section in stead of the lateral roughness k_{sl} and the central roughness k_{sb}. The total discharge expressed in terms of the effective roughness k_{se} can be described by:

$$Q = \frac{18\,Rv\sqrt{S_f}\,h^{3/2}}{2.3}\left[\frac{4}{5} m h \left(\ln\frac{12\,h}{k_{se}} - \frac{2}{5}\right) + B \ln\frac{12\,h}{k_{se}}\right] \qquad (4.25)$$

equating equation 4.24 and 4.25:

$$\frac{4}{5} m h \left(\ln\frac{12\,h}{k_{se}} - \frac{2}{5}\right) + B \ln\frac{12\,h}{k_{se}} = \frac{4}{5} m h \left(\ln\frac{12\,h}{k_{sl}} - \frac{2}{5}\right) + B \ln\frac{12\,h}{k_{sb}} \qquad (4.26)$$

rearranging the terms gives:

$$\ln k_{se} = \frac{0.8\,m \ln k_{sl} + (B/h) \ln k_{sb}}{0.8\,m + (B/h)} \qquad (4.27)$$

Equation 4.27 shows the influence of the side slopes and the central part of the trapezoidal canal on the effective roughness of the whole cross section. For small values of the B/h ratio the effect of the lateral part on the flow characteristics in the cross section is as important as the central part. The influence of the lateral part for large values of the B/h ratio is considered negligible as assumed for wide canals and the effective roughness of the cross section is governed mainly by the bottom roughness.

As an example the discharge of a trapezoidal canal with composite roughness will be calculated. The geometrical characteristics of the canal are the following:
- bottom width (B) = 8 m

- water depth (h) = 2 m
- side slope (m) = 2
- area (A) = 24 m^2
- hydraulic radius (R) = 1.42 m
- bottom slope = 0.0001
- lateral roughness (k_{sl}) = 0.02 m
- central roughness (k_{sb}) = 0.10 m
- ratio of velocities (Rv) = 0.90 (from equation 4.14)

The discharge is calculated by using equation 4.24. Replacing all data in that equation gives:
$Q = 13.0\ m^3/s$

The effective hydraulic roughness k_{se} computed by equation 4.27 gives:
$k_{se} = 0.06$ m

and the effective Chézy coefficient (eq. 4.10)results in:
$C_e = 44\ m^{1/2}/s$

replacing this value in the Chézy equation (eq. 4.8), the discharge gives:
$Q = 12.6\ m^3/s$

Now the discharge will be calculated for an identical canal, but with a reversed roughness condition. This means that the lateral equivalent roughness $k_{sl} = 0.10$ m and the central equivalent roughness $k_{sb} = 0.02$ m. Following the same procedure as in the previous example, the discharge by using equation 4.24 is:
$Q = 14.6\ m^3/s$

The effective roughness for the entire cross section results in (eq. 4.27):
$k_{se} = 0.03$ m

The equivalent Chézy coefficient computed by equation 4.10 results in:
$C_e = 50\ m^{1/2}/s$

and the discharge is (eq.4.8):
$Q = 14.3\ m^3/s$

Discharges computed by both equations are similar. Small differences are due to the estimation of the ratio of velocities Rv by equation 4.14. The proposed method does not take into account the transfer of momentum. The local velocity in each stream tube is assumed to depend only on the local water depth and local roughness condition in the bottom of each tube. The ratio of velocities Rv is meant to adjust the difference between both methods for the computation of the discharge.

4.2.3.2 Correction for the distribution of velocities: although the discharges of both methods (eqs. 4.8 and 4.24) are the same, it is uncertain whether the velocities distribution over the cross section represent realistic values. Local velocities in the central part of the canal computed by the proposed method are strongly affected by the water depth, because no transfer of momentum has been considered. It means that the velocities in the central part of the trapezoidal canal will overestimate the effect of the roughness of that part on the effective roughness for the total cross section. In case of a trapezoidal canal with a smooth bottom and relative rough side slopes the effective Chézy coefficient will be excessively smooth (high value of Chézy coefficient). In the opposite case of a trapezoidal canal composed of a rough bottom and relative smooth side slopes, the effective Chézy coefficient will be excessively rough (low value of the Chézy coefficient). For that reason the effective Chézy coefficient (equation 4.10) has to be modified with a factor which takes into account that effect. The factor should take into account the distribution of velocities across the trapezoidal cross section with composite roughness. It is proposed to modify the equivalent Chézy coefficient and thus the discharge with a factor depending on the ratio of velocities Rv previously explained. Experimental data will be used later to verify this approach. The modified effective Chézy coefficient is proposed to be:

$$C_e' = f_c \, C_e \tag{4.28}$$

with:

$$f_c = Rv \qquad \text{for} \quad k_{sl} > k_{sb} \tag{4.29}$$

and,

$$f_c = \frac{1}{Rv} \qquad \text{for} \quad k_{sl} < k_{sb} \tag{4.30}$$

where:

f_c = correction factor for the effective Chézy coefficient
C_e' = modified effective Chézy coefficient

For this modified effective Chézy coefficient the value of the effective hydraulic roughness k_{se}' can be calculated by using the equation:

$$C_e' = 18 \log \left(\frac{12 \, R}{k_{se}'} \right) \tag{4.31}$$

In terms of the Manning coefficient (n) the effective roughness k_{se}' can be expressed as (Henderson, 1966):

$$n_e = 0.034\ (3.3 * k_{sc}')^{1/6} \qquad (4.32)$$

where:

k_{sc} = effective hydraulic roughness (m)
n_e = effective Manning coefficient.

Figure 4.9 and 4.10 show the velocity distribution in the cross section of an laboratory trapezoidal canal with different composite roughness along the wetted perimeter. Each figure shows the velocity distribution which is computed for each streamtube as:

$$v_i = C_i \sqrt{h_i\ S_f} \qquad (4.33)$$

where:

v_i = local velocity in the streamtube
C_i = Chézy coefficient
h_i = local water depth
S_f = energy gradient

The velocity distributions were calculated for different values of the Chézy coefficient, namely a theoretical velocity distribution computed by a measured Chézy coefficient, a velocity distribution computed by a effective Chézy coefficient without correction (eq.4.10) for the composite roughness distribution and a velocity distribution computed with a modified Chézy coefficient (eq. 4.28). Details of the experimental procedure for the measurement of the Chézy coefficients in a canal with composite roughness is given in section 4.2.3.3.

The method was applied for two cases of composite roughness: rough surface on the bottom -relatively smooth surface on side slope and relatively smooth surface on the bottom and rough on the side slope. Details of the geometrical and hydraulic characteristics of those experiments are given in annex C (tables C.3 and C.4). Figure 4.9 shows the velocity distribution in the canal with rough side slopes and a smooth bottom. The estimated Chézy coefficient (equation 4.10) is rather large (very smooth) and its value deviates much from the measured Chézy coefficient (theoretical). Once the Chézy coefficient is modified by using equation 4.28 both velocity distributions are similar. In figure 4.10 the opposite case is presented, namely the velocity distribution in a trapezoidal canal with smooth side slopes and a rough bottom. The estimated Chézy coefficient by using equation 4.10 results in a relative small value (very rough). Once the value is corrected by the equation 4.28, the resulting velocity distribution does not deviate much from the theoretical distribution. A better description of the velocity distribution over the cross section composed by composite roughness will provide a more appropriate factor f_v for correcting the Chézy coefficient in equation 4.28.

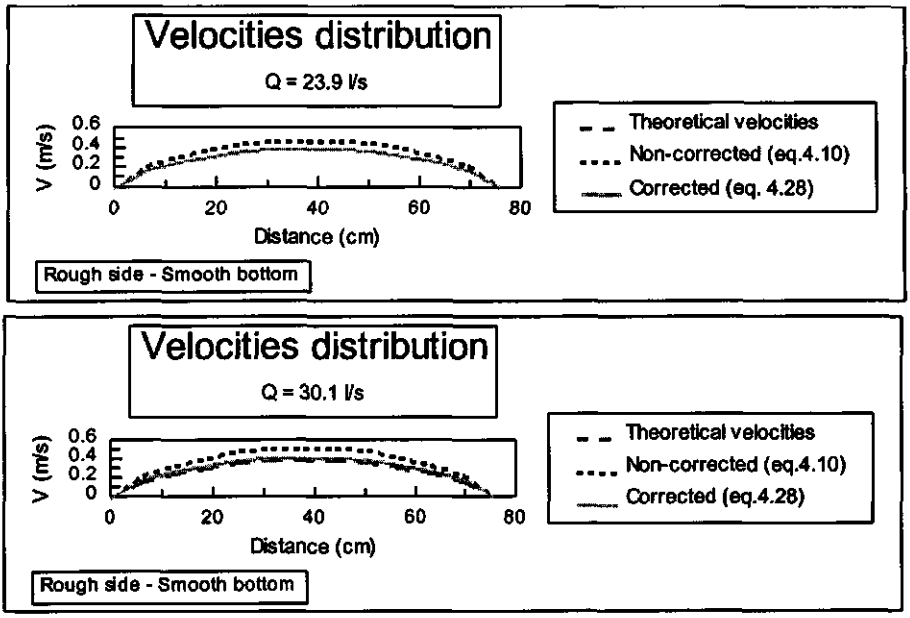

Figure 4.9 Velocity distribution in a trapezoidal canal with composite roughness: rough side slopes (k_{ss}= 19.4 mm) and smooth bottom (k_{sb} = 0.21 mm)

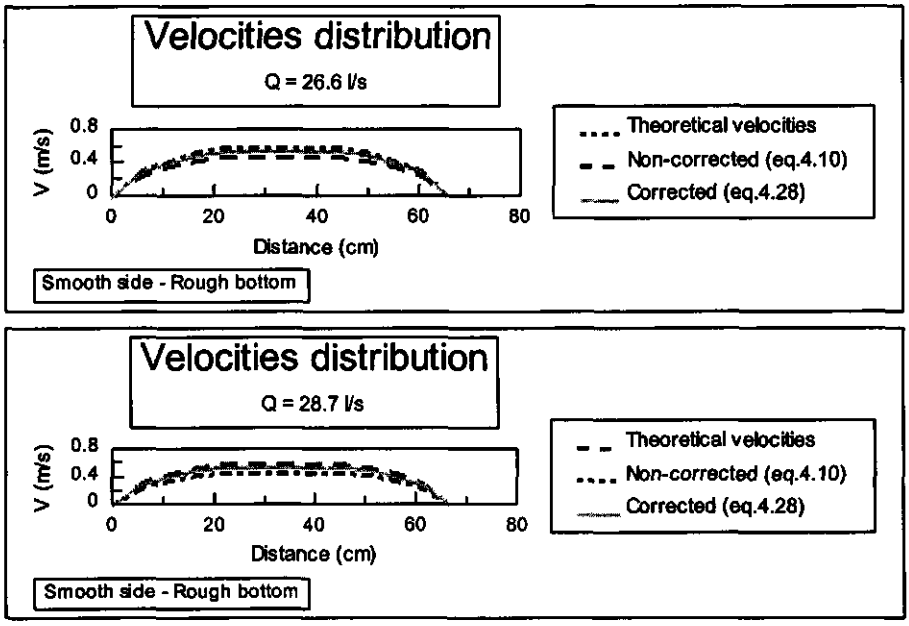

Figure 4.10 Velocity distribution in a trapezoidal canal with composite roughness: smooth side slopes (k_{ss} = 0.21 mm) and rough bottom (k_{sb} = 19.4 mm)

In order to predict the composite roughness in irrigation canals, the methods mentioned in section 3.2.1.4 (methods 1, 2, 3a, 3b and 4) and the new method (method 5) will be compared with a selected set of laboratory data, which has been collected in the hydraulic laboratory at Wageningen Agricultural University (WAU), the Netherlands.

4.2.3.3 Experimental set-up: the aim of the experiments is to investigate the friction factor in a trapezoidal canal having different roughness on side and bottom. The experiments were carried out in a tilting flume, which was equipped with devices for measuring discharges, water levels and velocities.

Details of the flume, measurement devices and experimental procedures are the following:
Flume: a trapezoidal flume with a length of 12 m, bottom width 0.25 m and side slope m = 1.5 has been built. The flume, which was constructed from wood, has an adjustable, longitudinal slope. The water is supplied by a pump and enters the flume after passing a calibrated flow meter. The discharge returns from the flume to a reservoir via a pipe loop.

Measurement devices: the discharge in the flume has been measured by a magnetic flow meter which gives the actual value of the pipe flow before it enters the flume. The flow meter has an accuracy of 1%.The velocities are measured by a propeller meter. The propeller meter has a diameter of 30 mm. The water depth in the flume has been measured by static tubes and point gauges. The readings are accurate to the nearest 0.1 mm. The instruments can be moved together with a movable platform, to which they were connected. The static tubes were connected with stilling wells.

Experimental procedure: the flow conditions have been measured in one selected cross section of the flume (section 6 in figure 4.11). The bottom width, water depth, discharge, mean velocity and bottom slope have been measured for the selected cross section. The energy slope at the selected cross section has been taken as the average energy slope between the selected cross section and two other cross sections (section 2 and 10 in figure 4.11). These sections are four meter from section 6 in downstream and upstream direction respectively. The water depth has been measured at section 2, 6 and 10 for different discharges Q and for all cases (single and composite roughness). From the measured water depth and discharge the mean velocity at each cross section has been calculated. Next the specific energy at cross section 2, 6 and 10 has been calculated by the equation:

$$E = h + \frac{V^2}{2*g} \qquad (4.34)$$

where:

h = water depth
V = mean velocity (V = Q/A)
g = gravity acceleration

E = specific energy

The downstream energy slope (S_{fdo}) between section 2 and 6 and the upstream energy slope (S_{fup}) between section 6 and 10 are computed from the measured data by using the equation:

$$S_f = S_o - \frac{dE}{dx} \tag{4.35}$$

where:

V = mean velocity
R = hydraulic radius
S_f = energy slope
S_o = bottom slope

The average slope of S_{fdo} and S_{fup} has been taken as the energy slope at the test section (section 6). The above mentioned procedure has been repeated for all cases (smooth, rough and combinations). The results of the computation are presented in annex C.

Using the available data, the Chézy coefficient C can be computed be using:

$$C = \frac{V}{\sqrt{R * S_f}} \tag{4.36}$$

where:

C = Chézy coefficient
V = mean velocity
R = hydraulic radius
S_f = energy slope

The hydraulic roughness k_s for all cases (single and composite roughness) was computed from the measured values by using:

$$C = 18 \log \left| \frac{12\ R}{k_s + \frac{3.3\nu}{u_*}} \right| \qquad \text{Transition regime} \tag{4.37}$$

or

$$C = 18 \log\left(\frac{12\,R}{k_s}\right) \qquad \text{Rough regime} \qquad (4.38)$$

where:

u_* = shear velocity
ν = kinematic viscosity
R = hydraulic radius
C = Chézy coefficient
k_s = equivalent hydraulic roughness

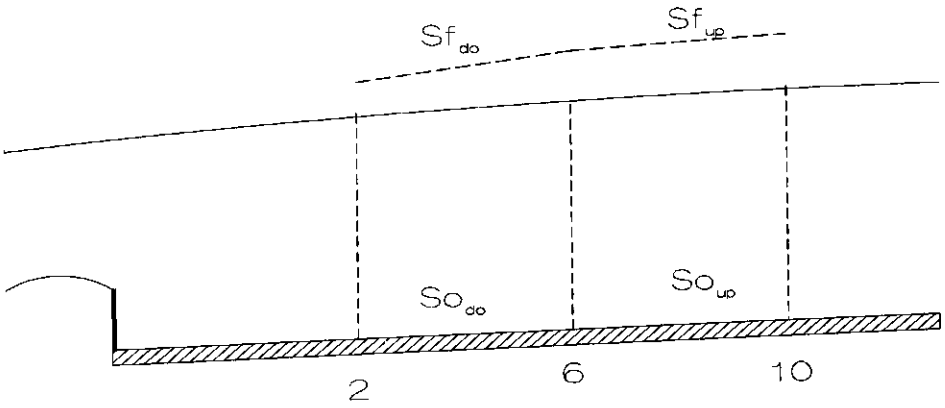

Figure 4.11 Details of the energy slope computation

Analyses of results: Four cases of roughness distribution along the perimeter of the trapezoidal canal have been investigated, namely:

- constant roughness along the whole perimeter:
  - * Case 1: relatively smooth;
  - * Case 2: roughened with uniform gravel;
- Case 3: relatively smooth side slopes and the bottom roughened with uniform gravel;
- Case 4: the side slopes roughened with uniform gravel and a relatively smooth bottom.

The particle size distribution of the gravel used for the artificial roughness is shown in figure 4.12.

Figure 4.13 shows details of the trapezoidal flume and the measurement devices. Also details of the roughness distribution with smooth side slopes and a rough bottom (case 3) are also shown in that figure.

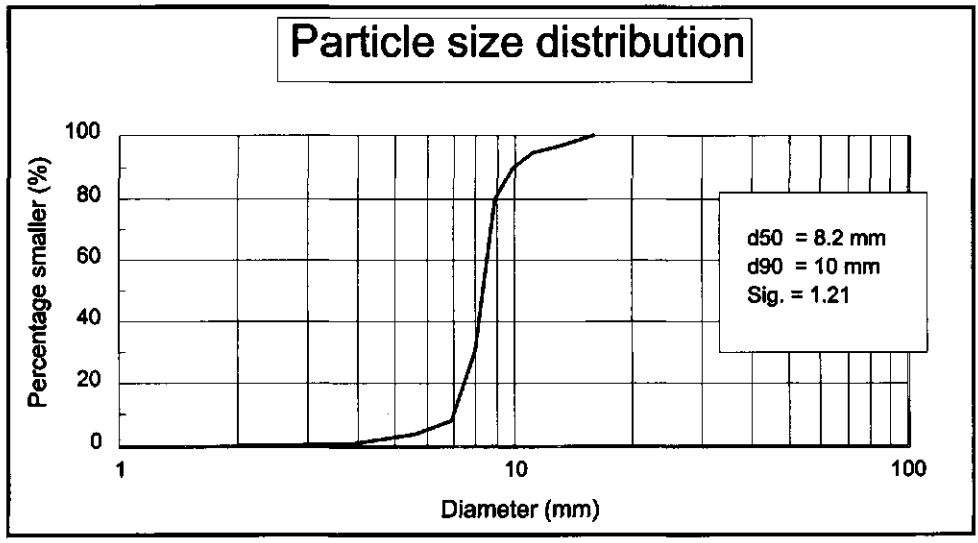

Figure 4.12 Particle size distribution of the gravel

Cases 1 and 2 (single roughness) provide the equivalent hydraulic roughness k_s for wood and gravel respectively. The experimental procedure previously described has been used to determine the equivalent roughness in the two cases. The mean value and the standard deviation for the set of calculated equivalent roughness k_s have been determined for each case.

A total of 40 records were collected from the laboratory experiments. Table 4.5 shows a summary of the characteristics of the collected data. In Table C.1 from appendix C shows details of the collected data for case 1 (smooth side slope and smooth bottom).

Table 4.5 Characteristic of the collected data for single roughness at WAU

Test	#	Width	Side	B/h	V	Fr	$k_s \pm \sigma$
Case 1	14	25.0	1.530	1.5-2.8	0.3-0.6	0.1-0.5	0.21 ± 0.07
Case 2	26	24.5	1.585	1.3-2.8	0.1-0.4	0.1-0.2	19.4 ± 2.14

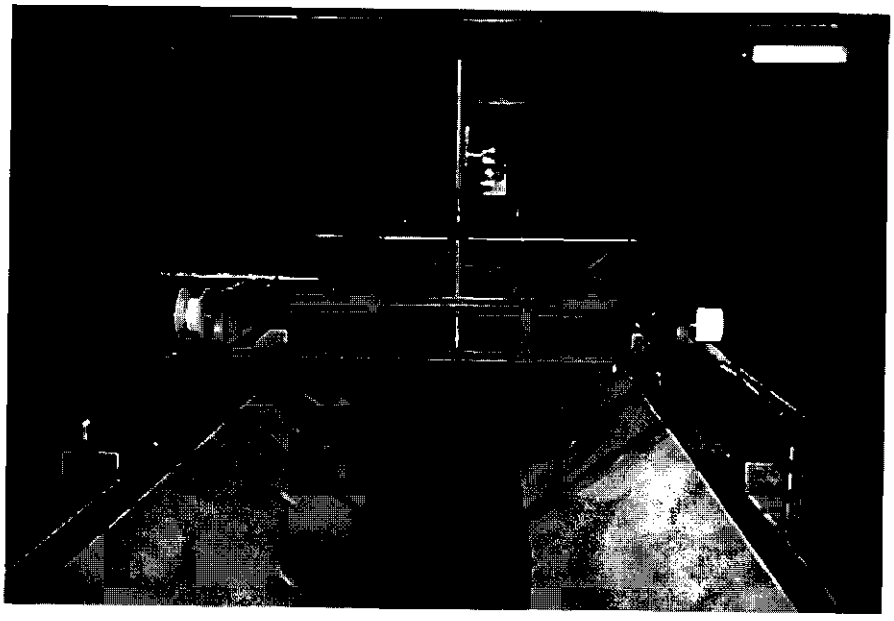

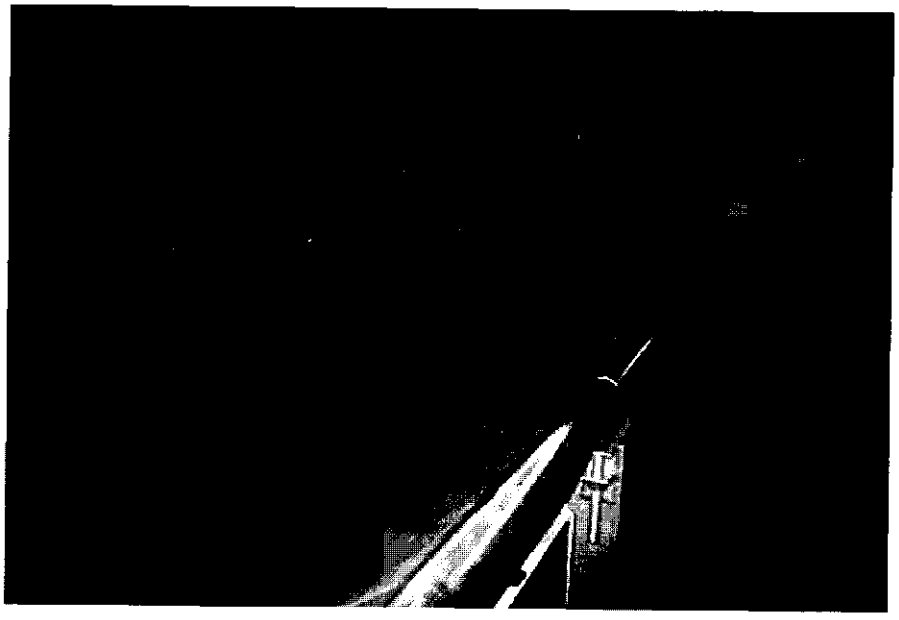

Figure 4.13 Details of the case 3 of composite roughness (smooth side - rough bottom) in the trapezoidal flume at WAU

In case 1, the flow conditions were in transition regime (see equation 4.37). Two collected data values were neglected because they were in the smooth regime which has no effect of the roughness on the resistance to flow. The mean value for the equivalent roughness k_s resulted in 0.21 mm with a standard deviation equal to 0.07 mm. The mean value k_s is relatively smaller than the recommended k_s values for wood (0.3 mm$\leq k_s \leq$ 0.6 mm) mentioned by Henderson (1966) and Chow (1983). Although a relative large value of the standard deviation was found, the effect on the computation of the Chézy coefficient (eq.4.9) is small. The estimated error for computing the Chézy coefficient in the range of variation for the equivalent roughness k_s is in the order of $\pm$ 3%.

Table C.2 from appendix C shows details of the collected data for case 2 (rough side slopes and rough bottom). In case 2, the flow conditions were in the rough regime (see eq. 4.38). The mean value for the equivalent roughness of the gravel k_s and the standard deviation resulted in 19.5 mm and 2.15 mm respectively. Relating the mean value for the equivalent roughness to the size of the gravel, resulted that the $k_s = 2\ d_{90}$ which is rather similar to the suggested values for the surface roughness k_s = 2-3 d_{90} (Krüger, 1988)

The determined composite roughness for wood and gravel is used in case 3 and 4. Details of the data for those cases are described in table C.3 and C.4 (Appendix C). A total of 51 records with composite roughness (case 3 and 4) were collected from the laboratory tests. Table 4.6 and 4.7 show a summary of the characteristics of the collected data.

Flow conditions in case 3 and 4 were in the transition regime (eq. 4.37) and rough regime (eq. 4.38). Froude numbers were smaller than 0.4 and the mean velocity smaller than 0.5 m/s. The values of the effective roughness for the whole set of data were between the boundary values of the equivalent hydraulic roughness (0.02 mm$\leq k_{se} \leq$ 19.2 mm)

Table 4.6 Characteristic of the collected data with composite roughness at WAU

Test	Bottom width (cm)	Side slope	k_{sl} (mm)	k_{sb} (mm)	k_{sb}/k_{sl}	# records
Case 3	21	1.56	0.2 (*)	19.3 (*)	96	33
Case 4	27	1.53	19.3 (*)	0.2 (*)	0.01	18

(*) determined during the laboratory test of case 1 and case 2 as previously explained

Table 4.7 Hydraulic characteristic of the collected data at WAU

	B/h	k_{sb}/k_{sl}	V m/s	Fr	Chézy coeff.	Manning coeff.
Minimum	1.07	0.03	0.14	0.02	36.5	0.0116
Maximum	4.10	96	0.48	0.36	55.9	0.0191

4.2.3.4 Comparison of composite roughness predictors in trapezoidal canal: in order to predict the composite roughness in trapezoidal canals, the methods mentioned in paragraph 3.2.1.4 (methods 1, 2, 3a, 3b and 4) and the new method proposed (method 5) will be compared to the set of laboratory data collected from experiments carried out at WAU.

The comparison of the methods for predicting the composite friction factor with the laboratory data is based on a relative basis. Due to the fact that the existing methods for estimating the composite roughness are expressed in terms of the Manning coefficient n, the same parameter will be used to evaluate the roughness coefficient of the cross section. The predicted Manning coefficient for each method is calculated by using the equations described in section 3.2.1.4 (equation 3.31, 3.33, 3.35, 3.37 and 3.42) and the proposed equation 4.28.

Accuracies of the methods are based on the following criteria:

- the number of well-predicted values within a error band, which is given by:

$$\frac{\text{Measured value}}{K} \leq \text{Predicted value} \leq \text{Measured value} * K \qquad (4.39)$$

$$\text{Accuracy} = \frac{\text{number of well predicted values}}{\text{number of total values}} * 100 \qquad (4.40)$$

where:

K = error factor

- the ratio between the average value of the predicted Manning coefficients and the average value of the measured Manning coefficients. It can be expressed as:

$$Rn = \frac{\frac{\sum (n_p)_i}{N}}{\frac{\sum (n_m)_i}{N}} \qquad (4.41)$$

where:

Rn = ratio between n-measured and n-predicted

n_m = measured Manning coefficient

n_p = predicted Manning coefficient

N = number of data in each case

- the standard error of the predicted values, which is given by:

$$s_n = \sqrt{\frac{\sum (n_p - n_m)^2}{N}} \qquad (4.42)$$

where:

s_n = standard error of the predicted values
n_p = predicted Manning coefficient
n_m = measured Manning coefficient
N = total number of values

The comparison of the various selected methods with the measured values is shown in figure 4.14. The figure shows the number of well-predicted values for several error factors. Details of the comparison of each method for an error factor of 1.15 are shown in figure 4.15.

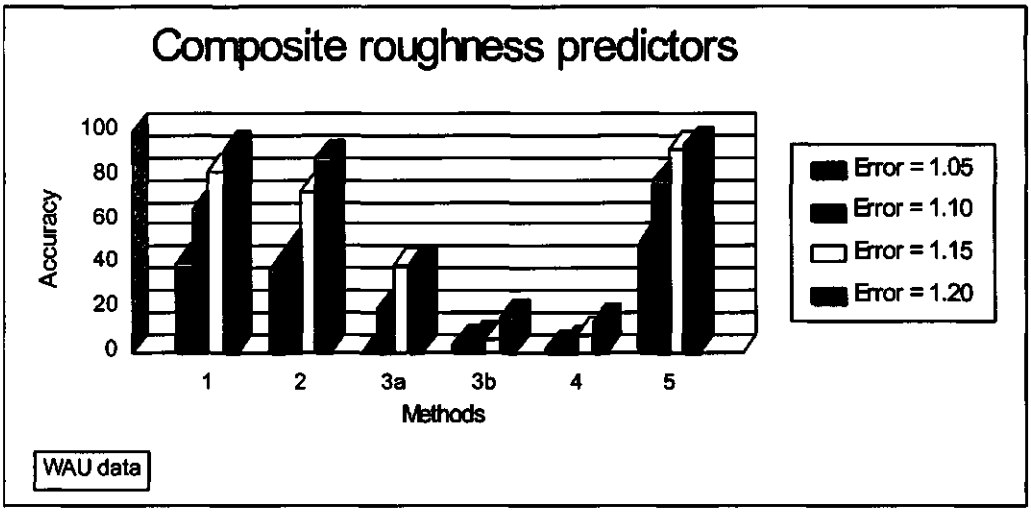

Figure 4.14 Comparison of well-predicted values for several values of the error factor by using the WAU data

Results of the ratio of the average values of the Manning's coefficient and the standard error of the predicted values are shown in table 4.8.

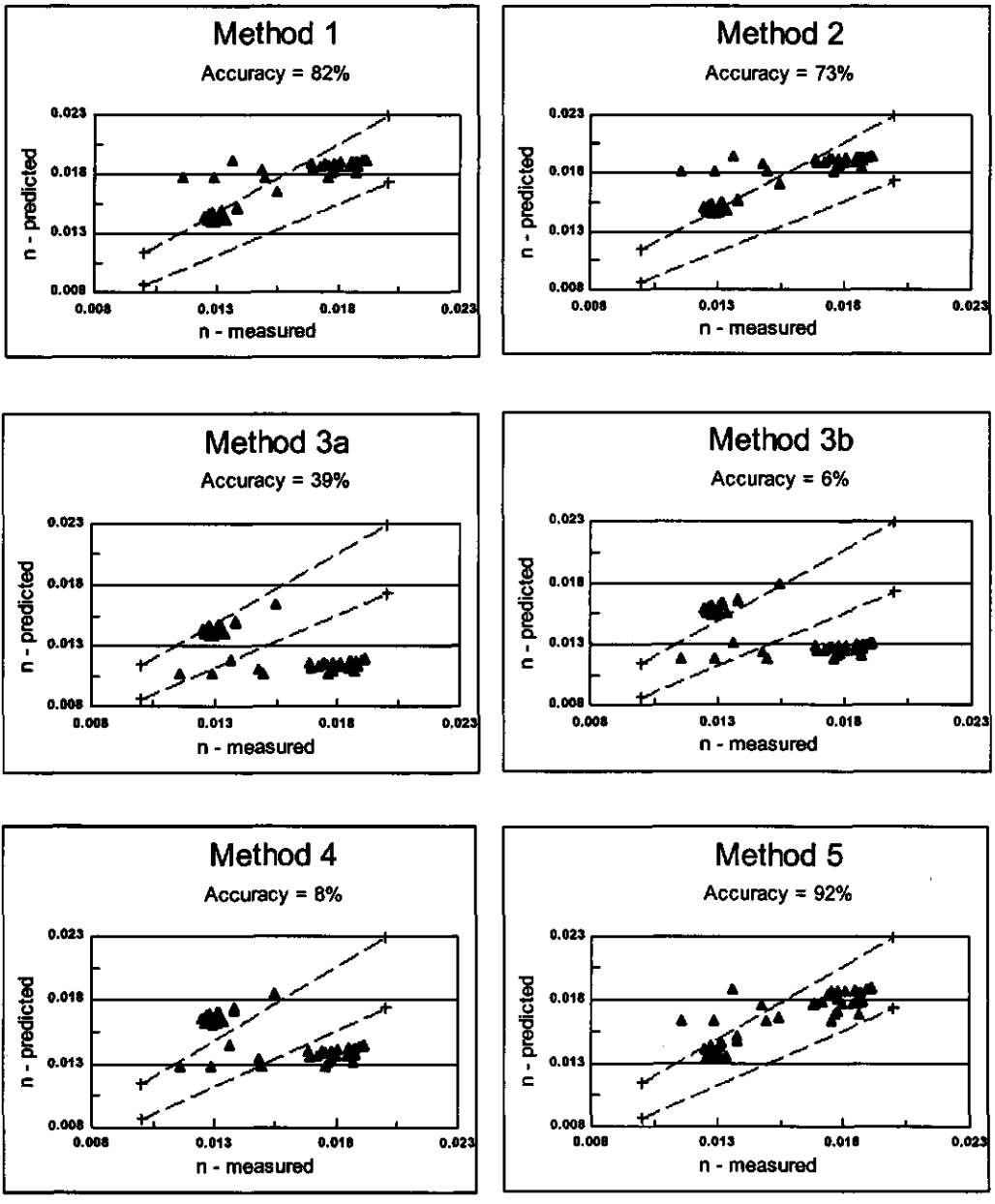

Figure 4.15 Comparison of the various methods for computing the composite roughness with the WAU data at an error factor of 1.15

Table 4.8 Ratio of the average values of Manning's coefficient and the standard error of the predicted values for the WAU data

			Method					
	Case (s)	Measured	1	2	3a	3b	4	5
Mean Manning coefficient (n)	3	0.0175	1.07	1.08	0.65	0.72	0.79	1.02
	4	0.0131	1.11	1.15	1.10	1.22	1.27	1.08
Std. Error (* 10^{-3})	3	*******	2.0	2.2	6.3	5.2	4.1	1.6
	4	*******	0.5	0.9	0.4	1.7	2.3	0.6
	3 and 4	*******	1.6	1.8	5.0	4.3	3.6	1.4

The referred methods (1, 2, 3a, 3b, 4 and 5) were also compared to a selected set of data from Krüger (1988). The criteria for selecting the data from the Krüger data were the following:

- trapezoidal cross section;
- Froude number less than 0.5
- bottom width-water depth ratio smaller than 8

A total of 30 records were selected from the compilation of Krüger (1988). Table 4.9 and 4.10 show a summary of the selected data.

Table 4.9 Characteristic of the selected data

Test	Bottom	Side slope	k_{sl} (mm)	k_{sb} (mm)	k_{sb}/k_{sl}	# records
1	24.5	1	0.054 (*)	1.047 (*)	19.8	4
2	23.3	1	16.4 (**)	0.054 (*)	0.003	10
3	24.0	1	16.4 (**)	1.047 (*)	0.07	8
4	24.6	2	0.054 (*)	1.047 (*)	19.8	8

(*) determined during the laboratory test by using a similar procedure to the one described for the WAU data

(**) No explicit value is given by Krüger (1988) It was calculated by using the same relation found for the WAU data $k_s = 2\ d_{90} = 16.4$ mm.

Table 4.10 Hydraulic characteristic of the selected data

	B/h	k_{sb}/k_{sl}	V	Fr	Chézy coeff.	Manning coeff
Minimum	1.7	0.003	0.20	0.34	39.6	0.0108
Maximum	7.9	19.8	0.48	0.48	58.7	0.0151

The comparison between the methods and the selected data from Krüger (1988) has been made in a similar way as the one used for the comparison with the WAU data. Figure 4.16 shows the accuracy of the different methods when compared with the measured values for several values of error factor (1.05, 1.10, 1.15 and 1.20). Details of the comparison for all the methods at an error factor of 1.15 are shown in figure 4.17.

Results of the ratio of the average value of Manning's coefficients and the standard error of the predicted values for the Krüger data are shown in table 4.11 .

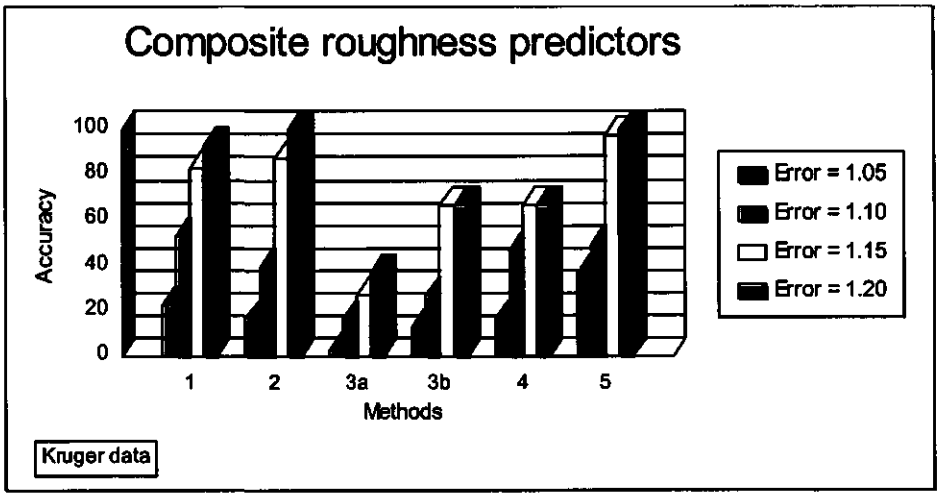

Figure 4.16 Comparison of well-predicted values for several values of the error factor by using the Krüger data

Table 4.11 Ratio of the average value of Manning's coefficient and the standard error of the predicted values for the Krüger data

			Method					
	Case	Measured	1	2	3a	3b	4	5
Mean Manning coefficient (n)	1	0.0116	0.94	0.95	0.93	1.04	1.04	0.90
	2	0.0149	1.01	1.05	0.53	0.59	0.64	0.98
	3	0.0154	1.11	1.12	0.80	0.90	0.92	1.12
	4	0.0127	0.86	0.87	0.86	0.92	0.93	0.92
Std. Error (* 10^{-3})	1	*******	0.8	0.7	0.8	0.6	0.6	1.2
	2	*******	0.9	1.1	7.0	6.1	5.4	0.6
	3	*******	1.7	1.9	3.1	1.6	1.3	1.9
	4	*******	1.8	1.7	1.8	1.0	0.9	1.1
	All	*******	1.4	1.4	4.5	3.6	3.2	1.3

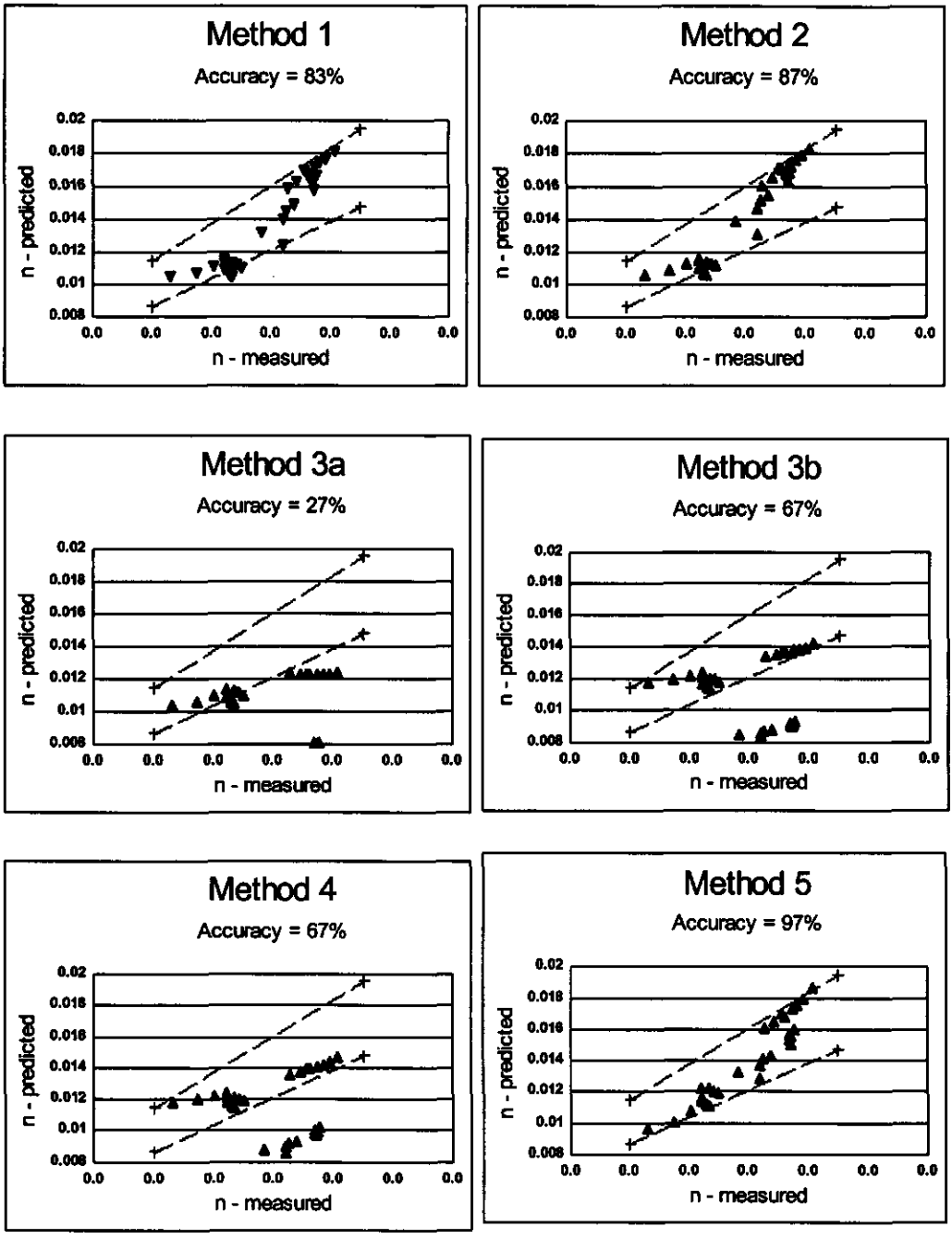

Figure 4.17 Comparison of the methods for computing the composite roughness with the Krüger data at an error factor of 1.15

From the comparison of the five methods to predict the composite roughness in trapezoidal cross sections with laboratory data, some conclusions can be drawn:

- based on the overall performance of the different methods with the two sets of experimental data the methods can be ranked in descending order as: 5, 1, 2, 4, 3a and 3b;
- method 1, 2, 3a, 3b and 4 were developed for river conditions, in which the channel is composed by a main canal and two parallel flood plains. The water depths in both main canal and flood plains are assumed to be constant;
- method 5 takes into account the effect of the water depth on the roughness coefficient; it does not take into account the transfer of momentum;
- method 5 behaves better than the other methods for error factors smaller than 1.2. This method predicts the two sets of collected data with an accuracy larger than 90% for an error factor of 1.15. The narrowest range of the ratio for estimating the average value of the Manning coefficient is between $0.90 \leq Rn \leq 1.12$, which corresponds with method 5. The minimum value for the standard error of the predicted values was also observed for method 5;
- methods 1 and 2 behave similarly. The assumptions for both methods give similar results (see equations 3.31 and 3.33); they weigh the side part of the canal in the same way as the central part without taking into account the differences in velocities and water depths.
- methods 3b and 4 are rather similar. They only differ in the description of the mean velocity in the sub-sections.

4.2.3.5 Prediction of composite roughness in rectangular canal: for rectangular cross sections the existing methods to estimate the composite roughness can not be directly used. There are no clearly defined areas to be associated with each type of roughness along the wetted perimeter. Therefore it is proposed to estimate the composite roughness in a rectangular cross section according to the same principles as used by the side wall correction method. The side wall correction is a calculation procedure initially proposed by Einstein (1942) to determine the shear stress at the bottom as well as the values of shear velocity, friction factor, etc. This method does not introduce any correction for the effect of the side walls on the velocity distribution and sediment transport characteristics (ASCE, 1977). Section 4.3.3.3 will describe that the velocity distribution for a rectangular cross section is not strongly affected by the side walls. Water flow in those canal are highly turbulent. Viscous forces between streamtubes are negligible. There is a nearly uniform velocity distribution in the width direction of the rectangular canal. Therefore the side wall correction procedure can be used for estimating the composite roughness in rectangular cross sections.

A non-wide rectangular canal with bottom width B and water depth h can be replaced by a "wide canal" with a bottom width B_* ($B_* = B + 2\,h$) and a water depth R ($R = A/P$) as shown in figure 4.18. The total discharge for the "wide rectangular canal" can be expressed by:

$$Q = 2\ C_L\ h\ R\ \sqrt{R\ S_f} + C_b\ B\ \sqrt{R\ S_f} \tag{4.43}$$

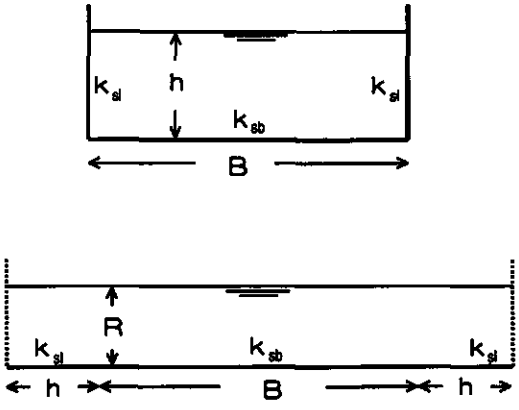

Figure 4.18 Non-wide rectangular canal and its schematization as wide canal.

Replacing the total discharge in terms of equivalent composite roughness and Chézy coefficient as a function of the surface roughness and water depth gives:

$$Q = 2\left(18\ \log\left(\frac{12\ R}{k_{sl}}\right)\right)\ h\ R\ \sqrt{R\ S_f} + \left(18\ \log\left(\frac{12\ R}{k_{sb}}\right)\right)\ B\ R\ \sqrt{R\ S_f} \tag{4.44}$$

Expressing the total discharge in terms of an equivalent composite surface roughness by:

$$Q = \left(18\ \log\left(\frac{12\ R}{k_{sc}}\right)\right)\ (B + 2\ h)\ R\ \sqrt{R\ S_f} \tag{4.45}$$

and equating both equations and rearranging the terms gives:

$$\log k_{sc} = \frac{2\ \log k_{sl} + \frac{B}{h}\ \log k_{sb}}{2 + \frac{B}{h}} \tag{4.46}$$

Expressed in terms of the Manning's coefficient results in:

$$n_e = \frac{2 + \frac{B}{h}}{\frac{2}{n_l} + \frac{B}{h}\frac{1}{n_b}} \qquad (4.47)$$

where:

Q = total flow discharge (m^3/s)
B = bottom width (m)
h = water depth (m)
R = hydraulic radius (m)
S_f = energy slope
C_L = Chézy coefficient for the lateral part
C_b = Chézy coefficient for the central part
k_{se} = equivalent composite roughness for the entire wetted perimeter
k_{sl} = equivalent roughness for the lateral part
k_{sb} = equivalent roughness for the bottom part
n_e = equivalent Manning's coefficient for entire cross section
n_l = Manning's coefficient for lateral part
n_b = Manning's coefficient for the central part

The method described to estimate the composite roughness in canals with rectangular cross section has been tested with a selected set of laboratory data from Krüger (1988). The criteria for selecting the data were similar to those used in the case of the trapezoidal cross sections. A total of 37 records was used. Table 4.12 shows a summary of the characteristics of the selected data.

Table 4.12 Characteristic of the selected data for rectangular cross section

	B/h	k_{sb}/k_{sl}	V	Fr	Chézy coeff.	Manning coeff
Minimum	1.3	0.05	0.17	0.28	31.8	0.0105
Maximum	8.0	151.0	0.54	0.46	61.3	0.0174

The comparison of the proposed method to estimate the composite roughness in rectangular cross sections with the selected data is similar to the one given in 4.1.3.2. The Manning's coefficient is used to evaluate the roughness coefficient. Figures 4.19 shows the results of that comparison. The proposed method predicts 92% of the measured values of the composite roughness within a range of error of 7.5%.

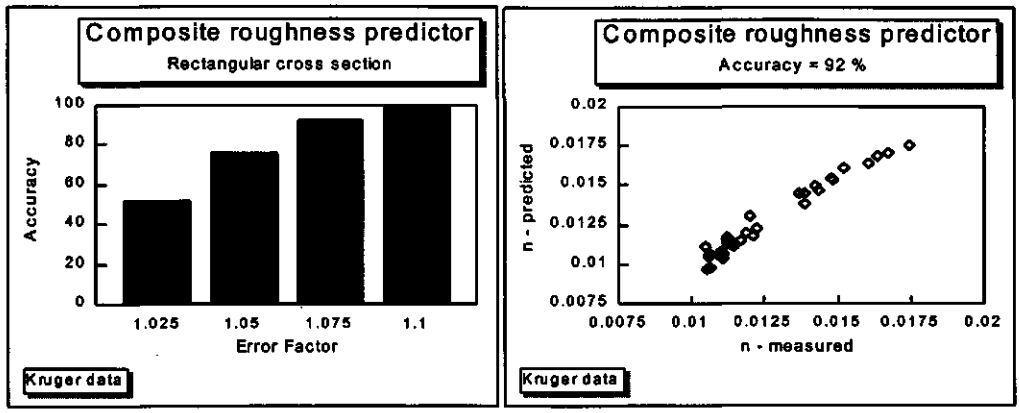

Figure 4.19 Accuracies for several error factors and predictability at an error factor of 1.075 of the proposed method for estimating the composite roughness in rectangular canals.

Summarizing the composite roughness in an irrigation canal can be estimated for each case of composite roughness by:

Rigid boundaries: the composite roughness is associated with the different types of material on the sides and bottom of the canal (fig. 4.20a). Values of roughness coefficients for the side and bottom can be determined depending on the type of material on the bottom and sides respectively. The composite equivalent roughness can be directly estimated by applying equations 4.29.

Movable bottom bed: flow conditions might change the roughness characteristics of the bed by developing bed forms. For two cases of composite roughness with movable bottom bed, the estimation of the hydraulic roughness can be done by:

- *bed form on the bottom and flat surface on the sides* (fig. 4.20b): roughness on the bottom can be estimated from the bed form characteristics. The hydraulic roughness of the side slope can be estimated depending on the type of material and the composite roughness for the entire cross section is found by equations 4.29;
- *bed form on the bottom and vegetated side slopes* (fig. 4.20c): the flow resistance for vegetated side slopes has been related with the degree of obstruction by the growing of weed. Weed growth will increase the roughness of the cross section. Querner (1993) gives a typical behaviour of the variation of the relative obstruction degree and the relative roughness coefficient during the growing period (figure 4.21). Only tendencies and no absolute values for the relative obstruction degree and relative roughness coefficient during the growing period are presented in this figure. This means that the friction factor (e.g. the Chézy coefficient) can be affected by a weed factor F_w to obtain the actual roughness coefficient. No explicit value for F_w is given. This factor depends on local flow conditions, vegetation characteristics (growing period, type etc). Petryk

(1975), Nitschke (1983), Querner (1993) mention variations for the weed factor between 0.1 (very densely overgrown canal) and 1 (ideally clean canal). Table 4.13 shows some values of the weed factor F_w , which is based on the data and local conditions as presented by Nitschke (1983). These values are here mentioned as an example, they are only applicable for the specific flow conditions and vegetation described in that research.

The variation of the obstruction degree and weed factor during a certain period will also depend on the maintenance degree. As example some values for the weed factors are given (table 4.14). Three scenarios with different types of maintenance policies will be considered:

- *no maintenance*: no weed clearing
- *well maintained*: weed clearing when the degree of obstruction reaches 25% (approx. after 2 months)
- *ideally maintained*: continuous weed clearing

Table 4.13 Weed factor for different conditions of obstruction degree

Obstruction degree	Weed factor F_w
< 5 %	1.0
5 - 10 %	0.9
10 - 15 %	0.8
15 - 25 %	0.7
25 - 35 %	0.5
35 - 50 %	0.4
50 - 75 %	0.2
> 75 %	0.1

Table 4.14 Weed factors according to the type of maintenance

	Weed factor	
Type of maintenance	Maximum	Minimum
No maintenance	1.0	0.1
Well maintained	1.0	0.7
Ideally maintained	1.0	1.0

By using the information related to the obstruction degree (weed factor), the actual roughness can be calculated by:

$$\text{Actual roughness} = \text{Initial roughness} * F_w \qquad (4.48)$$

In terms of the Chézy coefficient:

$$\text{Actual Chézy coefficient} = \text{Chézy coefficient without weed-effect} * F_w \qquad (4.49)$$

where:

F_w : weed factor depending of the degree of obstruction

The composite roughness under those conditions can be estimated by computing the initial roughness of the whole cross section, depending on whether there is a single roughness or a composite roughness along the wetted perimeter or based on the type of roughness of the bottom and sides as mentioned before. Next the actual roughness is reduced by the weed factor F_w by applying equation 4.45 or 4.46.

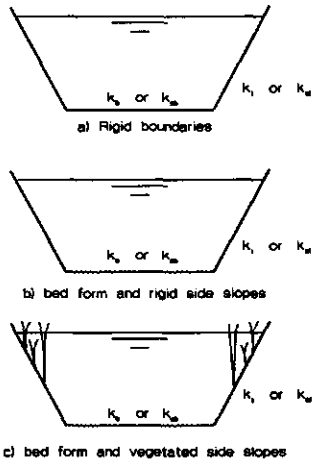

Figure 4.20 Types of composite roughness in trapezoidal irrigation canals

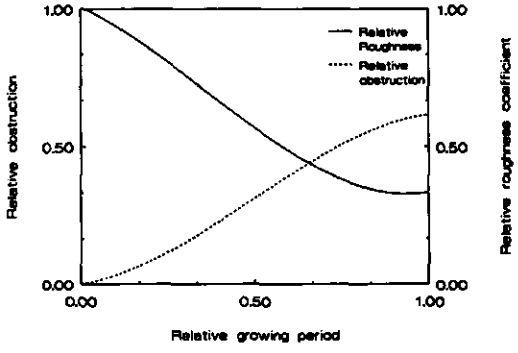

Figure 4.21 Variation of the relative obstruction and relative roughness coefficient during the weed growing period

4.3 Methods to estimate sediment transport in irrigation canals

Sediment transport methods are established for different conditions and the use of the equations should be restricted to the conditions for which they were tested. However a comparison of the different methods for similar flow conditions and sediment characteristics, both in irrigation canals and from field and laboratory data will be a useful tool to evaluate the suitability of each method under these specific conditions.

A way to evaluate the predictor methods for sediment transport is to compare the results to measured sediment transports. Once the hydraulic and sediment quantities (e.g. mean velocity, flow depth, sediment size, etc) are known, the sediment transport rates can be predicted. Next these predicted rates will be compared with the measured values of sediment transport.

4.3.1 Laboratory and field data

The assessment of the methods for predicting the sediment transport rate will be based upon a comparison of field and laboratory data. The compilation of data by Brownlie (1981) will be used for this purpose.

The information on these data is provided in the following format:

- discharge Q (l/s);
- width of the canal B in m;
- flow depth h in m;
- slope S (10^{-3});
- median diameter d_{50} in mm;
- geometric standard deviation of particle distribution σ;
- relative density s;
- concentration c in ppm by mass;
- temperature in t °C;
- bed form according to the description of Vanoni (1975). For lower regime, the bed forms are described as: plane bed, ripples and dunes.

The criteria for selecting the data are based on the flow conditions and sediment characteristics normally encountered in irrigation canals. These criteria are the same as described in paragraph 4.2.1.

A total of 169 records has been selected from the available data of Brownlie. Table 4.15 shows a summary of the selected data. Figure 4.22 shows the characteristics of the data base selected.

Table 4.15 Summary of data selected

Investigator and year	Data code	No. of records
Davies, T. R. (1971)	DAV	10
Guy, H.P. et al (1966)	GUY	43
Mutter, D. G (1971)	MUT	18
Pratt, C. J. (1970)	PRA	7
Barton, J. et al (1955)	BAL	4
Onishi, Y. et al (1972)	OJK	4
Colby, B. R et al (1955)	NIO	15
Mahmood, et al (1979)	ACOP	51

4.3.2 Evaluation of the methods to predict the sediment transport

The comparison of predicted and measured values will be done by:

- plotting the measured values against the predicted values for each method and by calculating the accuracy of the predicted values according to the following relation:

$$\frac{\text{Measured value}}{K} \leq \text{Predicted value} \leq K * \text{Measured value} \qquad (4.50)$$

where:
K = error factor

Thus, the accuracy of each method is calculated by the number of predicted values within the range with a error factor K, divided by the total number of data used in the comparison.

- Mean arithmetic and mean geometric of the discrepancy ratio d_r. The latter ratio is defined as:

$$d_r = \frac{\text{predicted value}}{\text{measured value}} \qquad (4.51)$$

$$\text{Arithmetic mean} = \sum \frac{d_r}{n} \qquad (4.52)$$

$$\text{Geometric mean} = \sqrt[n]{(d_{r_1} * d_{r_2} * .... * d_{r_n})} \qquad (4.53)$$

where:

n = number of data

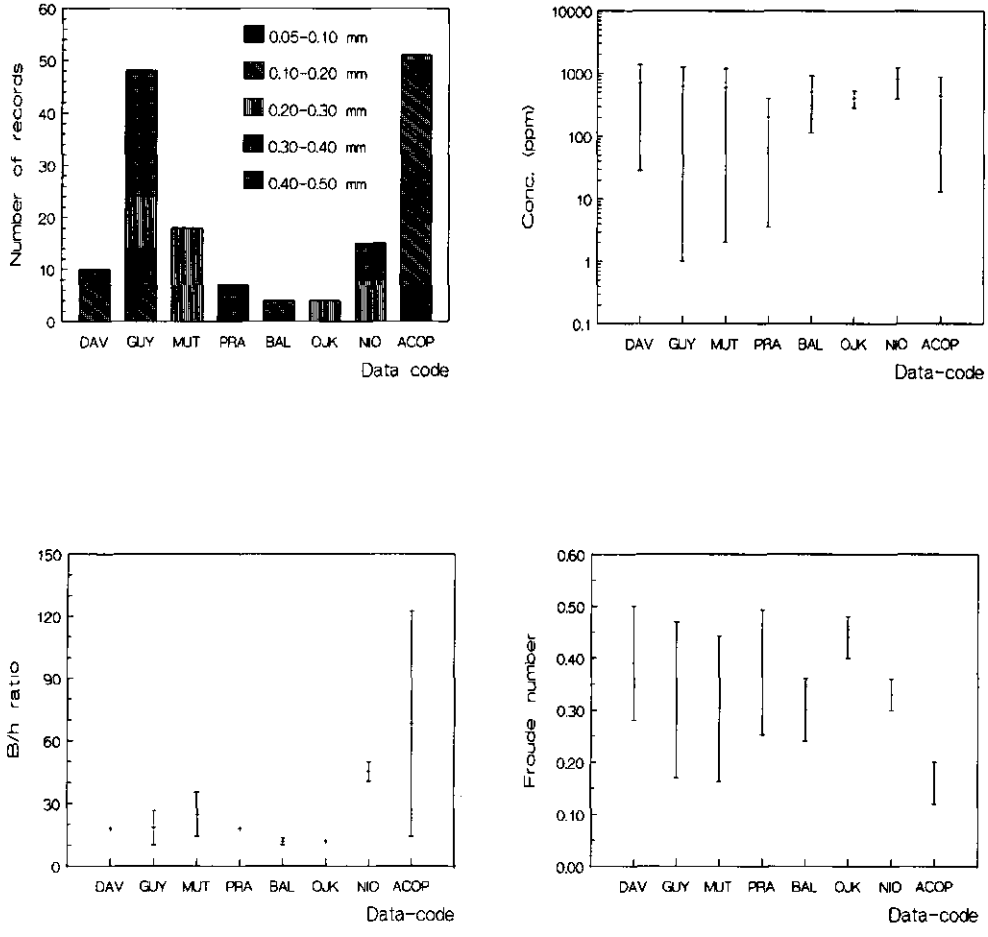

Figure 4.22 Range of median diameter d_{50}, concentration, B/h ratio and Froude numbers in each data code of the selected data

The Ackers and White (A-W), Brownlie (BRO), Engelund-Hansen (E-H), van Rijn (RIJ) and Yang (YAN) methods to predict sediment transport have been evaluated. These methods are compared to field and laboratory data, in which the flow condition and sediment characteristics are similar to those prevailing in irrigation canals. From the evaluation some remarks can be drawn:

- prediction of the sediment transport in irrigation canals within an error factor smaller than 2 is hardly possible. Even in case of the most reliable method, only 61% of the measured values are predicted with the tolerance of an error factor of 2. For error factors smaller than 2, the predictability of the methods is considerably less. Figure 4.23 shows the results of the comparison for error factor values of 1.1, 1.50, 1.75, 2, 2.5, and 3.00. Figure 4.24 shows the comparison of the predictors in terms of the arithmetic and geometric means;
- the Brownlie predictor method has a tendency to underpredict the sediment transport, while the Engelund-Hansen predictor overpredicts in most cases. Figure 4.25 shows the overpredictability degree of each method when compared with measured values. The overpredictability is given by the number of predicted values larger than the measured values divided by the total number of values;
- there is a general tendency of the methods to overpredict the sediment transport for low concentrations. In terms of goodness to fit to measured low concentration values, most methods do not perform well. Ackers and White and Brownlie are the best methods to predict the sediment transport rate for ranges of flow concentration smaller than 500 ppm. Figure 4.26 shows the results of the accuracy of each method for different concentration levels.
- conversely all the methods predict better when compared with higher concentrations as shown in figure 4.27. Ackers and White, Yang and Engelund and Hansen methods produce the best predictions for flow concentrations larger than 500 ppm.
- based on the overall performance of each method according to all the evaluation criteria, the Ackers and White and Brownlie methods seem to be the best to predict sediment transport in irrigation canals (figures 4.23 and 4.24). Figures 4.27 and 4.28 show the performance of both methods when compared with measured value for an error factor of 2;
- All the predictors performed well when compared with GUY and NIO data codes. The predictions of sediment transport was not well at all when compared with the MUT data code. Figure 4.29 shows the accuracy degree of the different predictors when compared with the data of each code.

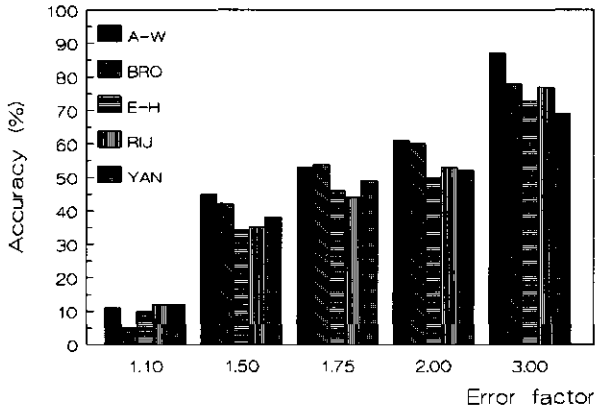

Figure 4.23 **Range of accuracy of the sediment transport predictors for different error factors**

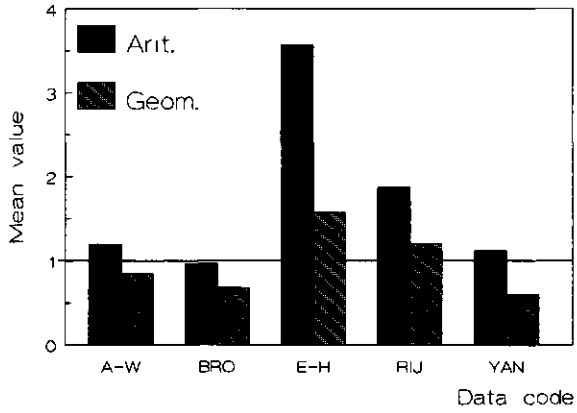

Figure 4.24 **Arithmetic and geometric mean values of the discrepancy ratio**

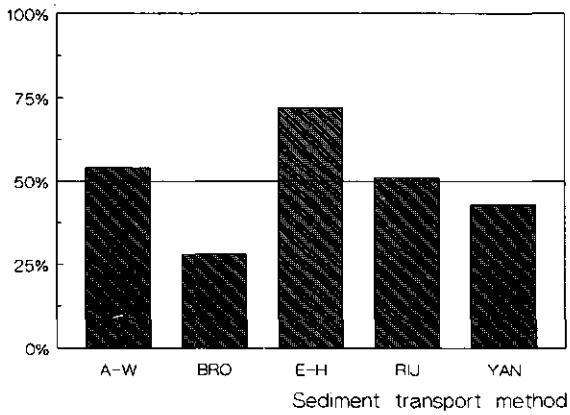

Figure 4.25 **Overpredictability degree of the sediment transport methods**

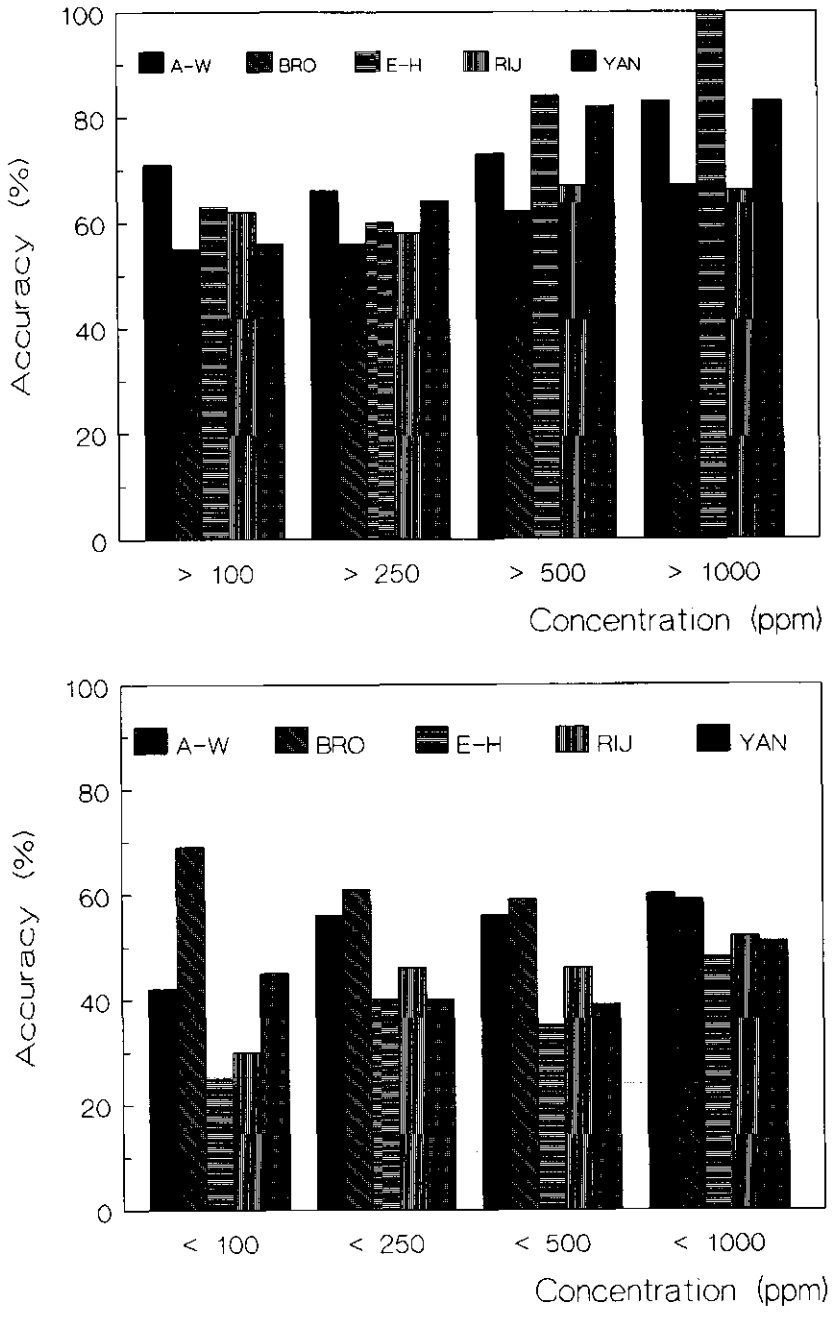

Figure 4.26 **Accuracy of the methods for different levels of sediment concentration**

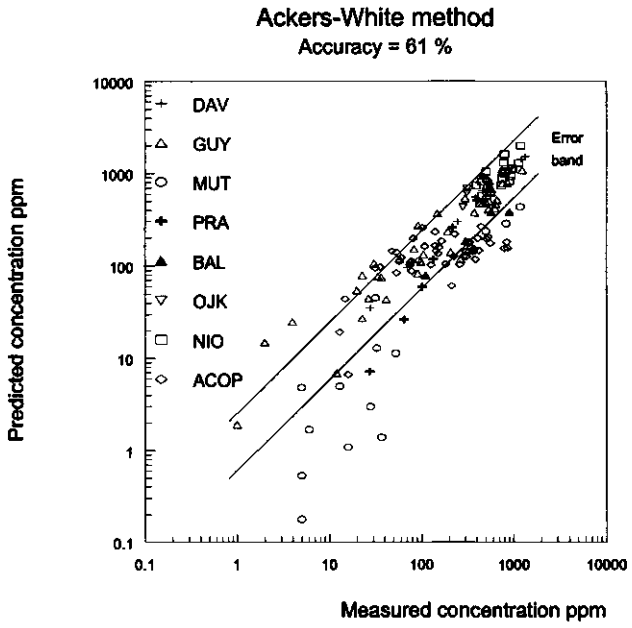

Figure 4.27 Accuracy of the Ackers and White sediment transport predictor for an error factor of 2

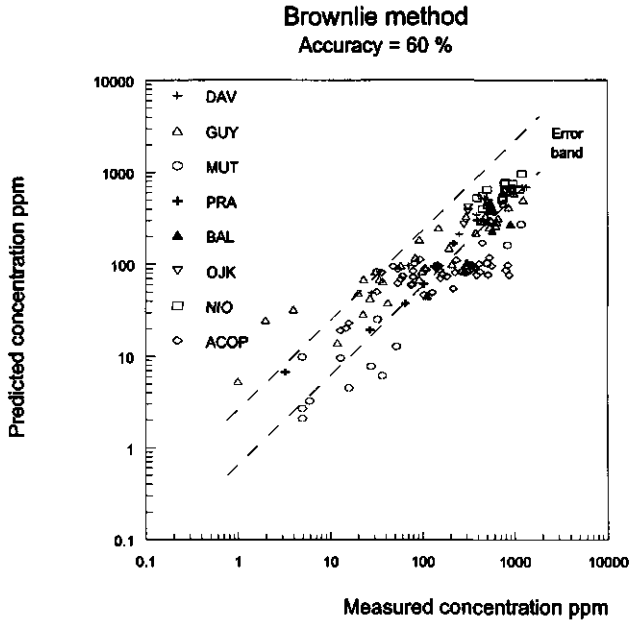

Figure 4.28 Accuracy of the Brownlie sediment transport predictor for an error factor of 2

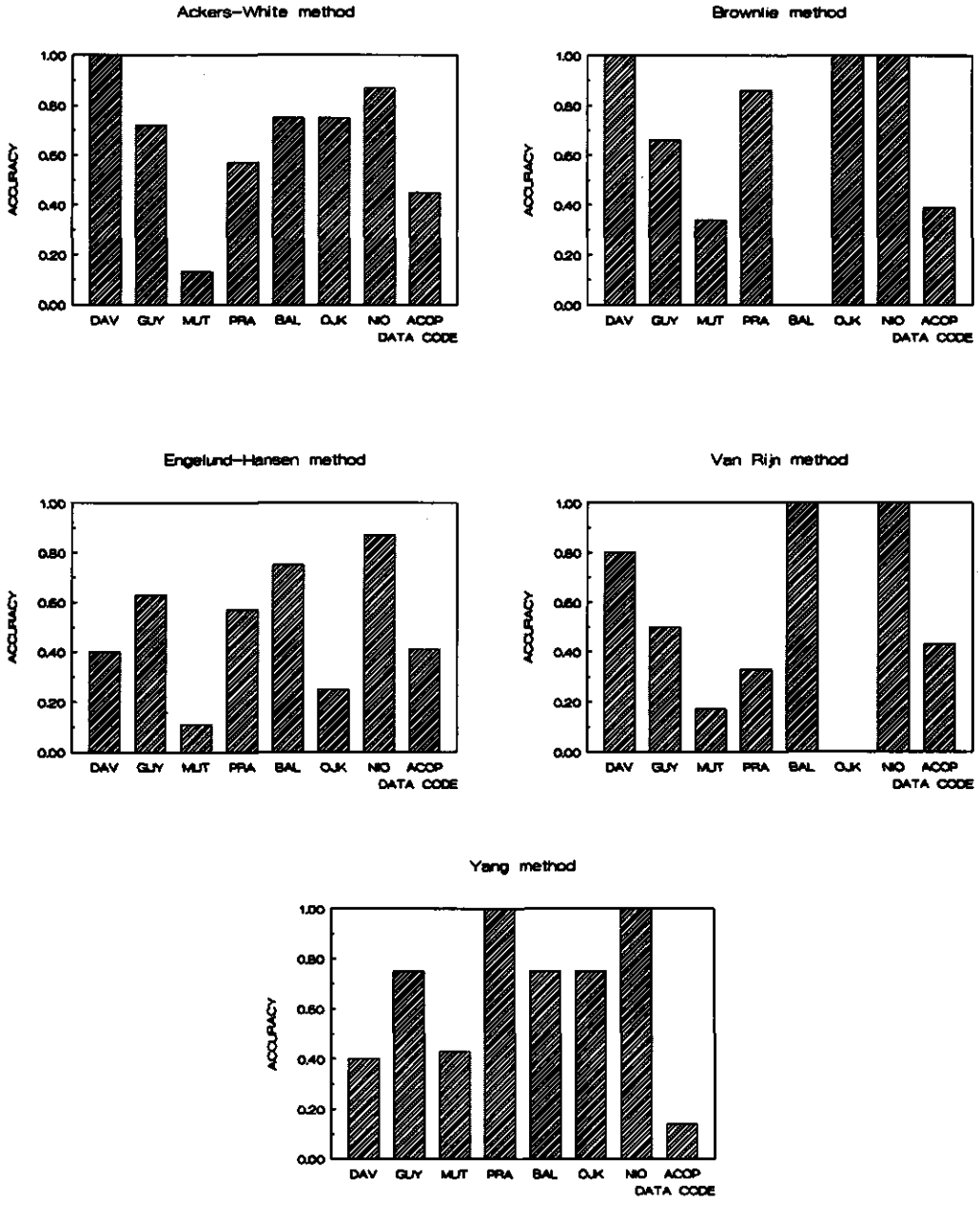

Figure 4.29 Accuracy degree of the different predictors when compared with each data code

4.3.3 Sediment transport computation in non-wide canals

The use of a sediment transport relationship that involves the velocity as variable often has been used without consideration of the variation in channel geometry, distribution of the flow velocity and distribution of the sediment transport in the cross section (Simons 1992). Sediment transport formulae have been developed for wide canals. They consider a canal with an infinite width without taking into account the effect of the side banks on the water flow and on the sediment transport. The effect of the side banks on the velocity distribution in lateral direction is neglected and therefore the velocity distribution and the sediment transport is considered to be constant in any point of the cross section. Under that assumption an uniformly distributed shear stress on the bottom and an identical velocity distribution and sediment transport in any point over the width of the canal is assumed. In that way these variables can be easily expressed per unit width. For other kinds of channels (non-wide channels) the shape will have an effect on the variables associated with the water flow and sediment transport. The existence of side banks and the varying water depth on the side slope will cause a non uniform distribution over the width for both the shear stress and the velocity and as a consequence also for the sediment transport.

Generally, the most common shape of irrigation canals is the trapezoidal cross section. These canals are not considered as wide canals. Recommended values for the ratio of bottom width and water depth (B/h) in irrigation canals are smaller than 8 (Dahmen, 1994). For that cross section, the imposed boundary condition for the velocity and the varying water depth on the sides will affect the shear stress and the velocity and sediment distribution in y-direction. In other words the variables related to the water flow and the sediment transport vary in y-direction. These effects will be larger for smaller values of the B/h ratio.

The cross section integrated approach is based on the assumption of a quasi two-dimensional model. This approach will be named procedure 3. The trapezoidal cross section is composed by a series of parallel stream tubes (fig. 4.30). Within each stream tube the velocity distribution is considered to be uniform and therefore can be described in an one-dimensional way. The sediment transport in each stream tube is considered as a function of the water flow in that stream tube only without taking into account the diffusion in y-direction. The total sediment transport in a trapezoidal cross section can be calculated by:

$$Q_s = \sum (q_s)_i \, dy \qquad (4.54)$$

where:

Q_s = total sediment discharge
q_s = sediment discharge of the stream tube i per unit width
dy = width of the stream tube

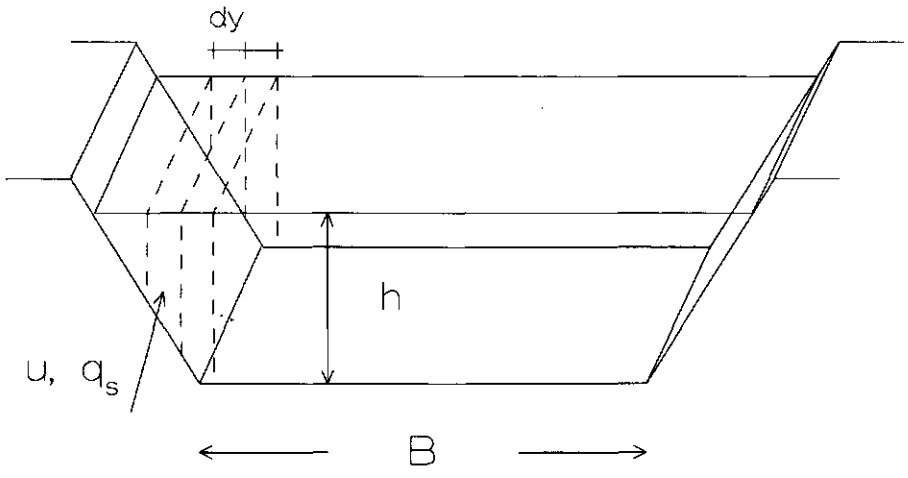

Figure 4.30 Schematization of stream tubes in a trapezoidal cross section

In most empirical formulae for one-dimensional uniform flow in non-wide channels the hydraulic radius is universally used as the single quantity to describe the geometry of the cross section and the mean velocity. The non-uniform distribution of the velocity (u) is replaced by a mean velocity (V) over the whole cross section (figure 4.31).

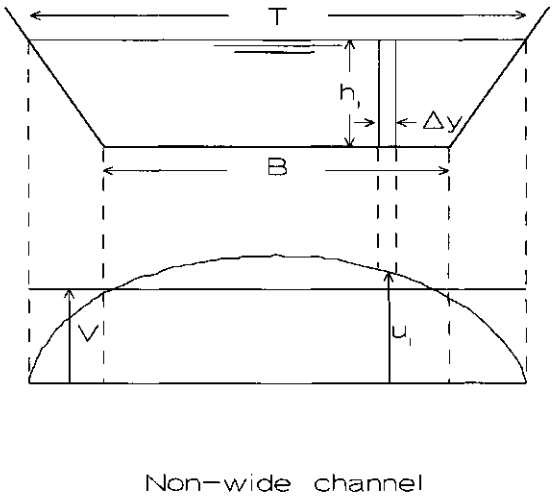

Figure 4.31 Velocity distribution in a non-wide canal

However, the sediment transport per unit width given by $q_s = M\ V^N$ is not the average of the sediment transport of each local velocity in the cross section $q_s = M\ u^N$. The difference between them is due to the non-linear relationship between the sediment transport and the velocity, so that a correction factor α for the sediment transport must be introduced in order to equal both values of sediment transport capacity. It is proposed to estimate the total sediment transport for the total cross section by (fig 4.32):

$$Q_s = \alpha\ B\ q_s \qquad \text{with} \qquad q_s = f\ (V) \tag{4.55}$$

where:

α = correction factor for calculating the total sediment transport in a non-wide canal.
B = bottom width
V = mean velocity
Q_s = sediment transport capacity for the whole cross section
q_s = sediment transport capacity per unit width

Referring to figure 4.32, the sediment transport passing the whole cross section can be also computed by:

$$Q_s = \int_T M\ u^N\ dy \tag{4.56}$$

Equating equations 4.55 and 4.56:

$$\alpha = \frac{\int_T M\ u^N\ dy}{B\ M\ V^N} \tag{4.57}$$

M and N are coefficients, which depend on the flow conditions and sediment characteristics. In a given cross section these coefficients vary for flow conditions, which are close to the threshold for initiation of motion (for Ackers and White and Brownlie predictors). Outside this region the coefficients are relatively constant (see paragraph 4.3.3.2). For Engelund and Hansen predictors these coefficients are constant in any point of the cross section. By assuming constant coefficients M and N for the entire cross section then equation 4.50 becomes:

$$\alpha = \frac{\int_T \left(\frac{u}{V}\right)^N dy}{B} = \frac{\sum \left(\frac{u}{V}\right)^N \Delta y}{B} \tag{4.58}$$

The correction factor α for computing the total sediment transport is a function of the velocity distribution in the cross section and the exponent N in the relationship of the velocity and the sediment transport predictor.

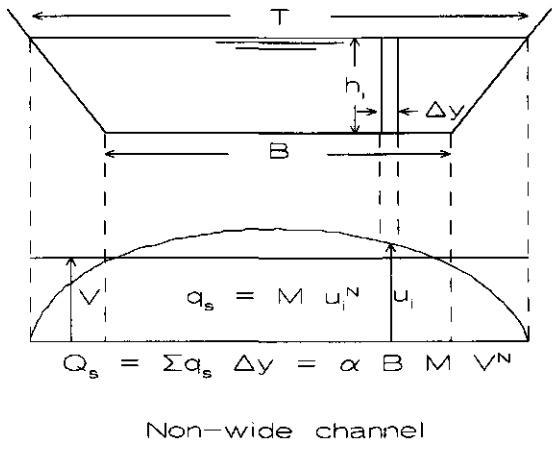

Figure 4.32 Total sediment transport in a non-wide trapezoidal canal

4.3.3.1 Velocity distribution in the lateral direction: In section 4.2.3.1 was proposed a distribution of velocities over a trapezoidal cross section composed of different roughness along the wetted perimeter. This distribution of velocities does not take into account the lateral transfer of momentum. Due to the strong relationship between the sediment transport and the velocity a more accurate description of the distribution of velocities over a trapezoidal cross section (single roughness) is needed.

The distribution of the velocity in the cross section of an open canal can be estimated by using the 2-D equation of motion expressed in the x- and y-direction. That equation can be given by:

$$\frac{\partial u}{\partial t} + u\frac{\partial u}{\partial t} + v\frac{\partial u}{\partial y} + g\frac{\partial}{\partial x}(h + z) + \frac{1}{\rho\ h}\tau_{bx} - \frac{1}{\rho\ h}\left(\frac{\partial(h\ \tau_{xx})}{\partial x} + \frac{\partial(h\ \tau_{xy})}{\partial y}\right) = 0 \qquad (4.59)$$

where:

u, v	= depth averaged velocity in x and y direction (m/s)
x, y	= length co-ordinates (m)
h	= water depth (m)
g	= acceleration due to gravity (m/s^2)
ρ	= water density (kg/m^3)
τ_{bx}, τ_{by}	= bottom shear stress in x and y direction respectively (N/m^2)
τ_{xy}, τ_{xx}	= effective shear stress (N/m^2)

The effective shear stress at the interface between two stream tubes affects the velocity distribution in y-direction. The effective shear stress τ_{xy} in the x-direction perpendicular to the y-direction can be expressed as (Ogink, 1985):

$$\tau_{xy} = \rho \nu_t \left(\frac{\partial u}{\partial y} + \frac{\partial v}{\partial x}\right) \tag{4.60}$$

where:

ν_t = effective viscosity coefficient (m^2/s)

Equation 4.59 can be solved numerically by using a finite difference method, which can transform the equation to:

$$(h_{n-1} + 4\,h_n - h_{n+1})\,u_{n-1} - 8\,h_n\,u_n + (-h_{n-1} + 4\,h_n + h_{n+1})\,u_{n+1} = \frac{4\,g}{\nu_t}\left(1 - \frac{h_s}{R}\right)\left(\frac{Q\,\Delta y}{A\,C}\right)^2 \tag{4.61}$$

For a given trapezoidal cross section in a canal with bottom slope S_0, the velocity distribution can be determined by solving numerically the equation. Details for determining the velocity distribution in the width direction is given in appendix D.

4.3.3.2 Determination of the exponent N: Sediment transport predictors can be schematized by using a simple relation between q_s and V in the following way:

$$q_s = M\,V^N \tag{4.62}$$

where:

q_s = sediment transport per unit width
V = mean velocity
M, N = parameters depending on the water flow and sediment characteristics.

Derivation of the exponent N can be done by:

$$\frac{dq_s}{dV} = M\,N\,V^{N-1} \tag{4.63}$$

and therefore,

$$N = \frac{V}{q_s}\frac{dq_s}{dV} \tag{4.64}$$

Here the exponent N will be determined for the following sediment transport predictors: Ackers and White, Brownlie and Engelund and Hansen. Appendix D shows details of the determination of N for those predictors.

Ackers and White sediment transport predictor: in the Ackers and White sediment transport predictor the exponent N is not constant. It depends on the flow conditions and sediment characteristics. Figure 4.33 shows the relationship between the dimensionless mobility parameter F_{gr} and the exponent N for flow conditions in irrigation canals. Flow conditions close to the initiation of motion are strongly affected by the flow velocity and sediment diameter and the exponent N is in that region considerably higher. Far away from the initiation of motion the exponent N varies slightly with the flow conditions and only depends on the sediment diameter. For these flow conditions variations of the exponent N are in the range between 7.5 and 8 for a median diameter equal to 0.1 mm and between 3.4 and 3.8 for a diameter of 0.5 mm. Details of the determination of the exponent N in this predictor is given in appendix D. The exponent N of the Ackers and White sediment transport is represented by:

$$N = 1 + \frac{m' F_{gr}}{F_{gr} - A} \tag{4.65}$$

where:

F_{gr} = dimensionless mobility parameter
A = value of F_{gr} at nominal initial movement
m' = exponent in the sediment transport parameter G_{gr}

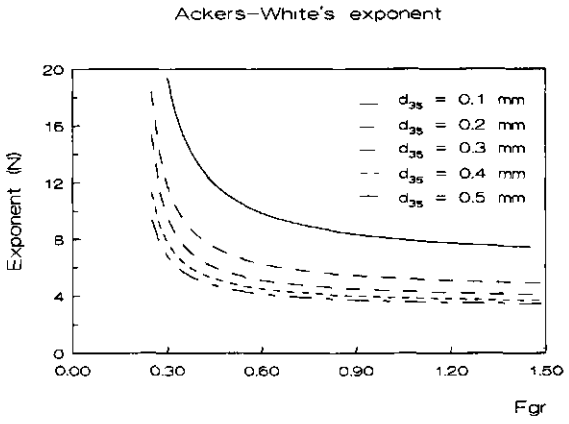

Figure 4.33 Relationship between the exponent N and the mobility parameter F_{gr} for the Ackers and White predictor

Brownlie sediment transport predictor (1981): The exponent N of the Brownlie sediment transport predictor is not a constant value. It depends on several variables such as the critical flow condition for initiation of motion, the actual flow condition and sediment characteristics. The computations are performed for a nearly uniform sediment distribution ($\sigma_s = 1.4$). It can be represented as:

$$N = 1 + \frac{1.978\ F_g}{F_g - F_{gcr}} \tag{4.66}$$

where:

F_g = grain Froude number

F_{gcr} = critical grain Froude number

A sensitivity analysis for other sediment distributions is done on a relative basis in which several sediment distributions are compared with the value used for the geometric standard deviation ($\sigma_s = 1.4$). It is measured in terms of an error, which reads:

$$\text{Error} = \left(\frac{N_{1.4} - N_x}{N_{1.4}}\right) * 100 \tag{4.67}$$

where:

$N_{1.4}$ = exponent N calculated by using a value of $\sigma_s = 1.4$

N_x = exponent N calculated by using a different value of σ_s

Figure 4.34 shows the results of the sensitivity analysis for the geometric standard deviation σ_s. The largest error values are observed for flow conditions, which are close to the initiation of motion. Far away from that flow condition the errors are considerably smaller. It means that the relationship between the exponent N and the flow conditions will behave similar for other sediment distributions.

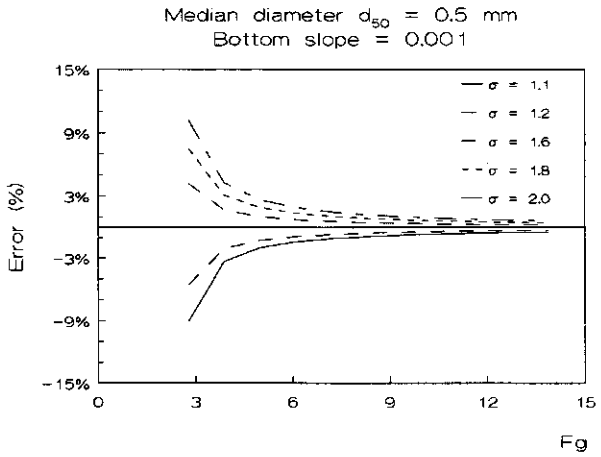

Figure 4.34 Sensitivity analysis for the geometric standard deviation σ_s in the Brownlie sediment transport predictor

Figure 4.35 shows the relationship between the exponent N and the grain Froude number for sediment diameters between 0.1 mm and 0.5 mm. Far away from the flow conditions for initiation of motion the exponent N behaves relatively constant with a little influence of the median diameter and flow condition. The variation for the exponent N for a range of bottom slopes between 0.00005 and 0.001 and a range of median diameters between 0.1 mm and 0.5 mm is as follows: 3.3-3.6 for a median diameter equal to 0.1 mm and 3.25-3.45 for a median diameter of 0.5 mm.

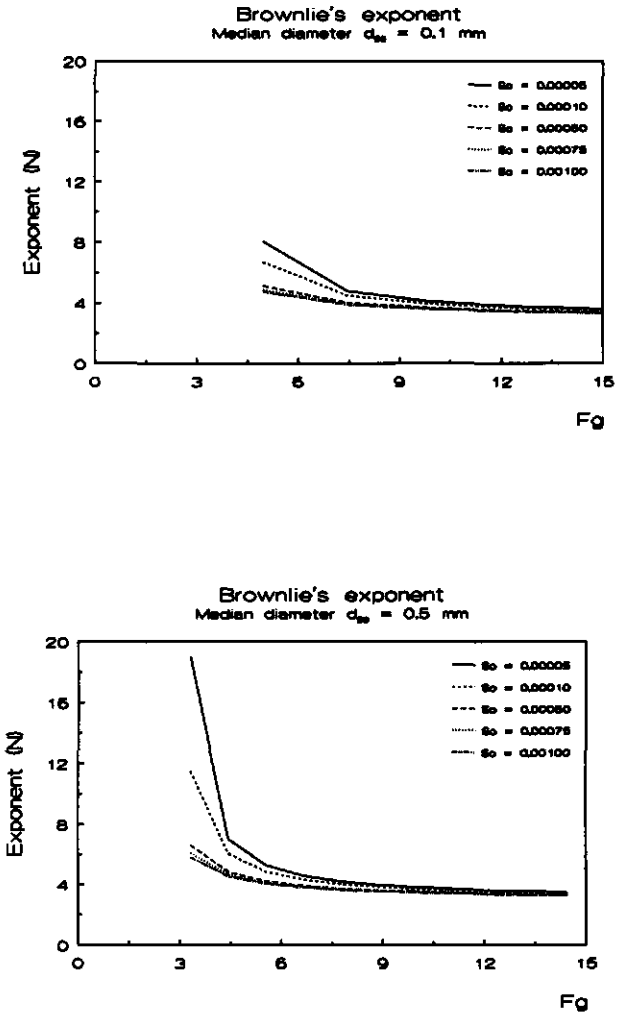

Figure 4.35 Relationship between the exponent N and the grain Froude number for different values of sediment diameter and flow conditions in the Brownlie sediment transport predictor

Engelund-Hansen sediment transport predictor (1967): the Engelund and Hansen function for the sediment transport is given by:

$$q_s = \frac{0.05\ V^5}{(s-1)^2\ g^{0.5}\ d_{50}\ C^3} \qquad (4.68)$$

where:

q_s = total sediment discharge (m^2/s)
V = mean velocity (m/s)
C = Chézy coefficient ($m^{1/2}/s$)
s = relative density
d_{50} = mean diameter (m)

Comparing equation 4.62 and equation 4.68 results in the observation that the exponent N for the Engelund and Hansen predictor is a constant value for a given cross section and is equal to (if C= constant):

$$N = 5 \qquad (4.69)$$

4.3.3.3 Determination of the correction factor (α) for the sediment transport computations in non-wide canals: once the velocity distribution of the non-wide canal has been determined and the sediment transport predictor has been selected, the correction factor α for the sediment transport computation can be determined. The correction factor α will be determined for a schematized non-wide canal with the following characteristics:

- bottom width (B) = 6 m
- Chézy coefficient (C) = 40
- mean velocity (V) = 0.5 m/s
- bottom width-water depth ratio (B/h) = 3
- side slopes (m) = 0, 1, 2 and 3
- exponent (N) of the sediment transport predictor = 4

The procedure to determine the correction factor α can be summarized as follows:

- divide the cross section in stream tubes and compute the depth averaged velocity distribution in the lateral direction by using the procedure described in section 4.3.3.1
- calculate the correction factor (α) by applying equation 4.58.

The number of stream tubes to be used in the procedure described above is determined by a sensitivity analysis for that variable. Figure 4.36 shows the results of the calculation of the correction factor α and the number of stream tubes. The accuracy of the calculated α value does not improve for more than 17 stream tubes. Therefor the number of stream tubes to be used in the calculation of the correction factor α will be 17.

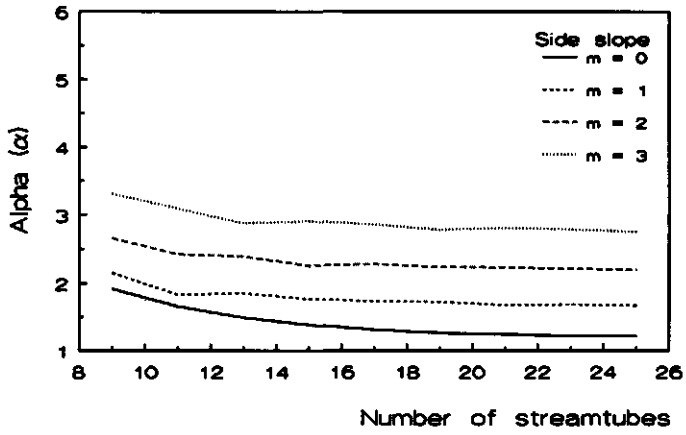

Figure 4.36 Relationship between the number of stream tubes and the correction factor α

The determination of the correction factor α depends on several independent variables which influence either the flow condition or the sediment transport calculations. A sensitivity analysis of these variables is necessary to find the degree of dependency between the correction factor α and these independent variables. The variables to be analysed are: bottom width-water depth ratio (B/h), exponent in the sediment transport predictor (N), bottom width (B), bottom slope (S_0) and roughness coefficient (C).

Bottom width-water depth ratio: the correction factor α for the sediment transport was calculated for a range of B/h ratio between 2 and 7. That range is normally used in irrigation canals (Dahmen, 1994). Figure 4.37 shows the variation of the correction factor α for different values of the B/h ratio. For rectangular cross sections the B/h ratio does not influence the correction factor. In rectangular cross sections the pattern of the velocities distribution behaves similar for that range of B/h ratio's, which is explained due to the turbulent flow in the canal. For non-rectangular cross sections the correction factor is strongly affected by the B/h ratio and the side slope. The varying water depth on the sides affects the velocity distribution in the cross section and therefore the water flow and sediment transport. This effect will be larger for small B/h ratios and larger m for the side slope.

Exponent N of the sediment transport predictor: the non-linear relationship between sediment transport and flow velocity has a large influence on the value of the correction factor α. The smallest effect of that independent variable on the correction factor is observed for a rectangular cross section (m = 0) due to the small deviation of the velocity distribution from the mean velocity. Large deviation of the velocity distribution from the mean velocity as observed for the side slope m = 3 will produce a large effect on the correction factor α. The relationship between the exponent N and the correction factor is shown in figure 4.38.

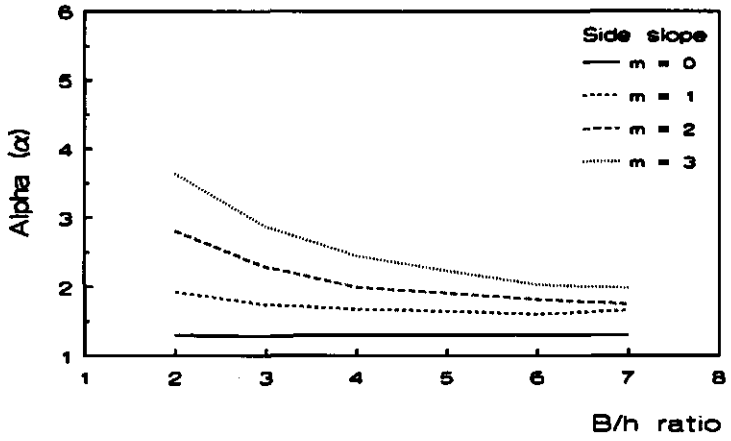

Figure 4.37 Relationship between the bottom width-water depth ratio (B/h) and the correction factor α as a function of the side slope m

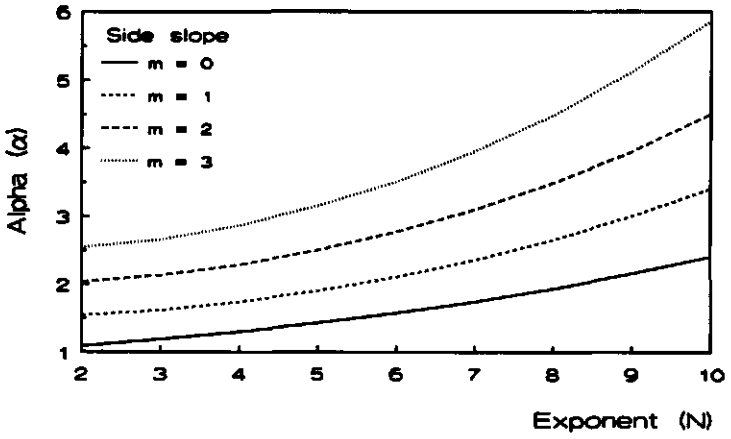

Figure 4.38 Relationship between the exponent N of the sediment transport predictor and the correction factor α

Bottom width: the influence of the bottom width on the value of the correction factor α has been evaluated for a range of bottom widths between 2 m and 8 m. The evaluation shows that the bottom width has no systematic influence on the calculation of the correction factor α. Figure 4.39 shows the errors of calculation of the correction factor for other values of bottom width when compared with a bottom width of 6 m. That error can be described as:

$$e = \left(\frac{\alpha_x - \alpha_6}{\alpha_6}\right) * 100 \qquad (4.70)$$

where:

e = computation error

α_x = correction factor α calculated by using a bottom width different of 6 m

α_6 = correction factor α calculated by using a bottom width equal to 6 m

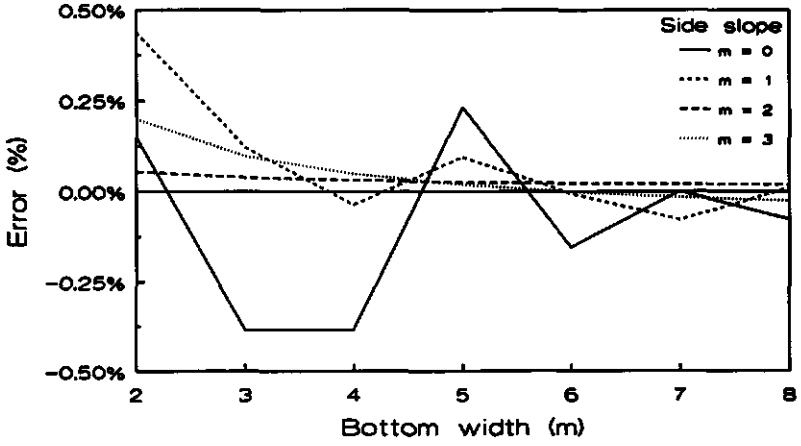

Figure 4.39 Computation error in the correction factor α for different values of the bottom width

Roughness coefficient: variation of the Chézy coefficient in the range between 25 and 65 and its influence on the correction factor for the sediment transport computations has also been evaluated. The influence of this independent variable is measured on a relative basis. The correction factor calculated by using different values of the Chézy coefficient is compared with the ones calculated with a Chézy coefficient equal to 40 as described below. There is no systematic influence of the Chézy coefficient on the value of the correction factor. Variation of that variable affects in a similar way both the velocity distribution in width direction and the mean velocity. Figure 4.40 shows the results of the influence of the roughness coefficient on the correction factor α.

$$e = \left(\frac{\alpha_x - \alpha_{40}}{\alpha_{40}}\right) * 100 \qquad (4.71)$$

where:

e = computation error

α_x = correction factor α calculated by using a Chézy coefficient different of 40

α_x = correction factor α calculated by using a Chézy coefficient different of 40
α_{40} = correction factor α calculated by using a Chézy coefficient of 40.

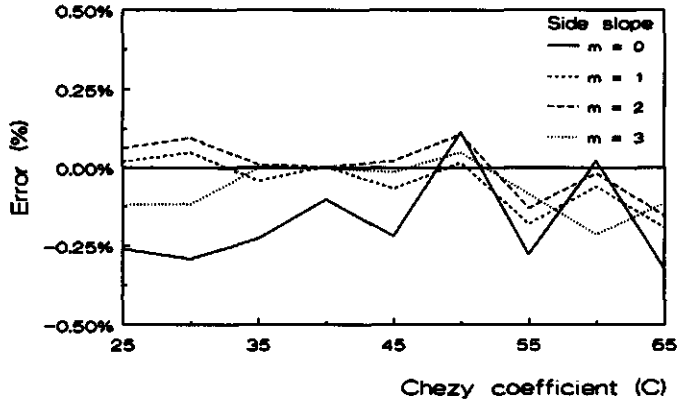

Figure 4.40 Computation error in the correction factor α for different values of the Chézy coefficient

Bottom slope: another independent variable affecting the flow conditions in canals is the bottom slope. Its effect on the correction factor α is evaluated in terms of the computation error when other bottom slopes are used in stead of the bottom slope of the schematized canal. The effect of the bottom slope on the correction factor is also measured in relative terms as shown in figure 4.41. No influence of the bottom slope on the correction factor can be observed. Variations of the bottom slope affect in the same way both the mean velocity and the velocity distribution in the width direction.

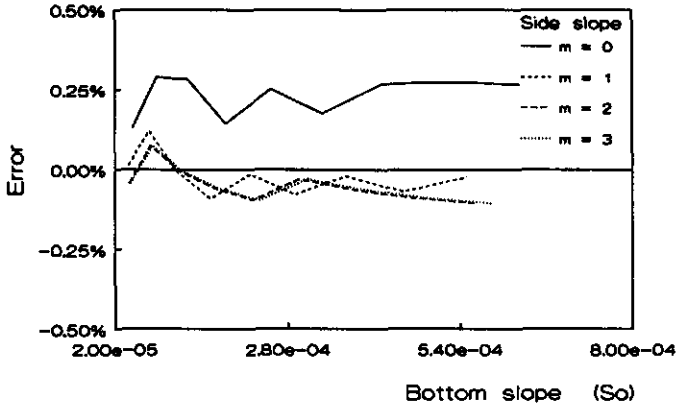

Figure 4.41 Computation error in the correction factor α for different values of the bottom slope

The previous paragraphs show that the correction factor α depends on several variables like bottom width-water depth ratio (B/h), side slope (m) and the sediment transport predictor which is represented by the exponent N. By using multiple linear regression several relationships can be found to determine the correction factor α as function of these independent variables. These relationships can be described as:

- for rectangular cross sections (m = 0) the correction factor α only depends on the kind of sediment transport predictor as shown figure 4.42.
- for trapezoidal cross sections the correction factor depends on the B/h ratio and the kind of sediment transport predictor (exponent N). Figure 4.43 to 4.45 show these relationships for side slopes of 1, 2 and 3 respectively.

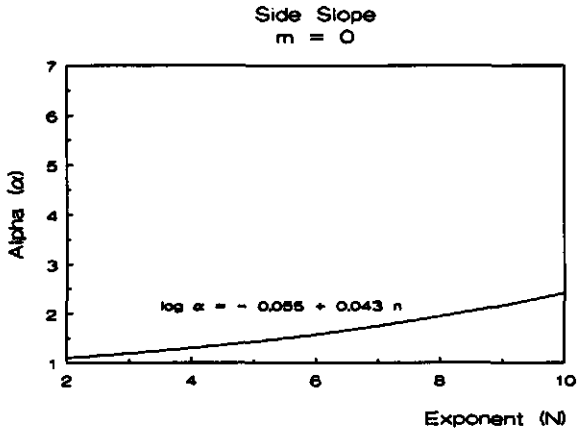

Figure 4.42 Relationship between the correction factor α and the exponent N for rectangular cross sections of non-wide canals

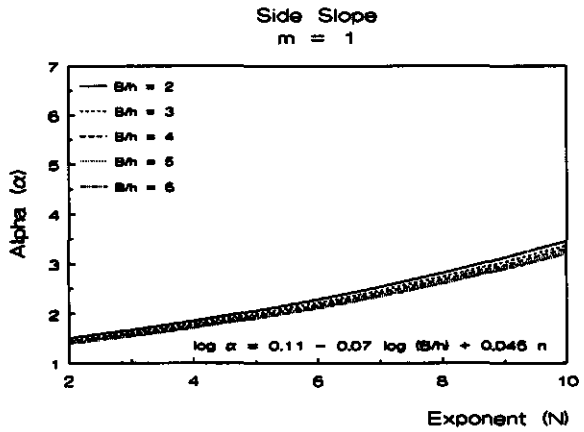

Figure 4.43 Relationship between the correction factor α and the exponent N for several B/h ratio's for a trapezoidal cross section (m = 1) of non-wide canals

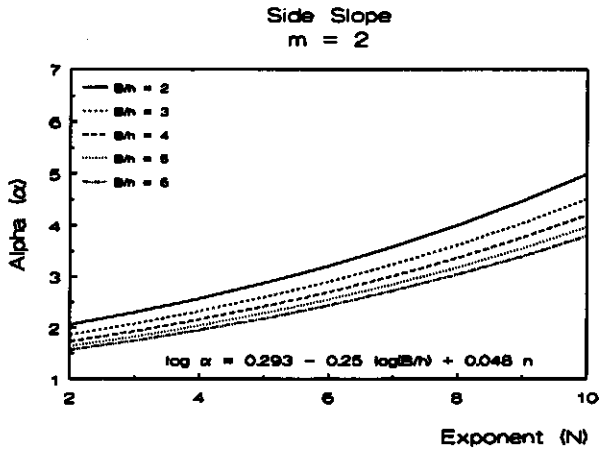

Figure 4.44 Relationship between the correction factor α and the exponent N for several B/h ratio's for a trapezoidal cross section (m = 2) of non-wide canals

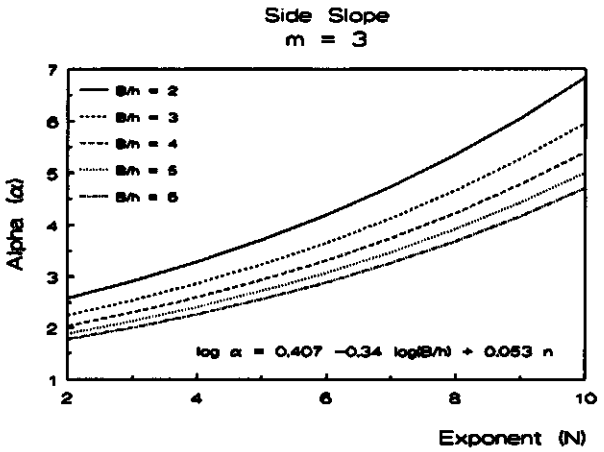

Figure 4.45 Relationship between the correction factor α and the exponent N for several B/h ratio's for a trapezoidal cross section (m = 3) of non-wide canals

4.3.4 Comparison of the procedures for computing the total sediment transport

Several procedures will be described to compute the total sediment discharge in open channels. These procedures are named:

Procedure 1: the sediment discharge per unit width (q_s) is calculated by using the hydraulic radius as representative variable for the water flow. The average width of the canal is assumed

to be the representative width of the canal and the total sediment transport is determined by the multiplication of these variables:

$$Q_s = q_s * B_{av.} \quad \text{with} \quad q_s = f(R) \tag{4.72}$$

Procedure 2: determination of the sediment transport per unit width (q_s) by using the water depth as representative variable of the water flow. Next the total sediment transport Q_s is calculated by multiplying the sediment transport per unit width (q_s) by the bottom width (B):

$$Q_s = q_s * B \quad \text{with} \quad q_s = f(h) \tag{4.73}$$

Procedure 3: it is proposed to calculate the total sediment transport by using the procedure described before, which is based on the computation of the sediment transport in stream tubes (cross section integrated approach):

$$Q_s = \int_{i=1}^{n} q_{s_{(i)}} \, dy \tag{4.74}$$

In order to compare procedures 1 and 2 and the proposed approach (procedure 3) for the computation of the total sediment transport in non-wide canals, application of the mentioned procedures on a selected set of laboratory data has been carried out. A correct method to compute the sediment transport will be necessary to avoid increasing inaccuracies. That method should take into account the effect of the cross section on the velocity distribution and the non-linear relationship between the velocity and the sediment transport. In the application the Ackers and White, Brownlie and Engelund and Hansen method have been used to compute the sediment transport.

The criteria for selecting the data are again based on the flow conditions and the sediment characteristics prevailing in irrigation canals. These criteria are:

- the selected data should contain all required quantities for computing the sediment transport;
- sediment sizes smaller than 0.5 mm;
- Froude number smaller than 0.5;
- B/h ratio smaller than 8.

A total of 102 records have been selected from the compilation of Brownlie (1981). It is noted that only data with rectangular cross section have been used. The data are shown in table 4.16. Figure 4.46 shows the characteristic values of sediment sizes, Froude number, B/h ratio and sediment concentration of the selected data.

Table 4.16 Data selected

Investigator and year	Data code	Records
Barton, J. R. and Lin, P. N. (1955)	BAL	9
Davies, T. R. (1971)	DAV	10
E. Pakistan Water and Power (1967)	EPA	11
Gov. of Pakistan (1966-69)	EPB	33
Guy, H. P. et al (1966)	GUY	6
Laursen, E. M. (1958)	LAU	7
Nomicos, G. (1957)	NOM	7
Nordin, C. F. (1976)	NOR	14
Pratt, C. J. (1970)	PRA	5

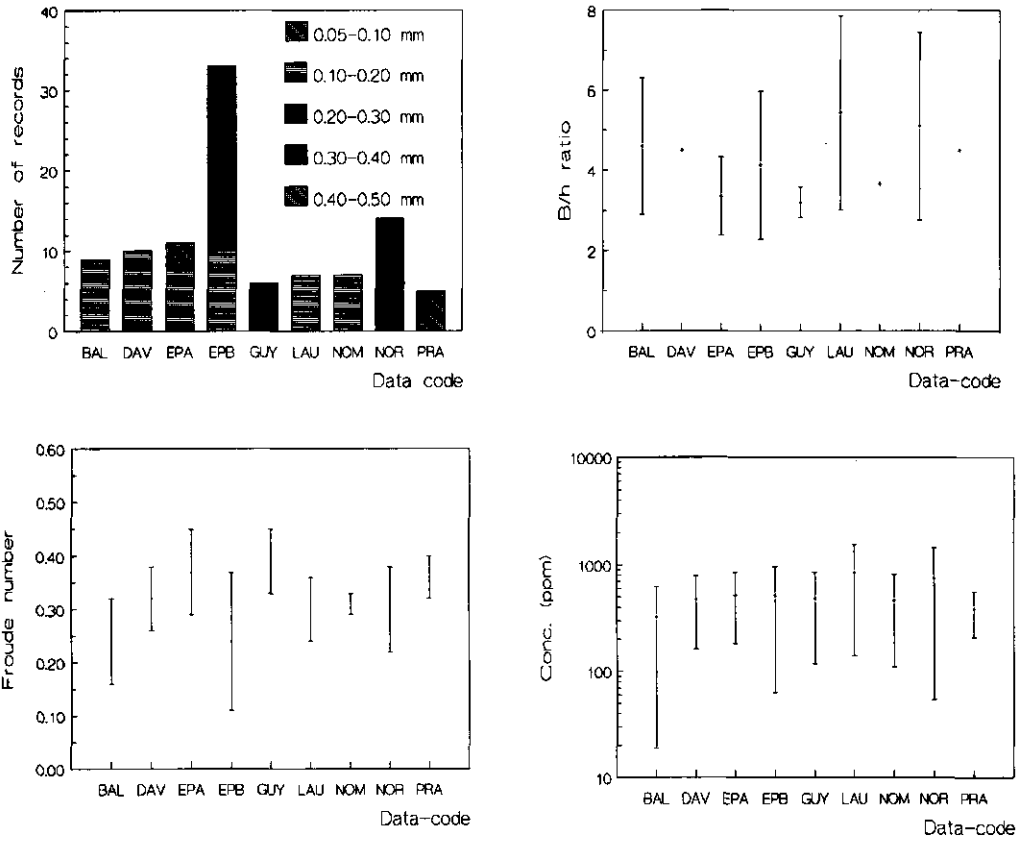

Figure 4.46 Characteristic values of the selected data

The procedures 1, 2 and 3 have been compared on a relative basis. The measured sediment transport was compared with the predicted sediment transport calculated by using one of the described procedures. The predictability of each procedure is measured in terms of the well-predicted values of the sediment transport within a certain accuracy range. It can be expressed as:

$$\frac{\text{Measured value}}{f} \leq \text{Predicted value} \leq \text{Measuredvalue} * f \tag{4.75}$$

$$\text{Accuracy} = \frac{\text{number of well-predicted values}}{\text{total values}} \tag{4.76}$$

where:

f = error factor

Figure 4.47 shows the results of the accuracy for all procedures and sediment transport methods and for different levels of error factor (f), when compared with the selected data. Based on the overall comparison procedure 3 behaves better than the other two procedures for all the sediment transport predictors. The best performance of procedure 2 is observed for the Brownlie predictor method and the best performance of procedure 1 is observed for the Engelund and Hansen predictor method. The Brownlie method (BRO) has a tendency to underpredict the sediment transport for the flow conditions in irrigation canals, which is compensated by the higher predictability of procedure 2. The underpredictability of the Brownlie predictor has been shown before, namely during the comparison of the various sediment transport predictors against some selected laboratory and field data. In that part the Ackers and White (A-W), Brownlie (BRO), Engelund and Hansen (E-H), van Rijn (RIJ) and Yang (YAN) sediment transport calculations have been compared with the selected data. Figure 4.25 shows the relative number of overpredicted values of the sediment transport when compared with measured values. The Brownlie predictor has a tendency to underpredict the sediment transport, while the Engelund and Hansen predictor overpredicts in most cases. The Ackers and White method overpredicts in a very few cases only. For the Ackers and White method procedure 3 behaves much better than the other two procedures for all the levels of the error factor. For the Brownlie method procedure 2 has a slightly better performance for a large error factor (f = 2.5) than procedure 3. In an opposite way procedure 1 has a performance comparable with procedure 3 for the Engelund and Hansen method. The over-predictability of the Engelund and Hansen method (fig 4.25) is compensated by the low prediction of procedure 1. Figure 4.48 shows the ratio of sediment transport computation of each procedure related to procedure 3. Procedure 3 predicts the sediment transport in a range between procedure 1 and 2. The better predictability of the procedure 3 in comparison with procedures 1 and 2 is obvious. Figure 4.49 shows the performance of the procedures 3 when applied with Ackers and White, Brownlie and Engelund and Hansen predictors.

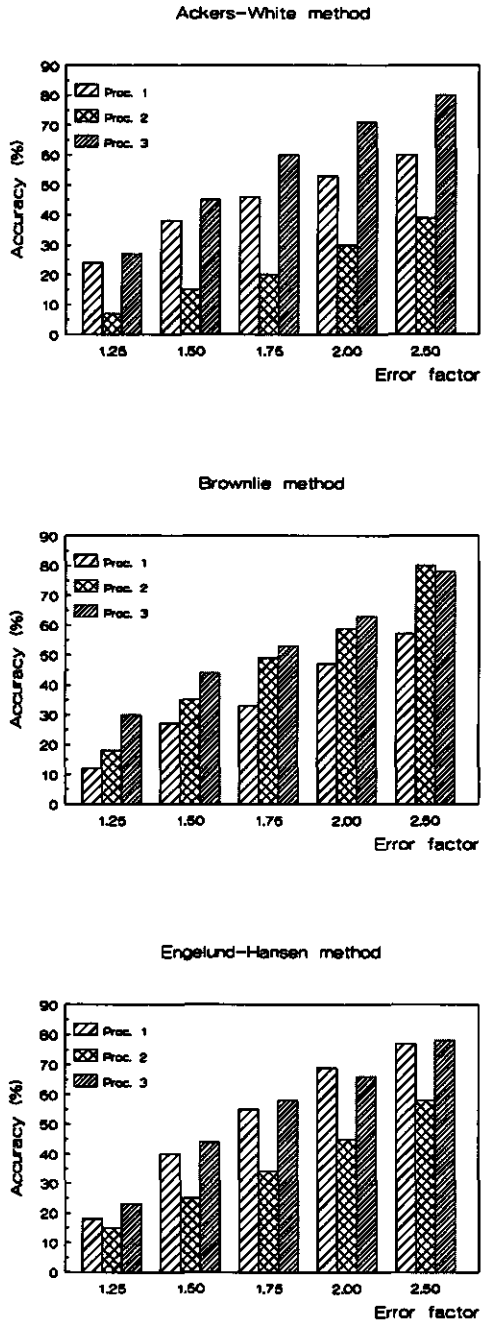

Figure 4.47 Comparison of the three procedures to compute sediment transport in non-wide canals

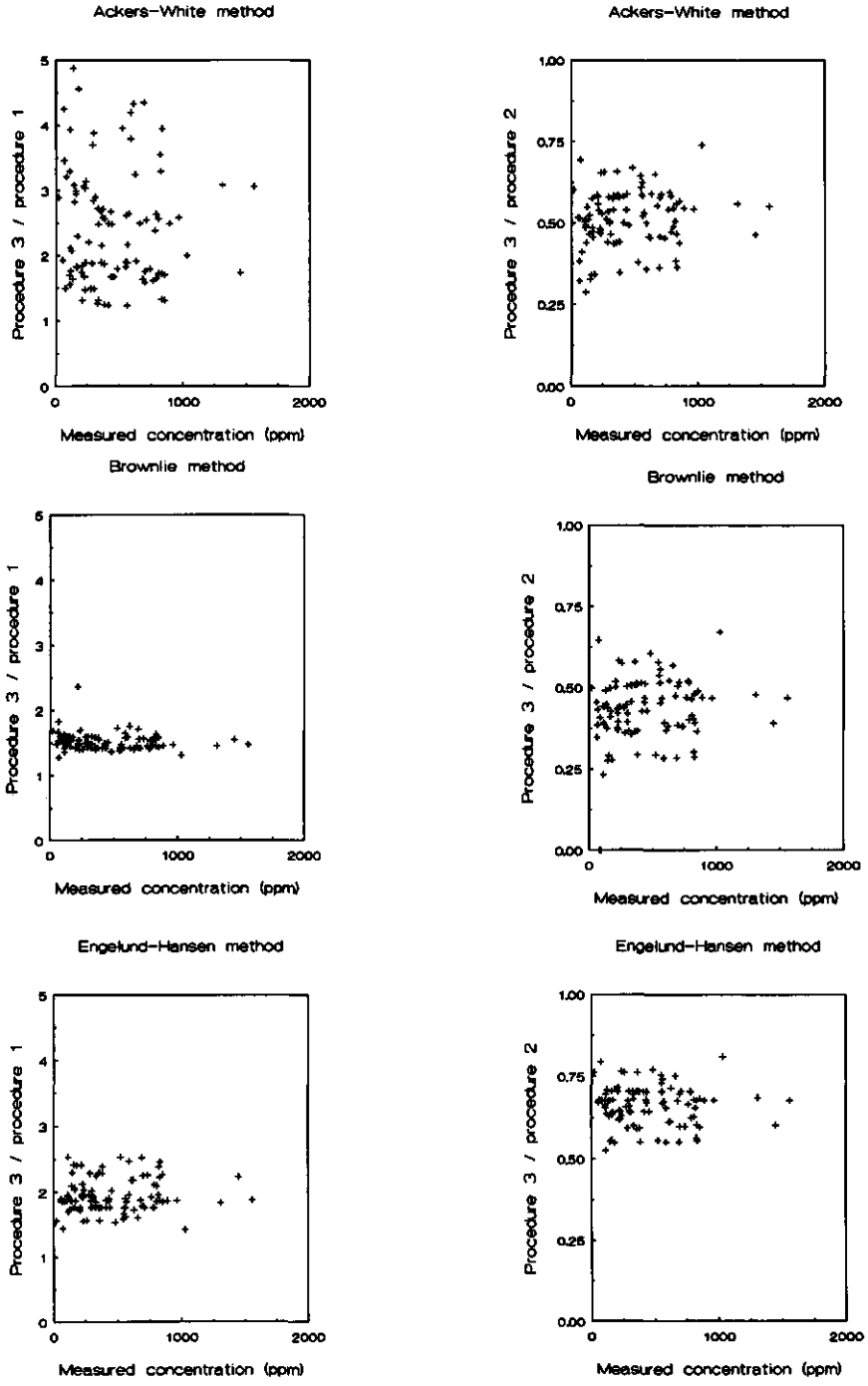

Figure 4.48 Ratio of sediment transport calculations between procedures 1, 2 and 3.

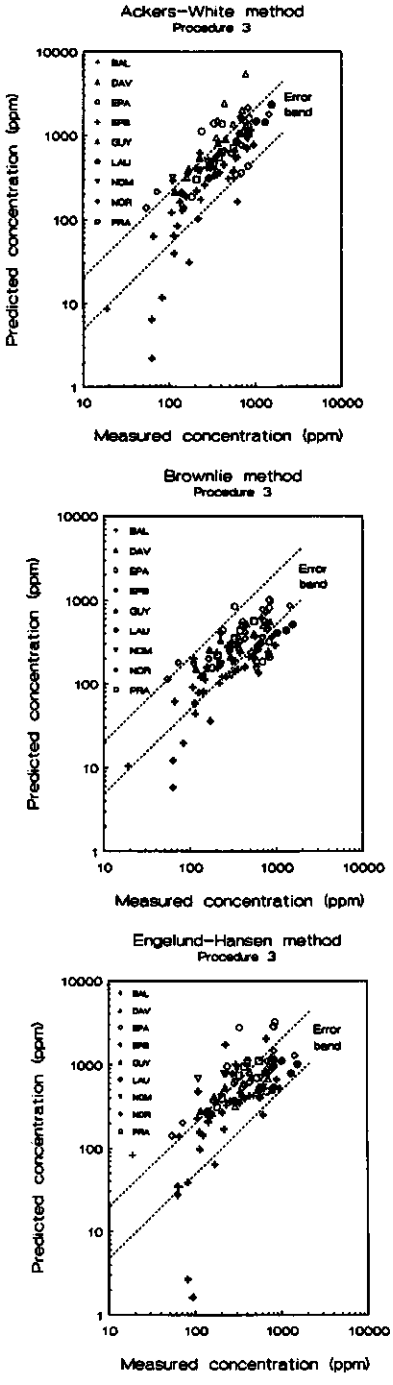

Figure 4.49 Performance of procedure 3 to compute the total sediment transport by the Ackers and White, Brownlie and Engelund-Hansen predictors at an error factor 2.

4.4 Conclusions

Applications of the existing sediment transport concepts under flow conditions and sediment characteristics encountered in irrigation canals were carried out in the previous sections. Those applications were intended to evaluate the suitability of those concepts on some particular conditions. In that way the increase of the unavoidable uncertainties and inaccuracies during the computations of the sediment transport can be minimized.

From the applications of the sediment transport concepts for the conditions prevailing in irrigation canals some conclusions can be drawn:

- all the bed forms described for the lower regime (ripples, mega-ripples and dunes) can be expected in irrigation canals;
- bed form types were better described by the van Rijn method. More than 75% of the observed types of bed form were well-predicted with the van Rijn method;
- existing friction factor predictors take only into account the bottom friction. For non-wide canals the side banks will have an important effect on the friction factor, therefore a weighed value of the friction factor will be required;
- the van Rijn method for predicting the friction factor behaved best when compared with measured values of the friction factor. More than 90% of the measured values were well-predicted with this method within an error band of 30%;
- the proposed method for predicting the effective roughness in a trapezoidal canal with different roughnesses along the wetted perimeter behaved better than the existing methods. More than 90% of the measured values were well-predicted by this method. Also the minimum value of the standard error and the narrowest range of variation of the predicted value were observed for the proposed method;
- the existing methods for predicting effective roughness in a rectangular canal with different roughnesses along the wetted perimeter can not be explicitly applied;
- the proposed method for estimating the effective roughness in a rectangular canal with composite roughness along the wetted perimeter predicted more than 95% of the measured values within a error band of 15%;
- existing predictors of the sediment transport capacity of wide canals do not take into account the geometry and its effect on the velocity distribution over the cross section;
- sediment transport capacity is still not well described by the existing predictors. For the best prediction methods, only 60% of the measured values were well-predicted within an error band of 100%;
- the Ackers and White and Brownlie methods are the best to predict the sediment transport capacity under the prevailing flow conditions and sediment characteristics in irrigation canals;
- the proposed method for computing the sediment transport capacity in a non-wide canal (rectangular and trapezoidal cross sections) behaved better than the other methods.

5 MATHEMATICAL MODEL FOR SEDIMENT TRANSPORT IN IRRIGATION CANALS

5.1 General

Clogging of turnouts and siltation of the canal system are some of the main problems of the operation and maintenance of irrigation systems. Annually high investments are required for rehabilitation and to keep them suitable for their purpose. In an irrigation network the sediment transport has to be properly estimated in time and space. A proper prediction of the sediment deposition along the entire canal during the irrigation season will contribute to make it possible that the canals are operated in such a way that irrigation needs are met and at the same time a minimum deposition is expected.

Although, it is difficult to predict the quantity of sediment that will be deposited in irrigation canals (Brabben, 1990), the numerical modelling of sediment transport offers the possibility of predicting and evaluating the sediment transport under very general flow conditions (Lyn, 1987). A mathematical model which includes the sediment transport concepts for the specific conditions of irrigation canals is an important and timely tool for designer and managers of those systems. Previous chapters presented a detailed analysis of the relevant processes and a physical and mathematical description of the sediment transport concepts under the specific conditions of irrigation canals. It will be the basis of the mathematical model for simulating the sediment transport in these canals. Hereafter a description of the mathematical model for the computation of sediment transport under changing flow conditions in an irrigation canal is presented. Based on that a model is developed to predict sediment transport and the deposition or entrainment rate for various flow conditions and sediment inputs during the irrigation season.

5.2 Numerical solution of water flow equations

Water flow in irrigation canals has been schematized as quasi-steady flow in which the governing equations can be represented as described in paragraph 3.1 by:

- continuity equation:

$$\frac{\partial Q}{\partial x} = 0 \quad \therefore \quad Q = \text{constant} \tag{5.1}$$

at points of confluences:

$$Q \pm q_l = 0 \tag{5.2}$$

- dynamic equation:

$$\frac{dh}{dx} = \frac{S_0 - S_f}{1 - F_r^2} \tag{5.3}$$

where:

Q = flow rate (m^3/s)
q_l = inflow/outflow discharge (m^3/s)
h = water depth (m)
S_0 = bottom slope
S_f = energy line slope
Fr = Froude number
x = length coordinate in x direction (m)

Several methods are available to solve the dynamic equation of gradually varied flow for prismatic canals. Among those methods, Henderson (1966), Chow (1983), Depeweg (1993) and Rhodes (1995) show a comprehensive description of the graphical-integration, direct integration, direct step, standard step, Newton-Raphson solution and the predictor-corrector method. The predictor-corrector method is proposed and will be applied in several steps:
- start at downstream end point ($x = x_0$)
- compute the derivative (eq. 5.3) at point $x = x_i = x_0$ for given S_0, S_f, and Fr

$$\left(\frac{dh}{dx}\right)_i = \frac{(S_0 - S_f)_i}{(1 - Fr^2)_i} \tag{5.4}$$

- calculate the water depth at point $x = x_{i+1}$

$$h_{i+1} = h_i + \left(\frac{dh}{dx}\right)_i (x_{i+1} - x_i) \tag{5.5}$$

- compute: $(S_f)_{i+1}$, $(Fr)_{i+1}$
- calculate the derivative at point $x = x_{i+1}$

$$\left(\frac{dh}{dx}\right)_{i+1} = \frac{(S_0 - S_f)_{i+1}}{(1 - F_r^2)_{i+1}} \tag{5.6}$$

- calculate the mean derivative

$$\left(\frac{dh}{dx}\right)_{mean} = \frac{\left(\frac{dh}{dx}\right)_i + \left(\frac{dh}{dx}\right)_{i+1}}{2} \tag{5.7}$$

- calculate the new value of h_{i+1} by:

$$h_{(i+1)2} = h_i + \left(\frac{dh}{dx}\right)_{mean} (x_{x+1} - x_i) \tag{5.8}$$

- check the accuracy of the predictor-corrector method by:

$$|h_{(i+1)1} - h_{(i+1)2}| \leq e \tag{5.9}$$

where:

e = accuracy degree. In the model an accuracy degree of e = 0.005 m was assumed.

Figure 5.1 shows a schematization of the predictor-corrector method for the numerical solution of equation 5.3.

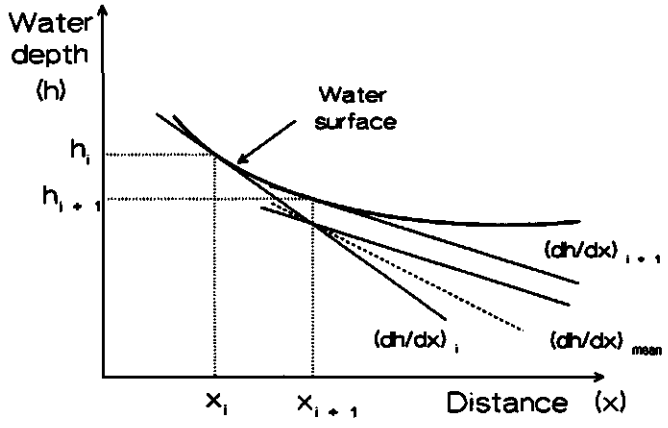

Figure 5.1 Predictor-corrector method for water flow

The numerical solution of the one-dimensional flow equations requires certain conditions that can be summarized as:

- condition describing the geometric variables of the canal: bottom width, side slope, bottom slope, length;
- condition related to the bed roughness (equivalent height roughness, fixed or movable boundaries, single or composite roughness, obstruction degree due to vegetation on the side banks);

- water level or discharge-water level relationship at the outflow boundary;
- discharge at the inflow boundary;
- internal conditions related to:
  * lateral discharge q_l (bifurcations and/or confluences): a balance of the water flow at points with lateral discharge (equation 5.2)is required;
  * presence of hydraulic structures: in most cases water level at both sides of structures can not be computed using the Saint Venants equations. Hydraulic computation of a water profile in the canal is uncoupled of the hydraulic computation of the structures. A specific hydraulic equation to calculate the water surface elevation at the upstream side of the structure is required. Those equations are not valid for all the possible operating conditions. They should be applied for the hydraulic conditions as will be specified below for some types of flow structures. Equations for flow control structures are depending on the water flow and variables related with geometry and location of the structures. Water level at the upstream side of the structure will be used as downstream boundary condition for computing the water profile in the upstream reach of the canal.

Several types of structures are specified in the mathematical model. The location of those structures defines the boundary between two reaches of the canal. The types of structures included in the mathematical model are: overflow type (broad and sharp crested weir), undershot type (sharp edge orifice with rectangular cross section), siphons, culverts with submerged type condition, flumes and drops.

Overflow type: This type of structures is defined by: width of the weir crest (B) and level of the crest weir (z_w). Two types of overflow types were described: broad and sharp rectangular crested weirs.

For broad crested weirs in modular flow ($h_2 < 0.7\ h_1$) the upstream water level (z_u) is computed by (fig. 5.2.a):

$$z_u = z_w + \left(\frac{Q}{1.67\ B}\right)^{2/3} + \frac{V_1^2}{2\ g} \qquad (5.10)$$

and for submerged flow ($h_2 > 0.7\ h_1$):

$$z_u = z_w + \left(\frac{\mu\ Q}{1.67\ B}\right)^{2/3} \qquad (5.11)$$

For sharp crested weirs (fig. 5.2.b) the nappe passing trough the weir has to be free with an air-filled area below the outflowing jet in such a way that atmospheric pressure prevails in that area. Under those flow conditions the upstream water level is (z_u) calculated as:

$$z_u = z_w + \left(\frac{Q}{1.92\ B}\right)^{2/3} + \frac{V_1^2}{2\ g} \qquad (5.12)$$

where:

Q = flow discharge (m^3/s)
V_1 = upstream mean velocity (m/s)
B = width of the crest (m)
μ = correction factor for submerged flow ($0 \leq \mu \leq 1$)
z_w = crest level (m)
z_u = upstream water level (m)
g = gravity acceleration (m/s^2)

Undershot type: underflow structure types commonly used in irrigation canals are sliding, flat or radial gates with a rectangular opening (fig 5.2.c). Those gates are characterized by: width of the rectangular opening (B), height of the opening (W). Flow conditions in those structures can be described by the same hydraulic equation. Differences are included in the discharge coefficient (c_d) which will depend on upstream and downstream water level and type of gate (flat or radial).

$$z_u = z_b + \left[\ y_2 + \frac{1}{2\ g}\left(\frac{Q}{c_d\ B\ W}\right)^2\right] \qquad (5.13)$$

where:

Q = flow discharge (m^3/s)
B = width of the opening (m)
W = height of the opening (m)
y_2 = downstream water depth (m)
z_b = bottom level (m)
z_u = upstream water level (m)
c_d = discharge coefficient
g = gravity acceleration (m/s^2)

Culverts and inverted siphons: frictionless water flow in inverted syphons and culverts with a submerged outlet are described (fig 5.2.d). Those structures are characterized by the number of pipes and the pipe diameter. Upstream water level is computed by:

$$z_u = z_d + 2.1\ \frac{V^2}{2\ g} \qquad (5.14)$$

where:

V = mean velocity in the pipe (m/s)

z_d = downstream water level (m)
z_u = upstream water level (m)
g = gravity acceleration (m/s^2)

Flumes: critical depth flumes with an upstream head-discharge relationship with the form $Q = K\ h^n$ were also incorporated into the mathematical model (fig. 5.2.e). Flumes are characterized by the values of K and n of the head-discharge relationship and by the floor level of the flume. The upstream water level is calculated by:

$$z_u = z_f + \left(\frac{Q}{K}\right)^{\frac{1}{n}} \tag{5.15}$$

where:
Q = flow discharge (m^3/s)
K, n = constants of the head-discharge relationship (m)
z_f = bottom level of flume (m)
z_u = upstream water level (m)

Drops: This structure is included as different bottom levels at the boundary of the reaches.

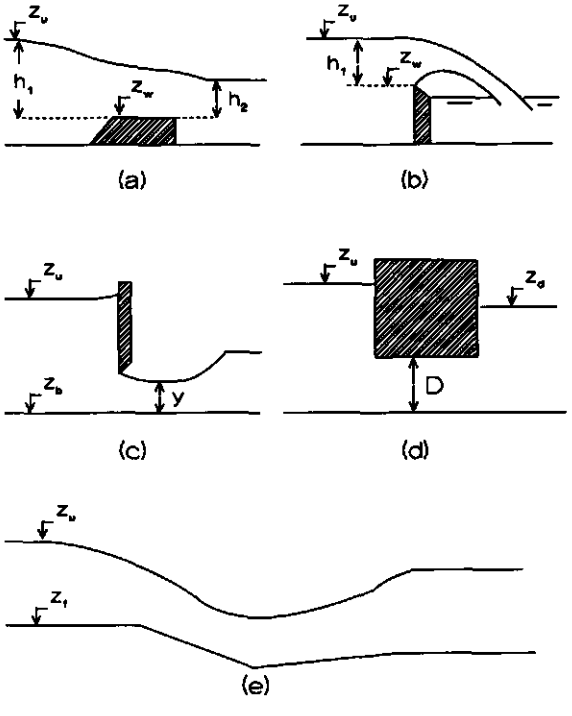

Figure 5.2 Schematization of flow control structures

5.3 Morphological changes of the bottom level

For one-dimensional computations, fixed side banks and occurrence of deposited or picked-up sediments on the bottom of the irrigation canals is assumed. The interrelation between the water movement and the morphological changes on the bottom level can be summarized by the following equations:

$$\frac{dh}{dx} = \frac{S_0 - S_f}{1 - Fr^2} \tag{5.16}$$

and

$$\frac{\partial Qs}{\partial x} + B\,(1 - P)\,\frac{\partial z}{\partial t} = 0 \tag{5.17}$$

These equations will be solved alternatively. First the water flow equation (eq. 5.16) is solved to determine the flow profile for given boundary conditions related to water level and discharge. Details of that procedure are shown in the previous paragraph. Next, the output values of equation 5.16 are used to solve equation 5.17 for the calculation of the mass balance for the total sediment transport. The first term in equation 5.17 represents either the total entrainment or the total deposition rate between two points along the x-axis of the canal. It will depend on a balance between the transport capacity of the canal and the existing sediment load along the x-axis of the canal. The second term represents the net flux of sediment across a horizontal plane near the bed that will lead to a change of the bottom level of the canal.

Several finite difference methods based on explicit and implicit schemes have been used to solve equation 5.17. Cunge (1980), de Vries (1987) and Vreugdenhil (1982 and 1989) describe the Lax, modified Lax, Lax-Wendroff and the 4-points implicit schemes as methods to solve the morphological equation. The modified Lax scheme can be used quite successfully, though is not claimed to be the best method (Abbot & Cunge, 1982). This method can be expressed as:

$$z_{i,j+1} = z_{i,j} - \frac{1}{B\,(1 - P)}\left[\frac{Qs_{i+1,j} - Qs_{i-1,j}}{2\,\Delta x} - \frac{1}{2\,\Delta t}\left[\,(\alpha_{i+1,j} + \alpha_{i,j})\,(z_{i+1,j} - z_{i,j}) - (\alpha_{i,j} + \alpha_{i-1,j})\,(z_{i,j} - z_{i-1,j})\,\right]\right] \tag{5.18}$$

This numerical scheme can not be applied to the downstream and upstream boundaries. An adapted scheme to the downstream boundary is described by:

$$z_{i,j+1} = z_{i,j} - \frac{1}{B\,(1 - P)}\left[\frac{Qs_{i+1,j} - Qs_{i-1,j}}{2\,\Delta x} + \frac{1}{2\,\Delta t}\left[\,(\alpha_{i,j} + \alpha_{i-1,j})\,(z_{i,j} - z_{i-1,j})\,\right]\right] \tag{5.19}$$

and for the upstream boundary by:

$$z_{i,j+1} = z_{i,j} - \frac{1}{B\,(1-p)}\left[\frac{Qs_{i+1,j} - Qs_{i-1,j}}{2\,\Delta x} - \frac{1}{2\,\Delta t}\left[\,(\alpha_{i+1,j} + \alpha_{i,j})\,(z_{i+1,j} - z_{i,j})\,\right]\right] \tag{5.20}$$

in which the subscripts i and j mean:

$$i \equiv i\,\Delta x \quad \text{and} \quad j \equiv j\,\Delta t \tag{5.21}$$

and:

Qs = sediment discharge (m^3/s)
p = porosity
B = bottom width (m)
Δx = distance (m)
z = bottom level (m)
Δt = time step (m)
α = parameter used for stability and accuracy of the numerical scheme.

The stability of the scheme is given by (Vreugdenhil, 1989):

$$\sigma^2 \le \alpha \le 1 \tag{5.22}$$

Accuracy of this scheme is increased if (Vreugdenhil, 1982):

$$\alpha \approx \sigma^2 + 0.01 \tag{5.23}$$

in which σ is called the Courant number and is described by:

$$\sigma = N\,V\,\frac{Qs/Q}{1 - Fr^2}\,\frac{\Delta t}{\Delta x} \tag{5.24}$$

where:

N = exponent of velocity in the sediment transport equation $s = f(V^N)$
Q = discharge (m^3/s)
Qs = sediment discharge (m^3/s)
V = mean velocity (m/s)
Δt = time interval (s)
Δx = distance (m)
Fr = Froude number

Figure 5.3 shows a schematization of the deposition or entrainment computation at the bottom of the canal.

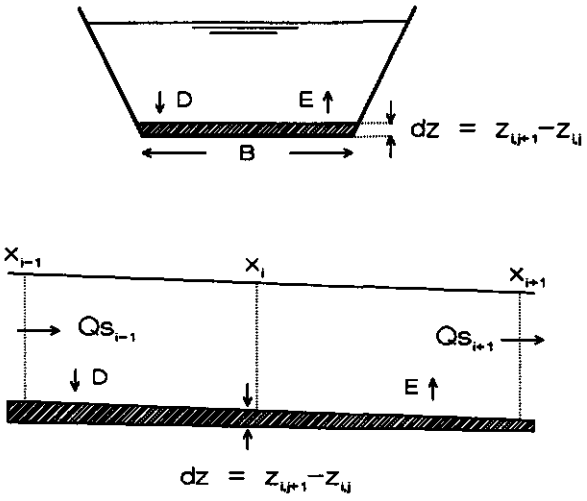

Figure 5.3 Schematization of computations of changes on the bottom level

Figures 5.4 to 5.6 show some schematizations for different flow conditions in a canal and they illustrate the way of computation for the sediment mass balance after one time step. Let us take a uniform flow as example (fig.5.4). In case the sediment transport capacity of the canal Q_{se} is lower than the actual sediment transport Q_s ($\partial Qs/\partial x < 0$) deposition is expected up to a point where Q_s reaches the equilibrium sediment transport. An adaptation length will be expected for the adjustment of the actual sediment transport to the sediment transport capacity of the canal. From this point onwards the sediment transport will remain constant. For Q_{se} larger than Q_s two possibilities can occur depending on whether motion of sediment on the bottom occurs or not. Motion of sediment is evaluated in terms of the mobility parameter θ and the critical mobility parameter θ_{cr}. In the first case ($\theta > \theta_{cr}$) entrainment of particles and increasing sediment transport occurs until the adaptation to the sediment transport capacity of the canal. For the second case the actual sediment load is conveyed without changes.

For gradually varied flows a distinction between backwater and drawdown effects has to be made. Figure 5.5 shows the backwater effect on the sediment transport in a canal. For Q_s larger than the Q_{se} ($\partial Qs/\partial x < 0$) deposition will occur to reach adaptation to the sediment transport capacity of the canal ($Q_{se} = Q_s$). From that point onward a continuous deposition, in downstream direction may be expected. For Q_s lower than the Q_{se} ($\partial Qs/\partial x > 0$), the actual sediment transport can either remain constant along the canal ($\theta < \theta_{cr}$) or increase up to Q_{se} equal to Q_s ($\theta > \theta_{cr}$). A continuous deposition in downstream direction is expected. The drawdown effect is shown in figure 5.6. For Q_s larger than Q_{se} deposition will occur up to the equilibrium condition ($Q_{se} = Q_s$). From that point onwards a continuous entrainment is expected. In case of Q_{se} larger than Q_s either the latter remains constant ($\theta < \theta_{cr}$) or increases to reach Q_s ($\theta > \theta_{cr}$) and a continuous entrainment in downstream direction will occur.

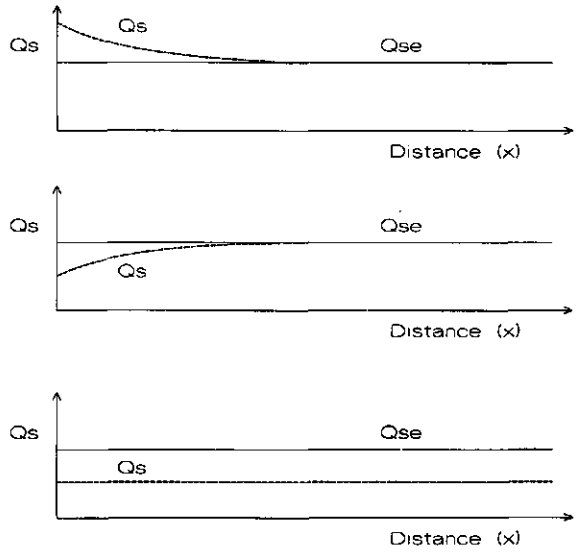

Figure 5.4 **Sediment transport for uniform flow**

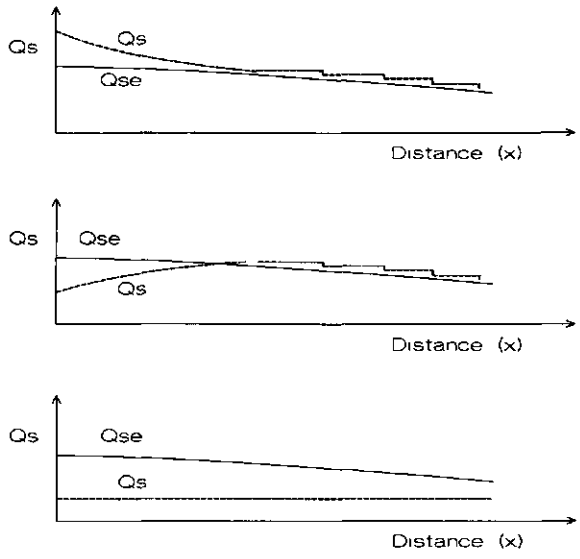

Figure 5.5 **Sediment transport for gradually varied flow (backwater effect)**

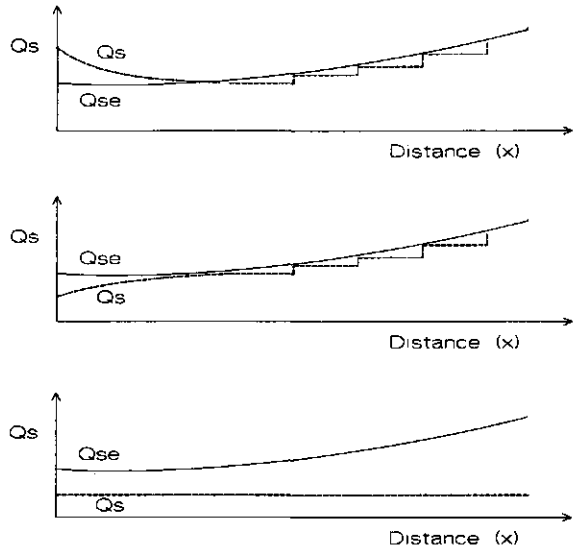

Figure 5.6 Sediment transport for gradually varied flow (drawdown effect)

The numerical solution of the one-dimensional sediment mass balance equation requires some boundary conditions for water flow and sediment. These conditions are:

- condition describing the geometrical variables of the canal during a time step: bottom width, bottom slope, bottom level.
- condition describing the water flow stage along the entire canal during a time step: discharge, mean velocity, roughness condition, water depth, energy slope;
- incoming sediment characteristics (sediment load and sediment size) at the upstream boundary;
- sediment discharge along the entire canal;
- changes in bottom width and/or bottom level, confluences and bifurcations can be incorporated by applying continuity for water discharge and sediment.

For the computation of the sediment discharge along the entire canal the adaptation of the entering sediment load to the sediment transport capacity of the reaches has to be considered. The adaptation of the actual sediment load to the sediment transport capacity is given in terms of sediment concentration C by Gallapatti's depth-integrated model (see part 3.3.2.2) by:

$$C = C_e - (C_e - C_0) \exp - \frac{x}{L_A} \quad \text{with} \quad L_A = f\left(\frac{u_*}{V}, \frac{w_s}{u_*}, h\right) \tag{5.25}$$

where:

C = actual sediment concentration at distance x
C_e = equilibrium sediment concentration
C_0 = sediment concentration at the head of the reach
x = distance along the x-direction ($x \equiv i\,\Delta x$)
L_A = adaptation length
w_s = fall velocity
u_* = shear velocity
V = mean velocity
h = water depth

In order to determine the actual sediment concentration along the x - direction, the values of the variables C_0, L_A, Δx and C_e must be known. The first one, the initial concentration C_0 does not depend on the local flow condition. It depends on the source of water and/or the sediment trap located at the head of the irrigation network. At boundaries between reaches the sediment load passing through the downstream part of the upstream reach will become C_0 for the next reach.

In a gradually varied flow the values of C_e, h, V, u_* and f are functions of x. These variables may be known in advance at any point in the x-direction if the water flow equation are solved firstly (uncoupled technique). That means that in any point of the canal, i = 0, 1,....., n are given C_e, h, V, u_* and the dimensionless parameters u_*/V and w_s/u_*.These variables will be determined according to the following procedure:

- the Δx-value is fixed according to the desired degree of accuracy for the numerical solution (eqs. 5.22-5.24) and the need for representing the adaptation of the actual non-equilibrium condition to the sediment transport capacity of the canal. The Δx-value should be much smaller than the required length for adaptation of the actual sediment transport to the sediment transport capacity of the canal.An adaptation length of 99% was adopted which represents the required length (L_{99}) for a 99% adaptation to the transport capacity of the canal. The adaptation length L_{99} is determined as:

$$\frac{(C - C_e)}{(C_0 - C_e)} = 0.01 \qquad (5.26)$$

then, substituting in equation 5.25 results:

$$L_{99} = \ln (100)\, L_A = 4.61\, L_A \qquad (5.27)$$

- computation of the L_A-value. For the local flow conditions the values of w_s/u_*, u_*/V and the water depth (h) are known in advance. Minimum values for L_A are given for the largest values of the dimensionless parameter w_s/u_*. Typical flow conditions in irrigation canals are able to initiate suspension of the sediment particles (see fig. 3.2)

Therefore the large value of the dimensionless parameter w_s/u_* can be represented by (van Rijn, 1984b):

$$\theta'_{cr} = \frac{16}{D_*} \frac{w_s^2}{(s-1)\, g\, d_{50}} \quad \text{for} \quad 1 \leq D_* \leq 10 \tag{5.28}$$

and:

$$\theta'_{cr} = \frac{16\, w_s^2}{(s-1)\, g\, d_{50}} \quad \text{for} \quad D_* \geq 10 \tag{5.29}$$

replacing θ_{cr}' in terms of the shear velocity gives:

$$\frac{u_*^2}{(s-1)\, g\, d_{50}} = \frac{16}{D_*} \frac{w_s^2}{(s-1)\, g\, d_{50}} \quad \therefore \quad \frac{w_s}{u_*} = \frac{\sqrt{D_*}}{4} \tag{5.30}$$

and:

$$\frac{u_*^2}{(s-1)\, g\, d_{50}} = \frac{16\, w_s^2}{(s-1)\, g\, d_{50}} \quad \therefore \quad \frac{w_s}{u_*} = \frac{1}{4} \tag{5.31}$$

where:

θ_{cr}' = critical mobility parameter for initiation of suspension (van Rijn, 1984)
w_s = fall velocity (m/s)
u_* = shear velocity (m/s)
V = mean flow velocity (m/s)
D_* = particle diameter parameter
s = relative density
g = gravity acceleration (m/s^2)
d_{50} = median diameter (m)

Those maximum values of the parameter w_s/u_* satisfy the requirements for validity of the depth-integrated model (Ribberink, 1986)

The dimensionless parameter u_*/V can be determined by:

$$\frac{u_*}{V} = \frac{g^{0.5}}{C} \tag{5.32}$$

where:

C = Chézy coefficient ($m^{1/2}/s$)
u_* = shear velocity (m/s)
V = mean flow velocity (m/s)
g = gravity acceleration (m/s^2)

Once the motion of sediment has been initiated the values of the Chézy coefficient can be estimated depending on the type of roughness along the wetted perimeter by:

$$C = 18 \log \frac{12\ R}{k_s} \qquad \text{for single roughness} \qquad (5.33)$$

and

$$C_e' = f_c\ (18 \log \frac{12\ R}{k_{se}}) \qquad \text{for composite roughness} \qquad (5.34)$$

where:

k_s = hydraulic roughness of a canal with single roughness
k_{se} = hydraulic roughness of a canal with composite roughness (eq. 4.27)
C_e' = modified effective Chézy coefficient for a canal with composite roughness
f_c = correction factor for the Chézy coefficient
R = hydraulic radius

Different lengths (in meter) for 99% of adaptation from non-equilibrium to the sediment transport capacity of irrigation canals are shown in figure 5.7. From that figure estimated Δx-values can be drawn for expected values of water depth, Chézy coefficient and fall velocity w_s of the sediment.

the value of the depth-averaged equilibrium concentration C_e can be determined by using the selected sediment transport predictors such as: Ackers-White, Brownlie or Engelund-Hansen predictors. Those formulae compute the sediment transport per unit width (q_s) which is completely determined by the local flow conditions and the sediment properties. The total sediment transport across the section Q_{se} is calculated by:

$$Q_s = \alpha\ B\ q_s \qquad (5.35)$$

and the C_e-value is calculated by:

$$C_e = \left(s\ \frac{Q_s}{Q} \right) 1000000 \qquad (5.36)$$

where:

q_s = sediment transport per unit width (m^2/s)
Q_s = total sediment transport (m^3/s)
Q = total water discharge (m^3/s)
B = bottom width (m)
α = correction factor
s = relative sediment density
C_e = equilibrium concentration (ppm)

Internal conditions along the canal were taken into account for computing the sediment transport distribution at boundaries between reaches of canals and/or branches at bifurcations or confluences.

Changes in bottom width and/or bottom level and confluences were incorporated by applying continuity for water discharge and sediment discharge in the following way:
- changes in the bottom width and /or bottom level by:

$$Q_1 = Q_2 \qquad \text{and} \qquad Q_{s_1} = Q_{s_2} \tag{5.37}$$

- confluences:

$$Q_1 + Q_2 = Q_3 \qquad \text{and} \qquad Q_{s_1} + Q_{s_2} = Q_{s_3} \tag{5.38}$$

Bifurcations were also incorporated by applying continuity for water and sediment discharge as described before, but the distribution of water and sediment at the branches will depend on the local flow pattern. The distribution of sediment at the branches can be proportional to the discharge or not. No analytical solution for the sediment distribution at bifurcations is yet available (de Vries, 1987).

$$Q_1 = Q_2 + Q_3 \qquad \text{and} \qquad Q_{s_1} = Q_{s_2} + Q_{s_3} \tag{5.39}$$

with:

$$Q_{s_2} = \theta\, Q_{s_1} \qquad \text{and} \qquad Q_{s_2} = (1 - \theta)\, Q_{s_1} \tag{5.40}$$

where θ represents the ratio of distribution related to the incoming sediment rate.

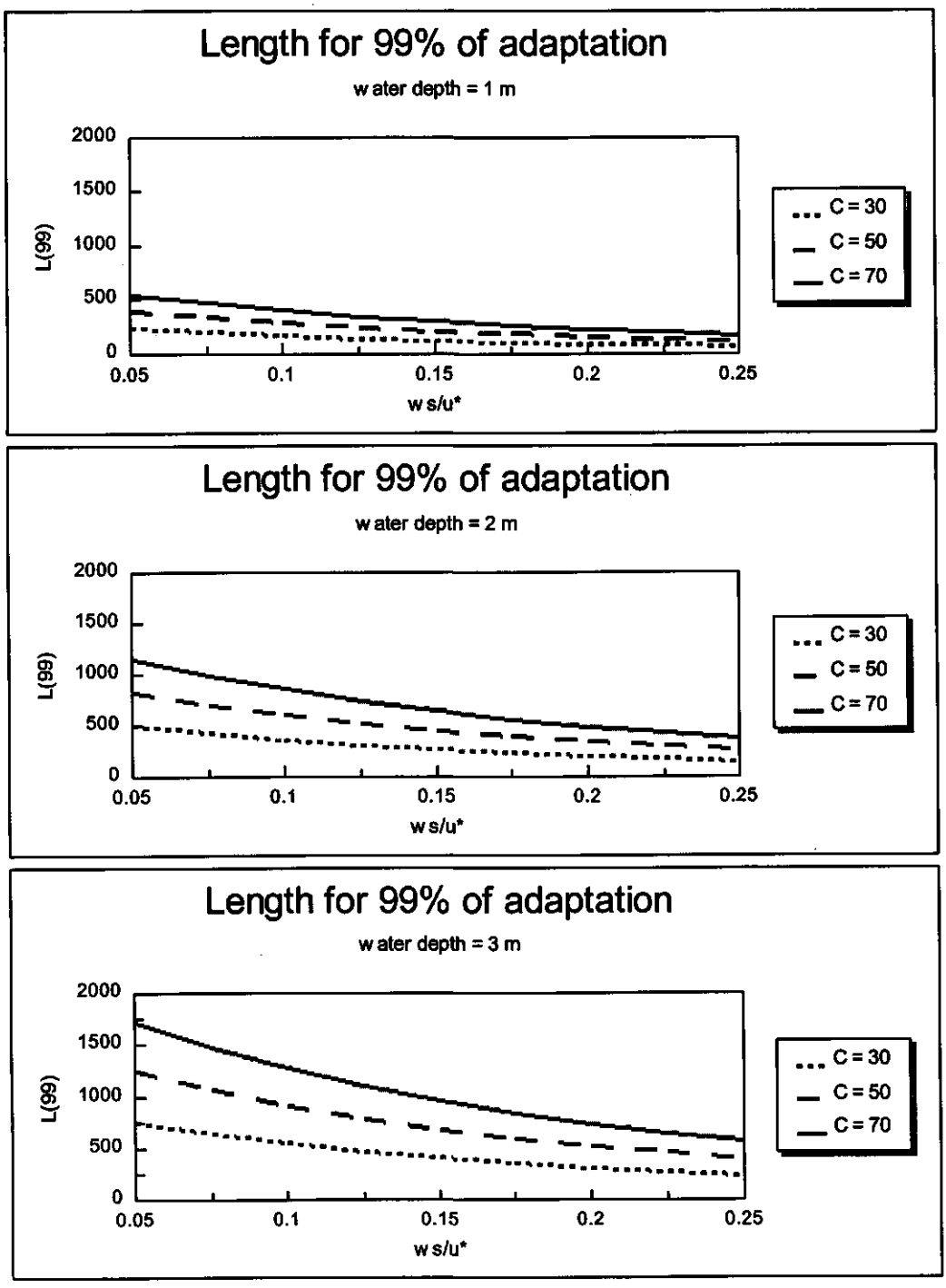

Figure 5.7 Lengths for 99% of adaptation as function of the Chézy coefficients and water depth

Figure 5.8 shows a schematization of the internal boundaries for water flow and sediment transport.

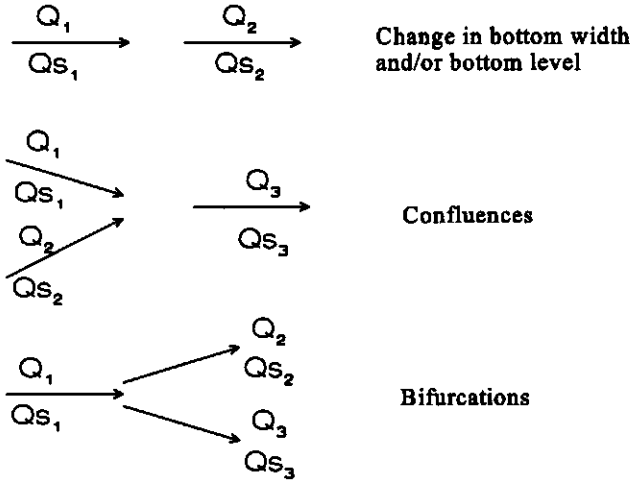

Figure 5.8 Internal condition for mass balance of water flow and sediment

The type of flow control structure was taken into account for determining the sediment discharge at the boundaries between reaches. The sediment mass balance was considered at the upstream and downstream end of the flow control structure. Additional internal condition was introduced for sharp and broad crested weirs. Those flow control structures have a poor sediment passing capacity (Bos, 1989). Only suspended sediment load was assumed to pass through those types of structures. The suspended load was computed by using the procedure described by van Rijn (1984a and 1984b) as described in part 3.2.

The entrainment and deposited rates in a reach of a canal can be derived from the sediment mass balance in the reach, thus :

- the entrainment rate for a quasi-steady flow may be derived by:
  for $\theta \geq \theta_{cr}$

$$E = \frac{\partial Q_s}{\partial x} = \frac{Q}{s} \frac{\partial C}{\partial x} \qquad (5.41)$$

or

$$E = \frac{Q}{s} \frac{(C_{i+1} - C_i)}{\Delta x} \qquad (5.42)$$

for $\theta < \theta_{cr}$

$$\frac{\partial Q_s}{\partial x} = 0 \quad \therefore \quad E = 0 \tag{5.43}$$

The total entrainment rate can be computed from:

$$E_t = E\ \Delta x \tag{5.44}$$

where:

E = entrainment rate in m^3/ms
E_t = total entrainment rate in m^3/s
Q_s = total sediment transport in m^3/s
Δx = distance between two sections in m
s = relative density

The net deposition rate for steady flow condition may be derived by:

$$D = \frac{\partial Q_s}{\partial x} = \frac{Q}{s}\frac{\partial C}{\partial x} \tag{5.45}$$

or

$$D = \frac{Q}{s}\frac{(C_{i+1} - C_i)}{\Delta x} \tag{5.46}$$

The total deposition rate is computed as:

$$D_t = D\ \Delta x \tag{5.47}$$

where:

D = deposition rate in m^3/ms
D_t = total deposition rate in m^3/s
Δx = distance between two sections in m
s = relative density

5.4 General description of the mathematical model

In order to compute the sediment transport in irrigation canals, a computer program "SETRIC" (**SE**diment **TR**ansport in **I**rrigation **C**anals) was developed. The computer program was written in QuickBASIC.

5.4.1 Functional description

The SETRIC computer program can simulate the water flow, sediment transport and changes of bottom level in an open network composed of a main canal and several laterals with/without tertiary outlets. Several flow conditions along the irrigation season can be simulated. Figure 5.9 shows the flow diagram for calculating the change of the bottom level in a canal during one time step.

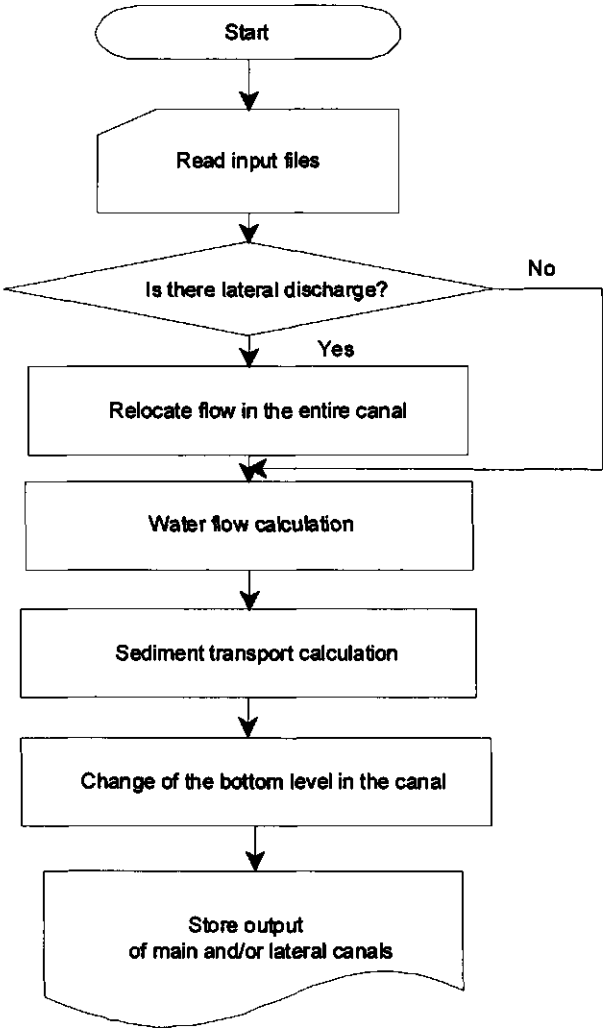

Figure 5.9 Flow diagram of SETRIC computer program for calculating water flow, sediment transport and changes in bottom level in main and/or lateral canals

Flow diagrams of the SETRIC computer program for the water flow and sediment transport calculations in a reach of a canal are also shown in figure 5.10 and 5.11.

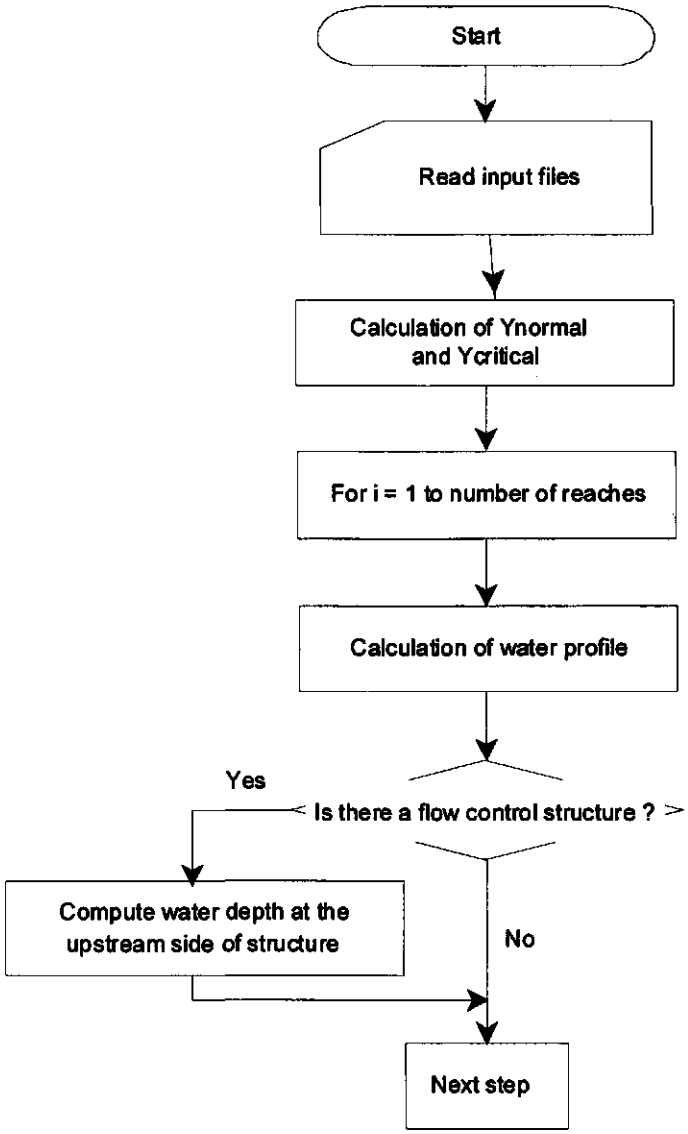

Figure 5.10 Flow diagram of the SETRIC computer program for calculating water flow in main and lateral canals during a time step

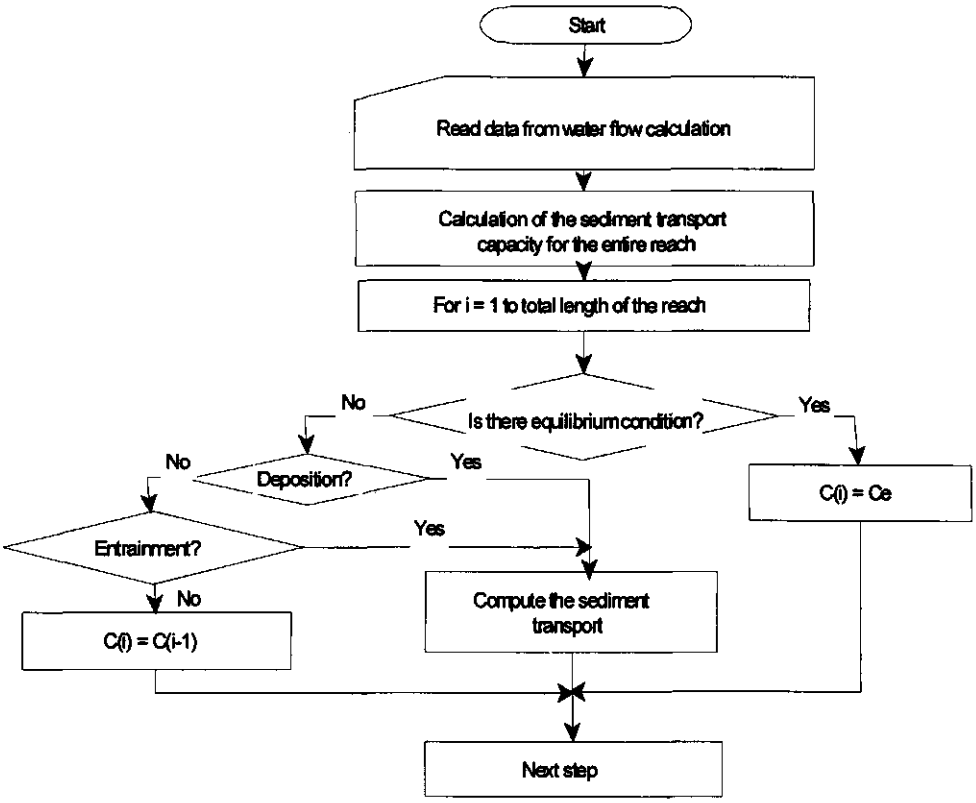

Figure 5.11 Flow diagram of the SETRIC computer program for calculating sediment transport in main and lateral canals during a time step

The background for the hydraulic and sediment transport computations has been described in the previous paragraphs. The general description of the computer program is:

- Water flow: a sub-critical, quasi-steady, uniform or non-uniform flow (gradually varied flow) can be modelled. For the gradually varied flow, backwater as well as drawdown curves can be calculated. The program computes the water flow only in the subcritical regime, therefore the water profiles for gradually varied flow included in the computer program are: H2, M1, M2, C1, S1 and A2;
- Cross section: the water flow can be simulated in open channels, with a rectangular or trapezoidal cross section;
- Only friction losses are considered. No local losses due to changes in bottom level, cross section or discharge are taken into account;

- Changes in the bottom level are considered;
- An irrigation network composed by primary and secondary canals with tertiary outlets is included. Each canal can consist of several reaches or sections;
- Canal sections are characterized by the geometrical dimensions, which include the following parameters:
  * initial coordinate: relative location of the canal section. The most upstream part is defined as x = 0 m;
  * length (l): length of the section (m);
  * bottom width (B): width of the bottom (m);
  * side slope (m): 1 vertical : m horizontal;
  * roughness is defined by the equivalent roughness coefficient (k_s);
  * bottom slope (S_0);
  * bottom elevation at the beginning of the canal section (z_b).
- Location of control structures and/or lateral flow will define boundaries between reaches. Also changes in geometrical dimensions of the reaches will define such boundaries;
- Lateral discharge (as inflow or outflow) can be simulated. These lateral discharges must be located at the end of any canal section of the main and secondary canal;
- Control section at the downstream end of the main canal and secondary canals can be set. The type of structure located at the downstream end of each section determines the water level;
- Several flow control structures can be incorporated into the program. They are schematized by:
  * overflow type: crest width, crest level;
  * undershot type: width and height of the rectangular opening;
  * submerged culverts and inverted siphons: number and diameter of pipes;
  * flumes: constants of the upstream head-discharge relationship;
  * drops: incorporated as different bottom level at the boundaries between two reaches;
  * Sediment characteristics are defined by:
    - sediment concentration (ppm) at the upstream end of the main canal;
    - sediment size is characterized by the mean diameter d_{50}. The range of values is 0.05 mm $\leq d_{50} \leq$ 0.5 mm. An uniform sediment size distribution has been assumed. Geometrical standard deviation equal to 1.4 was used as default.
- Simulation periods take into account the variation of irrigation water requirement during the growing season. Water requirements are mainly determined by the cropping pattern and also for leaching accumulated salts in the soil and for compensating water losses. Variations of irrigation requirement depend on the expected cropping pattern and the stage of the crops. The growing season is divided into four stages depending on the crop development and climate conditions (FAO, 1984). Irrigations requirements will change during the irrigation season therefore the water supply will change in order

to follow those changes in area and time. Operation policies of an irrigation system will match the delivery of water supply with the irrigation requirements. In the program each period is characterized by a number of days and a number of hours per day. The program assumes a maximum of four different periods in which the discharges along the system can be varied. Operation policies will be schematized during the simulation time. Figure 5.12 shows the theoretical and schematized periods during the irrigation period.

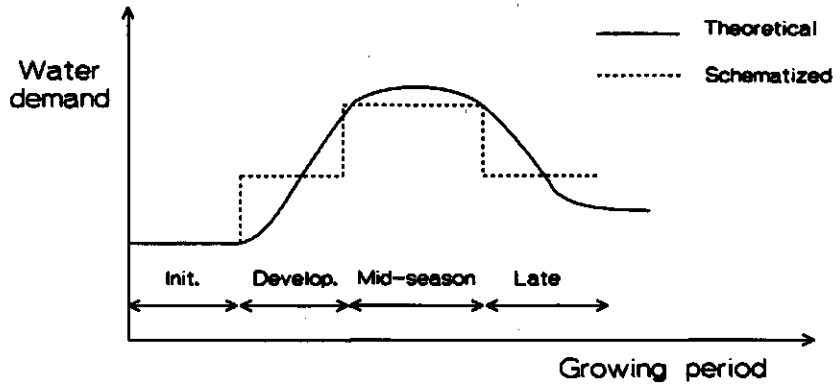

Figure 5.12 Crop water requirements: theoretical and schematized

- Variations of the roughness conditions in time were incorporated into the program. Sedimentation of canals during the irrigation season will induce the development of bed forms. Different flow conditions will produce different types of bed form in a particular canal. The friction factor is computed time to time for each local flow condition and for each cross section in which the canal system was schematized. Composite roughness is also considered in the computation of the total friction factor for the entire cross section;
- Maintenance activities were also included into the program. Those maintenance activities are referred to by the obstruction degree due to weed growth on the banks and its effect on the roughness condition of the canal. From that point of view three types of maintenance were included into the program:
  * ideally maintenance: negligible obstruction degree in time;
  * well maintained: a maximum obstruction degree of 10 % is assumed;
  * poor maintained: more than 75% obstruction degree is assumed.

Figure 5.13 shows the expected variations of the friction factor depending on the types of maintenance.

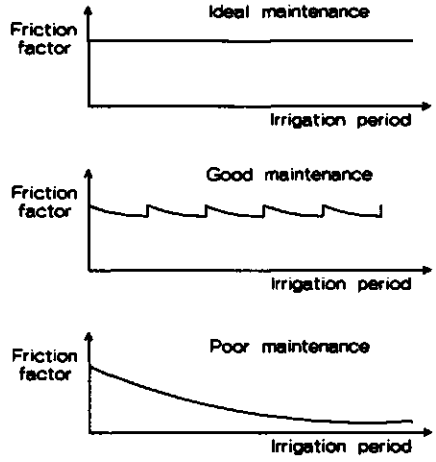

Figure 5.13 Variations of the friction factor for different types of maintenance activities

5.4.2 Input data

For the computation of the water flow and sediment transport, the computer program requires several input data that can be described as follows:

- *Simulation period*: characteristics of the period to be simulated are required. Those characteristics include:
  * number of periods in which the irrigation season is divided;
  * type of maintenance to be expected during the irrigation season;
  * details of each period: number of days per period and irrigation hours per days.
- *Canal dimensions*: for main and secondary canals a set of data related to the geometrical dimensions are required:
  * for each canal: number of sections, kind of roughness data;
  * for each section: location, length, bottom width, roughness coefficient, side slope, bottom slope, bottom elevation.
- *Main and lateral discharges*: the schedule of irrigation flows during the irrigation period is required. Discharge (in m^3/s) of the water flow entering the upstream part of the main canal for each period of the irrigation period has to be specified. In the same way a lateral discharge (in m^3/s) can be defined at the upstream part of each lateral for each period of the irrigation season. Inflow (+) and outflow (-) can be entered in the computer program;
- *Sediment data*: data related to the sediment entering into the main canal are required. Mean sediment concentration and mean diameter of the particles must be entered. The computer program computes internally the sediment concentration entering into the lateral canals;
- *Control sections*: control sections located at the downstream end of the main and lateral canals are specified. The input data to be entered in each canal are: water level and

location of each control section. If flow control structures are located at boundaries between reaches of canals then the type of structure and its characteristics has to be specified. The computer program computes internally the upstream water level of the structure. That water level will act as control level for the next reach of the canal.

5.4.3 Output data

The computer program has several possibilities to present the output data of the water flow and suspended sediment transport calculations. Results are shown in tables or graphs depending on the selected option. The results can be presented on the monitor or on paper by selecting the appropriate option.

Tables: The program can show the following tables:

- General information:
  - * results related to the water flow: normal and critical depth, discharge;
  - * results related to sediment transport: fall velocity, length step, minimum and maximum shear stress, shear velocity.
- Concentrations: this table shows the water depth, equilibrium concentration and actual concentration for the entire canal;
- Bottom level: the initial bottom level and the change in bottom elevation at the end of the selected period are presented in this table.

5.5 Conclusions

A mathematical model for predicting water and sediment discharges and variations in the bottom level of the canal has been presented. The model is based on an uncoupled solution of the water flow and sediment transport equations, which was explained in the previous sections of this chapter. This model can be used for simulating the sediment deposition in an irrigation network under changing flow conditions and sediment characteristics during the irrigation season. The model can be used for evaluating the effects of the inter-relation between the irrigation practice and the sediment deposition. First the direct effect of the irrigation practices on the sediment deposition: changes in the discharge, changes in sediment load, flow control structures, controlled deposition, operation and maintenance activities, diverted sediment load to the farmlands etc. Second the effect of the sediment deposition on water level variation (overtopping of canals), water distribution at outlets, flow control structures etc.

Nevertheless, the mathematical model's performance has to be confirmed. Results should be compared with field measurements in order to confirm whether the physical processes are well represented in the mathematical model or there is a deficiency as a result of the assumptions for describing those processes. Monitoring of the sediment deposition in an irrigation network is urgently needed to evaluate the model and to investigate the response in time and space of the bottom level to determine water flows and sediment characteristics. Influences of the type

and operation of flow control structures, geometrical characteristics of the canals, water flow and incoming sediment characteristics on the deposition, which the mathematical model predicts, will contribute to a better understanding of the sediment transport processes under the prevailing flow conditions in irrigation canals.

6 APPLICATIONS OF THE MATHEMATICAL MODEL FOR SEDIMENT TRANSPORT IN IRRIGATION CANALS

6.1 General

The amount of water and sediment load, which enter into an irrigation canal will change during the growing season and moreover during the life time of the irrigation system. Variations in crop water requirement, water supply, size of the area to be irrigated, planned cropping pattern and sediment concentration frequently occur during the life time of the irrigation system. The design of the irrigation canals and flow control structures permits to some extent flexibility in the delivery of different water flows at certain fixed water levels and the conveyance of the incoming sediment under the assumption of an equilibrium condition for transporting the sediment load. Once the flow conditions deviate from the design values, the flow velocity and thus the capacity for transporting the sediment load will vary in time and space along the irrigation canal. Then, the initial assumption related to the conveyance of the sediment load in equilibrium condition is not anymore valid for these changing flow conditions. Sediment transport in irrigation canals will be mainly in non-equilibrium conditions for these changing operation conditions. Therefore, the sediment transport will strongly depend on the variation of the initial conditions of the flow and incoming sediment load during the irrigation season or the life time of that canal. For that reason the sediment transport should be viewed in a more general context which takes into account the in time and place varying operation of the irrigation system.

The sediment transport model offers the possibility to predict the behaviour of the sediment deposition in time and space, for particular flow condition and incoming sediment load. In this chapter some applications of sediment transport modelling in irrigation canals will be described. The applications are meant to show the applicability of the developed model and to improve the understanding of the sediment transport process for situations usually encountered in irrigation systems.

The sediment deposition in an irrigation canal during a certain period will be simulated for each of the different applications. The initial geometrical and hydraulic conditions of the irrigation canal and the incoming sediment characteristics will be given for each application. The sediment transport capacity of the irrigation canal is computed according to the predictor method described in the chapters 3 and 4. Based on the results the sediment load can be either transported without any deposition along the entire canal or can be adjusted from a non-equilibrium condition to the sediment transport capacity of the canal. The adjustment towards the sediment transport capacity is according to the Gallapatti's depth-integrated model.

A sediment mass balance in each reach of the canal will give either the net deposition or the net entrainment between the two boundaries of that specific canal reach. In case the incoming

sediment load is larger than the sediment transport capacity of the canal, deposition will occur. In case the incoming sediment load is less than the transport capacity of the canal two possibilities can occur depending on whether motion of sediment occurs or not. In the first case entrainment of the previously deposited sediment occur until the adaptation to the sediment transport capacity of the canal. For the second case the sediment load is conveyed without any change. Different cases for the adjustment of the incoming sediment load to the sediment transport capacity of the canal are shown in section 5.2.

The model for the sediment transport will be used to evaluate the following effects in irrigation canals:

- changes of the discharge;
- changes in the incoming sediment load;
- controlled sediment deposition;
- sediment transport predictors;
- flow control structures;
- maintenance activities;
- operation activities.

The effect of changes in the incoming sediment load on the sediment transport will include the effect of variations in the incoming sediment concentration and in the median sediment size during the irrigation season. All these changes are related to the sediment concentration and sediment size as assumed for the equilibrium conditions.

As sediment deposition and the removal of the sediment belong to the most important problems in irrigation canals, the effect of controlled deposition of sediment by deepening or widening of one or some reaches of the canal has been simulated.

In chapter 4 the different sediment predictors have been described and compared for equilibrium conditions. Here the effect of the various sediment transport predictors, like Ackers and White, Brownlie and Engelund and Hansen, on the sediment deposition will be compared. Sediment deposition during a certain period and under non-equilibrium conditions will be simulated. Adaptation of the non-equilibrium condition to the equilibrium condition will be done for each sediment transport predictor.

An irrigation canal has to deliver water at the right amount, at the required time and at the proper elevation to the command area. The water is kept at the right level for varying discharges by flow control structures, which can be divided into two main groups, namely undershot and overflow structures. The selection of the structure depends on various operational aspects, one of which is the ability of the structure to pass sediment. The influence of the two types of structures on the sediment deposition and the distribution of the sediment deposition along the entire canal will be compared by using the model.

Maintenance is the set of actions to keep an irrigation system in perfect operating conditions and to provide at all time its function. Silt deposition, weed infestation, erosion of banks, seepage or clogging of offtakes do not allow the delivery of the required water in the right amount and at the right elevation. Maintenance activities related to silt deposition and weed infestation will be evaluated in terms of the effect of the maintenance on the hydraulic performance of the irrigation canal. The maintenance will be simulated by assuming optimal maintenance and non maintenance at all during the irrigation season, meaning that in the first case the roughness remains constant and that in the second case the roughness increases in time. For each maintenance scenario the sediment deposition or sediment entrainment will be evaluated.

An irrigation system is operated to obtain a maximum of crop production in view of the on-farm and project costs and benefits. Operation activities are aimed to deliver water to the users at the right time and at the proper volume and consist of several operational procedures. However, the diversity of constraints makes the selection of a general procedure very difficult, if not impossible. The operation policy for a certain irrigation system requires the evaluation of several scenarios to determine the reliability of each scenario in view of the water delivery. One of the aspects to be considered is the risk of sediment deposition in the canal system. The effects of various operation schedules on the sediment deposition will be simulated.

For most of the above described simulation cases a single irrigation canal is assumed. For the application case of operation activities an irrigation canal composed of several reaches is assumed. Also several assumptions for the hydraulic conditions and sediment characteristics during the simulation period are made. The main assumptions for these applications are:

- characteristics of the incoming sediment (sediment size and sediment concentration) are kept constant during the whole simulation period;
- no erosion of the initial bottom level is allowed. Only previously deposited sediment can be entrained during the simulation period;
- side slopes are stable;
- initial roughness conditions of the canal (s) are characterized by a single roughness along the wetted perimeter;
- weed infestation is only considered as roughness element;
- variations in time of the roughness conditions can occur due to: change of flow conditions, occurrence of bed forms on the bottom and obstruction by weed infestation (if so);
- the water level at the downstream end of the main canal is kept constant;
- the water level at the downstream end of internal reaches is governed by the hydraulic conditions either by a flow control structure or by the water level of the downstream reach;
- the sediment transport capacity of the water flow and the actual sediment load are referred to in terms of equilibrium concentration and actual concentration of sediment

respectively. The concentration is expressed in ppm (parts per million) as the weight of sediment per unit volume of the water-sediment mixture.

The initial geometrical, hydraulic and sediment characteristics will be given for the specific conditions of each case.

6.2 Changes of the discharges

A key problem for operating an irrigation canal is to determine the flow conditions for which the water requirement is met with minimum deposition. The reduction of the water flow in the irrigation canal (i.e. caused by: reduction in water requirements, reductions in water supply or variations in cropping pattern) and the need to deliver water at a certain level to the command irrigated area is one of the most important causes of sediment deposition in irrigation canals.

The effect of a reduction in discharge, with a controlled water level at the downstream end of the canal, on the sediment deposition is simulated in an irrigation canal. The irrigation canal is designed to transport a certain amount of water and sediment in equilibrium conditions. It means that no deposition and no erosion will take place while the design flow condition prevails in the irrigation canal. Afterwards reductions of the discharge are simulated. For new values of the discharge the flow condition and sediment transport capacity in the canal will change. A non-equilibrium condition for transporting the incoming sediment load will appear. The sediment transport during a certain time period is simulated and it is assumed that the incoming sediment load characteristics will remain constant for all the different discharges. The Ackers and White predictor is used to compute the sediment transport both for equilibrium and non-equilibrium condition (see equation 5.25). Next the sediment deposition for each discharge reduction is calculated. The initial geometrical, hydraulic and sediment characteristics of the irrigation canal are the following:

- length (L) = 10000 m
- bottom width (B) = 10 m
- side slope (m) = 2
- equiv. roughness (k_s) = 0.01 m
- bottom slope (So) = 0.00008
- bottom level (begin) = 40.00 m
- bottom level (end) = 39.20 m
- design discharge (Q) = 25.75 m^3/s
- simulation period = 90 days
- sediment size (d_{50}) = 0.15 mm
- equilibrium sediment concentration at inlet = 253 ppm
- flow control structure = undershot type
- water level at the end = 41.65 m
- flow condition = nearly uniform flow

- water depth = 2.45 m

Reductions of the discharge are specified in terms of a relative discharge (Rd) which reads:

$$Rd = \frac{\text{actual discharge}}{\text{design discharge } (Q = 25.75 \text{ m}^3/\text{s})} \quad (6.1)$$

Details of these computations are shown in the figures 6.1 to 6.3. For the design discharge of 25.75 m^3/s (relative discharge equal to 1) the sediment transport capacity of the irrigation canal is equal to the incoming sediment load (fig. 6.1) and will remain constant during all time. Therefore, the incoming sediment load will be conveyed without deposition in the irrigation canal (equilibrium condition).

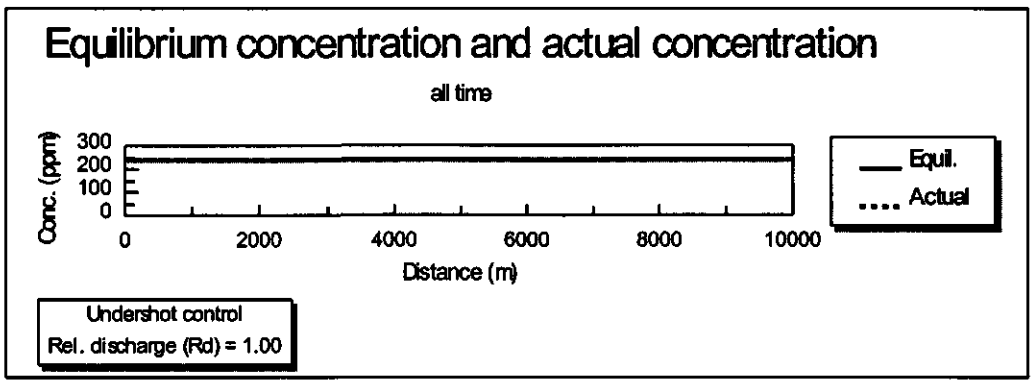

Figure 6.1 Equilibrium concentration and actual concentration for the sediment transport in equilibrium condition

Once the discharge is decreased (i.e. Rd = 0.74 and Rd = 0.8) as shown in figure 6.2, a gradually varied flow will prevail along the entire canal because the water level remains constant at the downstream end of the canal. The sediment transport capacity at the head of the canal will decrease as a consequence of the reduction in the discharge but also a continuous decrease of the sediment transport capacity in downstream direction will take place. A continuous deposition will occur along the canal under that condition of gradually varied flow. Large deviation from the design value of the discharge will cause large deviation between the incoming sediment load and the sediment transport capacity of the canal. A relative discharge Rd of 0.74 shows a larger difference between the sediment transport capacity and the incoming sediment than the difference in case of a relative discharge Rd of 0.88.

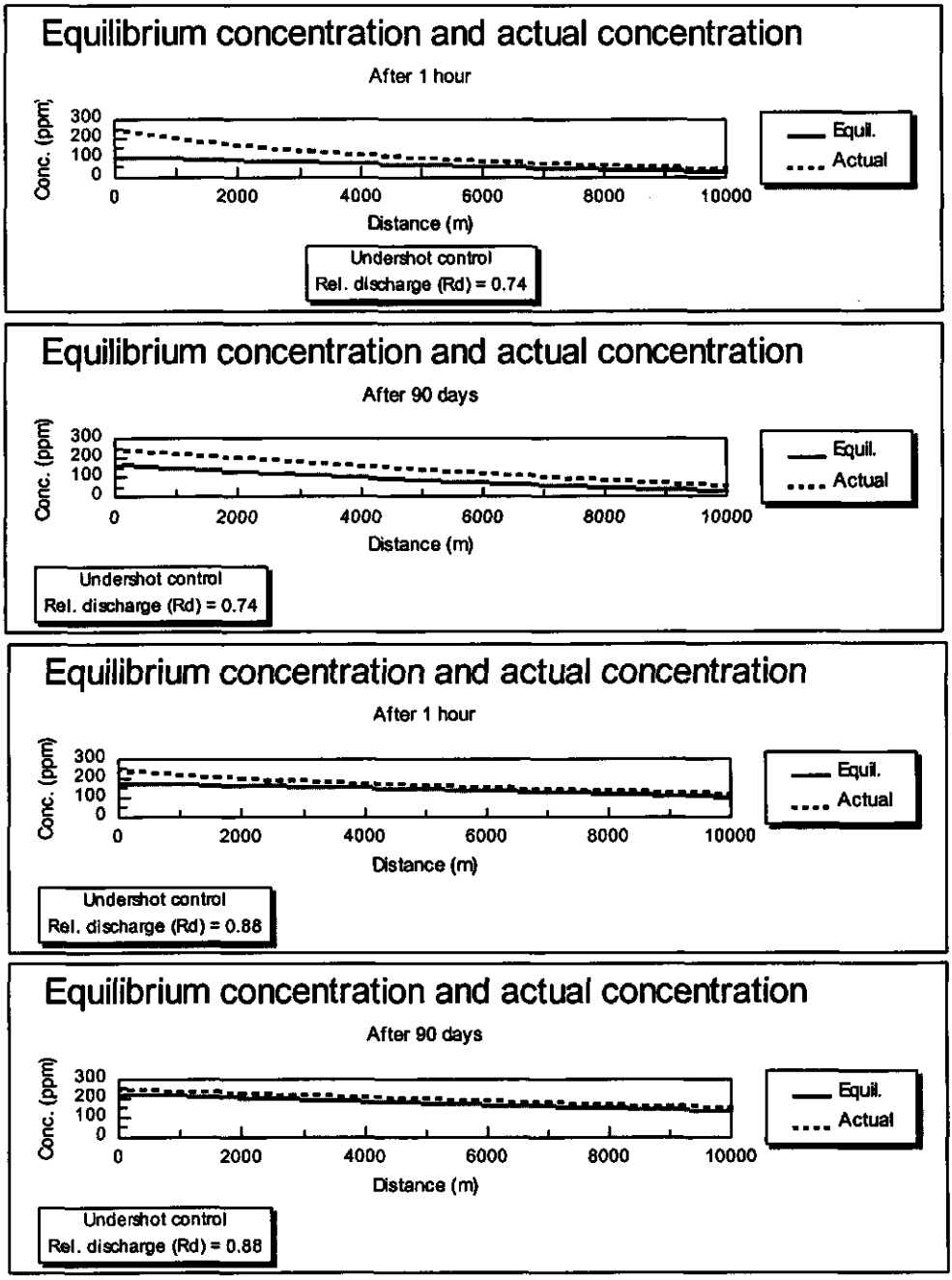

Figure 6.2 Equilibrium concentration and actual concentration at the beginning and at the end of the simulation period for different values of the relative discharge

Although the amount of sediment mass entering into the canal is reduced in the same way as the reduction of discharge, the sediment deposition is considerably larger for smaller discharges. Due to the fact that the total incoming sediment load during the simulation period is different for each relative discharge Rd a relative deposition value was used to describe the sediment deposition in the irrigation canal. The relative deposition is expressed in terms of the percentage of the total sediment deposited in the entire canal during the simulation period and the total sediment load entering in the irrigation canal during the same period. It can be expressed as:

$$\text{Relative deposition (\%)} = \frac{\text{total deposition}}{\text{total incoming sediment load}} * 100 \qquad (6.2)$$

Figure 6.3 shows the amount of total deposited sediment and the relative sediment deposition when compared with the total amount of sediment entering into the canal during 90 days. For reductions of discharge to 80% of the design value, more than 40% of the incoming sediment load will be deposited in the irrigation canal.

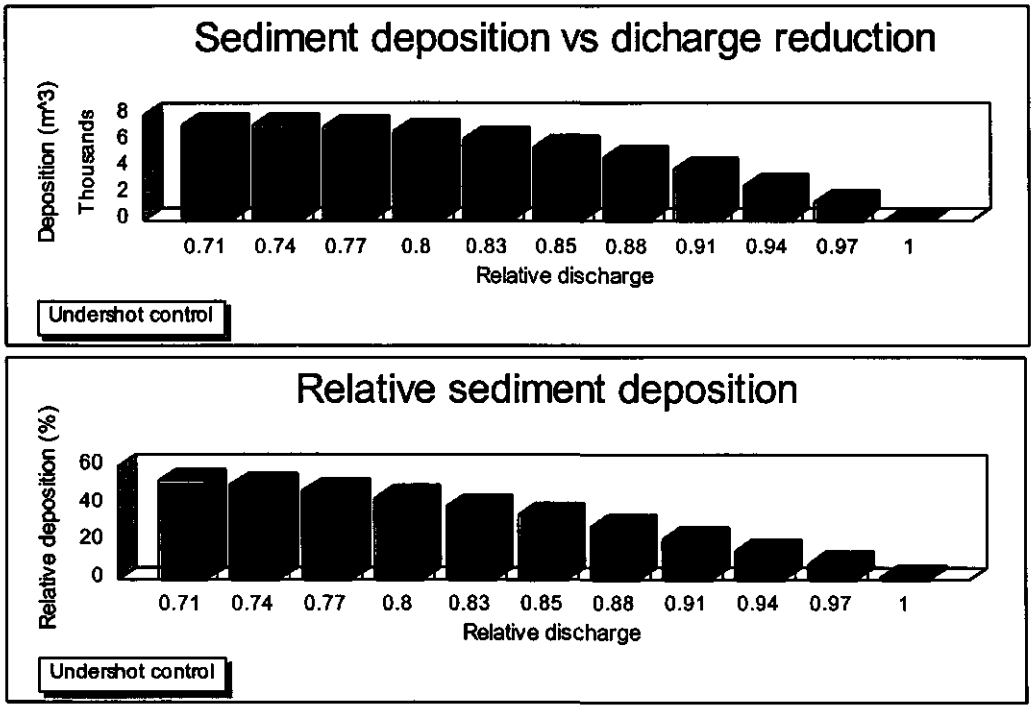

Figure 6.3 Sediment deposition and relative sediment deposition after 90 days along the irrigation canal as function of the relative discharge

6.3 Changes in the incoming sediment load

Another important issue for estimating the sediment deposition during an irrigation period is related to the incoming sediment concentration and the median sediment size. In many cases water for irrigation is coming from rivers. Seasonal changes in sediment concentration and median sediment size are frequent in rivers and therefore the sediment concentration in the water entering the irrigation canals also varies. The sediment concentration depends on the specific conditions of the river. Variations of the sediment concentration in the river are expected during an irrigation season and moreover during the lifetime of the irrigation system. Estimation of the sediment deposition for variations in the incoming sediment concentration can be done by assuming deviations of the sediment concentration from the equilibrium concentration. Non-equilibrium conditions can also appear by deviations of either the sediment concentration or the median sediment size of the incoming sediment load from the design value of those sediment characteristics. To study the influence of these sediment characteristics on the deposition of the sediment along an irrigation canal, the sediment transport with different sediment characteristics will be studied.

First the influence of the variation of the sediment concentration on the sediment deposition in the irrigation canal is studied. A proper irrigation canal is designed for transporting a sediment load in equilibrium condition, meaning that the incoming sediment load is transported without deposition along the entire canal. Afterwards the sediment deposition is studied by using a different sediment concentration. It is assumed that the initial flow condition and median diameter of the sediment remain constant for all the cases with a new sediment concentration. Larger values of the incoming sediment concentration than the equilibrium sediment concentration capacity of the irrigation canal will result in non-equilibrium conditions and sediment deposition will take place. The Ackers and White sediment transport predictor is used to estimate the sediment transport capacity of the irrigation canal.

The sediment load along the canal is in non-equilibrium condition as explained in the previous sections. Sediment deposition is calculated by computing the sediment mass balance between the two boundaries of the canal reach. These computations were done for all the length steps and during all the time steps in which the simulation period was divided. The mathematical model described in chapter 5 was used for these computations.

The characteristics of the irrigation canal are the following:

- length (L) = 10000 m
- bottom width (B) = 10 m
- side slope (m) = 2
- equiv. roughness (k_s) = 0.01 m
- bottom slope (So) = 0.00008
- bottom level (begin) = 40.00 m
- bottom level (end) = 39.20 m

- discharge (Q) = 25 m^3/s
- simulation period = 90 days
- sediment size (design value of d_{50}) = 0.15 mm
- equil. sed. load (design value) = 236 ppm
- flow control structure = undershot type

Variations of the sediment concentration were expressed in terms of the ratio of the actual sediment load related to the sediment transport capacity of the canal (equilibrium condition):

$$\text{Relative sediment load} = \frac{\text{actual sediment load}}{\text{equil. sed. load (236 ppm)}} \tag{6.3}$$

Due to the fact that the total incoming sediment load during the simulation period is different for each relative sediment load, a relative deposition value was used to describe the sediment deposition in the irrigation canal. The relative deposition is expressed in terms of the percentage of the total sediment deposited during the simulation period and the total sediment load entering the irrigation canal during the same period. It can be expressed as:

$$\text{Relative deposition} = \frac{\text{total deposition}}{\text{total incoming sediment load}} * 100 \tag{6.4}$$

Details of the simulation results for the sediment deposition are shown in figure 6.4. Sediment deposition in the irrigation canal highly depends on the characteristics of the incoming sediment. For a relative sediment load of 1.1 a nearly equilibrium condition for the sediment transport is present. The sediment load along the entire canal does not deviate much from the sediment transport capacity of the canal. The variation of the sediment load per unit length along the entire canal is small, therefore the sediment deposition is also small. A large deviation of the sediment concentration from the design value will result in a large variation of the sediment load per unit length of canal and a large deposition in the canal. About 15% of the total incoming sediment load will be settled in the canal when the incoming sediment load increases by 10% (relative sediment load equal to 1.1) from the design value of the equilibrium concentration. For 100% variation in the incoming sediment concentration (relative sediment load equal to 2) about 30% of the incoming sediment load is expected to settle into the canal.

Second the influence of the variations of the sediment size on the sediment deposition in the irrigation canal was simulated. The procedure for computing the sediment deposition for the different cases of sediment size was similar to the one used in the previous example, but now the sediment size was varied in stead of the sediment concentration. The variation of the sediment size can be expressed in terms of the ratio of the actual median sediment size and the design value of the median diameter of the sediment (equilibrium condition), which can be expressed as:

$$\text{Relative median sediment size} = \frac{\text{actual median sediment}}{\text{equil. median sed. size } (d_{50} = 0.15 \text{ mm})} \qquad (6.5)$$

A similar behaviour as for the case of variations in the sediment concentration is observed for changes in the relative median sediment size of the incoming sediment (figure 6.5).

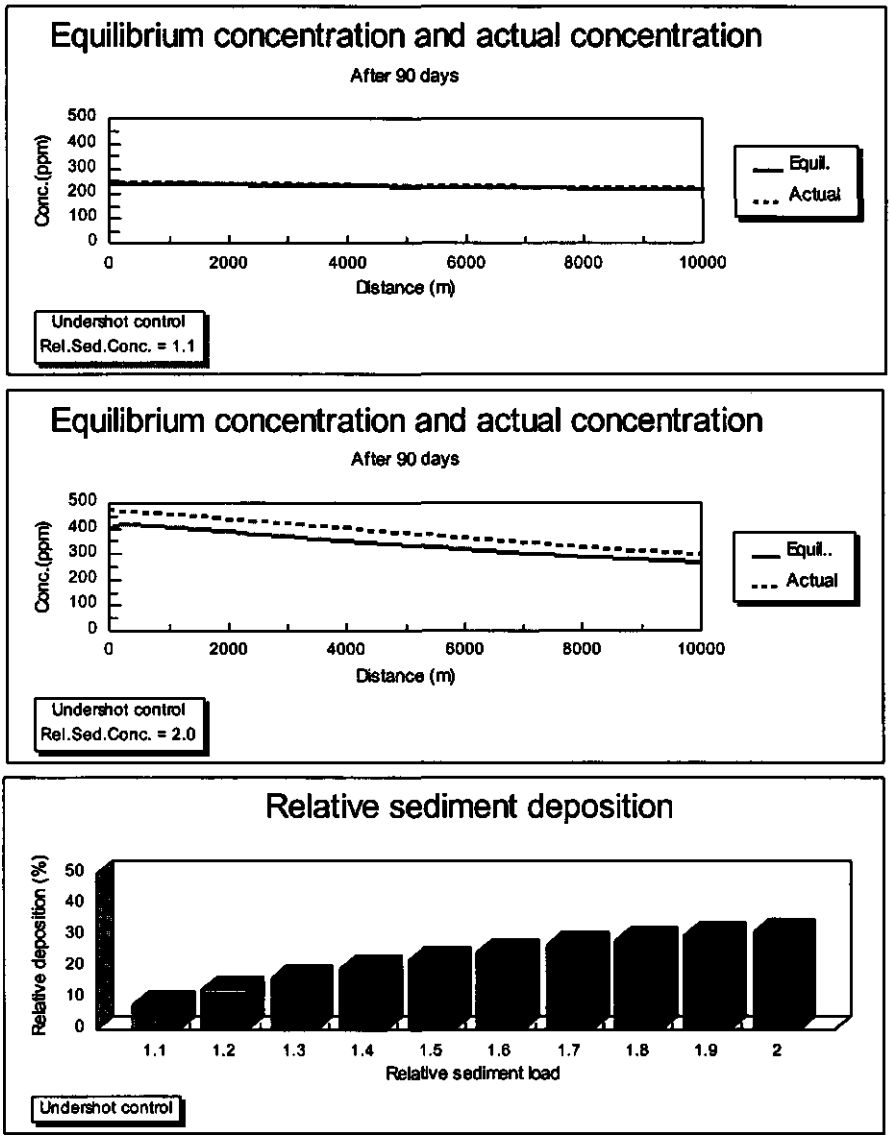

Figure 6.4 Total sediment deposition and relative sediment deposition after 90 days as function of the variation in the relative sediment load

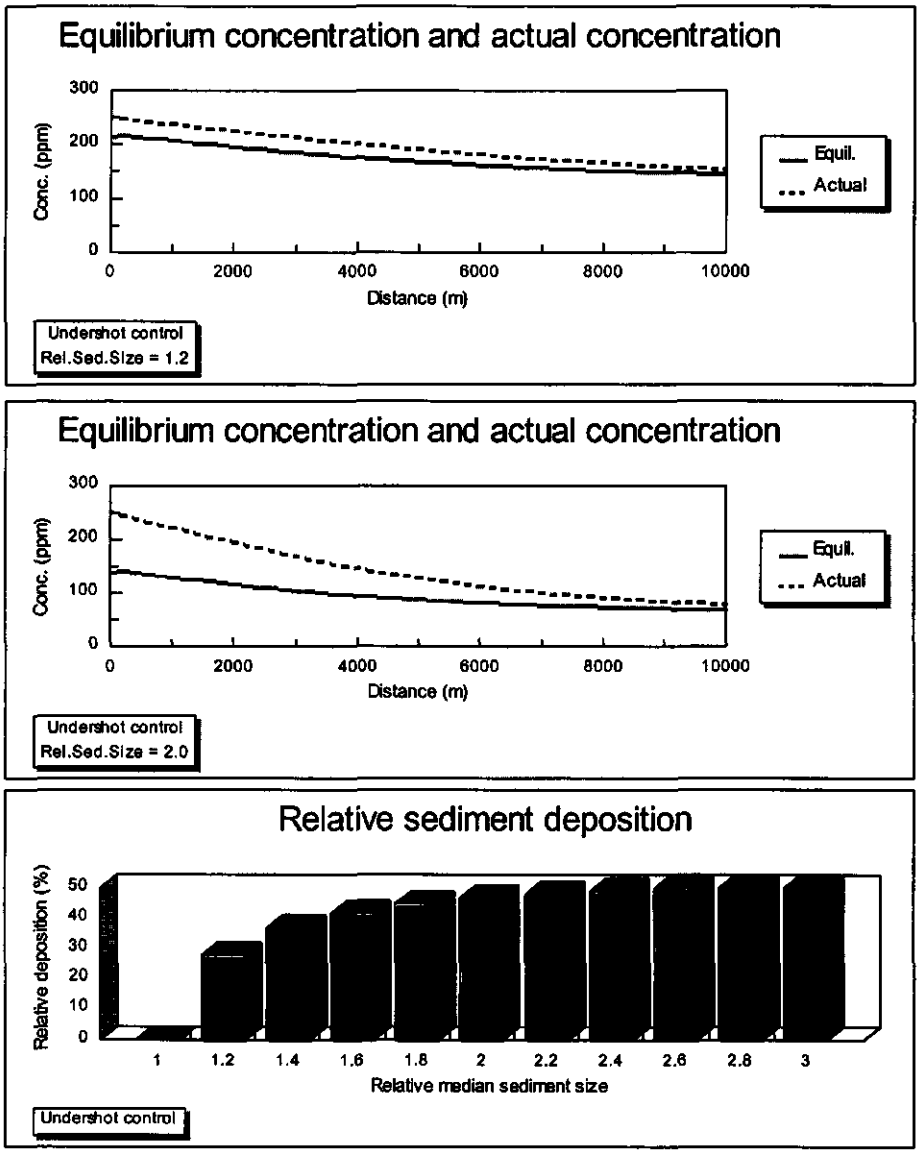

Figure 6.5 Total sediment deposition and relative sediment deposition after 90 days as function of variation in relative median sediment size

A small deviation from the equilibrium median sediment size (i.e. relative median sediment size of 1.2) produce small variation in the equilibrium sediment transport capacity of the canal. The incoming sediment load is gently adapted to the new equilibrium condition. For larger relative sediment sizes (i.e. relative median sediment size of 2.0) the adaptation of the incoming sediment load to the equilibrium condition is more abrupt than in the previous case and therefore the variation of the sediment load per unit length is larger as well. For instance a total of about 25% of the total incoming sediment during the simulation period is deposited

in the first case while a total of about 45% of the incoming sediment load is deposited when the sediment size deviates 100% of the design median diameter.

6.4 Controlled sediment deposition

Once the sediment enters the irrigation network it can be eliminated in different ways: by deposition along the entire canal, by deposition in a trap within the reach of the canal where it can be periodically removed at minimum cost or by distribution over the irrigated land.

Uncontrolled deposition of sediment in the entire canal would produce clogging of turnouts, reduction of conveyance capacity, large variation in water level in the canal, variation in water depth-discharge relationship of structures and high cost for canal desilting.

Controlled deposition can be obtained by designing a siltation trap within the irrigation canal by deepening or widening of some reaches of the canal (silting canal). This solution can be an attractive for controlling the sediment deposition. An appropriate consideration on the location of the sediment deposition is important for the design and operation of an irrigation system.

The options for controlling the sediment deposition will be attractive because they would reduce the effects of the sediment deposition on water flow and would reduce the desilting cost by reducing the number of locations where desilting routines have to be carried out. Two case studies will be described in which the cross section of an irrigation canal is modified in order to reduce the sediment transport capacity in such a way that the major part of the sediment deposition can be isolated in some reaches of the irrigation canal. In this example an irrigation canal will be used in which sediment deposition is expected to occur during the irrigation season.

The characteristics of the irrigation canal are the following:

- length (L) = 10000 m
- bottom width (B) = 10 m
- side slope (m) = 2
- equiv. Roughness (k_s) = 0.01 m
- bottom slope (So) = 0.00008
- bottom level (begin) = 40.00 m
- bottom level (end) = 39.20 m
- discharge (Q) = 25 m^3/s
- simulation period = 90 days
- sediment size = 0.15 mm
- sediment concentration = 300 ppm
- flow control structure = undershot type

The irrigation canal is unable to transport the sediment load to the fields during the entire period, therefore sediment deposition is expected to occur. No measures for controlling the sediment deposition have been taken and therefore the sediment deposition is expected to occur along the entire length of the irrigation canal. Figure 6.6 shows the sediment transport capacity the incoming sediment load and the sediment deposition during the simulation period.

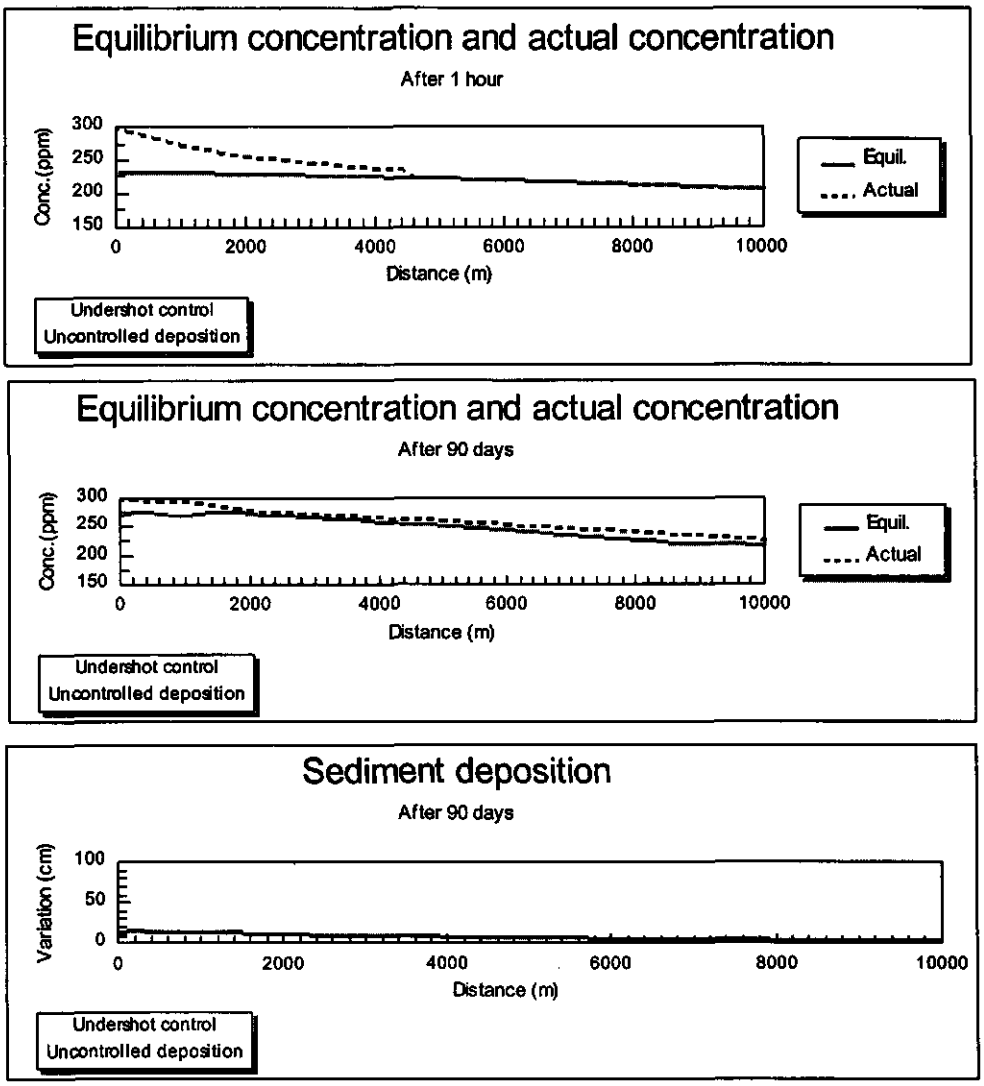

Figure 6.6 Sediment transport and sediment deposition in an irrigation canal with uncontrolled deposition

At the beginning of the simulation period (after 1 hour), a non-equilibrium condition prevails. The incoming sediment load will adapt to the sediment transport capacity of the canal by depositing sediment mainly in the first half of the irrigation canal. At the end of the simulation period (after 90 days) the bottom level of the irrigation canal is raised by the sediment

deposition. The sediment transport capacity increases during that time period but not enough to match the incoming sediment load. Sediment deposition is observed in the entire canal.

Two scenarios are proposed to concentrate the sediment deposition at the head reach of the canal. Those scenarios are intended to reduce the transport capacity in that reach of the canal only. The two scenarios will transform the head of the irrigation canal in a sort of settling basin within the canal. They can be described as:

- *scenario 1*: widening the bottom width of the first 1000 m of the canal from 10 m to 14 m;
- *scenario 2:* deepening the canal over the first 1000 m of the canal from the initial level to a 0.50 m lower level over the whole length of this reach.

These proposed changes in the geometry of the irrigation canal are simple modifications of the original cross section. No additional considerations for optimizing economical cost and sediment deposition are done. The other geometrical and hydraulics characteristics are kept constant for the simulation of the sediment deposition in both scenarios.

The two scenarios are compared with the irrigation canal without any control of the sediment, in terms of the capability to trap the sediment in the first 1000 m. A relative deposition value was used for the comparison. The relative deposition was expressed as:

$$\text{Relative deposition} = \frac{\text{Volume of deposited sediment in the first 1000 m}}{\text{total volume of entering sediment}} \qquad (6.6)$$

Results of the comparison are given in figure 6.7. For the specific flow and sediment transport conditions scenario 2 (by deepening) traps more sediment than scenario 1 (by widening). Scenario 2 has trapped 4 times more sediment than the irrigation canal without control.

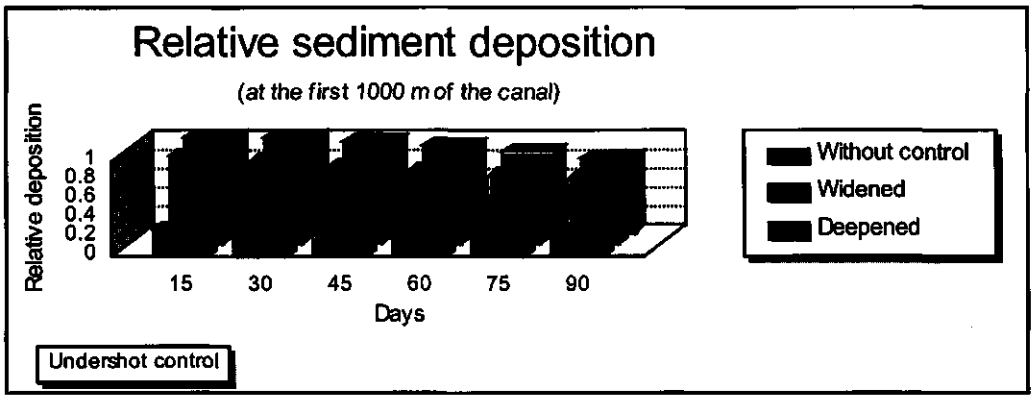

Figure 6.7 Relative sediment deposition of the two scenarios for controlling the sediment deposition

The results of the simulation of the sediment deposition due to the deepening of the first reach of t he canal are shown in figure 6.8. The figure presents the behaviour of the sediment transport capacity and the incoming sediment load at the beginning of the simulation period.

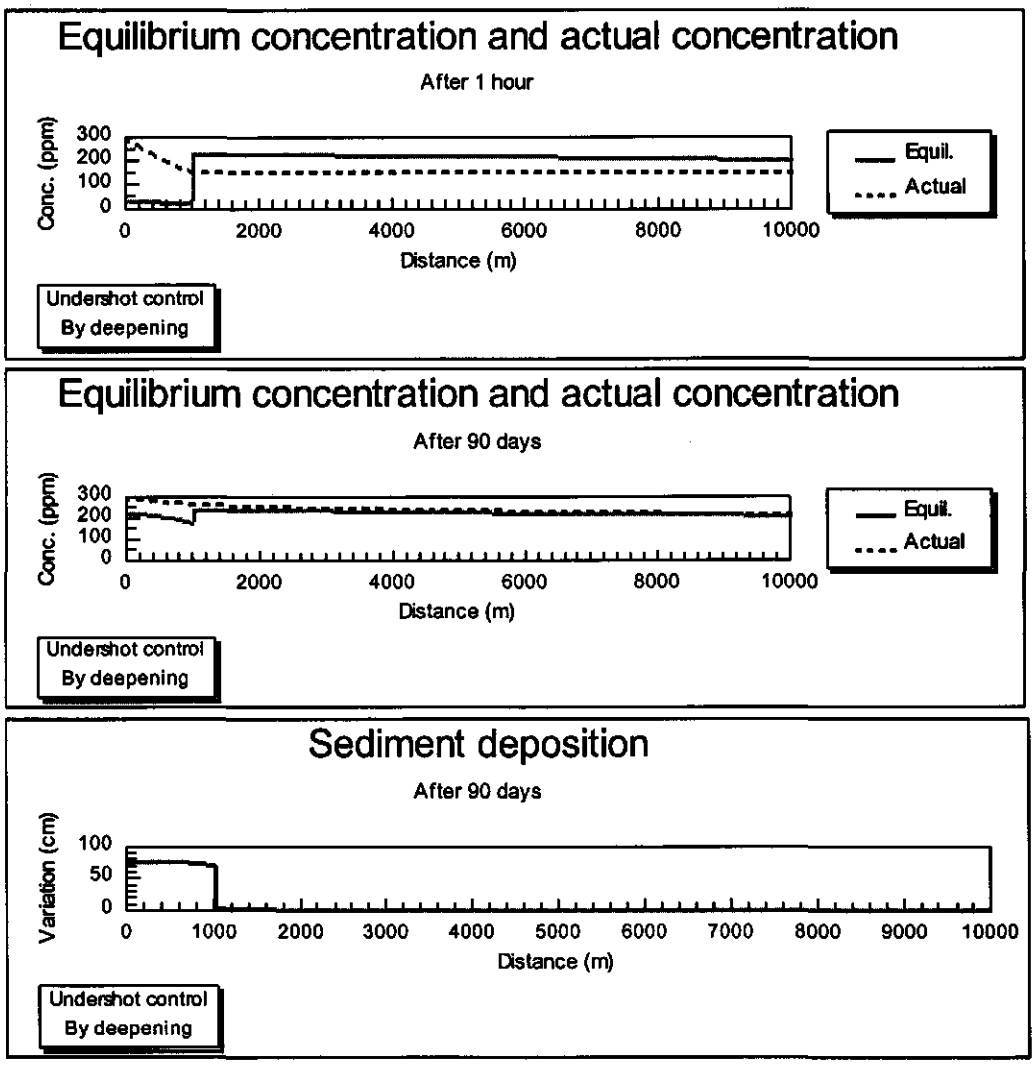

Figure 6.8 Sediment transport and sediment deposition in an irrigation canal with controlled deposition (by deepening the bottom of the canal over the first 1000 m of the canal

The incoming sediment load is reduced in the first 1000 m of the canal. From that point onward the sediment load could be transported without any deposition or erosion in the last 9000 m. The sediment deposition in the first reach will increase the sediment transport capacity in that part of the canal. At the end the simulation period the difference between the sediment

transport capacity at the head of the irrigation canal and the incoming sediment load is smaller. Sediment deposition was mainly concentrated in the first 1000 m of the irrigation canal.

Results of the simulation by widening the bottom width of the irrigation canal are shown in figure 6.9. The behaviour of the non-equilibrium condition for the sediment transport was rather similar to the one described previously. Less deposition was observed in the case with widening than by deepening the bottom of the irrigation canal.

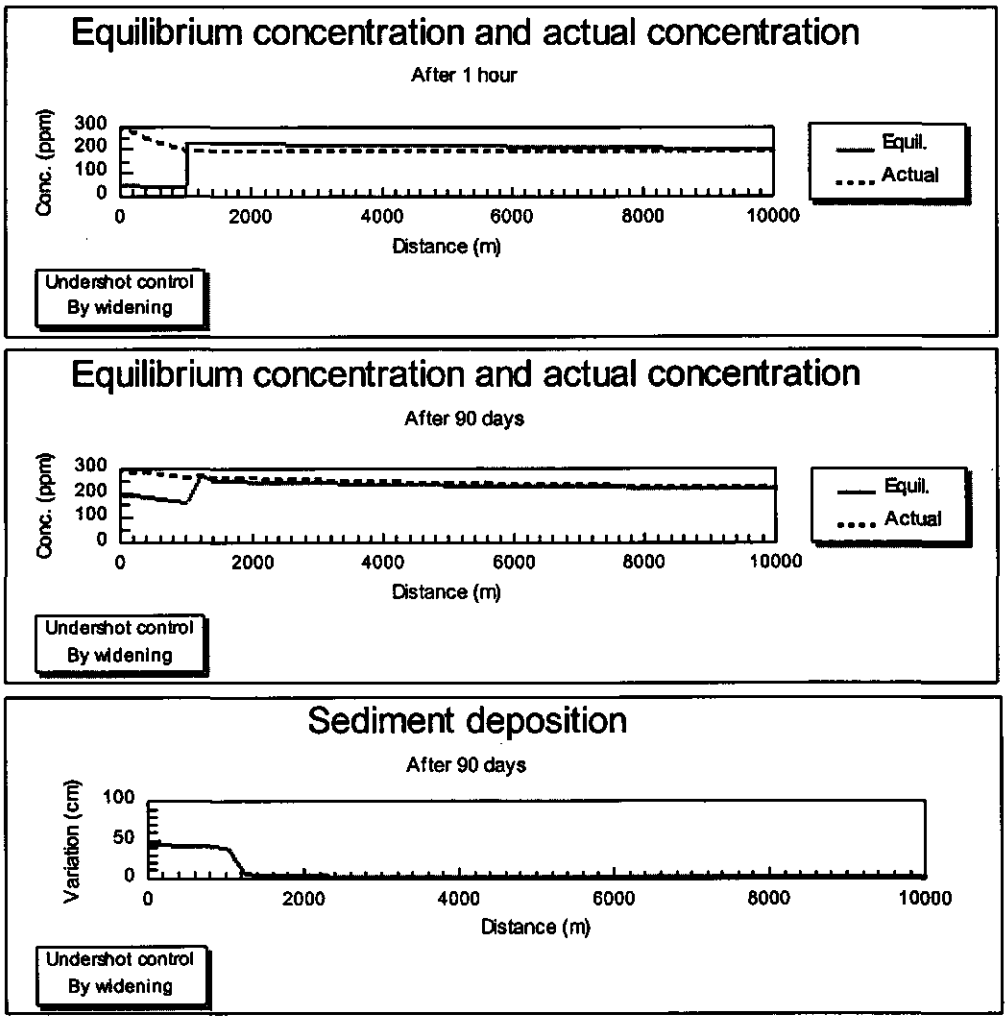

Figure 6.9 Sediment transport and sediment deposition in an irrigation canal with controlled deposition (by widening the bottom width over the first 1000 m of the canal

6.5 Sediment transport predictors

In section 4.2.2 several sediment transport predictors were compared for predicting the sediment transport capacity based on a set of field and laboratory data. Flow conditions and sediment transports in that set of data were supposed to be as uniform flow and in equilibrium condition. But the flow conditions in irrigation canals can vary incessantly both in space and time during the irrigation season and therefore the assumed equilibrium condition of the sediment transport can not be hold during these varying flow conditions.

Sediment transport predictors will be evaluated in terms of the effect of the estimation of the sediment transport capacity on the sediment deposition of an irrigation canal under non-equilibrium conditions. The Ackers and White (A-W), Brownlie (BRO) and Engelund and Hansen (E-H) predictors will be separately used to estimate the sediment transport capacity of an irrigation canal. Afterwards the adaptation of the non-equilibrium condition to the transport capacity of the canal and thus the sediment load in the entire canal is estimated. A balance of sediment mass between the boundaries of a reach will give the net deposition or the net entrainment between these points. The sediment deposition was simulated for a period of 90 days by using the Ackers and White, Brownlie and Engelund and Hansen predictors. The initial geometrical, hydraulic and sediment characteristics of the irrigation canal are as follows:

- length (L) = 10000 m
- bottom width (B) = 10 m
- side slope (m) = 2
- equiv. roughness (k_s) = 0.01 m
- bottom slope (So) = 0.00008
- bottom level (begin) = 40.00 m
- bottom level (end) = 39.20 m
- design discharge (Q) = 25 m^3/s
- simulation period = 90 days
- sediment size (d_{50}) = 0.15 mm
- equilibrium sediment concentration at inlet = 300 ppm
- flow control structure = undershot type
- water level at the end = 41.65 m
- water depth = 2.45 m
- flow condition = nearly uniform flow
- sediment transport condition = non-equilibrium

The hydraulic conditions during the simulation period gave a low sediment transport capacity for the Engelund and Hansen predictor and a larger one for Brownlie and Ackers and White predictors. Therefore the expected deposition in the irrigation canal will be larger in case of Engelund and Hansen and Brownlie predictor than for the Ackers and White predictor. Figures 6.10 and 6.11 show the behaviour of the sediment transport capacity and the sediment load at the beginning of the simulation period for each sediment transport predictor.

For all the sediment transport predictors the transport of the incoming sediment load is in non-equilibrium condition. The incoming sediment load is larger than the sediment transport capacity and therefore sediment deposition will occur. Once the sediment is deposited the bottom level will change together with the bottom slope. The initial sediment transport capacity of the canal will increase towards a new equilibrium condition.

The smallest difference between the sediment transport capacity at the beginning of the simulation period and the incoming sediment load is given by the Ackers and White predictor.

Figure 6.10 shows the equilibrium concentration and the actual concentration at the beginning and at the end of the simulation period according to the Ackers and White predictor. The initial sediment transport capacity at the upstream end of the canal by using the Ackers and White predictor (236 ppm) is not so different from the incoming sediment concentration (300 ppm) at the inlet. After 90 days the sediment transport capacity of the canal changed to 291 ppm, it means 23% more than the initial concentration. Once the sediment transport capacity reaches the incoming sediment load a minimum deposition will be expected due to the presence of a gradually varied flow in the irrigation canal.

On the other hand the largest difference is observed for the Engelund and Hansen predictor. Figure 6.11 shows the equilibrium concentration and the actual concentration at the beginning and at the end of the simulation period according to the Engelund and Hansen predictor. The initial sediment transport capacity at the beginning of the simulation period and at the upstream end of the irrigation canal is 61 ppm. After 90 days that concentration changed to 132 ppm, it means 100% higher than the initial concentration. The fast response of the Engelund and Hansen predictor is explained by the larger changes in the bottom level observed than the observed changes of the bottom level for the Ackers and White predictor (figure 6.10). The changes of the sediment transport capacity are bigger for large differences between the initial concentration and the incoming sediment concentration. The changes in the sediment transport capacity and changes in bottom level by using the Brownlie predictor behaved between the two predictors previously mentioned.

Deposition of sediment was observed for all the sediment transport predictors. The variation of the bottom level and a the relative deposition when compared with the Ackers-White sediment transport predictor is shown in figure 6.12. The relative deposition is expressed by:

$$\text{Relative deposition} = \frac{\text{Total deposition by the selected predictor}}{\text{Total sediment by the Ackers and White predictor}} \qquad (6.7)$$

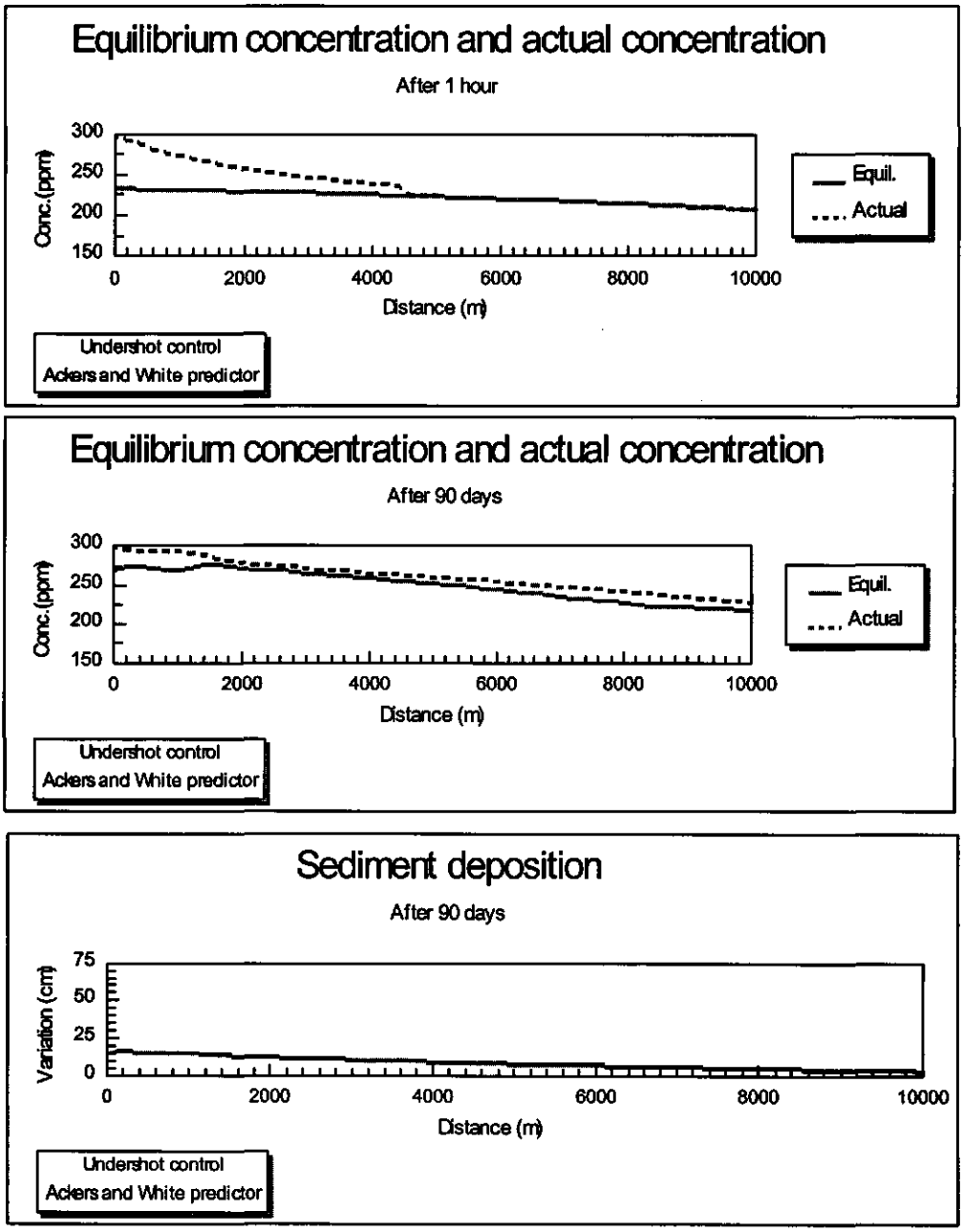

Figure 6.10 Equilibrium concentration and actual concentration at the beginning and at the end of the simulation period according to the Ackers-White's sediment transport predictor

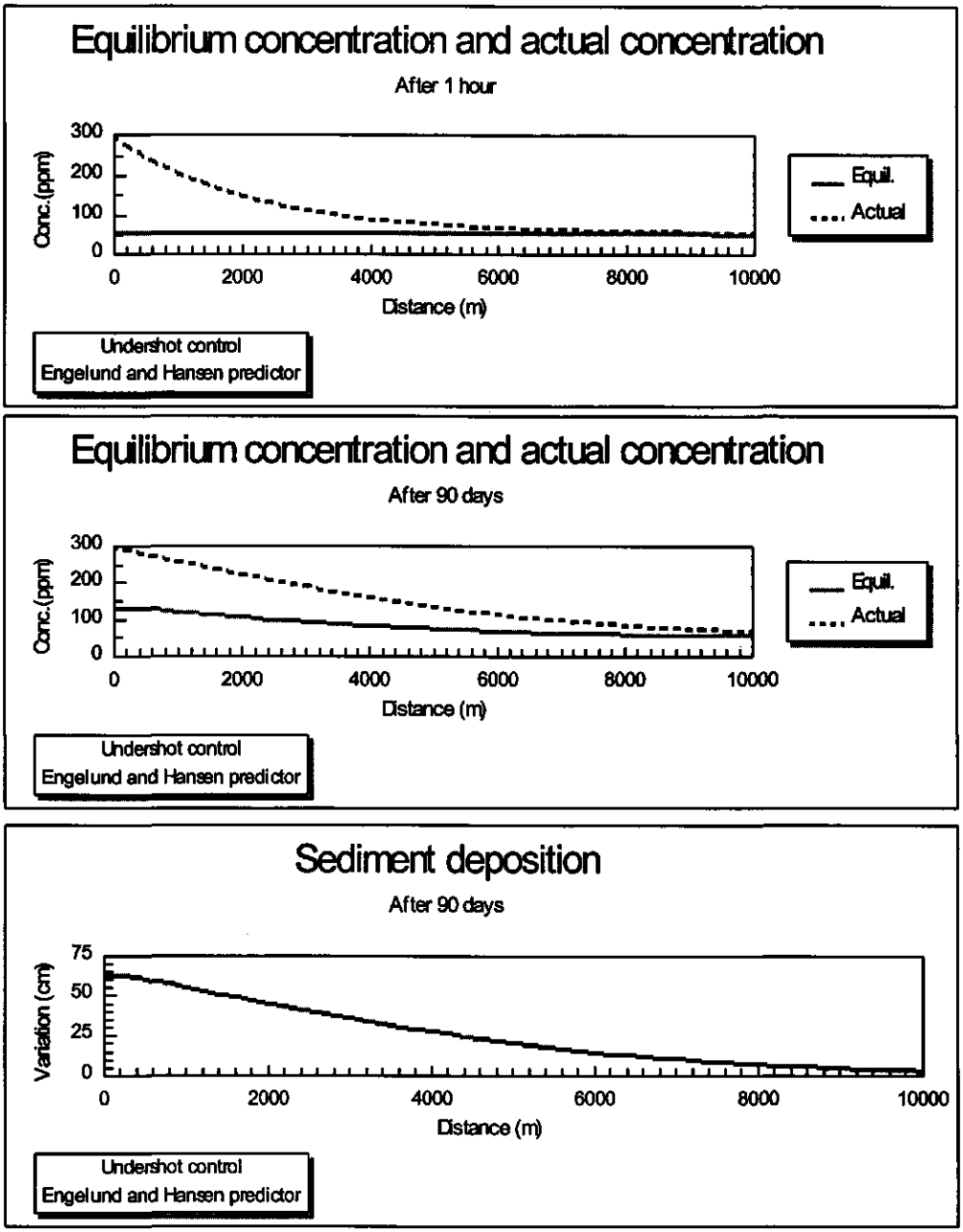

Figure 6.11 Equilibrium concentration and actual concentration at the beginning and at the end of the simulation period according to the Engelund-Hansen's sediment transport predictor

Large differences in the computed sediment deposition were observed among the sediment transport predictors. By using the Engelund and Hansen predictor, the estimated sediment deposition was three times larger than the estimated deposition by using the Ackers and White predictor and two times larger the estimated sediment deposition by using the Brownlie predictor. These differences are related to the capability for predicting the sediment transport capacity of certain flow conditions. An underprediction in the sediment transport capacity will overpredict the sediment deposition within the irrigation canal during certain period and in the other way around an overprediction of the sediment transport capacity will lead to either an underprediction of the sediment deposition or no deposition at all in time and space within the irrigation canal. Reliability of the prediction of the sediment deposition in irrigation canals will require an appropriate description of the carrying sediment capacity of these canals.

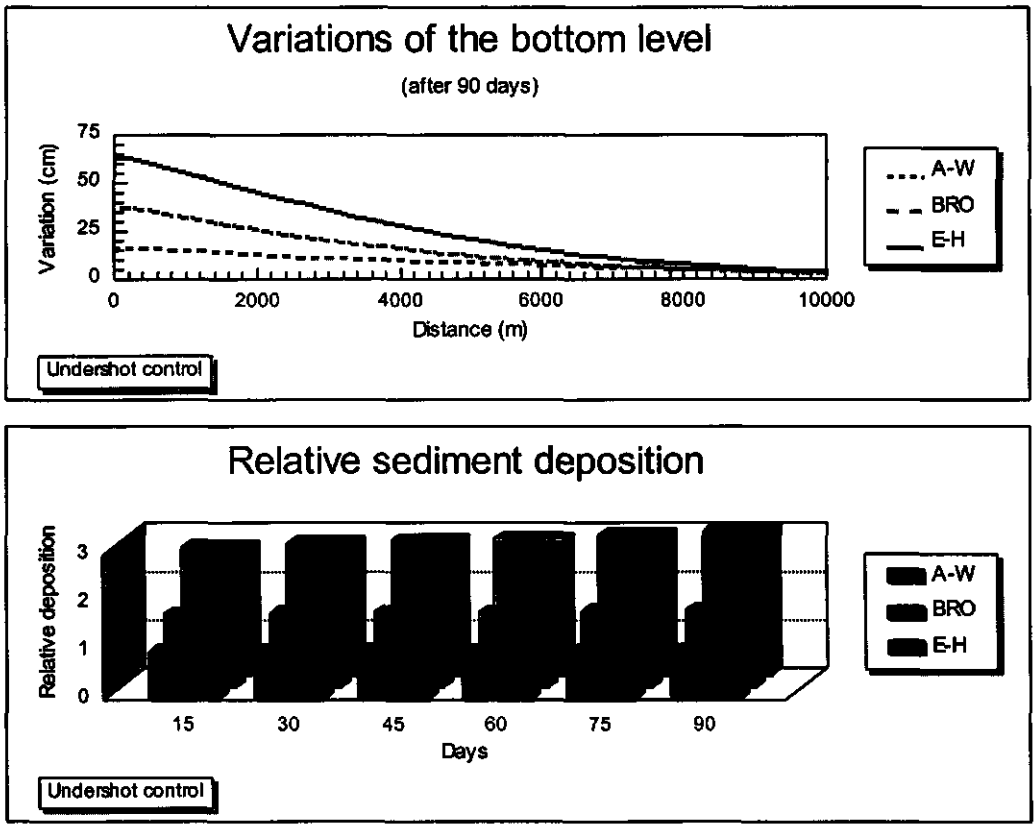

Figure 6.12 Variation of the bottom level and relative sediment deposition after 90 days in irrigation canal according three sediment transport predictors

6.6 Flow control structures

One of the criteria for designing irrigation canals is the command criterion. It means that the irrigation canal must deliver the water supply at the right elevation to the commanded area. Flow control structures are needed to keep the water level at a certain target for every discharge during the irrigation season. Selection of flow control structures depends on the operational objectives of the irrigation system and is based on several criteria in which the sediment passing capacity of those structures is one of the important criteria to be considered.

Two cases with different types of flow control structures will be considered namely undershot and overflow type. For both cases the sediment deposition and the distribution of the sediment deposition along the entire canal will be compared. The Ackers and White (A-W), Brownlie (BRO) and Engelund and Hansen (E-H) sediment transport predictors will be used to estimate the sediment transport capacity of the canal.

The geometrical, hydraulic and sediment characteristics of the irrigation canal are the same as in the previous sections and are described as:

- length (L) = 10000 m
- bottom width (B) = 10 m
- side slope (m) = 2
- equiv. Roughness (k_s) = 0.01 m
- bottom slope (So) = 0.00008
- bottom level (begin) = 40.00 m
- bottom level (end) = 39.20 m
- discharge (Q) = 25 m^3/s
- simulation period = 90 days
- sediment size = 0.15 mm
- sediment concentration = 300 ppm

The two types of flow control structure are defined as:

- *undershot type (case 1);*
- *overflow type (case 2).*

Although the selection of the structure depends on various operational aspects, only the ability of the structure to pass sediment is studied. Bed load and suspended load are supposed to pass trough the undershot type while only the suspended load is able to pass the overflow type and the bed load is supposed to be trapped by the obstacle imposed by the structure. Due to the fact that the water level at the downstream end of the canal is kept constant in both cases, no differences in the hydraulic conditions of both cases are expected. Both flow control structures are placed at the downstream end of the irrigation canal to control the water level at 41.65 m above the reference level.

To compare the total deposition of the sediment in the two cases a relative sediment deposition is used. It is expressed as:

$$\text{Relative sediment deposition} = \frac{\text{total sediment deposition in case 2}}{\text{total sediment deposition in case 1}} \qquad (6.8)$$

The distribution of the sediment deposition along the canal was evaluated by using a relative change of bottom level which is expressed as:

$$\text{Relative change of bottom level} = \frac{\text{variation of bottom level in case 2}}{\text{variation of bottom level in case 1}} \qquad (6.9)$$

Results of the simulation after 90 days, the sediment deposition in each case and the relative deposition of both cases are shown in figure 6.13. The sediment deposition in case 2 is larger than in case 1. The bed load passing capacity of case 1 is larger than case 2. An important difference between the two cases is the distribution of the sediment deposition.

Figure 6.14 shows the observed variation of the bottom level in both cases along the entire canal. Also the ratio between the variation of the bottom level in both cases is shown in figure 6.14.

For the considered simulation period, the distribution of sediment deposition shows large differences at the downstream part of the irrigation canal. In the upstream part of the canal (first 9600 m) there is no appreciable difference between both cases. In case 2 the bed load could not pass the flow control structure. The sediment transport capacity upstream of the overflow type (case 2) is only composed by the suspended transport capacity. In case 2 the sediment deposition process is due to two mechanism:

- first the sediment transport capacity of the irrigation canal is unable to convey the incoming sediment load of 300 ppm, therefore a sediment deposition process will occur at the upstream part of the canal. That sediment deposition will move in downstream direction.
- second, the flow control structure located at the downstream end of the irrigation canal is unable to pass the bed load transport therefore a sediment deposition process will start at the downstream end of the canal. It will move in an upstream direction.

In case 1 the sediment deposition is only due to the first mechanism. It was assumed that the undershot structure type (case 1) is able to pass both the bed load transport as the suspended load transport.

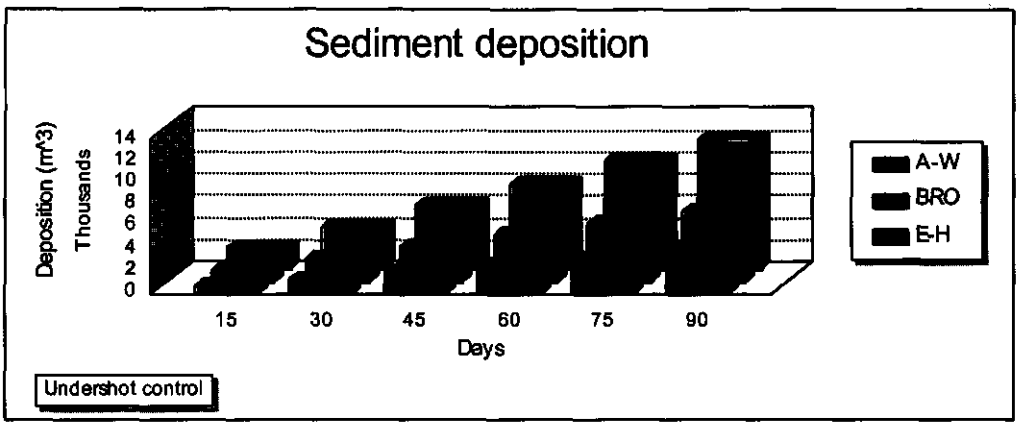

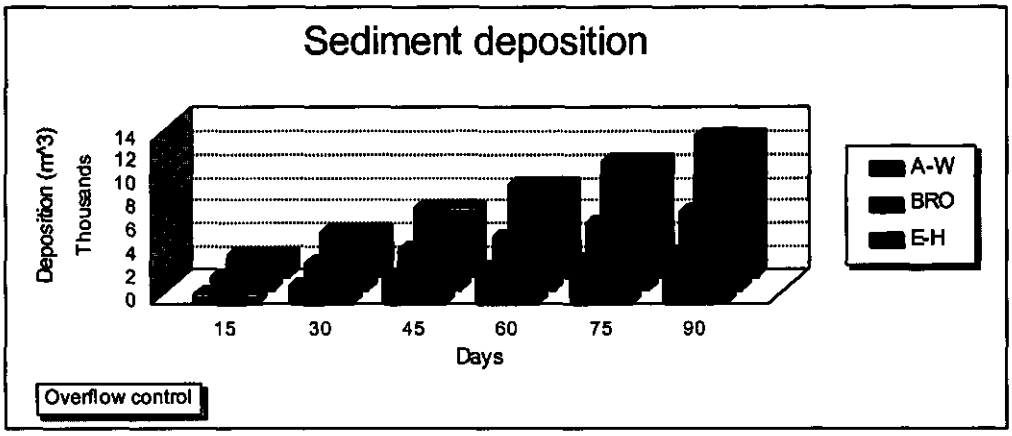

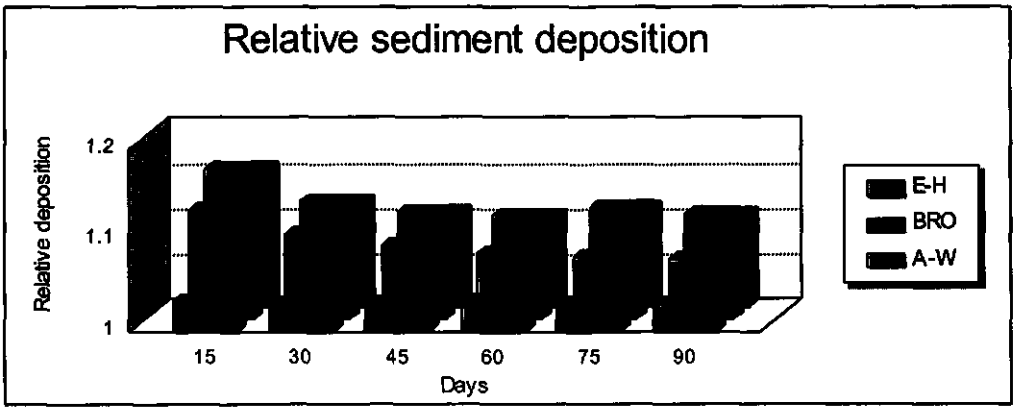

Figure 6.13 Total sediment deposition and relative sediment deposition in two types of flow control structures

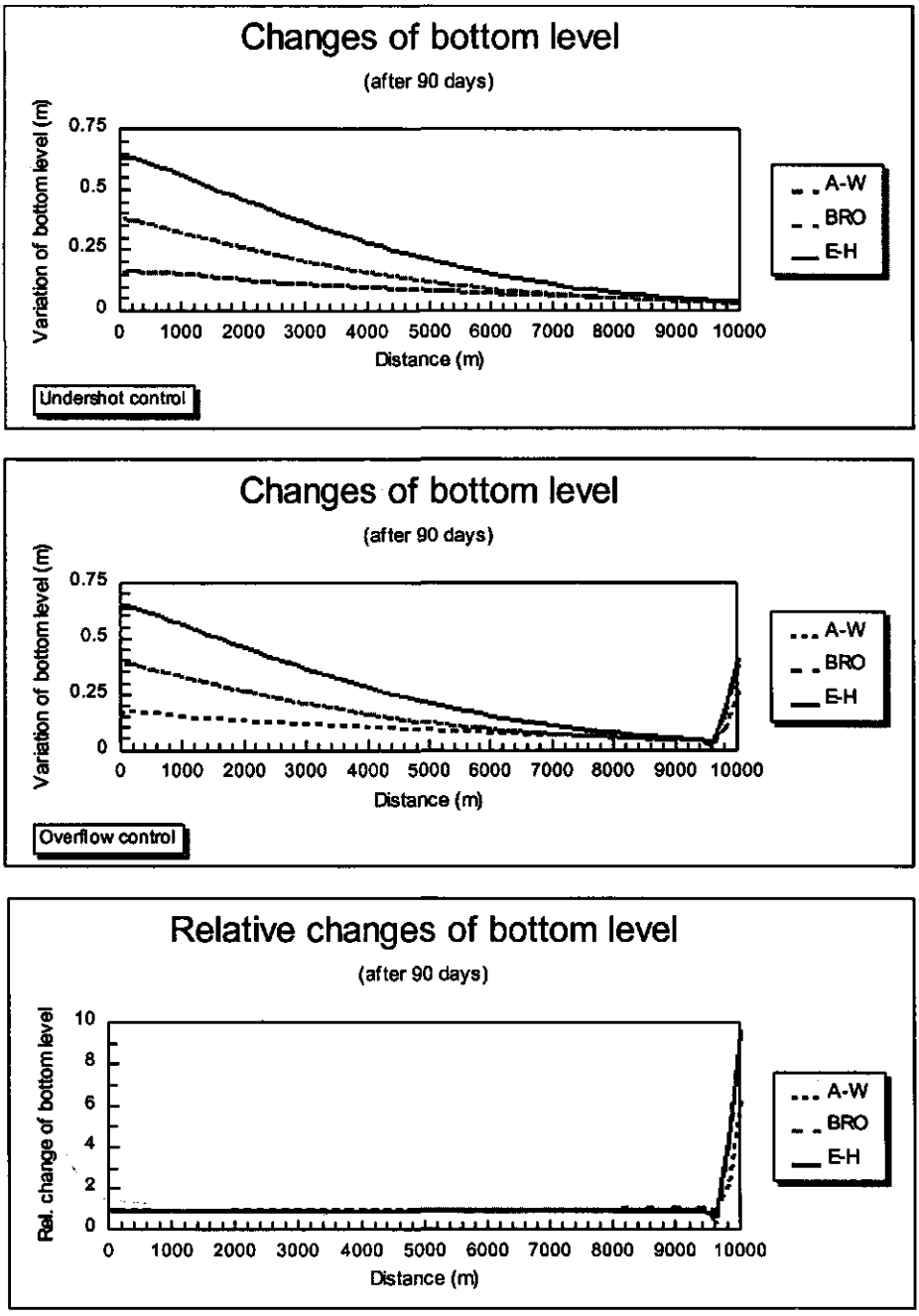

Figure 6.14 Comparison of changes in bottom level for two types of flow control structures

6.7 Maintenance activities

Maintenance in an irrigation canal comprises the set of activities for keeping the canal in good operating conditions and for ensuring that it is able to provide at all time its assigned objectives. Silt deposition, weed infestation, erosion of the banks, water infiltration and clogging of offtakes do not allow to deliver the required amount of water in the right amount and at the right elevation to the irrigated area. In this section the maintenance activities are related only to the silt deposition and weed infestation of the irrigation canal. Maintenance activities will be evaluated in terms of the effect of the type of maintenance on the hydraulic conditions and from the latter one on the sediment transport capacity of an irrigation canal. Effects of the vegetation on the sediment transport are not considered. Two types of maintenance were simulated in an irrigation canal with a nearly uniform flow condition. First an irrigation canal was used for transporting a certain amount of water and sediment load under a policy of ideal maintenance of weed infestation. It means that the roughness condition of the cross section is constant most of the time. Later on the water flow and the sediment transport in the irrigation canal was simulated under the policy of no maintenance during the simulation period. The Ackers and White sediment transport predictor was used to compute the sediment transport capacity of the irrigation canal. Sediment deposition or sediment entrainment for each scenario of type of maintenance was calculated. No erosion beyond the initial bottom level of the irrigation canal is assumed. The initial hydraulic condition is characterized by a nearly uniform flow with a small backwater curve (M1 profile). Initial geometrical, hydraulic and sediment characteristics of the irrigation canal are the following:

- length (L) = 10000 m
- bottom width (B) = 10 m
- side slope (m) = 2
- equiv. Roughness (k_s) = 0.01 m
- bottom slope (So) = 0.00008
- bottom level (begin) = 40.00 m
- bottom level (end) = 39.20 m
- discharge (Q) = 25 m^3/s
- simulation period = 90 days
- sediment size = 0.15 mm
- sediment concentration = 300 ppm
- flow control structure = undershot type
- water level at the canal end = 41.65 m

Two scenarios related to the expected type of maintenance during the simulation period were used. They can be described as:

- *scenario 1*: sediment deposition in an ideally maintained irrigation canal meaning that no obstruction is allowed. A nearly constant value of the roughness coefficient is expected during the simulation period. Variations of the Chézy coefficient are only due

to the occurrence of bed forms in the bottom of the irrigation canal and to the changes in flow conditions caused by the sediment deposition;

- *scenario 2*: sediment deposition in an irrigation canal without any maintenance at all. Variations of the Chézy coefficient are due to the occurrence of bed forms, to the changes in flow conditions caused by the sediment deposition and to the lack of maintenance. For the last one it is assumed that the lack of maintenance causes a linear reduction of the Chézy coefficient till 55% of the initial value.

Figure 6.15 shows the variation of the Chézy coefficient during the simulation period for each scenario. In an ideally maintained canal the Chézy coefficient is approximately constant. The vertical scale of the figure 6.15 was on purpose modified to show the small variation in time and space of the Chézy coefficient due to the presence of bed forms on the bottom and to the variation of the water depth along the irrigation canal. For an irrigation canal without maintenance the Chézy coefficient will largely vary due to weed growth on the side slope, but also by the occurrence of bed forms on canal bottom.

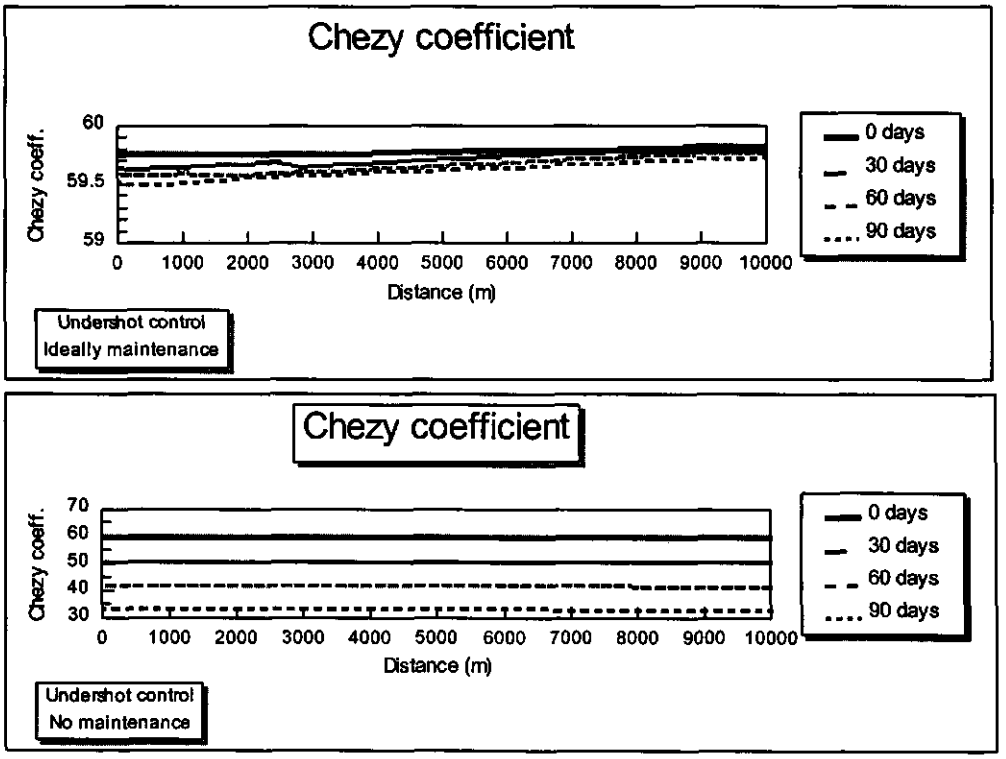

Figure 6.15 Variation of the Chézy coefficient during the simulation period in two type of maintenance activities: ideally maintenance and not maintenance

In case of an ideally maintained canal the flow conditions in the irrigation canal will slightly change during the simulation period. Water levels and mean velocities do not change so much when compared with the initial flow conditions of the simulation period as shown in the upper part of figures 6.16 and 6.17. A small backwater curve is present during the simulation period. Mean velocities are decreasing in downstream direction during most of the time.

Large reductions of the value of the Chézy coefficient in case of a non-maintained irrigation canal will largely affect the flow conditions in the canal. The water depth along the canal will rise and therefore the flow condition will change from a slightly developed backwater profile (M1) to a well developed drawdown water profile (M2). Mean velocities along the canal will increase in downstream direction. The lower parts of figures 6.16 and 6.17 show the behaviour of the water level and mean velocities for this type of maintenance. Also the vertical scale of the ideally maintained canal in figure 6.17 was on purpose changed in order to highlight the small variations in time and space of the hydraulic characteristics in the canal.

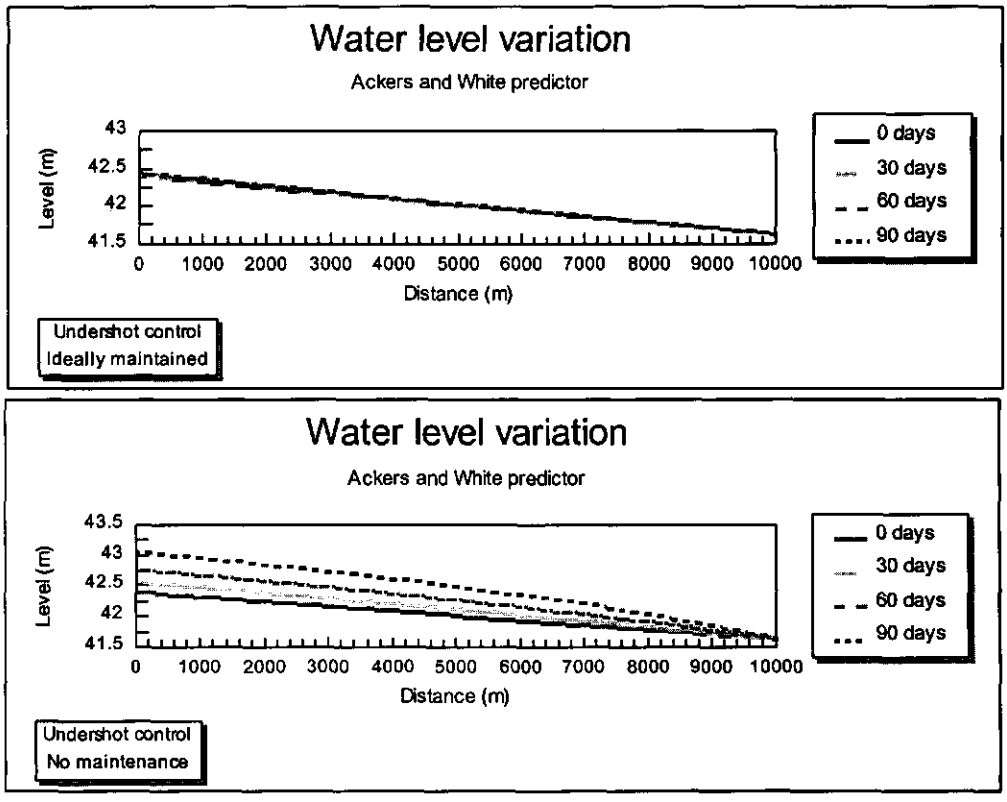

Figure 6.16 Variation of the water level during the simulation period in two type of maintenance activities

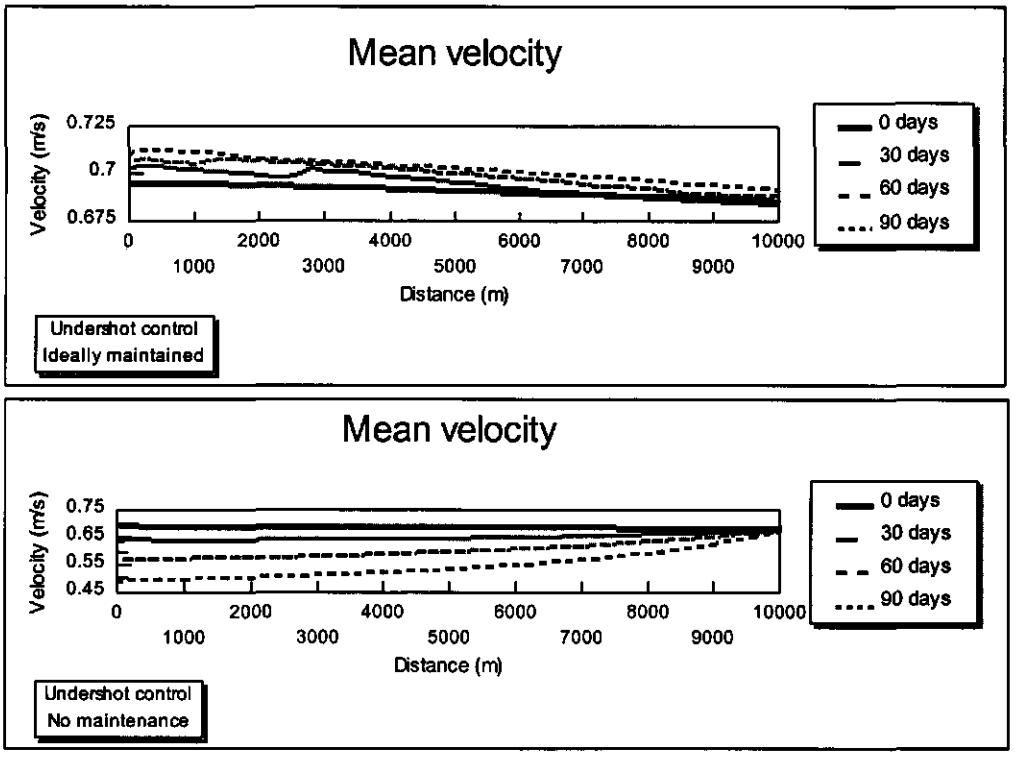

Figure 6.17 Variation of the mean velocities during the simulation period with and without maintenance

As a result of the behavior of the flow conditions during the simulation period the sediment transport capacity and the sediment load of the irrigation canal in each case of maintenance will also change. Figure 6.18 shows the sediment transport in the irrigation canal at the beginning and at the end of the simulation period. At the beginning of the simulation period (after 1 hour) the behavior of the sediment transport capacity and the sediment load in both cases of maintenance is similar. Initial flow conditions and sediment transport are the same in both cases. At the end of the simulation period the behavior of the sediment transport was different in both cases. In the ideally maintained canal the sediment transport capacity at the downstream end of the canal increases but not enough to match the incoming sediment load. Incoming sediment load will approach to the sediment transport capacity of the canal by depositing sediment along the entire irrigation canal. The sediment transport capacity of the canal will slightly decrease in downstream direction and sediment deposition will occur in the entire canal. In the canal without maintenance the sediment transport capacity at the head of the irrigation canal increases till it reaches the incoming sediment load after 30 days of the simulation period. At the end of the simulation period the sediment transport capacity of the entire canal is larger than the incoming sediment load and therefore can be transported without any deposition along the irrigation canal. Again the vertical scale has been changed to show the large variation of the sediment transport capacity.

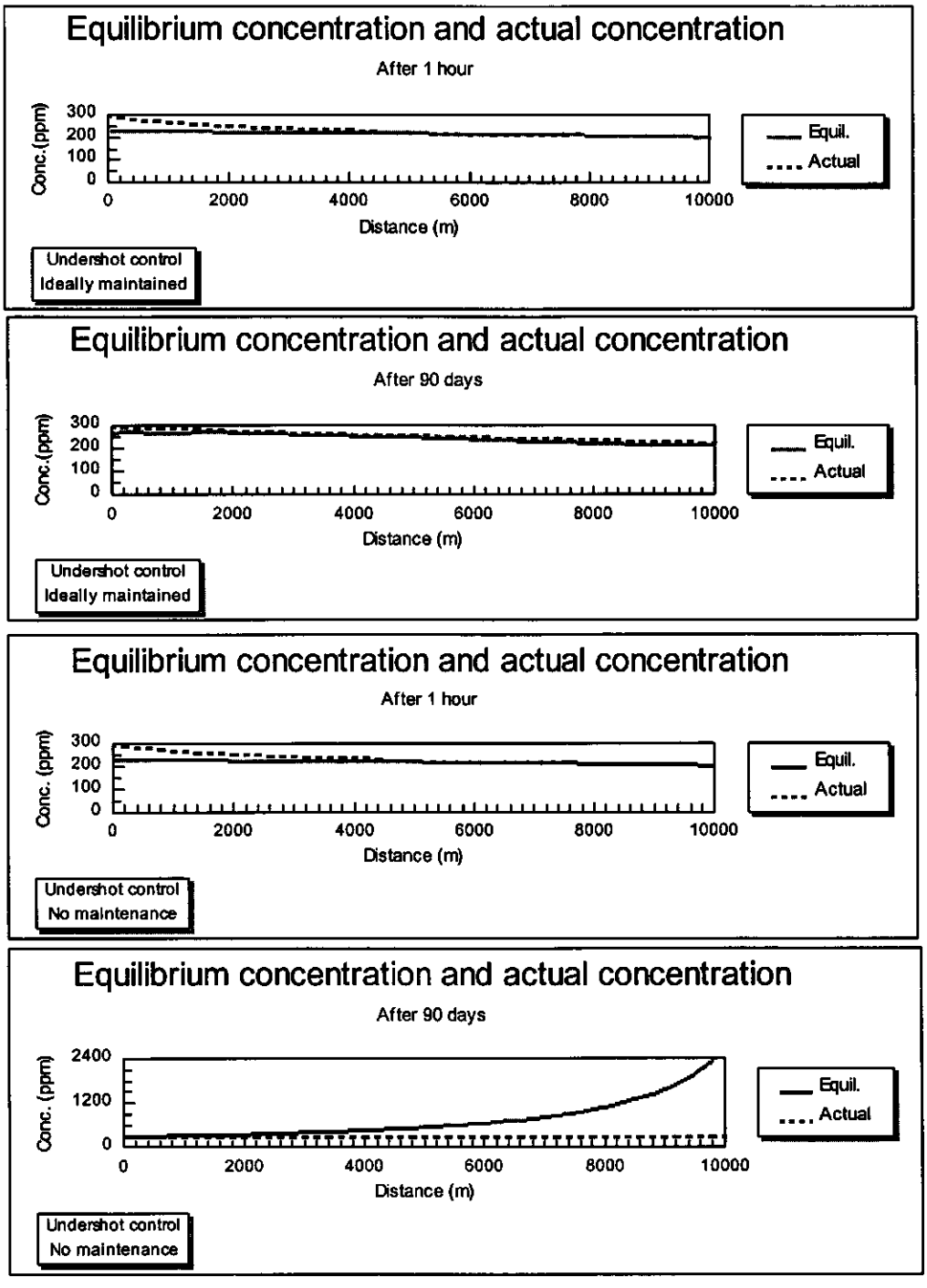

Figure 6.18 Variation of the sediment transport capacity and the sediment load during the simulation period with and without maintenance

Details of the variation in both the sediment transport capacity and the sediment load are shown in figures 6.19 and 6.20. Figure 6.19 shows the variation in time of the sediment transport capacity along the irrigation canal with and without maintenance.

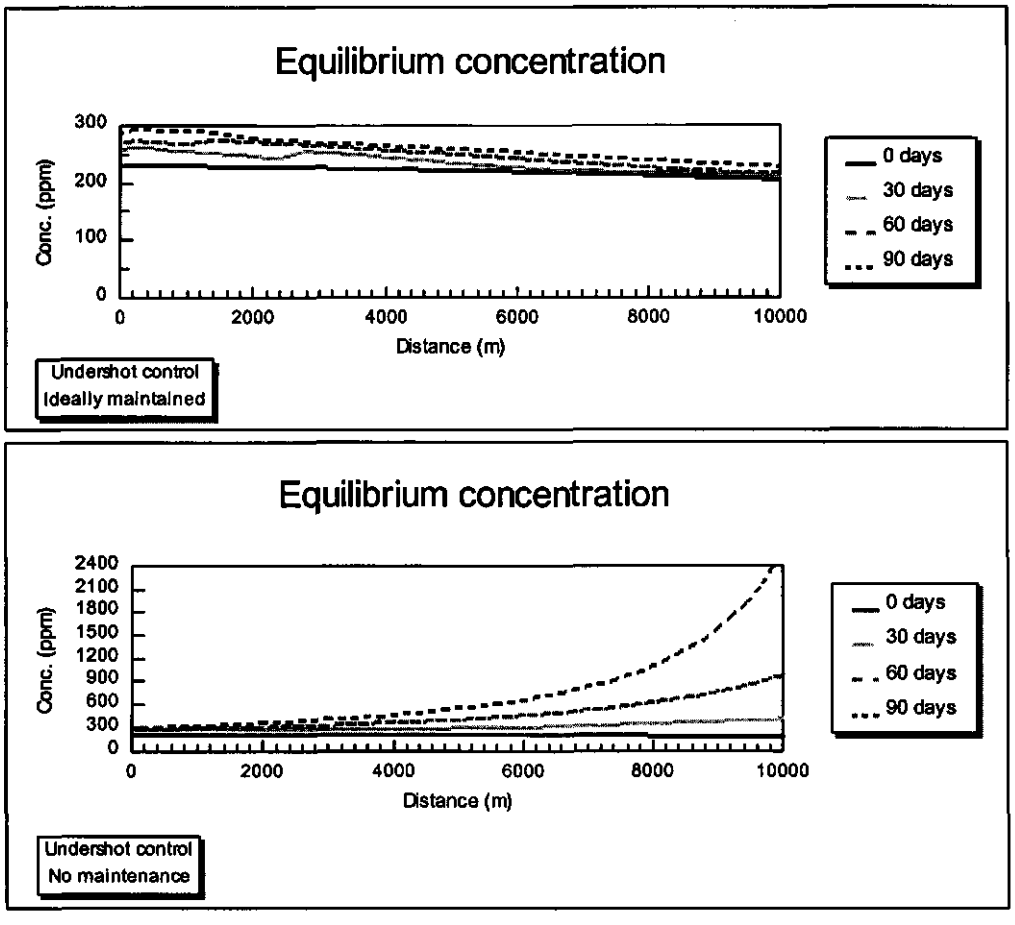

Figure 6.19 Variation of the sediment transport capacity during the simulation period with and without maintenance

In scenario 1 with an ideally maintained canal the sediment transport capacity will slightly increase in a specific cross section when compared with the initial sediment transport capacity at the beginning of the simulation period. On the other hand the sediment transport capacity of the canal will decrease in downstream direction. The sediment transport capacity at a specific location will increase due to effect of the sediment deposition on the mean velocity but the sediment transport capacity will decrease in downstream direction due to the backwater effect imposed by the control section at the end of the irrigation canal. The sediment transport capacity at the beginning of the irrigation canal reaches the incoming sediment concentration after 60 days. From that time onwards the sediment load is transported in downstream direction

with a continuous deposition due to the decreasing sediment transport capacity in that direction. For an irrigation canal without maintenance the sediment transport capacity will increase at any cross section but will also increase in downstream direction. The change of the flow conditions during the simulation period from a backwater curve to a drawdown curve will produce also changes in the mean velocities and shear velocities which will increase in downstream direction. Although the water depth is decreasing in downstream direction the energy slope increases in such a way that the resultant shear velocity also increases in downstream direction. The sediment transport capacity in the canal without maintenance reaches the incoming sediment load after 30 days. From that time onwards a continuous entrainment of the previously deposited sediment will take place. The vertical scale has been modified to show the large variation in the sediment transport capacity of the irrigation canal. Figure 6.20 shows the variation in time of the sediment load along the irrigation canal for both cases of maintenance activities.

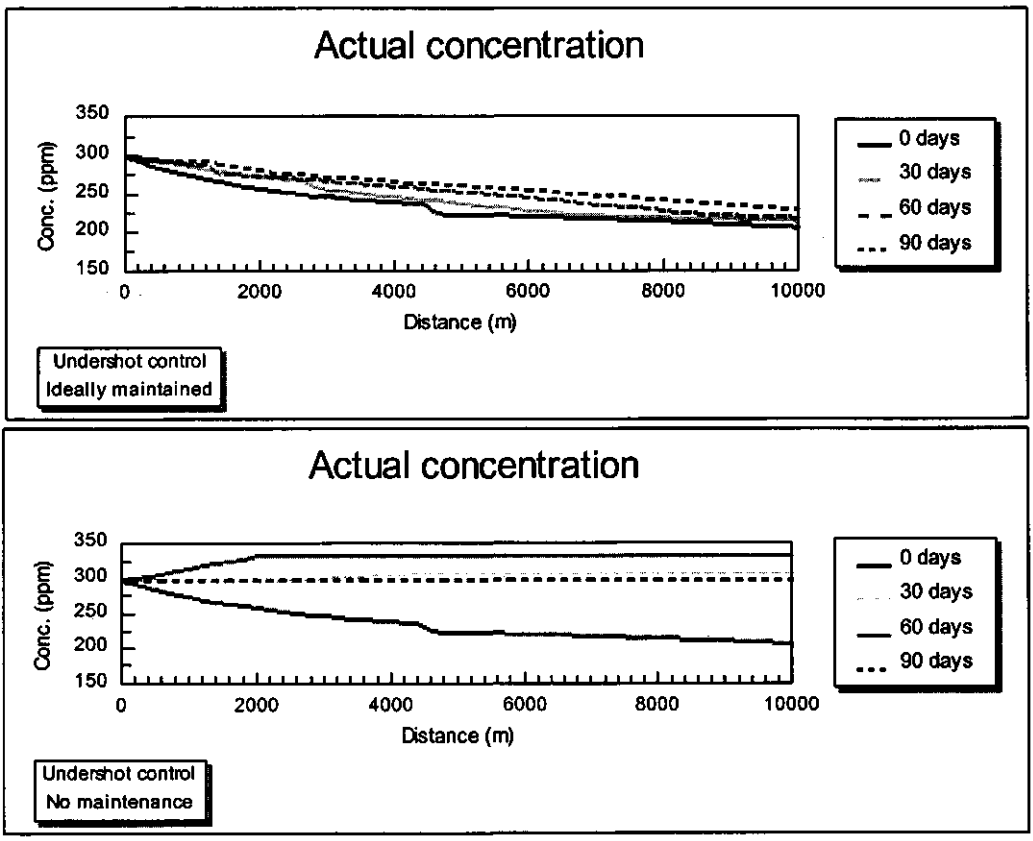

Figure 6.20 Variation of the sediment load during the simulation period with and without maintenance

The sediment deposition in scenario 1 increases during the simulation period. While the backwater curve remains in the irrigation canal a continuous deposition will occur until the sediment transport capacity in the entire canal reaches a larger value than the incoming

sediment load. From that time onward the incoming sediment load will be transported without deposition. This will not happen in the existing irrigation canal during the simulation period.

In scenario 2 sediment deposition occurs from the beginning of the simulation period until 30 days. Afterwards the entrainment of the previously deposited sediment occurs. Once the initial bottom level was reached the sediment load remained constant in time and space.

Figure 6.21 shows the variation in time of the total sediment deposition in the irrigation canal for both scenarios. For an ideally maintained canal a continuous deposition occurs. The flow conditions and the sediment transport do not deviate much from the initial condition. A non-equilibrium condition for the sediment transport with a continuous deposition is present during the simulation period. For the non-maintained irrigation canal the varying flow condition produces sediment deposition in the first 30 days of the simulation period but afterwards this previously deposited sediment is entrained. No sediment deposition is observed at the end of the simulation period.

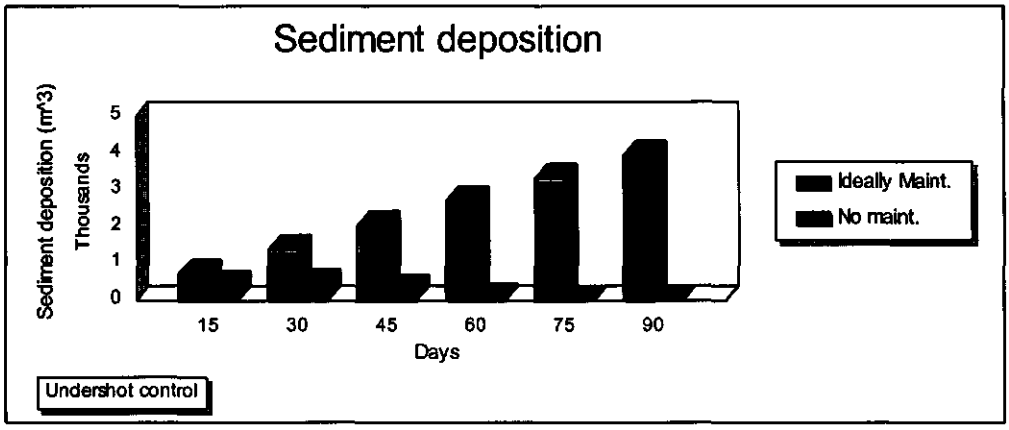

Figure 6.21 Variation of the sediment deposition during the simulation period for the two type of maintenance activities.

6.8 Operation activities

Operation of an irrigation system comprises all the activities for delivering the irrigation water to the user at the right time, at the correct elevation and at the proper volume. It can be done by several operation procedures. Each scheme can be operated under different conditions of availability of water, management of water supply, scheduling of water delivery, water control, water measurement, operating procedures, qualification of personal, institutional limitations, farm requirements, water rights, evaluation and monitoring and maintenance activities. The diversity of constraints makes the development of a general policy selection procedure difficult (Walker, 1993). Formulation of the operation policy for a certain irrigation system requires the evaluation of several scenarios in terms of the reliability of each scenario for water delivery. One of the aspects to be considered is the risk for sediment deposition in the canal system for each scenario. Effects of the type of operation on the sediment deposition are

simulated in an irrigation canal. For an analysis of the effect of the water distribution on the sediment deposition an irrigation system was schematized. The features related to the irrigation requirements, geometrical, hydraulic and incoming sediment characteristics can be described as follows: a main irrigation canal of 16 km will deliver water to two laterals and a reach located in the downstream part of the main canal. The main canal is composed of three reaches (AB, BC and CD). The first lateral (B_1) is located at 5 km of the upstream part. It will deliver water to the irrigated area B. The second lateral (C_1) is located 6 km downstream of the first lateral (B_1) which distributes water to the irrigated area C. The reach CD will convey the water to the downstream reach of the main canal which will be denoted as area D. The water flow is controlled by long crested weirs located at the division points of the main canal (nodes B, C and D). Two drops of 0.66 m and 0.60 m are at nodes B and C respectively. Table 6.1 shows the geometrical and hydraulic characteristics of the reaches of the main canal. Figure 6.22 shows the schematization of the irrigation system and a longitudinal profile of the main canal.

Table 6.1 Geometrical characteristics of main irrigation canal

Reach	Length L	Width B	Roughness k_s	Side slope m	Bottom slope S_0
(-)	(m)	(m)	(m)	(-)	(10^{-3})
A-B	5000	10	0.03	2	.08
B-C	6000	10	0.03	2	.08
C-D	5000	8	0.03	2	.10

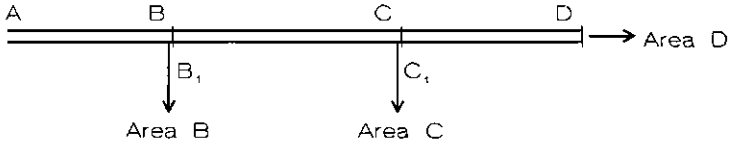

(a) Schematization of an irrigation system

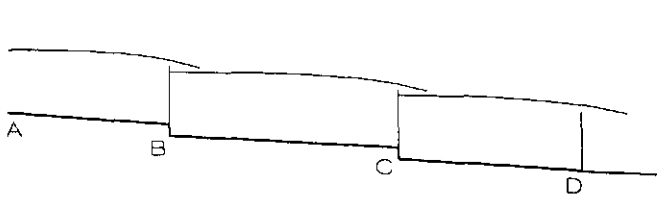

(b) Longitudinal profile of the main irrigation canal

Figure 6.22 Schematization of an irrigation system and longitudinal profile of the main canal

The irrigation season is characterized by three periods in which the water requirement per period for each of the irrigated areas was specified as described in table 6.2.

Table 6.2 Water needs along the irrigation season of the irrigated area

Irrigated area		Period					
		1		2		3	
		Duration	Needs	Duration	Needs	Duration	Needs
Area	ha	days	l/s/ha	days	l/s/ha	days	l/s/ha
B	5000	28	0.8	28	1	28	0.8
C	5000	28	0.8	28	1	28	0.8
D	15000	28	0.8	28	1	28	0.8

To match the water needs with the water supply several operation procedures for the main irrigation canal can be used. For simulating the effect of the operation procedures on the sediment deposition in the main canal four scenarios will be analyzed. All of them are able to meet the water requirements of the irrigated areas. The Ackers and White sediment transport predictor is used to compute the sediment transport capacity of the irrigation canal. Distribution efficiency in the main canal is assumed to be 100%. The incoming sediment load at the inlet during the whole irrigation season is characterized by:

- median diameter d_{50} = 0.15 mm
- sediment concentration = 300 ppm

The four scenarios can be described as:

- *scenario 1 (continuous flow)*: a continuous flow during the whole irrigation season;
- *scenario 2 (rotational flow)*: a rotational flow during day time is proposed for the laterals B_1 and C_1. It means that each lateral will receive water every day during 12 hours. For distinguishing from the other types of rotational flow this scenario will be named as rotational by hour;
- *scenario 3 (rotational flow)*: a rotational flow per day is proposed for the laterals B_1 and C_1. The water delivery will be rotated every day between those laterals. It will be named rotational by day;
- *scenario 4 (rotational flow)*: a rotational flow per week is proposed for the laterals B_1 and C_1. Every week one lateral will receive the water supply. It will be named rotational by week.

Details of the duration (D) of the water delivery, the frequency (F) or interval between two irrigation turns and the flow rate (Q) during the periods of the irrigation season in each reach of the main canal and laterals are given in table 6.3.

Table 6.3 Flow conditions during the irrigation season in each reach of the main irrigation canal and laterals

Scenario	Canal	Period								
		1			2			3		
		D	F	Q	D	F	Q	D	F	Q
		hrs	days	m^3/s	hr	days	m^3/s	hrs	days	m^3/s
1	A-B	24	Cont.	20	24	Cont.	25	24	Cont.	20
	B-C	24	Cont.	16	24	Cont.	20	24	Cont.	16
	C-D	24	Cont.	12	24	Cont.	15	24	Cont.	12
	B_1	24	Cont	4	24	Cont.	5	24	Cont.	4
	C_1	24	Cont.	4	24	Cont.	5	24	Cont.	4
2	A-B	24	Cont.	20	24	Cont.	25	24	Cont.	20
	B-C	24	Cont.	12-20	24	Cont.	15-25	24	Cont.	12-20
	C-D	24	Cont.	12	24	Cont.	15	24	Cont.	12
	B_1	12	1	8	12	2	10	12	2	8
	C_1	12	1	8	12	2	10	12	2	8
3	A-B	24	Cont.	20	24	Cont.	25	24	Cont.	20
	B-C	24	Cont.	12-20	24	Cont.	15-25	24	Cont.	12-20
	C-D	24	Cont.	12	24	Cont.	15	24	Cont.	12
	B_1	24	2	8	24	2	10	24	2	8
	C_1	24	2	8	24	2	10	24	2	8
4	A-B	24	Cont.	20	24	Cont.	25	24	Cont.	20
	B-C	24	Cont.	12-20	24	Cont.	15-25	24	Cont.	12-20
	C-D	24	Cont.	12	24	Cont.	15	24	Cont.	12
	B_1	24	7	8	24	7	10	24	7	8
	C_1	24	7	8	24	7	10	24	7	8

The sediment deposition during the irrigation season is simulated in the entire canal (ABCD) for each scenario. Details of the behaviour of the sediment transport at the end of each irrigation period for scenario 1 is shown in figures 6.23.

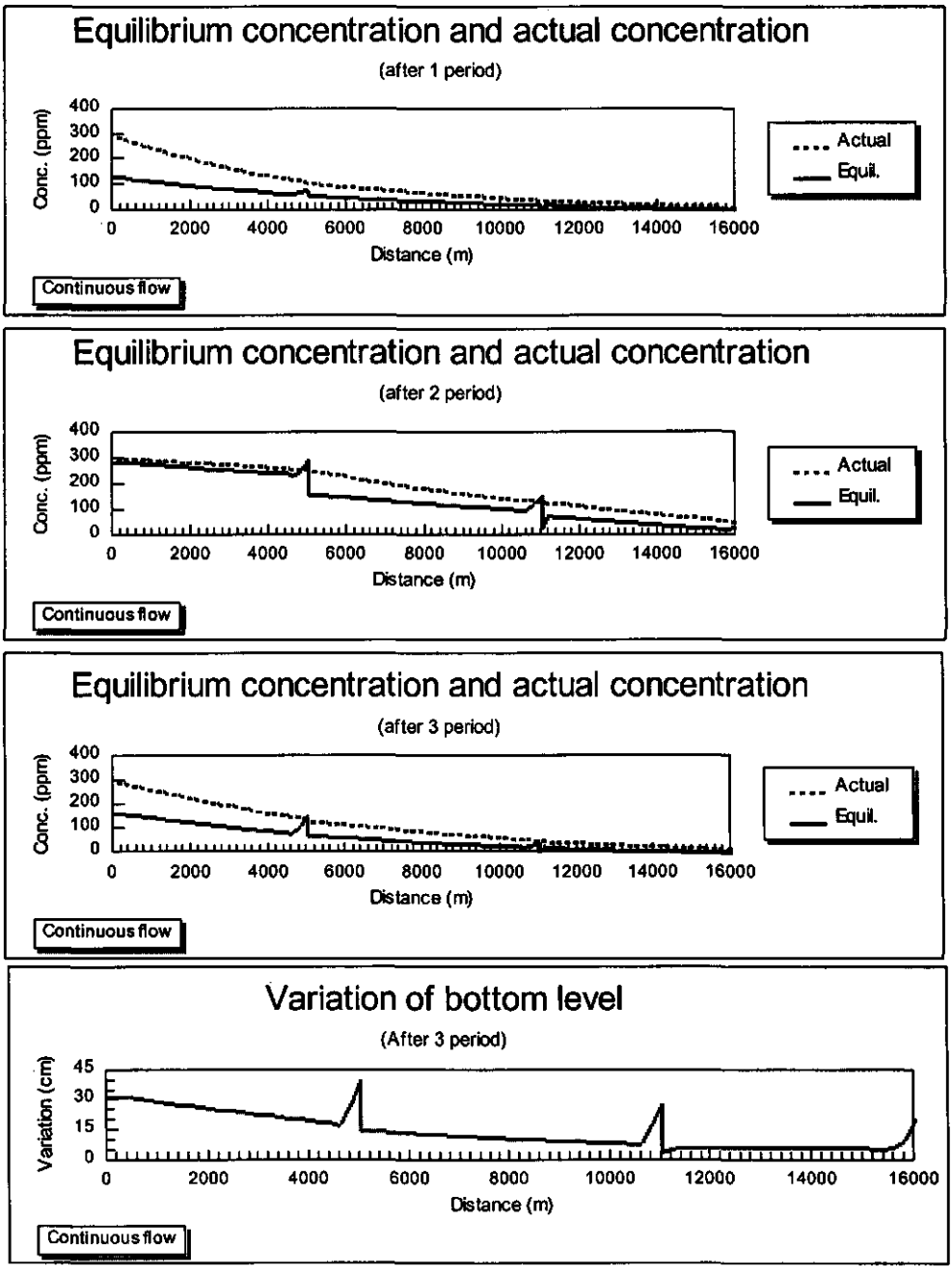

Figure 6.23 Variation of the equilibrium concentration and actual concentration at the end of each irrigation period and variation of the bottom level at the end of the simulation period (continuous flow)

In scenario 1 (fig. 6.23) the variation of the sediment transport capacity in time and space does not reach values larger than the incoming sediment load. Only at the end of the reaches, the

sediment transport capacity of the canal is larger than the sediment load due to the local deposition caused by the structure (overflow type). The mean velocities at those points are larger due to the smaller water depths there. Although the sediment transport capacity increases during the second period of the irrigation season a decreasing sediment transport capacity in downstream direction is observed along the entire main canal. Sediment deposition is observed during all the periods in the entire canal.

Figure 6.24 and 6.25 show the characteristics of the sediment transport on a day at the end of the irrigation period when the water is diverted to the lateral B_1 (fig. 6.24) or when the water is diverted to lateral C_1 (fig. 6.25).

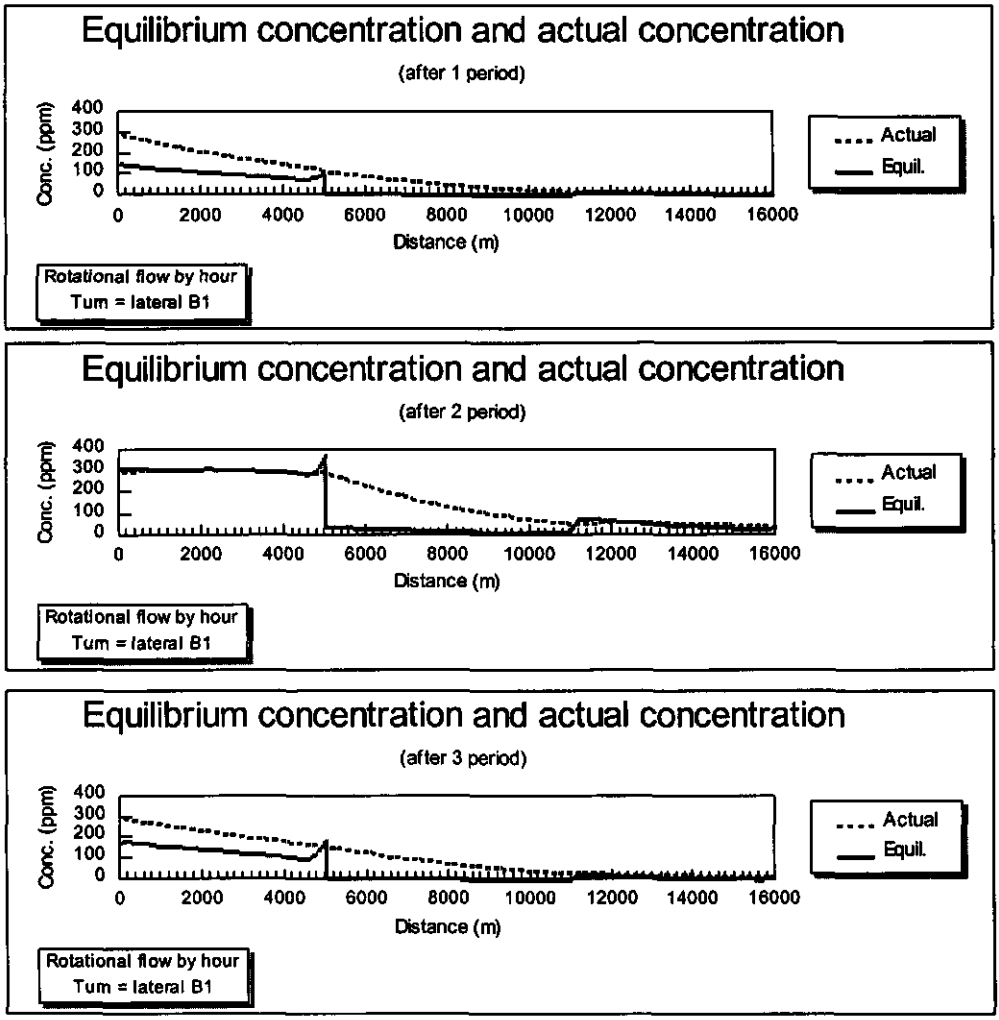

Figure 6.24 Variation of the equilibrium concentration and actual concentration at the end of each irrigation period during the first turn of irrigation (Rotational flow by hour)

In scenario 2 (figs. 6.24 and 6.25) the sediment transport capacity is changing in time due to two effects. First, the varying flow condition in the reach BC imposed by the rotational flow. Second, the varying flow condition during the simulation period imposed by the different periods of irrigation. Those effects produce alternatively processes of deposition and entrainment.

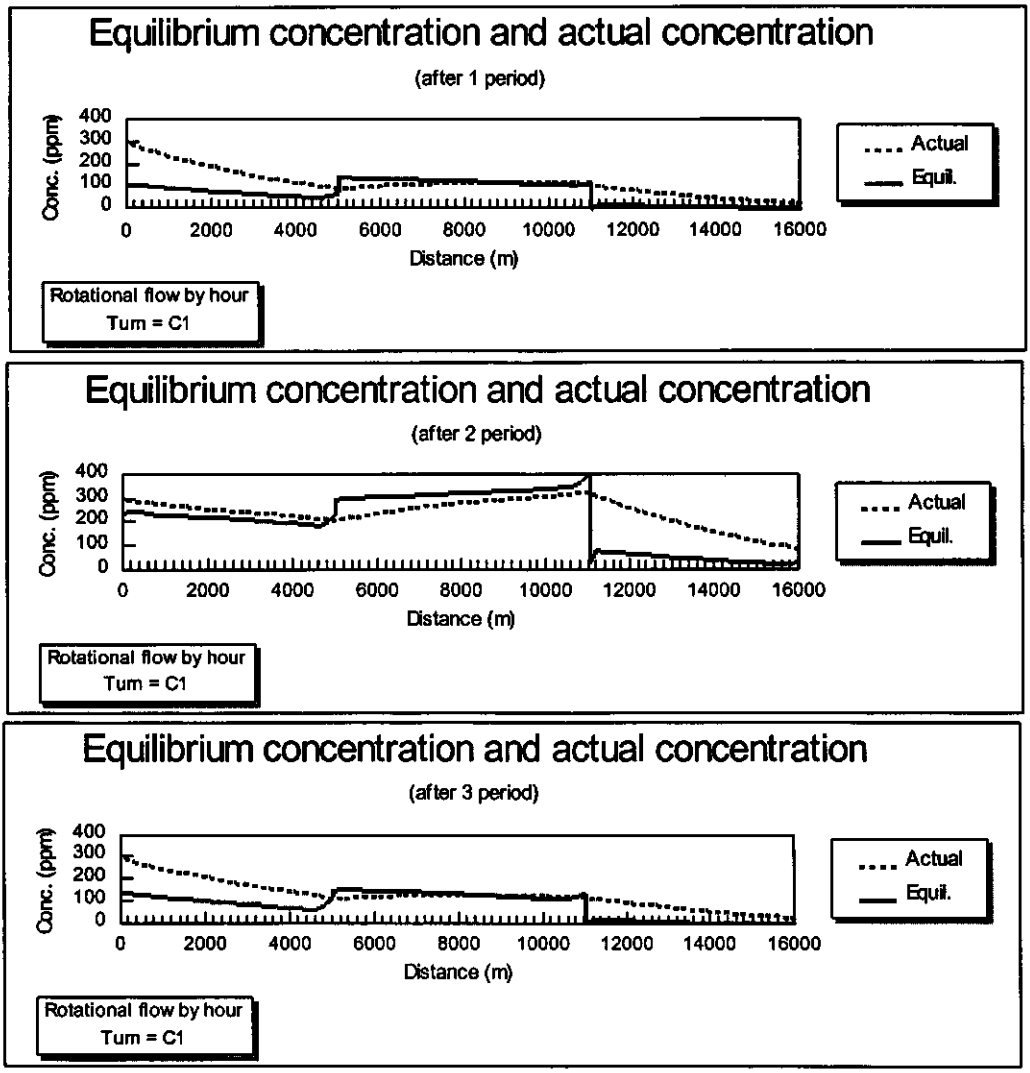

Figure 6.25 Variation of the equilibrium concentration and actual concentration at the end of each irrigation period during the second turn of irrigation (Rotational flow by hour)

In the reach AB the incoming sediment load is larger than the capacity of the sediment transport of this reach and deposition occurs. During the second period of irrigation there is an increase of the discharge. Sediment transport capacity increases till it reaches the incoming

sediment load. The sediment load is conveyed in a nearly equilibrium condition to the second reach BC with a minimum of deposition. The flow condition in reach BC is characterized by a gradually varied flow (backwater curve) with very small velocities decreasing in downstream direction along this reach. Deposition is observed in this reach during this part of the day. The increase of the discharge in the second period in the entire canal is not large enough to convey the sediment load entering the reach BC. Sediment concentration entering the next reach CD is small due to the large deposition in the previous reach. That sediment load is transported by the water flow. Small deposition is observed in the reach CD. In the second half of the day (fig. 6.25), the lateral B_1 is closed and the lateral C_1 is opened. The reach AB behaves rather similar to the previous turn but with a lower value of the sediment transport capacity due to the fact that the water level over the crest of the weir is slighly higher than the previous turn. The sediment transport capacity in reach BC is larger than the sediment load. In the second irrigation period the increase of the discharge in the reach BC produces a gradually varied flow (drawdown curve). Therefore an increasing sediment transport capacity in downstream direction and entrainment of the previous deposited sediment are observed. The sediment load entering the next reach (reach CD) is larger due to the entrained sediment in the previous reach. Under this flow condition, sediment deposition is observed during the whole irrigation season. Variation of the bottom level at the end of the simulation period for this type of operation (scenario 2) is shown in figure 6.26.

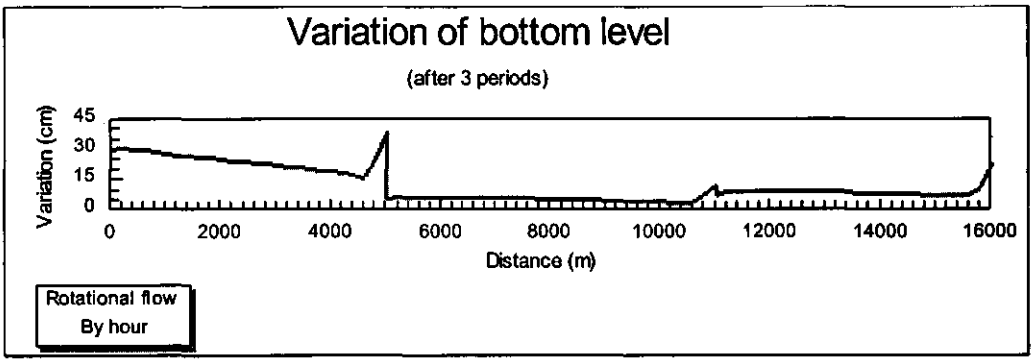

Figure 6.26 Variation of the bottom level during the simulation period (Rotational flow by hour).

In scenarios 3 and 4 the sediment transport behaves similar to the previous scenario with alternative periods of deposition and entrainment but at different time intervals due to the different intervals of irrigation. Figures 6.27 and 6.28 show the variation of the equilibrium concentration and actual concentration at the end of each period during the second turn of irrigation in those scenarios (Rotational flow by day and by week). As explained in the previous scenario the sediment tranport capacity during the second period of the irrigation season reaches values larger than the incoming sediment load. In those scenarios deposition and erosion of the previously deposited sediment is observed. The computed total sediment depositions in those scenarios do not show large differences among them. Differences are mainly observed in the location of the sediment deposition in the reaches.

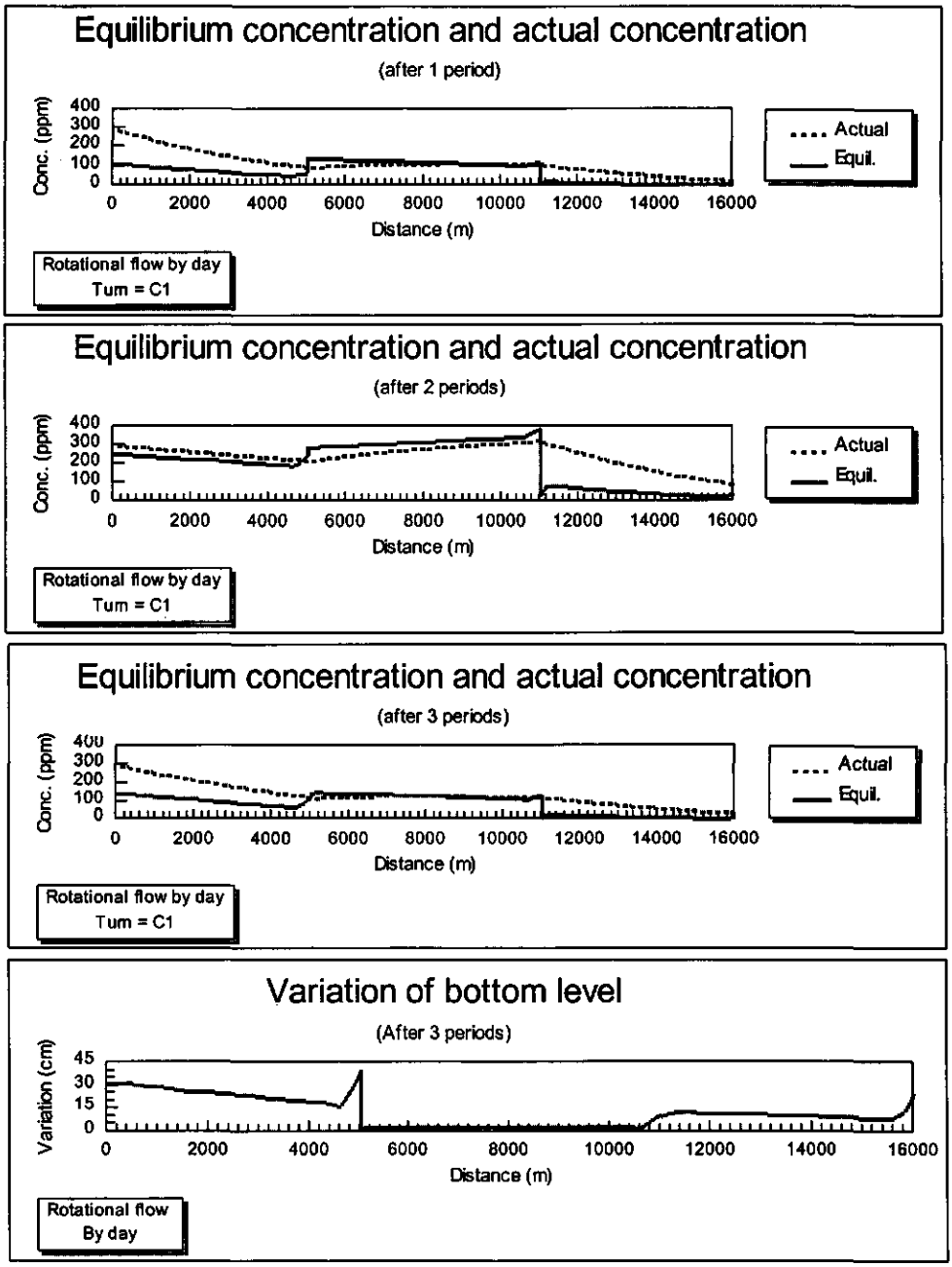

Figure 6.27 Variation of the equilibrium concentration and actual concentration at the end of each irrigation period and variation of the bottom level at the end of the simulation period (Rotational flow by day)

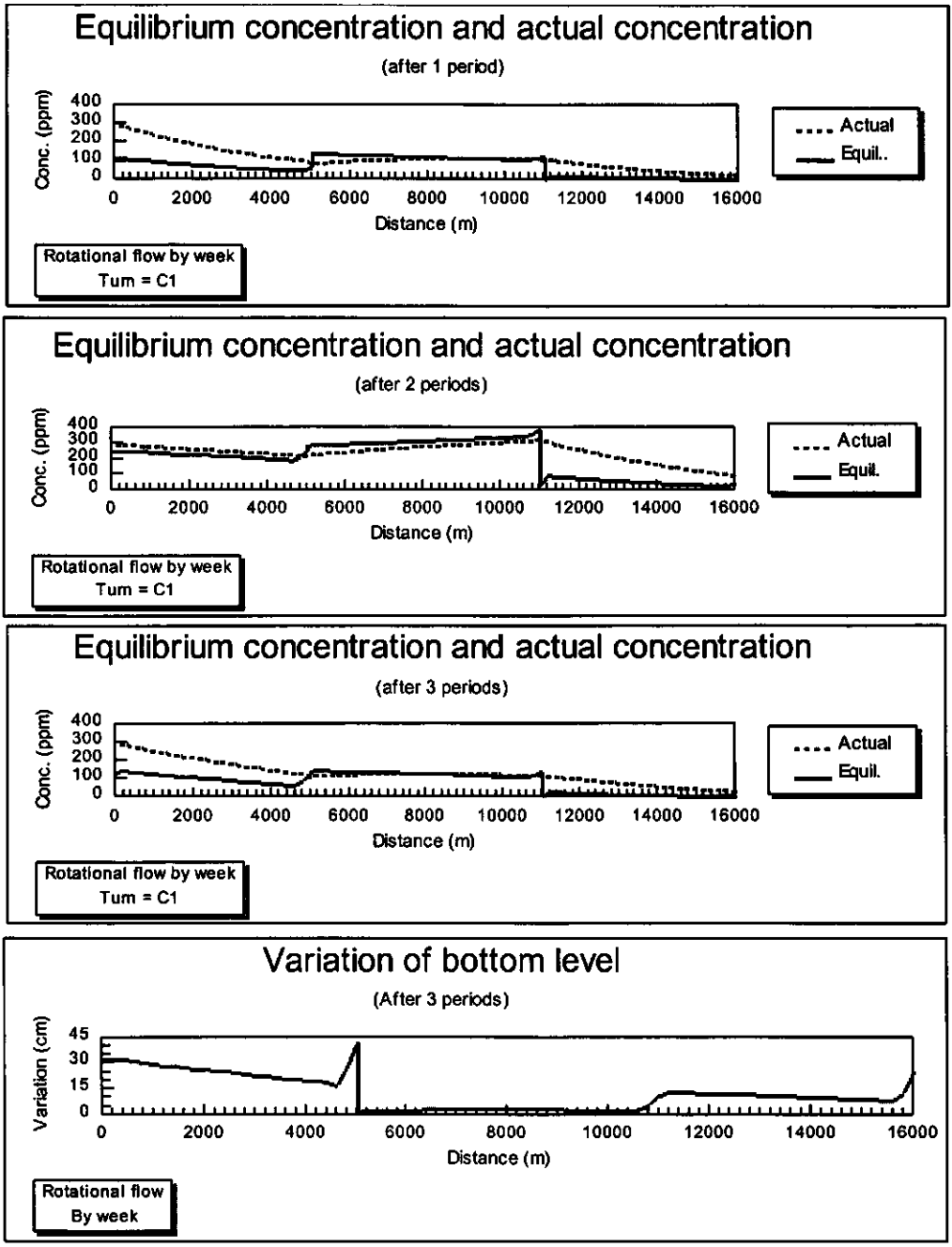

Figure 6.28 Variation of the equilibrium concentration and actual concentration at the end of each irrigation period and variation of the bottom level at the end of the simulation period (Rotational flow by week)

In order to compare the distribution of sediment deposition in each reach of the main canal a relative sediment deposition related to the deposition observed for continuous flow is used. The relative sediment deposition can be expressed as:

$$\text{Relative deposition} = \frac{\text{computed sediment deposition by scenario 1}}{\text{computed sediment deposition by scenarios 2, 3, or 4}} \qquad (6.10)$$

Figure 6.29 shows the relative deposition for each scenario. From that comparison some conclusions can be drawn:

- the largest total sediment deposition in the canal (all reaches) with 20 % more deposition than the other scenarios is observed in scenario 1. A relative deposition of about 1.2 is observed when compared with each scenario. The total sediment deposition in scenarios 2, 3 and 4 are rather similar;
- in the reach AB the sediment deposition in all scenarios is approximately similar. Differences in the sediment deposition are less than 5% among all scenarios. Those small differences were mainly due to the variation in time of the hydraulic head over the long crested weir located at node B which affects the sediment transport capacity of the reach, therefore the sediment deposition is also affected;
- in reach BC the computed sediment deposition in scenario 1 (continuous flow) is between 2 and 3.5 times the observed sediment deposition in scenarios 2, 3 and 4. In scenarios 2, 3 and 4 the sediment transport capacity during the second turn of irrigation (lateral C_1 is opened and lateral B_1 is closed) and during the second irrigation period increases beyond the incoming sediment load producing a degradation process of the previous deposited sediment;
- in reach CD the observed sediment deposition of scenario 1 (continuous flow) is approximately half time the observed sediment deposition in scenarios 2, 3 and 4. In scenario 2, 3 and 4 the sediment load leaving the reach BC is very small due to the relative large deposition observed in that reach therefore the incoming sediment load in reach CD can be transported with a minimum of deposition;
- the total sediment deposition in the entire canal and its distribution within the canal are important aspects to be considered in the selection of the operation strategy for the water delivery in an irrigation canal.

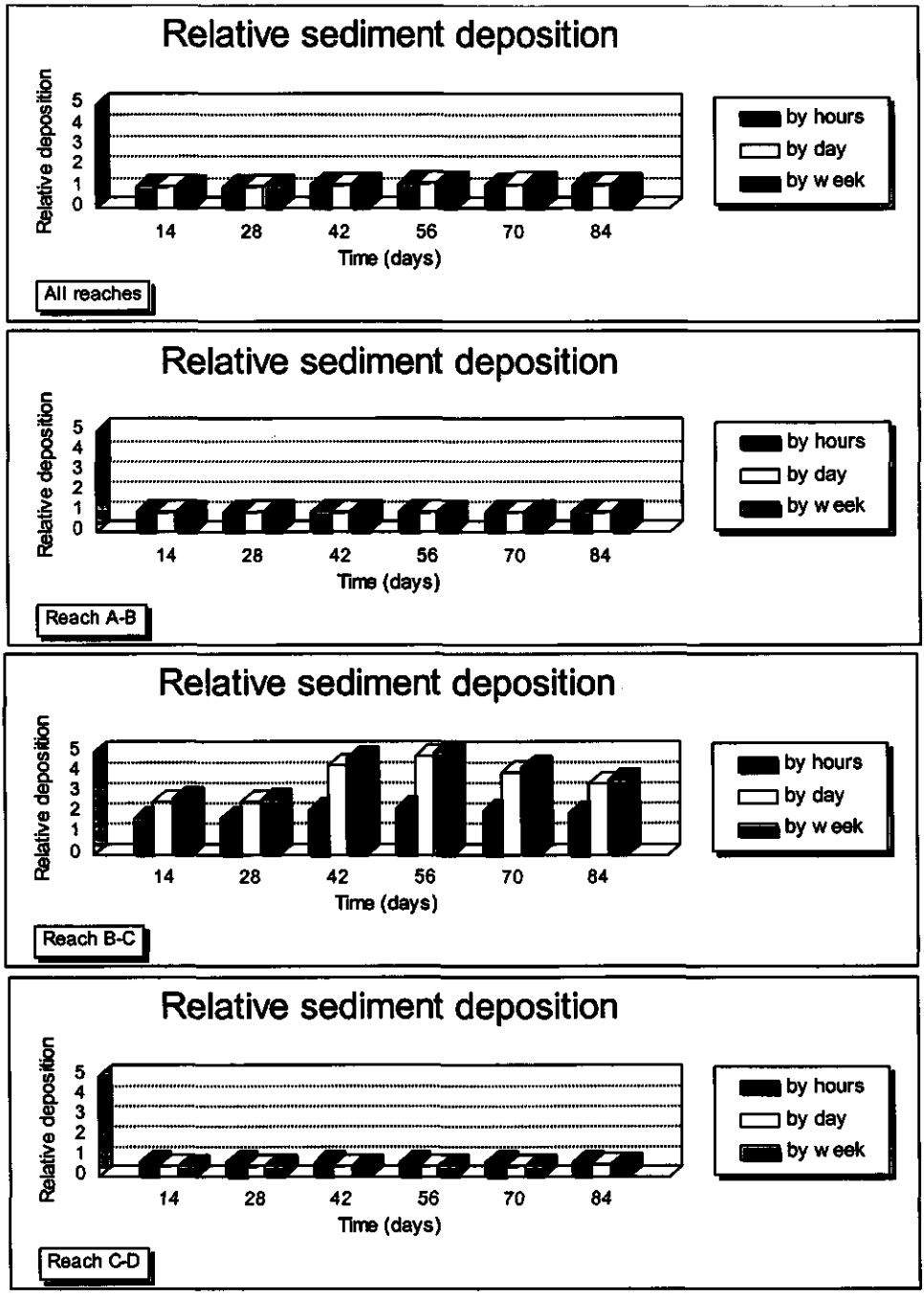

Figure 6.29 Relative sediment deposition in the reaches and the entire irrigation canal when compared with the sediment deposition observed in scenario 1 (continuous flow)

7 EVALUATION

7.1 General

Sediment problems in natural or artificial channels have been studied for many years. Although the problem of sedimentation in irrigation canals is not new, it is only during the last decades that it is worldwide recognized. During the past 50 years the rapid expansion of irrigation systems showed that many existing systems silted up and could not be operated in a proper way due to an insufficient transport capacity for the incoming sediment load at the canal headwork. This circumstance has attracted the attention of many irrigation engineers, who are looking for solutions to improve the operation capability of those systems.

Many researchers have contributed to the understanding and description of the physical processes that govern the sediment transport in open channels. However, researches have mainly focused on river, tidal and coastal engineering. There is still a need to know the flow characteristics and the behaviour of rivers and their changes due to natural or man-made modifications in their characteristics as for instances by dams, spillways, locks and weirs, navigation or flood control channels or intakes of irrigation systems.

Various efforts addressed the design of stable alluvial canals and sediment control structures at the head of irrigation networks. All the existing methods for the design of lined and unlined irrigation canals are based on the interrelating equations of input variables for certain water flow and sediment transport conditions. However, the input variables will widely vary during the irrigation season and moreover during the lifetime of the irrigation canals. Most of the time, non-equilibrium conditions prevail in the irrigation systems and therefore the initial assumptions for the design of stable canals are not valid anymore. Also lined canals experience sedimentation problems. Although lined canals are generally designed for a high sediment transport capacity; variations in either flow condition or in the incoming sediment load will produce non-equilibrium conditions for the transport of the sediment.

Sediment problems in irrigation canals should be analysed in a more general context in which different scenarios for water flow and sediment transport are considered. An up-to-date mathematical model will be very useful to predict the transport and the deposition of sediment in irrigation canals. The mathematical formulation used in the model requires the recognition and understanding of the governing physical processes. The reliability of the results largely depends on the degree of the applicability of the model to the specific flow conditions.

Applications of simulation models for sediment transport in rivers are frequently mentioned in the literature, but only a very few references are directly related to sediment transport in irrigation canals. Until nowadays a surprisingly small number of mathematical models dealing with sediment transport in irrigation canals can be found in the literature and so far none of

them has been concentrated on the specific conditions of irrigation canals. The existing models dealing with sediment transport are mainly focused on river conditions. Although certain similarities exist between irrigation canals and rivers, these models are not applicable to irrigation canals due to specific differences between rivers and canals, among others the use of the appropriate sediment transport formula and friction factor predictors, the effect of the side banks on the velocity distribution and sediment transport and the operation rules. The applicability of these sediment transport concepts should be related to the flow conditions and sediment characteristics prevailing in irrigation canals. An appropriate mathematical model based on a description of the sediment transport for the specific conditions of irrigation canals may become an important tool for designers and managers of irrigation systems.

7.2 Simulation of sediment transport in irrigation canals

A description and analysis of the sediment transport concepts under the specific conditions of irrigation canals will contribute to improve the understanding on these concepts; it will also help to decide on the applicability of the proper concepts for simulation of the sediment transport process for a given particular condition of water flow and sediment inputs. The aim of the evaluation of the simulation of sediment transport in irrigation canals is to present an analysis of the applicability of the relevant processes under the specific flow conditions prevailing in irrigation canals. Afterwards, a mathematical description of those processes will be used for evaluating the sediment transport in several cases related to irrigation practice.

Resistance to flow: friction factor estimation

The determination of the friction factor for a movable bed requires the knowledge of the implicit process of water flow and bed form development. A comparison with field and laboratory data will help to find an appropriate theory to describe the occurrence of bed forms and the effect on the friction factor.

From the performance of the methods to predict the occurrence of bed forms and the related friction factor, some conclusions can be drawn:

- the methods proposed by van Rijn (1984c) and by Simons and Richardson (1966) proved to be the best theories to predict bed form;
- all the bed forms described by the methods for the lower flow regime (ripples, mega-ripples and dunes) can be expected in irrigation canals;
- the prediction of the friction factor by using the described methods takes only into account the bottom friction; they assume a condition of a wide channel in which the effect of the sidewalls is considered to be negligible;
- the van Rijn method (1984c) for predicting friction factors gives the best results when compared with the selected data.

Another important feature related to the resistance of water flow in irrigation canals is the estimation of the composite hydraulic roughness of these canals, where the flow frequently encounters a varying roughness along the wetted perimeter. Not only differences in the roughness on the bottom and side banks occur in these canals, but also the development of bed forms on the bottom, different material on the bottom and sides of the canal or vegetation on the sides are typical situations for the flow conditions. The widely accepted procedures to compute the discharge in canals with composite roughness are mainly valid for river conditions, for which the cross-section is divided in sub-sections, namely in a main canal and two flood plains. The equivalent friction factor for the entire cross section is based on the friction factor of each sub-section and the discharge over the entire cross section is found by using this equivalent friction factor. The most common cross sections in irrigation canals are trapezoidal and rectangular cross sections with a relatively small value for the bottom width-water depth ratio.

By considering that the velocity distribution over the trapezoidal cross section is more governed by the varying water depth on the sides than by the imposed boundary condition at the side wall (zero velocity), it is proposed to estimate the composite roughness in a trapezoidal canal by using a theoretical velocity distribution over the cross section. The proposed new method uses an equivalent friction factor in terms of the Chézy coefficient.

The existing methods to predict the composite roughness in canals have been compared with the proposed method by using a selected set of laboratory data, which has been collected in the hydraulics laboratory at Wageningen Agricultural University (WAU), the Netherlands and a selected data set from the compilation of Krüger (1988). From the comparison of the methods to predict the composite roughness in trapezoidal cross sections, some conclusions can be drawn:

- existing methods are developed for river conditions, in which the channel is composed by a main channel and two parallel flood plains;
- the proposed method behaves better than the existing methods and predicts that 90% of the two sets of collected data are within an error band of 15%;
- the proposed method takes into account the effect of the varying water depth on the side slope on the roughness coefficient; it does not take into account the lateral transfer of momentum;
- a better description of the velocity distribution over a cross section with composite roughness will provide a more appropriate understanding of effect of different roughness along the wetted perimeter on the total resistance;
- the effect of vegetated side slopes on the total friction factor of the entire cross section has to be investigated.

A new, but different method is also proposed for canals with rectangular cross sections. The method is based on the same principle as used for the side wall correction procedure proposed by Einstein (1942). The proposed method to estimate composite roughness in canals with

rectangular cross sections was tested with a selected set of laboratory data from Krüger (1988). The method predicts that more than 90% of the values of the composite roughness are within an error range of 7.5% compared to measured values. Nevertheless, verification of the proposed method by further experiments and field measurements is recommended.

Sediment transport equations

It was described that for the flow conditions and sediment sizes usually encountered in irrigation canals, the sediment is transported both as bed load and suspended load, therefore any predictor to estimate sediment transport should take into account this fact. Sediment transport predictors should be able to compute either the total transport load (bed load + suspended load) or be able to compute bed load and suspended load separately.

Sediment transport equations are related to the way in which the sediment is transported. They are different under equilibrium and non-equilibrium conditions.

Sediment transport methods for equilibrium condition are established for different conditions to those encountered in practical applications and the use of those equations should be restricted to the conditions for which these methods are valid. There is no universally accepted equation to determine the total sediment transport capacity of canals. Some methods were compared with field and laboratory data in which the flow condition and sediment characteristics are similar to those encountered in irrigation canals. The compilation of data by Brownlie (1981) has been used for this purpose. From that evaluation, some remarks can be drawn:

- prediction of the sediment transport in irrigation canals within an error factor smaller than 2 is hardly possible. Even in case of the most reliable method, only 61% of the values are predicted with a tolerance of error of $\pm 100\%$ compared to the measured values;
- based on the overall performance of each method, the Ackers and White and Brownlie methods seem to be the best to predict sediment transport in irrigation canals.

Most of the sediment transport theories have been developed for open wide canals. Most of the man-made irrigation canals have a trapezoidal or rectangular cross section in which the ratio of bottom width and water depth (B/h) is smaller than 8. For that cross section, the imposed boundary condition for the velocity at the side bank, and the varying water depth will affect the shear stress, velocity and sediment distribution in lateral direction. An appropriate method to compute sediment transport will be necessary to reduce inaccuracies. The method should take into account the effect of the cross section on the velocity distribution and the non-linear relationship between the velocity and the sediment transport. A new method to compute the total sediment transport capacity for non-wide trapezoidal and rectangular cross sections is proposed. The new method is based on the assumption of a quasi two-dimensional model. The trapezoidal cross section is represented by a series of parallel stream tubes. Within each stream

tube the velocity distribution is considered to be uniform and therefore can be described in a one-dimensional way. The total sediment transport in a non-wide canal is proposed to be calculated by the product of the sediment transport per unit width, the bottom width of the canal and a correction factor α. The determination of the correction factor α depends on several independent variables which influence either the flow condition or the sediment transport calculations. The correction factor α depends on bottom width-water depth ratio (B/h), side slope (m) and the sediment transport predictor which is represented by the exponent N. These relationships are:

- for rectangular cross sections (m = 0): the correction factor α only depends on the sediment transport predictor;
- for trapezoidal cross sections: the correction factor depends on the B/h ratio and the sediment transport predictor (exponent N).

Comparison of the existing procedures for computing the total sediment transport capacity in the entire cross section in non-wide canals and the proposed method was carried out. A selected set of laboratory data based on the flow conditions and the sediment characteristics as found in irrigation canals were used for that purpose. The proposed method performed better than the existing procedures for computing the total sediment transport capacity in a non-wide canal.

An interesting phenomenon of non-equilibrium sediment transport in irrigation canals is the adjustment of the actual sediment transport to the sediment transport capacity of the canal. To simulate the sediment transport under non-equilibrium conditions, the Gallapatti's depth integrated model for adaptation of the suspended load was used. It was assumed that the adaptation length for bed load is the same as for suspended load. Therefore the Gallapatti's depth integrated model depth could be used to describe how the total sediment concentration (suspended load and bed load) approaches the transport capacity of the irrigation canal.

Once the sediment load is known in the entire canal, a sediment mass balance in each reach of the canal will give either the net deposition or the net entrainment between the two boundaries of a specific canal reach. In case the incoming sediment load is larger than the sediment transport capacity of the canal, deposition will occur. In case the incoming sediment load is less than the transport capacity of the canal two possibilities can occur depending on whether motion of bed sediment occurs or not. In the first case entrainment of the previous deposited sediment occurs until the adaptation to the sediment transport capacity. For the second case the sediment load is conveyed without any change. Internal boundary conditions as confluences, bifurcations, changes in bottom width and/or bottom level between reaches, flow control structures have to be taken into account to compute the sediment transport at boundaries between canal reaches and/or branches. At bifurcations it is assumed that the sediment distributions between the branches are related to the incoming sediment rate. The distribution of sediments at bifurcations depends on the local flow pattern. No analytical solutions are available yet. Sediment distributions for typical situations encountered in irrigation networks

are recommended. In this study a distinction between overflow and underflow type of structures is made. Underflow structures are able to convey the total sediment load (bed load and suspended load). At overflow only the suspended load is conveyed. More investigations for the passing capacity of typical flow control structures are recommended.

Applications of sediment transport computations in irrigation canals

In order to apply the sediment transport computations in irrigation canals a mathematical model has been developed. The model offers the possibility to predict the behaviour of the sediment in time and space for a particular flow condition and incoming sediment load. The model simulates the water flow, sediment transport and changes in bottom level in an irrigation network. The model is based on an uncoupled solution for the water flow equations and sediment transport equations, which includes all the previously described processes. The applications of the sediment transport model will improve the understanding of the sediment transport process for situations usually encountered in irrigation systems. The model for the sediment transport has been used to evaluate the following effects in irrigation canals:

- changes of the discharges;
- changes in the incoming sediment load;
- controlled sediment deposition;
- sediment transport predictors;
- flow control structures;
- maintenance activities;
- operation activities.

From the evaluation of those applications on the sediment transport in irrigation canals some conclusions can be mentioned. It is important to highlight that those conclusions can not be generalized so that they are only valid for the local flow conditions and sediment characteristics of each application.

Changes of discharges: a key problem for operating an irrigation canal is to determine the flow conditions that meet the water requirements with a minimum deposition. The reduction of the water flow in the irrigation canal and the need to deliver water at a certain level to the commanded irrigated area is one of the most important causes of sediment deposition in irrigation canals. For reductions of discharge to 80% of the design value more than 40% of the incoming sediment load was observed to deposit in the canal.

Changes of incoming sediment load: the effect of changes in the incoming sediment load on the sediment transport includes the effect of variations in the concentration and median sediment size during the irrigation season and are related to the sediment concentration and sediment size for the equilibrium conditions. Sediment deposition in irrigation canals highly depends on the characteristics of the incoming sediment. About 15% of the total incoming sediment load will be settled in the canal when the sediment concentration of the incoming sediment load increases

by 10% from the design value. For 100% variation in the incoming sediment concentration about 30% of the incoming sediment load is expected to settle in the canal. A similar behaviour as described for the case of variations in the sediment concentration is observed for changes in the median sediment size of the incoming sediment. For instance about 25% of the total incoming sediment during the simulation period will be deposited when the sediment size deviates 20% from the equilibrium sediment size and about 45% from the incoming sediment load will be deposited when the sediment size deviates 100% from the design median diameter.

Controlled deposition: as deposition and removal of the sediment belong to the most important problems in irrigation canals, the effect of controlled deposition by deepening or widening of one or some reaches of the canal has been simulated. Two scenarios are proposed to concentrate the sediment deposition at the head reach of the canal by reducing the transport capacity in that reach only. The two scenarios will transform the head of the irrigation canal into a kind of settling basin within the canal.

The proposed changes in the geometry of the irrigation canal are simple modifications of the former cross section. No additional considerations for optimizing economic costs and sediment deposition have been included. For the specific flow and sediment transport conditions the deepened section traps more sediment than the widened section. The deepened section trapped 4 times more sediment than the irrigation canal without sediment deposition control and 1.3 times more than the widened section.

Sediment transport predictors: the different sediment predictors have been compared for the sediment transport in equilibrium condition. Here, the effect of the various sediment transport predictors, like Ackers and White, Brownlie and Engelund and Hansen, on the sediment deposition are compared. Large differences in the computed sediment deposition were observed among the sediment transport predictors. These differences are related to the capability for predicting the sediment transport capacity for certain flow conditions. The hydraulic conditions during the simulation period gave a relatively low sediment transport capacity for the Engelund and Hansen predictor, and relatively large sediment transport capacity for Brownlie and Ackers and White predictors. Therefore the expected deposition in the irrigation canal will be larger in case of Engelund and Hansen and Brownlie predictor than Ackers and White predictor. By using the Engelund and Hansen's predictor the sediment deposition was 2 and 3 times more than with the Brownlie and Ackers and White's predictors respectively. This specific application shows an important issue, namely the need for an accurate prediction of the sediment transport capacity of irrigation canals, otherwise the uncertainty of deposition will be very large.

Flow control structures: an irrigation canal has to deliver water at the right amount, at the required time and at the proper elevation to the command area. The water is kept at the right level for varying discharges by flow control structures, which can be divided in two main groups, namely, undershot and overflow structures. The observed total deposition in both cases

is rather similar. Only between 5% and 10% more deposition was observed in case of the overflow type compared to the undershot type. The difference is related to the ability to pass sediment trough the structure. The difference is mainly concentrated in the upstream part of the structure. A better understanding of the sediment transport capacity of the flow through typical flow control structures in irrigation networks is required.

Maintenance activities: maintenance is the set of actions to keep an irrigation system in good operating conditions and to provide at all time its functioning. Maintenance activities related to silt deposition and weed growth were evaluated in terms of the effect of the maintenance on the hydraulic performance of the irrigation canal. The maintenance was simulated by assuming optimal maintenance and non-maintenance at all during the irrigation season, meaning that in the first case the roughness remains constant and that in the second case the roughness increases in time. No direct effect of the growth of the weed on the sediment transport is considered. Only the effect on the variation of the roughness condition is considered. More sediment deposition was observed in the ideally maintained canal than the non-maintained canal. For the schematized ideally maintained irrigation canal a continuous deposition was observed during all the time along the irrigation canal. In the non-maintained canal a sediment deposition period followed by an entrainment period was observed.

Operation activities: an irrigation system should be designed and operated in such a way that a maximum crop production in quality and quantity can be reached considering the on-farm and project cost and benefits. Effects of the type of operation on the sediment deposition are simulated in an irrigation canal of 16 km composed of three reaches and two lateral canals. For simulating the effect of the operation procedures on the sediment deposition in the main canal four scenarios are used. The four scenarios can be described as:

- *Scenario 1 (continuous flow)*: a continuous flow during the whole irrigation season;
- *Scenario 2 (rotational flow)*: a rotational flow during daytime for the laterals;
- *Scenario 3 (rotational flow)*: a rotational flow per day for the laterals;
- *Scenario 4 (rotational flow)*: a rotational flow per week for the laterals.

From the comparison some conclusions can be drawn:

- the largest total sediment deposition in the entire canal system (all reaches) for scenario 1 was larger than that of the other scenarios. Total sediment deposition in scenario 2, 3 and 4 was rather similar;
- large differences were observed in the distribution of the sediment deposition within the reaches of the main canal. Differences of the sediment deposition in each reach were in the order of 0.5 to 4 times among the different scenarios;
- total sediment deposition in the entire canal and its distribution within the canal are important aspects to be considered in the selection of the operation strategy for the water delivery in an irrigation canal.

By considering the results of the applications of the mathematical modelling, it can be concluded that the model is a useful tool for assessing the sediment deposition within irrigation canals under different flow conditions and sediment characteristics. Nevertheless, the mathematical model's performance has to be confirmed. Results should be compared with field measurements in order to confirm whether the physical processes are well represented in the mathematical model or there is a deficiency as a result of the assumptions for describing those processes. Monitoring of the sediment deposition in irrigation networks is required to evaluate the model under specific conditions and to investigate the response in time and space of the bottom level under specific water flows and sediment characteristics. Influences of the type and operation of flow control structures, geometrical characteristics of the canals, water flow and incoming sediment characteristics on the deposition pattern, will contribute to a better understanding of the sediment transport processes.

REFERENCES

Abbot M. & A. J. Cunge, 1982. *Engineering applications of computational hydraulics*. Ed. Pitman. Boston, USA.

Ackers P. & W. R. White, 1973. Sediment transport: new approach and analisys. *Journal of Hydraulic Division, ASCE*. Vol 99, No. 11. New York,USA.

Ackers P., 1992. 1992 Gerard Lacey memorial lecture: Canal and river regime in theory and practice: 1929-92. *Proc. Instn. Civ. Engrs. Wat., Marit. & Energy*. Technical note No. 619. United Kingdom.

Ackers P., 1994. Sediment transport in open channels: Ackers and White update. *Proc. Instn. Civ. Engrs. Wat. , Marit. & Energy*. Technical note No. 619. United Kingdom.

Adeff S. E., 1989. On the mechanic of suspended sediment and entrainment. *23rd IAHR congress*. Otawa, Canada.

Aguirre Pe J., 1988. *Hidraulica de sedimentos*. CIDIAT. Merida, Venezuela.

Ahmed,S. E. & M.B. Saad, 1992. Prediction of natural hydraulic roughness. *Journal of Irrigation and Drainage Division, ASCE*. Vol.118, No.4. New York, USA.

Ahmed S. A. et al, 1986. Sedimentation Problems in The Gezira Scheme. *International Conference on Water Resources Needs and Planning in Drought Prone Area*. Khartoum, Sudan.

Alam A. M. & J. F. Kennedy, 1969. Friction factor for flow in sand bed channels. *Journal of Hydraulic Division, ASCE*. No. 6. New York, USA.

Allen J. R., 1970. *Physical Process of Sedimentation*. London, United Kingdom

Altunin V. S & T.A. Aliev 1989. Characteristic of suspension flow in a canal. *23rd IAHR congress*. Otawa, Canada.

Ankum P., 1995. *Lectures notes on flow control in irrigation and drainage*. IHE. Delft, the Netherlands.

Armanini A. & G. Di Silvio 1988. A one dimensional model for the transport of a sediment mixture in non-equilibrium condition. *Journal of Hydraulic Research, IAHR*. Vol. 26, No. 3. The Netherlands.

Asaeda T. et al, 1989. Sediment entrainment in channel with rippled bed. *Journal of Hydraulic Division, ASCE*. Vol. 115, No. 3. New York, USA.

Asano T. et al, 1985. Characteristics of variation of Manning's roughness coefficient in a compound cross section. *21stIAHR congress*. Melbourne, Australia.

ASCE, 1963. Friction factor in open channels. *Journal of Hydraulic Division, ASCE*. Vol. 89, No. 2. New York, USA.

ASCE, 1966a. Initiation of Motion. Task committee on preparation of sedimentation manual. *Journal of Hydraulic Division, ASCE*. New York, USA.

ASCE, 1966b. Nomenclature for bed form in alluvial stream. Task committee on preparation of sedimentation manual. *Journal of Hydraulic Division, ASCE.* Vol 92, N0. 3. New York, USA.

ASCE, 1972a. Sediment control methods. *Journal of Hydraulic Engineering Division, ASCE.* Vol. 98, No. 7. New York, USA.

ASCE, 1972b. Control of sediment in canals. *Journal of Hydraulic Engineering Division, ASCE.* Vol. 98, No. 9. New York, USA.

ASCE, 1989. Research and needs in irrigation and drainage. Vol. 115, No.4. *Journal of Irrigation Division, ASCE.* New York, USA.

ASCE. 1993. Unsteady-flow modelling of irrigation canals. *Task Committee on Irrigation Canal Hydraulic Modelling. ASCE.* New York, USA.

Azis N. & S. N. Prasad 1985. Sediment transport in shallow flows. *Journal of Hydraulic Division, ASCE.* New York, USA.

Aziz N. et al, 1992. Suspended sediment concentration profile using conservation laws. *Journal of Hydraulic Research, IAHR.* Vol.30, No.4. Delft, The Netherlands.

Bagnold R., 1966. An approach to the sediment transport problem from general physics. *Geological Survey Prof. Paper 422.I.* Washington, USA

Bakry M. et al, 1992. Field Measured Hydraulic Resistance Characteristic in Vegetation Infested Canal. *Journal of Hydraulic Division, ASCE.* New York, USA.

Bakker, B. et al, 1989. Regime theories updated or outdated. *Delft Hydraulics.* Publication no. 416. Delft, The Netherlands.

Bateman A. et al, 1991. Roughness factor estimation from laboratory and field data. *24^{h} IAHR congress.* Madrid, Spain.

Bennett J., 1973. An Investigation of The Suspended Load Transport Efficiency in The Bagnold Equation.*Journal of Hydraulic Research, IAHR.* Bangkok, Thailand.

Bettess, R., W. R. White and C.E. Reeve, 1988. Width of regime channels. *International conference on river regime. Hydraulic research.* Wallingford, United Kingdom.

Bishop A. et al, 1965. Total bed material transport. *Journal of Hydraulic Division, ASCE.* Vol. 91, No. 2. New York, USA.

Biswas A., 1995. Water for the developing world in the 21 century: issues and implications. *ICID journal.* New Delhi, India.

Blench, T., 1970. Regime theory design of canals with sand beds. *Journal of Irrigation and Drainage Division, ASCE.* Vol. 96, No. 2. New York, USA.

Bogardi, J., 1974. *Sediment transport in alluvial streams.* Akademiai Kiado. Budapest, Hungary.

Bolton, P., 1983. Sediment discharge measurenments and calculations. *Report OD/TN 2, Hydraulic Research.* Wallingford, United Kingdom.

Bos M. G., 1989. *Discharge measurement structures.* ILRI publications 20. Wageningen, The Netherlands.

Bos M. G. & J. H. A. Wijbenga, 1997. Passage of sediment through flumes and over weirs. *Irrigation and drainage systems*. Vol. 11, No.1. Kluwer Academic Publishers. Dordrecht, The Netherlands.

Brabben T., 1990. Workshop on Sediment Measurement and Control, and Design of Irrigation Canals. *Hydraulic Research*. Wallinford, United Kingdom.

Breuser H. N., 1993. *Lecture notes on sediment transport*. IHE. Delft, The Netherlands.

Brownlie W., 1981. Prediction of flow depth and sediment discharge in open channels. California Institute Technology. W.M.Keck Lab. Rep. No. KH-R-54. California, USA.

Brownlie W., 1981. Compilation of alluvial channel data: laboratory and field. *California Institute of Technology*. Report No. KH-R-43B. California, USA.

Brownlie W., 1983. Flow depth sand bed channel. *Journal of Hydraulic Division, ASCE*. Vol 109, No. 7. New York, USA.

Bruk S., 1986. Sediment Transport and Control in Irrigation System. *International Conference on water Resources Needs and Planning in Drought Prone Area*. Khartoum, Sudan.

Carruthers I, et al, 1997. Irrigation and food security in the 21st century. *Irrigation and drainage systems*. Vol 11. Kluwer Academic Publishers. Dordrecht, The Netherlands.

Cioffi F. & F. Gallerano, 1991. Velocity and concentration profile of solid particles in a channel with a movable and erodible bed. *Journal of Hydraulic Research, IAHR*. Vol. 29, No. 3. Delft, The Netherlands.

Celik I. & W. Rodi, 1985. Mathematical Modelling of Suspended Sediment Transport. *21st IAHR Congress*. Melbourne Australia.

Celik I. & W. Rodi, 1988. Modelling Suspended Sediment Transport in non Equilibrium Situation. *Journal of Hydraulic Division, ASCE*. Vol 14. New York, USA.

Celik I. & W. Rodi, 1991. Suspended sediment transport capacity for open channel flow. *Journal of Hydraulic Division, ASCE*. Vol. 117, No. 2. New York, USA.

Chang Howard, 1985. Design of stable alluvial canals in a system. *Journal of Hydraulic Division, ASCE*. New York, USA.

Chang Howard, 1988. *Fluvial processes in river engineering*. John Wiley & Sons. New York, USA.

Chang Howard, 1990. Hydraulic design of erodible-bed channel. *Journal of Hydraulic Division, ASCE*. Vol. 117, No.1. New York, USA.

Chao-Lin Chiu, 1989. Velocity distribution in open channel flow. *Journal of Hydraulic Division, ASCE*. Vol. 115, No.5, pp 989-1001. New York, USA.

Chao-Lin Chiu & David Murray, 1992. Variation of velocity distribution along non-uniform open channel flow. *Journal of Hydraulic Division, ASCE*. Vol. 118, No. 7. New York, USA.

Chitale M., 1996. Keynote address on conflict for water. *IWSA International Specialized Conference on Management of Water Supply*. Mumbai, India.

Chitale, S. V., 1976. Shape and size of alluvial canals. *Journal of Hydraulic Division, ASCE*. Vol. 102, No. 7. New York, USA.

Chitale S. V., 1994. Lacey divergence equation for alluvial canal design. *Journal of Hydraulic Division, ASCE*. Vol 120, No.1. New York, USA.

Chow Ven Te, 1983. *Open channel hydraulics*. Mc Graw Hill International Book Company. Tokio, Japan.

Chuang Yang et al, 1989. Semi-coupled Simulation of Unsteady Non uniform Sediment Transport in Alluvial Canal. *23rd IAHR congress*. Otawa, Canada.

Chwen-Yuan G. & W. Hughes, 1984. Optimal cross section with freeboard. *Journal of Hydraulic Division, ASCE*. New York, USA.

Clemmens A. J., F. M. Holly & W. Schuurmans, 1993. Description and evaluation of Duflow. *Journal of Hydraulic Division, ASCE*. Vol. 119, No. 4. New York, USA.

Colby B., 1964. Practical computations of bed material discharge. *Journal of Hydraulic Division, ASCE*. Vol. 90, No. 2. New York, USA.

Coleman S. & B. Melville, 1994. Bed form development. *Journal of Hydraulic Division, ASCE*. Vol. 120, No. 5. New York, USA.

Correia L. et al, 1991. Laboratory verification of a coupled unsteady flow model. *24th IAHR congress*. Madrid, Spain.

Correia Luis et al, 1992. Fully coupled unsteady mobile boundary flow model. *Journal of Hydraulic Division, ASCE*. Vol. 118, No. 3. New York, USA.

Cunge J. A.& D. Simons, 1975. Mathematical model of unsteady flow in movable bed rivers with alluvial channel resistance. *IAHR*. Sao Paulo, Brazil.

Cunge J.A., F. M. Holly & A. Verwey, 1980. *Practical Aspects of Computational River Hydraulics*. Pitman Advanced Publishing Program. London, United Kingdom.

Dahmen E., 1994. *Lecture notes on canal design*. IHE. Delft, The Netherlands.

Dargahi Bijan, 1990. Controlling Mechanism of local scouring. *Journal of Hydraulic Division, ASCE*. Vol. 116, No. 10. New York, USA.

Davies T. R. H., 1982. Lower flow regime bedforms: rational classification. *Journal of Hydraulic Division, ASCE*. Vol 108, pp 343 360. New York, USA.

Depeweg H. W. Th. 1993. *Lecture notes on applied hydraulics: gradually varied flow*. IHE. Delft, The Netherlands.

DHI (Danish Hydraulics Institute), 1993. *Mike 11: technical reference guide*. Danish Hydraulics Institute. Copenhagen, Denmark.

DHL (Delft Hydraulics Laboratory) & Ministry of Transport, Public Works and Water Management, 1994. *SOBEK: technical reference guide*. Delft Hydraulics. Delft, The Netherlands

Dong Z. et al, 1991. Turbulence characteristics of open channels flow over rough beds. *24th IAHR congress*. Madrid, Spain.

Earles, J. D., 1973. Irrigation canal system capacity design criteria. *Journal of Irrigation and Drainage Division ASCE*. No. 9973. New York, USA.

Einstein H., 1950. The bed load function for sediment transportation in open channel flow. *U.S. Dep. of Agriculture, Bull. No. 1026*. Washington, USA.

Engelund F., 1966. Hydraulic resistance of alluvial stream. *Journal of Hydraulic Division, ASCE*. Vol 92, No. 2. New York, USA.

Engelund F. & Hansen E., 1967. *A monograph on sediment transport in alluvial streams*. Teknisk Forlag, Copenhagen, Denmark.

FAO, 1971. Irrigation practice and water management. *Paper No. 1, FAO*. Rome, Italy.

FAO, 1981. Arid zone hydrology. *Paper No. 37, FAO*. Rome, Italy.

FAO, 1984. Crop water requirements. *Paper No. 24, FAO*. Rome, Italy.

Fish, I. L., P. Lawrence & E. Atkinson, 1986. Sedimentation in the Chatra Canal, Nepal. *Report OD85. Hydraulic research Wallingford*. Wallingford, United Kingdom

Flymm L. E. & M. A. Marino, 1987. Canal design: optimal cross section. *Journal of Hydraulic Division, ASCE*. Vol. 113, no 3. New York, USA.

Franji K., 1984. Past and likely future developments in irrigation, drainage and flood control measures in developing countries. *ICID*. New Delhi, India.

Froehlich David, 1994. Width and depth-constrained best trapezoidal section. *Journal of Hydraulic Division, ASCE*. Vol.120, No.4. New York, USA.

Galappatti R., 1983. A Depth Integrated Model for Suspended Transport. *Report no 83-7. Delft University of Technology*. Delft, The Netherlands.

Garcia M. & G. Parker, 1991. Entrainment of bed sediment into suspension. *Journal of Hydraulic Division, ASCE*. Vol. 117. New York, USA.

Graff W. H. & L. Suszka, 1985. Unsteady flow and its effects on sediment transport. *21st IAHR congress*. Melbourne, Australia.

Griffith George, 1989. Form resistance in gravel channels with mobile bed. *Journal of Hydraulic Division, ASCE*. Vol 115, No 3. New York, USA.

Gyr A. & A. Schmid, 1990. The different ripple formation mechanism. *Journal of Hydraulic Research, IAHR*, vol 27, No. 1. Delft, The Netherlands.

Haque M. & K. Mahmood, 1983. Analytical determination of form friction form. *Journal of Hydraulic Division, ASCE*. New York, USA.

Haque M. & K. Mahmood, 1985. Geometry of ripples and dunes. *Journal of Hydraulic Division, ASCE*. New York, USA.

Hart W. E. et al, 1992. Flow in trapezoidal cross section. *Journal of Hydraulic Division, ASCE*. Vol.118, pp 971-976. New York, USA.

Henderson F. M., 1966. *Open Channel Flow*. Mac Millan Publishing Co. Inc. New York, USA.

Hey R. D.,1979. Flow resistance in gravel-bed rivers. *Journal of Hydraulic Division, ASCE*. Vol. 105, No 4, pp 365-379. New York, USA.

Hey R. & C. R. Thorne, 1986. Stable channels with mobile gravel beds. *Journal of Hydraulic Division, ASCE*. Vol. 112, No. 8. New York, USA.

Hofwegen P. J. van, 1992. *Lecture notes on principles of irrigation management*. IHE. Delft, The Netherlands.

Hofwegen P. J. van, 1993. *Lecture notes on irrigation and drainage system*. IHE. Delft, The Netherlands.

Holly F. & Jean-Luc Rahuel, 1989. Advances in numerical simulation of alluvial-river response to disturbances. *23rd IAHR congress*. Otawa, Canada.

HR Wallingford, 1992. *DORC: user manual*. HR Wallingford. Wallingford, United Kingdom.

Hsieh Wen Shen et al, 1990. Bed form resistance in open channel flows. *Journal of Hydraulic Division, ASCE*. Vol. 116, No.6. New York, USA.

Huang J., Liu Hexian, 1993. A Research on the Operation schemes for an Irrigation Project With Plenty of Sediment Inputs. *25th IAHR congress*. Tokyo, Japan.

Huang J. et al., 1993. A Study on the Sediment Transport in an Irrigation Scheme. *15th ICID congress*. The Hague, The Netherlands.

Husain Tahir, 1988. Flow simulation using channel network model. *Journal of Hydraulic Division, ASCE*. Vol. 114, No. 3. New York, USA.

IHE, 1998. Duflow-manual. IHE-Delft. Delft, The Netherlands.

Ikeda S., 1982a. Lateral bed load transport on side slopes. *Journal of Hydraulic Division Vol. 108, No. HY11, ASCE*. New York, USA.

Ikeda S., 1982b. Incipient motion of sand particles on side slopes. *Journal of Hydraulic Division Vol. 108, No. HY1, ASCE*. New York, USA.

Ikeda S. & T. Asaeda, 1983. Sediment suspension with rippled bed. *Journal of Hydraulic Division, ASCE*. New York, USA.

Ilo, C. G., 1975. Resistance to flow in alluvial channels. *Journal of Hydraulic Division, ASCE*. Vol. 101, No. 6. New York, USA.

Iman E. H. et al, 1991. Design of irrigation canals: integrated approach. *Journal of Hydraulic Division, ASCE*. Vol.117, No. 6. New York, USA.

Ingram J. J et al, 1991. Sediment discharge computation using point-sampled suspended sediment data. *Journal of Hydraulic Division, ASCE*. Vol. 117, No. 6. New York, USA.

Ionescu F., 1993. *Lecture notes on free surface flow processes*. IHE. Delft, The Netherlands.

Itakura, T. & T. Kishi, 1980. Open channel flow with suspended sediments. *Journal of Hydraulic Division, ASCE*. Vol. 106, No. 8. New York, USA.

Jansen P., 1994. *Principles of river engineering*. Delftse Uitgevers Maatsschappij. Delft, The Netherlands.

Jensen M., 1993. The impacts of irrigation and drainage on the enviroment. *15th ICID congress*. The Hague, The Netherlands.

Jinchi, H., W. Zhaohui, & Z. Eishun, 1993. A study on sediment transport in an irrigation district. *15th International congress on irrigation and drainage*. R. 108, pp 1373-1384. The Hague, the Netherlands

Jin Ren Ni & G. E. Wang, 1991. Vertical sediment distribution. *Journal of Hydraulic Division, ASCE*. Vol. 117, No. 9. New York, USA.

Jones W, 1995. The World Bank and irrigation. *World Bank publications*. The World Bank. Washington D.C., USA.

Jorissen R. E. & J. K Vrijling, 1989. Local scour downstream hydraulic constructions. *23rd IAHR congress*. Otawa, Canada

Kandula V. et al, 1983. Velocity distribution in smooth rectangular open channels. *Journal of Hydraulic Division, ASCE*. New York, USA.

Karim M. F. & J. F. Kennedy, 1987. Velocity and sediment concentration profile in river flow. *Journal of Hydraulic Division, ASCE*. Vol. 113, No. 2. New York, USA.

Karim M. F. & J. F. Kennedy, 1990. Menu of coupled velocity and sediment discharge relations for rivers. *Journal of Hydraulic Division, ASCE*. Vol. 116, No. 8, pp 159-176. New York, USA.

Kerssens P. Et al, 1979. Model for suspended sediment transport. *Journal of Hydraulic Division, ASCE*. Vol. 105, No. 5. New York, USA.

Kikakawa, H. et al, 1967. On the effects of suspended sediments to the bed roughness. *Proceeding 12th congress of International Association for Hydraulic Research*. Colorado, USA.

Kinori B. Z., 1970. *Manual of surface drainage engineering*. Elsevier Publishing Company. New York, USA.

Khattab A. F. et al, 1987. Design of earthern canals using regime type equation. *6th Afro-asian reg. cong. proc. ICID*. Cairo, Egypt

Klaassen G. J., 1995. *Lecture notes on introduction into numerical modelling of river morphology*. IHE, Delft, The Netherlands.

Knigth Donald et al, 1984. Boundary shear stress in smooth rectangular channels. *Journal of Hydraulic Division, ASCE*. New York, USA.

Kobayashi N. & Seung Nam Seo, 1985. Fluid and sediment interaction over a plane bed. *Journal of Hydraulic Division, ASCE*. New York, USA.

Kouwen N., 1969. Flow retardance in vegetated channels.*Journal of Irrigation and Drainage Division, ASCE*. Vol. 95, No.2. New York, USA.

Kouwen N., 1992. Modern approach to design of grassed channels. *Journal of Hydraulic Division, ASCE*. Vol. 118, No.5. New York, USA.

Krishnamurthy M. & B, Christensen, 1972. Equivalent roughness for shallow channels. *Journal of Hydraulic Division, ASCE*. Vol. 118, No.5. New York, USA.

Krüger, F., 1988. Flow laws in open channels. Doctoral thesis at the Dresden University of Technology. Dresden, Germany.

Krüger F. & G. Bollrich, 1989. Boundary shear distribution in rectangular and trapezoidal channels with uniform and non-uniform bed and wall roughness. *23rd IAHR congress*. Otawa, Canada.

Lau Y. L., 1983. Suspended sediment effect on flow resistance. *Journal of Hydraulic Division, ASCE*. New York, USA.

Lau Y. L., 1988. Hydraulic resistance of ripples. *Journal of Hydraulic Division, ASCE*. Vol. 114, No. 10. New York, USA.

Lau Y. L. & B.G. Krishnappan, 1994. Does reentrainment occur during cohesive sediment settling?. *Journal of Hydraulic Division, ASCE*. Vol. 120, No 2. New York, USA.

Laurensen E. M., 1986. Friction slope averaging in backwater calculation. *Journal of Hydraulic Division, ASCE*. Vol. 112, No. 12. New York, USA.

Lavelle W. & H. O. Mofjeld, 1987. Do critical stresses for incipient motion and erosion really exists?. *Journal of Hydraulic Division, ASCE*. Vol. 113, No. 3. New York, USA.

Lawrence E. F. & Miguel Marino, 1987. Canal design: optimal cross section. *Journal of Hydraulic Division, ASCE*. Vol. 113, No.3. New York, USA.

Lawrence, P., 1986. Measurement of discharge and sediment flows in Kansal Choe, 1985. *Report OD 79, Hydraulic Research*. Wallingford, United KIngdom.

Lawrence P., 1990. Canal Design, Friction and Transport Predictor. *Workshop on Sediment Measurement and Control, and Design of Irrigation Canals. Hydraulic Research*. Wallinford, United Kingdom.

Lawrence P., 1993. Deposition of Fine Sediments in Irrigation Canals. *15th ICID congress*. The Hague, The Netherlands.

Lyn D. A., 1987. Unsteady Sediment Transport Modelling. *Journal of Hydraulic Division, ASCE*. Vol. 113. New York, USA.

Lyn D.A., 1991. Resistance in flat bed sediment-laden flow. Vol. 117, no 1. *Journal of Hydraulic Division, ASCE*. New York, USA.

Maddock T., 1976. Equations for resistance to flow and sediment transport in alluvial channels. *Water Resources Research*. Vol. 12, No. 1. USA.

Magazine M. K. et al, 1988. Effect of bed and side roughness on dispersion in open channel. *Journal of Hydraulic Division, ASCE*. Vol. 114, No. 7. New York, USA.

Mahmood K., 1973a. Sediment Equilibrium Consideration in The Design of Irrigation Canal Network. *Proc. IAHR. International Symposium on River Mechanics*. Bangkok, Thailand.

Mahmood K., 1973b. Sediment routing in irrigation canal systems. *ASCE, National Water Resources Engineering Meeting*. Washington D.C., USA.

Mahmood K., 1975. *Unsteady flow in open channel*. Water Resources Publications. Colorado, USA.

Mantz P., 1992. Cohesionless, fine sediment bed form in shallow flows. *Journal of Hydraulic Division, ASCE*. Vol. 118, No. 5. New York, USA.

Marchi E., 1967. Resistance to flow in fixed bed channels with the influence of cross-sectional shape and free surface. *Proceeding 12th congress of International Association for Hydraulic Research*. Colorado, USA.

Mc Bean E. & S. Al-Nassri, 1988. Uncertainty in suspended sediment transport curves. *Journal of Hydraulic Division, ASCE*. Vol 114, No. 1. New York, USA.

Mc Lean S. R., 1991. Depth-integrated suspended load calculation. *Journal of Hydraulic Division, ASCE*. Vol. 117, no 1. New York, USA.

Meadowcroft I., 1988. The applicability of sediment transport and alluvial friction prediction in irrigation canals. *Report technical note OD-TN 34. HR Wallingford.* Wallingford, United Kingdom.

Melo J. M. & A. H. Cardozo 1993. Modelling non-equilibrium transport by unsteady flow. *25th IAHR congress.* Tokio, Japan.

Mendez N., 1995. Suspended sediment transport in irrigation canals. *M.Sc thesis. IHE.* Delft, The Netherlands.

Morse B. & R. Townsend, 1989. Modelling mixed sediment suspended load profile. *Journal of Hydraulic Division, ASCE.* vol 115, no 6. New York, USA.

Motayed A. & M. Krishnamurthy, 1980. Composite roughness of natural channels. *Journal of Hydraulic Division, ASCE.* Vol. 106, No.HY6. New York, USA.

Motohiko Umeyama, 1992. Vertical distribution of suspended sediment in uniform open-channel flow. *Journal of Hydraulic Division, ASCE.* Vol. 118, No. 6. New York, USA.

Motohiko Umeyama 1992. Velocity distribution in uniform sediment-laden flow. *Journal of Hydraulic Division, ASCE.* Vol. 118, No. 2. New York, USA.

Mukhamedov A. et al, 1991. Evolution of the influence of river bed section shape and roughness upon stream kinematic characteristics and its considerations in hydraulic calculation of canals and models. *24th IAHR congress.* Madrid, Spain.

Murphy Peter & E. Aguirre 1985. Bed load or suspended load. *Journal of Hydraulic Division, ASCE.* New York, USA.

Myers W. R. C., 1982. Flow resistance in wide rectangular channels. *Journal of Hydraulic Division, ASCE.* Vol. 108, pp 471-482. New York, USA

Nagakawa H. Et al, 1989. Convolution-integral modelling of non-equilibrium sediment transport. *Sediment transport modelling. Ed. by S. S. Y. Wang. ASCE.* New York, USA.

Naimed Ullah M., 1990. Regime and Sediment Transport Concepts Compared as Design Approaches. *Workshop on Sediment Measurement and Control, and Design of Irrigation Canals. Hydraulic Research.* Wallinford, United Kingdom.

Nakato T., 1990. Test of Selected Sediment Transport Formula. *Journal of Hydraulic Engineering, ASCE.* New York, USA.

Nalluri C & M. A. U. Kithsiri, 1992. Extended data on sediment transport in rigid bed rectangular channels. *Journal of Hydraulic Research, IAHR,* Vol. 30, No. 6. Delft, The Netherlands.

Naot Dan, 1984. Response of channel flow to roughness heterogeneity. *Journal of Hydraulic Division, ASCE.* New York, USA.

Nitschke E., 1983. The influence of overgrowing with herbs on hydraulics parameters of agricultural outfalls and ditches. *Proc. 20th Congress of IAHR.* Subject D, pp 173-180. Moscow, USSR.

Nokes R. I. & G. O.Hughes., 1994. Turbulent mixing in uniform channels of irregular cross section. *Journal of Hydraulic Research, IAHR,* Vol. 32, No. 1. Delft, The Netherlands.

Noutsopoulus, G & P. Hadjipanos, 1983. Discharge computations in compound channels. *Proc. 20th Congress of IAHR*. Subject D, pp 173-180. Moscow, USSR

Novak P., 1983. *Development in Hydraulic Engineering - 1*. Applied Science Publishers. London, United Kingdom.

Ogink H. J. M., 1985. The effective viscosity coefficient in 2-D depth-averaged flow models. *Proc. 21st IAHR congress*. Melbourne, Australia.

Omnia El-Hakin & A. Keller 1992. Velocity distribution inside and above branched flexible roughness. *Journal of Hydraulic Division, ASCE*. Vol.118, No. 6. New York, USA.

Paintal A. S., 1971. Concept of critical shear stress in loose boundary open channel. IAHR. No. 9. Delft, The Netherlands.

Parker G. & N. Coleman 1986. Simple model of sediment-laden flow. *Journal of Hydraulic Division, ASCE*. Vol. 112, No. 8. New York, USA.

Parker G. & P. Wikcock 1993. Sediment feed and recirculating flumes: fundamental differences. *Journal of Hydraulic Division, ASCE*. Vol. 119. No. 1. New York, USA.

Parviz M., 1994. General formulation of best hydraulic channel section. *Journal of Hydraulic Division, ASCE*. vol 120, No.1. New York, USA.

Paul T.C. & V.S. Sakhuya 1990. Why sediment deposit in lined channels?. *Journal of Hydraulic Division, ASCE*. Vol.116, No. 5. New York, USA.

Petryk S. & G. Bosmajian III, 1975. Analysis of flow through vegetation. *Journal of Hydraulic Division, ASCE*. Vol. 120, No. 5. New York, USA.

Prabhata Swamee, 1994. Normal-depth equations for irrigation canals. *Journal of Hydraulic Division, ASCE*. Vol. 120, No. 5. New York, USA.

Prabhata Swamee & B. Basak 1994. Design of open-channel-contraction transitions. *Journal of Hydraulic Division, ASCE*. vol 120. New York, USA.

Querner E., 1993. Aquatic weed control within an integrated water management framework. Doctoral thesis, *Agricultural University of Wageningen*. Wageningen, The Netherlands.

Ranga Raju K. G., 1981. *Flow through open channels*. Tata McGraw-Hill. New Delhi, India.

Raudkivi A. J., 1990. *Loose Boundary Hydraulics*. 3rd Edition. Pergamon Press. Great Britain.

Raudkivi A. J. & H. Witte 1990. Development of bed features. *Journal of Hydraulic Division, ASCE*. Vol. 116, No. 9. New York, USA.

Ribberink J. S., 1986. Introduction to a depth integrated model for suspended sediment transport (Galappatti, 1983). *Report No. 6-86. Delft University of Technology*. Delft, The Netherlands.

Rosso Mauricio et al, 1990. Flow stability and friction factor in rough channels. *Journal of Hydraulic Division, ASCE*. Vol. 116, No. 9. New York, USA.

Sakhuja, V. S., 1987. A compilation of methods for predicting friction and sediment transport in alluvial channels. *Report OD/Tn 2, Hydraulic Research*. Wallingford, United Kingdom.

Salazar J., 1990. Sedimentation process in settling basin. *M.Sc. thesis. IHE*. Delft, The Netherlands.

Sanmuganathan K., 1990. Sediment research at hydraulic research; the quantitative approach to design and performance prediction. *Workshop on sediment measurement and control, and the design of irrigation canal.* Edited by Tom Brabben. Wallingford, United Kingdom.

Sarma, K. V. N. et al, 1983. Velocity distribution in smooth rectangular open channels. *Journal of Hydraulic Division, ASCE.* Vol. 109, pp 270-289. New York, USA.

Shao X. & X. Zhenhuan, 1991. Vertical diffusion of sediments in open-channel turbulent flows. *24th IAHR congress.* Madrid, Spain.

Schultz B, 1997. Drainage for the 21st century: Policy issues and strategies for emerging problems. *7th ICID International drainage workshop: Drainage for the 21 century.* Proceedings. Vol.1. Penang, Malaysia.

Schuurmans W., 1991. *A model to study the hydraulic performance of controlled irrigation canals.* Ph.D. thesis. Technical University of Delft. Delft, The Netherlands.

Shen H. et al, 1990. Bed form resistance in open channel flows. *Journal of Hydraulic Division, ASCE.* Vol. 116, No. 6. New York, USA.

Shou-Shan F., 1989. An overview of computer stream sedimentation models. *Sediment transport modelling. Ed. By S. S. Y. Wang. ASCE.* New York, USA.

Siddig E. A., 1992. Alluvial canals adequacy. *Journal of Hydraulic Division, ASCE.* Vol. 118, No. 4. New York, USA.

Siddiqui I. H., 1979. *Irrigation Canals.* National Book Foundation. Lahore, Pakistan.

Simons D. B. & E. V. Richardsons, 1961. Forms of bed roughness in alluvial channels. *Journal of Hydraulic Division, ASCE.* No. 3. New York, USA.

Simons D. B. & E. V. Richardsons, 1966. Resistance to flow in alluvial channels. *Geological Survey Prof. Paper 422-I.* Washington, USA.

Simons D. & Fuat Senturk, 1992. *Sediment Transport Technology.* Water Resources Publications. Colorado, USA.

Singh V. & P. D. Scarlatos 1985. Sediment transport in vertically two dimensional man-made canals. *21st IAHR Congress.* Melbourne, Australia.

Sloff C. J., 1993. Analysis of Basic Equations for Sediment-Laden Flows. *Delft University of Technology.* Delft, The Netherlands.

Soulsby R. L. & G. O Mabbett, 1987. A criterion for the effect of suspended sediment on mean bottom velocity profile. *Journal of Hydraulic Research, IAHR,* Vol. 25, No. 3. Delft, The Netherlands.

Stevens M. A., 1989. Width of straight alluvial channel. *Journal of Hydraulic Division, ASCE.* Vol. 115, No.3. New York, USA.

Steven M. A. & C. F.Nordin, 1987. Critique of the regime theory for alluvial channel. *Journal of Hydraulic Division, ASCE.* Vol. 113, No. 11. New York, USA.

Takashi Asaeda et al, 1989. Sediment entrainment in channels with rippled bed. *Journal of Hydraulic Division, ASCE.* Vol. 115, No.3. New York, USA.

Talapatra S. C. & S. Ghosh, 1981. Sediment transport due to transient flow. *19th IAHR congress*. New Delhi, India.

Tawatchai T., 1989. Stability analysis of 2-dimensional depth-averaged model. *Journal of Hydraulic Division, ASCE*. Vol. 115, No. 9. New York, USA.

Teisson C., 1991. Cohesive suspended sediment transport:feasibility and limitations of numerical modelling. *Journal of Hydraulic Research, IAHR*, Vol. 29. No.6. Delft, The Netherlands.

Temple D., 1986. Velocity distribution coefficient for grass lined channels. *Journal of Hydraulic Division, ASCE*. Vol. 112, No. 3. *Journal of Hydraulic Division, ASCE*. New York, USA.

Toffaleti F. B., 1969. Definitive computations of sand discharge in rivers. *Journal of Hydraulic Division, ASCE*. No. 1. New York, USA.

Tsujimoto H. et al, 1991. Turbulent flow and suspended sediment transport in vegetated bed channel. *24th IAHR congress*. Madrid, Spain.

Umeyama M., 1992. Vertical distribution of suspended sediment in uniform open-channel flow. *Journal of Hydraulic Division, ASCE*. Vol. 118, No. 6, pp 936-941. New Yok, USA.

Vanoni V., 1974. Factors determining bed forms in alluvial streams. *Journal of Hydraulic Division, ASCE*. vol 100, No. 3. New York, USA.

Vanoni V. (Ed.), 1975. Sedimentation Engineering. *Manuals and reports on engineering practice No. 54. ASCE*. New York, USA.

Vanoni V., 1984. Fifty years of sedimentation. *Journal of Hydraulic Division, ASCE*. New York, USA.

Van Rijn L. C., 1982. Equivalent roughness of alluvial bed. *Journal of Hydraulic Division, ASCE*. New York, USA.

Van Rijn L. C., 1984a. Sediment Transport Part I: Bed load Transport. *Journal of Hydraulic Division, ASCE*. Vol. 110,No. 10. New York, USA.

Van Rijn L. C., 1984b. Sediment Transport Part II: Suspended Load Transport. *Journal of Hydraulic Division, ASCE*. Vol. 110, No. 11. New York, USA.

Van Rijn L. C., 1984c. Sediment transport part III: Bed form and alluvial roughness. *Journal of Hydraulic Division, ASCE*. Vol. 110, No. 12. New York, USA.

Van Rijn L. C., 1984d. Sediment pick-up functions. *Journal of Hydraulic Division, ASCE*. Vol. 110. New York, USA.

Van Rijn L. C., 1987. Mathematical modelling of morphological processes in the case of suspended sediment transport. *Delft Hydraulic Communication No. 382*. Delft, The Netherlands.

Van Rijn L. C. et al, 1990. Field verification of 2-D and 3-D suspended sediment models. *Journal of Hydraulic Division, ASCE*. vol 116, No. 10. New York, USA.

Van Rijn L. C.1993. *Lecture notes on principles of sediments transport in rivers, estuaries, coastal seas and oceans*. IHE. Delft, The Netherlands.

Vermeer K. & A. P. Termes, 1991. *Lecture notes on Mathematical Modelling 1* IHE. Delft, The Netherlands.

Vigilar G. G. & Panayiotis Diplas, 1997. Channels with mobile bed: formulation and numerical solution. *Journal of Hydraulic Division, ASCE.* Vol 123, No. 3. New York, USA.

Vlugter H., 1962. Sediment transportation by running water and design of stable alluvial channelss. *De Ingenieur.* The Hague, The Netherlands.

Vreugdenhil C. & J. H. A. Wijbenga, 1982. Computation of flow patterns in rivers. *Journal of Hydraulic Division, ASCE.* vol 108, No. 11. New York, USA.

Vreugdenhil C., 1989. *Computational Hydraulics.* Springer-Verlag. Berlin, Germany.

Vries M. de, 1965. Consideration about non-steady bed load transport in open channel.. Delft Hydraulics Laboratory. Publications No. 36. Delft, The Netherlands.

Vries M. de, 1975. A morphological time scale for rivers. *IAHR.* Sao Paulo, Brazil

Vries M. de, 1982. A Sensitivity Analysis Applied to Morphological Computations. *Report No. 85-2. Delft University of Technology.* Delft, The Netherlands.

Vries M. de, 1987. *Lecture notes on Morphological Computations.* Delft University of Technology. Delft, The Netherlands.

Waijjen E.G. van et al, 1997. Using a hydro-dynamic flow model to plan maintenance activities and improve irrigation water distribution: application to the Fordwah distributary in Punjab, Pakistan. *Irrigation and drainage systems.* Vol 11. Kluwer Academic Publishers. Dordrecht, The Netherlands.

Wang Shang-yi 1984. The principle and application of sediment effective power. *Journal of Hydraulic Division, ASCE.* New York, USA.

Wang S. (editor), 1989. Sediment transport modelling. *Proceeding of the international symposium ASCE.* New York, USA.

Wang S. & W. R. White 1993. Alluvial resistance in transition regime. *Journal of Hydraulic Division, ASCE.* Vol. 119, No. 6. New York, USA.

Wang Z.B., 1990. Limit concentration of suspended sediment. *Journal of Hydraulic Division, ASCE.* New York, USA.

Wang Z. B., 1991. Theoretical analysis on depth integrated modelling of suspended sediment transport. *Journal of Hydraulic Research, IAHR.* Vol. 30, No. 3. Delft, The Netherlands.

Wang Z. B. & RibberinK, J.S., 1986. The validity of a depth integrated model for suspended sediment transport. *Journal of Hydraulic Research, IAHR.* Vol. 24, No. 1. Delft, The Netherlands.

Webel G. & M. Schatzmann, 1984. Transverse mixing in open channel flow. *Journal of Hydraulic Division, ASCE.* New York, USA.

Westrich B. & M. Juraschek, 1985. Flow transport capacity for suspended sediment. *21st IAHR congress.* Melbourne, Australia.

White W. R. et al, 1979. A new general method for predicting the frictional characteristics of alluvial streams. Hydraulic Research Limited, Wallingford, United Kingdom.

White W. R., 1989. Regime principle applied to the design of mobile bed physical models. *23rd IAHR congress*. Otawa, Canada.

White R., R. Bettes & E. Paris, 1982. Anayitical approach to river regime. *Journal of Hydraulic Division, ASCE*. Vol. 108, No. 10. New York, USA.

Wikcock P., 1993. Critical shear stress of natural sediments. *Journal of Hydraulic Division, ASCE*. Vol. 119, No. 4. New York, USA.

Willis Joe C., 1985. Near bed velocity distribution. *Journal of Hydraulic Division, ASCE*. New York, USA.

Woo H. et al, 1988a . Performance test of some selected transport formulae. *Journal of Hydraulic Division, ASCE*. New York, USA.

Woo H. et al, 1988b. Suspension of large concentration of sand. *Journal of Hydraulic Division, ASCE*. Vol. 114, No. 10. New York, USA.

Worapansopak J., 1992. Control of Sediment in Irrigation Schemes. *M.Sc. thesis. IHE*. Delft, The Netherlands.

World Bank, 1986. Design and operating guidelines for structural irrigation networks. *Fourth draft. Irrigation II Division. South Asia Project Department. World Bank.* Washington DC, USA.

World Bank, 1989. Irrigation training in the public sector.*The World Bank.* Washington DC, USA.

World Bank, 1995. The World Bank and Irrigation. *World Bank Operation Evaluation Department. The World Bank.* Washington DC, USA.

Wormleaton, P. R., et al, 1982. Discharge assesment in compound channel flow. *Journal of Hydraulic Division, ASCE*. Vol. 108, pp 975-994. New York, USA.

Xia Renjie & B.Yen, 1994. Significance of averaging coefficient in open channel flow equation. *Journal of Hydraulic Division, ASCE*. Vol. 120, No. 2. New York, USA.

Yalin M.S., 1977. *Mechanics of Sediment Transport*. Pergamon Press. Oxford, Great Britain.

Yalin M.S., 1985. On the determination of ripple geometry. *Journal of Hydraulic Division, ASCE*. New York, USA.

Yang et al, 1989. Semi-coupled simulation of unsteady non-uniform sediment transport in alluvial channel. *23rd IAHR congress*. Otawa, Canada.

Yang C. T., 1973. Incipient motion and sediment transport. *Journal of Hydraulic Division, ASCE*. Vol. 99. No. 110. New York, USA.

Yang C. T., 1979. Unit stream power equation for total load. *Journal of Hydrology Division, ASCE*. Vol. 99. No. 110. New York, USA.

Yang C. T. & A. Molinas, 1982. Sediment transport and Unit stream power. *Journal of Hydraulic Division 40*. Amsterdam, The Netherlands.

Yen, B. C., 1972. Variation of bed form and flow resistance in alluvial channel. *Proceedings of 14th congress of international association for hydraulic research*. Vol 3 pp 83-90. Paris, France.

APPENDIX A: DESCRIPTION OF THE SELECTED METHODS TO ESTIMATE THE TOTAL SEDIMENT TRANSPORT CAPACITY IN IRRIGATION CANALS

Irrigation canals are designed and operated in such a way that in principle no deposition or erosion occurs during certain periods. Thus, an accurate prediction of the sediment transport of irrigation canals is required for the design as well as for the operation phase of the irrigation system.

There is no universally accepted equation to determine the total sediment transport capacity of canals. Many methods have been proposed to predict the sediment transport under a large range of flow conditions and sediment characteristics. Among these methods can be mentioned the methods of Einstein (1950), Colby (1964), Bishop et al. (1965), Bagnold (1966), Engelund and Hansen (1967),Toffaletti (1969), Ackers and White (1973), Yang (1973), Brownlie (1981), van Rijn (1984), etc. But, the predictability of all of them is still poor. Van Rijn (1984) stated that it is hardly possible to predict any sediment transport with an inaccuracy of less than 100%. In fact it is quite difficult to make firm recommendations about which formula to use in practice. However, a comparison of sediment transport methods under the typical flow conditions and sediment characteristics of irrigation canals could become a powerful tool to reduce inevitable errors and inaccuracy. It is not possible to check all the existing methods to predict sediment transport. In this study five of the most widely used methods to compute sediment transport are evaluated. These methods are:

- Ackers and White;
- Brownlie;
- Engelund and Hansen;
- Van Rijn;
- Yang.

Ackers and White method (1973): the Ackers and White (1973) method is based on flume experiments with a uniform or nearly uniform sediment size distribution, with an established movement including bed forms, flow conditions with water depths smaller than 0.4 m and in the lower flow regime ($Fr \leq 0.8$). The Ackers-White method describes the sediment transport in terms of three dimensionless parameters: D_* (grain size sediment parameter), F_{gr} (mobility parameter) and G_{gr} (transport parameter). They are:

- Dimensionless grain parameter D_*, which reflects the influence of gravity, density and viscosity, expressed by:

$$D_* = \left[\frac{(s-1)\,g}{\nu^2}\right]^{1/3} d_{35} \qquad (A.1)$$

- The dimensionless mobility parameter F_{gr}, which is described by the ratio of the relevant shear force on an unit area of the bed to the immersed weight of a layer of grains. The general equation for the transitional range ($1 \leq D_* \leq 60$) is:

$$F_{gr} = \frac{u_*^n}{\sqrt{g\ d_{35}\ (s-1)}} \left[\frac{V}{\sqrt{32}\ \log\left(\frac{10\ h}{d_{35}}\right)}\right]^{1-n} \tag{A.2}$$

with:

$$n = 1.00 - 0.56 \log D_* \tag{A.3}$$

- The dimensionless transport parameter G_{gr}, which is based on the stream power concept. The general equation for this parameter is:

$$G_{gr} = c \left(\frac{F_{gr}}{A} - 1\right)^m \tag{A.4}$$

with

$$A = \frac{0.23}{\sqrt{D_*}} + 0.14 \tag{A.5}$$

$$m = \frac{9.66}{D_*} + 1.334 \tag{A.6}$$

$$\log c = 2.86 \log D_* - (\log D_*)^2 - 3.53 \tag{A.7}$$

The Ackers and White function to determine the total sediment transport reads as:

$$q_s = G_{gr}\ s\ d_{35} \left(\frac{V}{u_*}\right)^n \tag{A.8}$$

where:

D_* = dimensionless grain parameter
s = relative density
g = gravity (m/s^2)
d_{35} = representative particle diameter (m)
h = water depth (m)
ν = kinematic viscosity (m^2/s)

F_{gr} = dimensionless mobility parameter
A = value of F_{gr} at the nominal, initial movement
G_{gr} = dimensionless transport parameter
c = coefficient in the transport parameter G_{gr}
m = exponent in the transport parameter G_{gr}
n = exponent in the dimensionless mobility parameter F_{gr}
u_* = shear velocity (m/s)
V = mean velocity (m/s)
q_s = total sediment transport per unit width (m^2/s)

Brownlie method (1981): Brownlie's method to compute the sediment transport is based on a dimensional analysis and calibration of a wide range of field and laboratory data, where uniform conditions prevailed. The transport (in ppm by weight) is calculated by:

$$q_s = 727.6\ c_f\ (F_g - F_{g_{cr}})^{1.978}\ S^{0.6601}\ \left(\frac{R}{d_{50}}\right)^{-0.3301} \tag{A.9}$$

- grain Froude number:

$$F_g = \frac{V}{[(s - 1)\ g\ d_{50}]^{0.5}} \tag{A.10}$$

- critical grain Froude number:

$$F_{g_{cr}} = 4.596\ \tau_{*_o}^{0.5293}\ S^{-0.1405}\ \sigma_s^{-0.1696} \tag{A.11}$$

- critical dimensionless shear stress

$$\tau_{*_o} = 0.22\ Y + 0.06\ (10)^{-7.7\ Y} \tag{A.12}$$

the Y value is computed from:

$$Y = (\sqrt{s - 1}\ R_g)^{-0.6} \tag{A.13}$$

- grain Reynolds number:

$$R_g = \frac{(g\ d_{50}^3)^{0.5}}{31620\ \nu} \tag{A.14}$$

where:

c_f = coefficient for the transport rate ($c_f = 1$ for laboratory conditions and $c_f = 1.268$ for field conditions)
F_g = grain Froude number
F_{gcr} = critical grain Froude number
τ_{*_o} = critical dimensionless shear stress
σ_s = geometric standard deviation
g = gravity acceleration (m/s^2)
S = bottom slope
d_{50} = median diameter (mm)
s = relative density
R_g = grain Reynolds number
R = hydraulic radius (m)
ν = kinematic viscosity (m^2/s)

Engelund and Hansen method (1967): the method of Engelund and Hansen is based on an energy approach and they established a relationship between transport and mobility parameters. The Engelund and Hansen function for the total sediment transport is calculated by:
- Dimensionless transport parameter ϕ

$$\phi = \frac{q_s}{\sqrt{(s - 1)\, g\, d_{50}^3}} \tag{A.15}$$

- Dimensionless mobility parameter θ

$$\theta = \frac{u_*^2}{(s-1)\, g\, d_{50}} \tag{A.16}$$

The relationship between those parameters is expressed by:

$$\phi = \frac{0.1\, \theta^{2.5}\, C^2}{2\, g} \tag{A.17}$$

and the total sediment transport is expressed by:

$$q_s = \frac{0.05\, V^5}{(s - 1)^2\, g^{0.5}\, d_{50}\, C^3} \tag{A.18}$$

where:
q_s = total sediment transport ($m^3/s.m$)
θ = dimensionless mobility parameter
ϕ = dimensionless transport parameter

V = mean velocity (m/s)
C = Chézy coefficient ($m^{1/2}/s$)
s = relative density
u_* = shear velocity (m/s)
d_{50} = mean diameter (m)
g = gravity acceleration (m/s^2)

The Engelund and Hansen function for calculating the total sediment transport was tested against laboratory data characterized by graded sediment ($\sigma_s < 1.6$) and median diameters d_{50} of 0.19 mm, 0.27 mm, 0.45 mm and 0.93 mm. The mentioned authors do not recommend their method for those cases, in which the median size is less than 0.15 mm and the geometric standard deviation is greater than approximately 2.

van Rijn method (1984a and 1984b): the total sediment transport by the van Rijn method can be computed by the summation of the bed and suspended load transport ($q_s = q_b + q_{sus}$). The van Rijn method presents the computation of the bed load transport q_b as the product of the saltation height, the particle velocity and bed load concentration. It assumes that the motion of the bed particles is dominated by gravity forces. This method was tested against data with the following characteristics:

- mean velocity = 0.31 - 1.29 m/s
- flow depth = 0.1 - 1.0 m
- median diameter = 0.32 - 1.5 mm

The bed load transport rate is calculated as:

$$q_b = u_b \, \delta_b \, c_b \tag{A.19}$$

- particle velocity u_b

$$u_b = 1.5 \, T^{0.6} \, [(s - 1) \, g \, d_{50}]^{0.5} \tag{A.20}$$

- saltation height δ_b:

$$\delta_b = 0.3 \, D_*^{0.7} \, T^{0.5} \, d_{50} \tag{A.21}$$

- bed load concentration c_b:

$$c_b = 0.18 \, c_o \, \frac{T}{D_*} \tag{A.22}$$

with:

$$T = \frac{(u_*')^2 - (u_{*,cr})^2}{(u_{*,cr})^2} \qquad (A.23)$$

$$u_*' = \frac{g^{0.5}\, V}{C'} \qquad (A.24)$$

$$D_* = \left[\frac{(s-1)\, g}{\nu^2}\right]^{1/3} d_{50} \qquad (A.25)$$

after replacing equations A.20 to A.25 in equation A.19 gives:

$$q_b = 0.053\ (s - 1)^{0.5}\ g^{0.5}\ d_{50}^{1.5}\ D_*^{-0.3}\ T^{2.1} \qquad (A.26)$$

where:

q_b = bed load transport (m^2/s)
u_b = particle velocity (m/s)
c_b = bed load concentration
c_o = maximum volumetric concentration = 0.65
T = bed shear parameter
D_* = particle parameter
u_*' = bed shear velocity related to grains (m/s)
C' = Chézy coefficient related to grains ($m^{1/2}/s$) = 18 log ($12h/3d_{90}$)
δ_b = saltation height (m)
s = relative density
d_{50} = mean diameter (m)
g = gravity acceleration (m/s^2)

The suspended load transport q_{sus}, according to van Rijn (1984b) is the depth integrated product of the local concentration and the flow velocity. The method is based on the computation of the reference concentration from the bed load transport.
It was tested against field and laboratory data with the following characteristics:

- mean velocity = 0.4 - 2.4 m/s
- flow depth = 0.1 - 17 m
- median diameter = 0.1 - 0.4 mm

The suspended load transport is calculated by:

$$q_{sus} = F\ V\ h\ c_a \tag{A.27}$$

- shape factor F:

$$F = \frac{(a/h)^{Z'} - (a/h)^{1.2}}{(1 - a/h)^{Z'}\ (1.2 - Z')} \tag{A.28}$$

- suspension parameter Z

$$Z = \frac{w_s}{\beta\ \kappa\ u_*} \tag{A.29}$$

- modified suspension parameter Z'

$$Z' = Z + \psi \tag{A.30}$$

- reference concentration c_a

$$c_a = \frac{0.015\ d_{50}\ T^{1.5}}{a\ D_*^{0.3}} \tag{A.31}$$

- reference level a

$$a = 0.5\ \Delta \quad \text{or} \quad a = k_s \quad \text{with} \quad a_{min} = 0.01\ h \tag{A.32}$$

- representative particle size of suspended sediment d_s

$$d_s = [1 + 0.011\ (\sigma_s - 1)\ (T - 25)]\ d_{50} \tag{A.33}$$

with:
- β - factor

$$\beta = 1 + 2\ (\frac{w_s}{u_*})^2 \tag{A.34}$$

- ψ - factor

$$\psi = 2.5 \left(\frac{w_s}{u_*}\right)^{0.8} \left(\frac{c_a}{c_o}\right)^{0.4} \qquad (A.35)$$

where:

F	= shape factor
V	= mean velocity (m/s)
u_*	= shear velocity (m/s)
c_a	= reference concentration
h	= water depth (m)
D_*	= dimensionless particle parameter
a	= reference level (m)
Z	= suspension number
Z'	= modified suspension number
β	= ratio of sediment and fluid mixing coefficient
ψ	= stratification correction
κ	= constant of von Karman
σ_s	= geometric standard deviation
d_{50}	= median diameter (mm)
d_s	= representative particle size of suspended sediment (m)
w_s	= fall velocity of representative particle size (m/s)
T	= transport stage parameter
Δ	= bed form height (m)
k_s	= equivalent roughness height (m)
$u_{*,cr}$	= critical bed shear velocity (m/s)

Yang method (1973): the Yang method is based on the hypothesis that the sediment transport in a flow should be related to the rate of energy dissipation of the flow. The rate of energy dissipation is defined as the unit stream power and it can be expressed by the velocity times slope (V * S). The theoretical basis for Yang's dimensionless unit stream power is provided by the turbulence theory. By integrating the rate of turbulence energy production over the flow depth, the suspended sediment transport can be expressed as function of the unit stream power. The total sediment transport can also be expressed in ppm by mass as a function of the unit stream power by:

$$\log c_t = I + J \log \left(\frac{V S - V_{cr} S}{w_s}\right) \qquad (A.36)$$

with the Yang's coefficients represented by:

$$I = 5.435 - 0.286 \log \left(\frac{w_s d_{50}}{\nu}\right) - 0.457 \log \left(\frac{u_*}{w_s}\right) \quad \text{(A.37)}$$

and:

$$J = 1.799 - 0.409 \log \left(\frac{w_s d_{50}}{\nu}\right) - 0.314 \log \left(\frac{u_*}{w_s}\right) \quad \text{(A.38)}$$

- the critical velocity for initiation of motion V_{cr}:

$$V_{cr} = 2.05\ w_s \quad \text{(A.39)}$$

The total load transport is calculated by:

$$q_s = 0.001\ c_t\ V\ h \quad \text{(A.40)}$$

where:

q_s = total load transport (kg/sm)
c_t = total sediment transport expressed in ppm by mass
V = mean velocity (m/s)
V_{cr} = velocity for initiation of motion (m/s)
h = water depth (m)
S = bottom slope
I, J = coefficients in Yang's function for the total sediment transport
w_s = fall velocity (m/s)
d_{50} = median diameter (m)
u_* = shear velocity (m/s)
ν = kinematic viscosity (m^2/s)

Equation A.36 and A.40 was verified with laboratory and field data in the following ranges:

- sediment size = 0.15 - 1.71 mm
- mean velocity = 0.23 - 1.97 m/s
- water depth = 0.01 - 15.2 m
- concentration = 10 - 585,000 ppm
- bottom slope = $0.043*10^{-3}$ - $27.9*10^{-3}$

Calculation of the total sediment transport capacity according to all methods

The total sediment transport capacity according to all methods is calculated step by step from certain variables given by the flow condition and sediment characteristics. These variables are:

ν = kinematic viscosity (m^2/s)
h = water depth
V = mean velocity (m/s)
S_0 = bottom slope
d_{35} = representative particle diameter (m)
d_{50} = representative particle diameter (m)
d_{90} = representative particle size
σ_s = geometric standard deviation
s = relative density

The computation for each sediment transport method is carried out as follows:

Ackers and White method:
compute the:
- dimensionless grain parameter D_* (eq. A.1);
- value of n (eq. A.3);
- shear velocity u_* (eq. 2.16);
- dimensionless mobility parameter F_{gr} (eq. A.2);
- values of A, m and c (equations A.5, A.6 and A.7)
- dimensionless transport parameter G_{gr} (eq. A.4);
- total sediment transport capacity q_s (eq. A.8)

Brownlie method:
compute the:
- dimensionless grain Froude number F_g (eq. A.10);
- dimensionless grain Reynolds number R_g (eq. A.14);
- value of Y (eq. A.13)
- dimensionless critical shear stress (eq. A.12);
- dimensionless critical grain Froude number F_{gcr} (eq. A.10);
- total sediment transport capacity q_s (eq. A.9)

Engelund and Hansen method:
compute the:
- Chézy coefficient from $C = V/(h\, S_0)^{0.5}$;
- total sediment transport capacity q_s (eq. A.18)

van Rijn method:
compute the:
- dimensionless grain parameter D_* (eq. A.25);

- Chézy coefficient related to the grains(C') by using $C' = 18 \log (12h/3d_{90})$
- effective bed shear velocity u_*' (eq. A.24);
- critical mobility parameter θ_{cr} (equations 2.18 to 2.20)
- critical bed shear velocity u_{*cr} (eq. 2.14)
- excess bed shear parameter T (eq. A.23)
- bed load transport (eq. A.26)
- bed form height (equationsB10 or B.12)
- reference level a (eq. A.32)
- reference concentration c_a (eq. A.31)
- representative particle size of the suspended sediment d_s (eq. A.33)
- fall velocity w_s for the representative particle size d_s
- overall bed shear velocity u_* (eq. 2.16)
- β factor (eq. A.34)
- ψ factor (eq. A.35)
- suspension number Z (eq. A.29) and the modified suspension number Z' (eq. A.30)
- shape factor F (eq. A.28)
- suspended load transport q_s (eq. A.27)
- total sediment transport by summation of the bed load transport (eq. A.26) and the suspended load transport (eq. A.27).

Yang Method:
compute the:

- fall velocity w_s of the representative sediment size (d_{50})
- overall bed shear velocity u_* (eq. 2.16)
- Yang's function coefficients I and J (equations A.37 and A.38))
- depth average velocity at initiation of motion V_{cr} (equation A.39)
- total sediment transport expressed in ppm by mass (equation A.36)
- total sediment transport capacity q_s (eq. A.40)

APPENDIX B: DESCRIPTION OF THE METHODS TO ESTIMATE THE FRICTION FACTOR

The methods selected to predict the friction factor in irrigation canals are:

- van Rijn (1984c);
- Brownlie (1983);
- White, Bettess & Paris (1979);
- Engelund (1966).

Those methods will be briefly described in the next paragraphs. In this study the Chézy coefficient is used to describe the friction factor in irrigation canals. Additional applications with the Darcy-Weisbach and Manning (Strickler) coefficient can be made by using the following relationships:

$$C = \sqrt{\frac{8\,g}{f}} \quad \text{or} \quad C = \frac{R^{1/6}}{n} \tag{B.1}$$

where:

C = Chézy coefficient ($m^{1/2}/s$)
f = Darcy-Weisbach's friction factor
n = Manning's coefficient ($m^{1/3}/s$)
R = hydraulic radius (m)
g = gravity acceleration (m/s^2)

van Rijn's method (1984): the Chézy coefficient is calculated according to the type of flow regime. Based on the bed-roughness conditions the hydraulic flow regime in open canals can be divided in: smooth, rough and a transition regime. Roughness conditions on the bottom are simulated by using an equivalent height of the sand roughness k_s, which is equal to the roughness of a sand that gives a resistance similar to the resistance of the bed form. The dimensionless value of $u_* k_s/\nu$ is used as the classification parameter to distinguish the type of flow regime. van Rijn (1993) described the type of hydraulic regimes as shown in table B.1.

Table B.1 Hydraulic regime types

Type of regime	Classification parameter $u_* k_s/\nu$
Smooth	$u_* k_s/\nu < 5$
Transition	$5 < u_* k_s/\nu < 70$
Rough	$u_* k_s/\nu > 70$

Depending on the bed condition the hydraulic regimes in irrigation canals can be determined as:

Plane bed: for plane beds (no motion) the equivalent height k_s is related to the largest particles of the bed material. van Rijn (1982) described the equivalent roughness height as $k_s = 3\ d_{90}$.

Assuming an uniform sediment size distribution in irrigation canals ($d_{90} \approx 1.5\ d_{50}$), the equivalent roughness height of the sediment for plane beds can be represented by:

$$k_s = 4.5\ d_{50} \tag{B.2}$$

where:

d_{50} = median diameter of the sediment (m)
k_s = equivalent height roughness (m).

The maximum values of the parameter $u_* k_s/\nu$ for plane bed (no motion) in irrigation canals is determined by using:

- $k_s = 4.5\ d_{50}$;
- u_* = critical Shield shear velocity (u_{*cr})

The results of this computations are shown in table B.2. The flow regime types for no-motion conditions are: smooth and transition.

Table B.2 $u_* k_s/\nu$ parameter for plane bed (no motion)

d_{50} (mm)	0.05	0.10	0.15	0.20	0.25	0.30	0.35	0.40	0.45	0.50
$u_{*(cr)} k_s/\nu$	2.8	5.1	8.2	11.5	14.9	18.5	21.3	25.8	30.6	35.7

Bed forms: for higher velocities, the occurrence of bed features changes the bed roughness. The effective roughness or the total equivalent height is represented by (van Rijn 1984c):

$$k_s = k_s' + k_s'' \tag{B.3}$$

where:

k_s = total equivalent height (m)
k_s' = equivalent height related to the grain (m)
k_s'' = equivalent height related to the bed form (m)

k_s' and k_s'' values can be determined by (van Rijn, 1982):

$$k_s' = 3\ d_{90} \approx 4.5\ d_{50} \tag{B.4}$$

and:

$$k_s'' = 20\ \gamma_r\ \Delta_r\ (\frac{\Delta_r}{\lambda_r}) \quad \text{(Ripples)} \tag{B.5}$$

or:

$$k_s'' = 1.1\ \gamma_d\ \Delta_d\ (1 - e^{-25\ \frac{\Delta_d}{\lambda_d}}) \quad \text{(Dunes)} \tag{B.6}$$

where:

γ_r = ripple presence (γ = 1 for ripples alone)
γ_d = form factor (γ_d = 0.7 for field conditions)
Δ_r = ripple height (Δ_r = 50 to 200 d_{50})
Δ_d = dune height
λ_r = ripple length (λ_r = 500 to 1000 d_{50})
λ_d = dune length

The resistance due to the grain roughness is small compared to the one caused by the geometry of the bed form. Many attempts have been made to describe the geometry of ripples and dunes.

Yalin (1985) described the geometry of ripples generated by a subcritical open channel flow with cohesionless and uniform bed material. He found that the length of the ripples was in the interval:

$$600\ D \leq \lambda_r \leq 2000\ D \tag{B.7}$$

where:

D = representative grain size (D = d_{50})
λ_r = ripple length

The "largest population" of the ripples lengths were found within the range:

$$900\ d_{50} \leq \lambda_r \leq 1000\ d_{50} \tag{B.8}$$

A value which represents well the length of the ripples can be given by:

$$\lambda_r \simeq 1000\ d_{50} \tag{B.9}$$

The ripple height was also described by Yalin (1985):

$$\Delta_r \simeq 50 \text{ to } 200\ d_{50} \tag{B.10}$$

where:

Δ_r = ripple height (m)

It is possible to assume for practical purposes that (for $\Delta_r = 100\ d_{50}$ and $\lambda_r = 1000\ d_{50}$):

$$\frac{\Delta_r}{\lambda_r} \approx 0.1 \quad \text{for} \quad 1 \leq D_* \leq 10 \quad \text{and} \quad T \leq 3 \tag{B.11}$$

Another bed form type in the lower regime (Fr < 0.8) is the dune type. The shape of the dunes is similar to the ripples, but the length and height greater than of ripples. Relationships for length and dune height based on flume and field data are given by van Rijn (1994). Both variables can be calculated by:

$$\frac{\Delta_d}{h} = 0.11 \left(\frac{d_{50}}{h}\right)^{0.3} (1 - e^{-0.5\,T}) (25 - T) \tag{B.12}$$

and

$$\lambda_d = 7.3\ h \tag{B.13}$$

where:

T = excess bed-shear stress parameter
λ_d = dune length (m)
Δ_d = dune height (m)
d_{50} = median diameter (m)
h = water depth (m)

Consider the influence of k_s' (related to the grain) on the total value of the equivalent roughness height k_s. The maximum influence of k_s' will occur for those bed forms with a minimum equivalent height. The minimum equivalent height related to the bed form is generated for ripples. The maximum influence of the equivalent height of k_s' over the total equivalent height for the specific conditions of irrigation canals is approximately 1.5 - 2 % (ripples occurrence).

$$\frac{k_s'}{k_s' + k_s''} = \frac{4.5\ d_{50}}{4.5\ d_{50} + 20\ \gamma_s\ \Delta_r \left(\frac{\Delta_r}{\lambda_r}\right)} \approx 2\ \% \tag{B.14}$$

For other bed forms the influence of the grains will be smaller than for ripples. For that reason and because the grain roughness is assumed to be constant during changes of the size of bed forms, the grain roughness can be neglected. Hence, the equivalent height related to the bed form is recommended to use. Therefore, for ripples the total equivalent roughness can be computed by replacing in equation B.5 as:

$$k_s = k_s'' = 20 * 1 * 0.1 * 100 * d_{50} = 200\ d_{50} \qquad \text{(B.15)}$$

Minimum values (ripples) for the parameter $u_* k_s/\nu$ in irrigation canals can be computed by:
- $k_s = 200\ d_{50}$;
- $u_* =$ critical Shield shear velocity u_{*cr}.

For those canals the values of the parameter $u_* k_s/\nu$ are shown in table B.3. Once the sediment on the bottom of an irrigation canal comes into motion the flow will be considered as hydraulically rough. Figure B.1 shows the types of flow regime in irrigation canals.

Table B.3 $u_* k_s/\nu$ parameter for ripples

d_{50} (mm)	0.05	0.10	0.15	0.20	0.25	0.30	0.35	0.40	0.45	0.50
$u_{*(cr)} k_s/\nu$	499	899	1450	2037	2650	3286	3782	4590	5445	6344

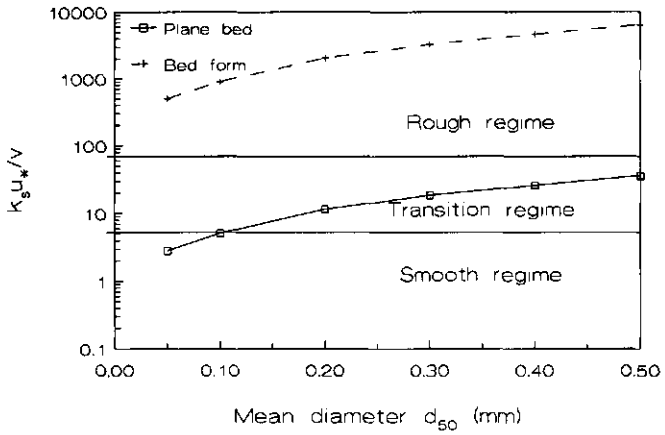

Figure B.1 Hydraulic regimes in irrigation canals

For smooth and transition flow regimes, the Chézy coefficient is a function of the flow condition only and it can be calculated by (van Rijn, 1993):

$$C = 18 \log\left(\frac{12\ h}{3.3\ \frac{\nu}{u_*}}\right) \qquad \text{Smooth flow regime} \qquad \text{(B.16)}$$

$$C = 18 \log \left(\frac{12\ h}{k_s + 3.3\ \frac{\nu}{u_*}} \right) \qquad \text{Transition flow regime} \qquad \text{(B.17)}$$

$$C = 18 \log \left(\frac{12\ h}{k_s} \right) \qquad \text{Rough flow regime} \qquad \text{(B.18)}$$

where:

C = Chézy coefficient ($m^{1/2}/s$)
h = water depth (m)
ν = kinematic viscosity (m^2/s)
u_* = shear velocity (m/s)
k_s = total equivalent roughness (m)

A good approximation of the Chézy coefficient for canals with ripples can be obtained by replacing he total equivalent height by the equivalent height related to the bed form k_s'' (eq. B.15) which can be represented by:

$$C = 18 \log \frac{h}{200\ d_{50}} \qquad \text{(B.19)}$$

The Chézy coefficient obtained from equation B.16 to B.18 considers only the bed forms on the bed without taking into account the friction factor of the side banks. Therefor it is necessary to find a weighed value of the Chézy coefficient for the friction of both bed and side banks.

Brownlie's method (1983): Brownlie (1983) proposed a technique to predict the flow depth (and therefore the friction factor) when the discharge and the slope are known. No explicit calculation of the Chézy coefficient is proposed, but once the resistance to flow is determined (equations B.20 and B.21) then the Chézy coefficient will be calculated by equation B.22. The Brownlie method is based on a dimensional analysis, basic principles of hydraulics and a verification with a large amount of field and flume data. Step by step, the Chézy coefficient in the lower flow regime can be predicted by using the following relationships:

$$q_* = \frac{Q}{B\ g^{0.5}\ d_{50}^{1.5}} = \frac{q}{g^{0.5}\ d_{50}^{1.5}} \qquad \text{(B.20)}$$

$$h = 0.372\ d_{50}\ q_*^{0.6539}\ S_0^{-0.2542}\ \sigma_s^{0.1050} \qquad \text{(B.21)}$$

and

$$q = C\ h\ \sqrt{h\ S_0} \quad \therefore \quad C = \frac{q}{h^{1.5}\ S_0^{0.5}} \qquad \text{(B.22)}$$

where:

Q = discharge (m^3/s)
q = unit discharge (m^2/s)
B = bottom width (m)
h = water depth (m)
S_0 = bottom slope
d_{50} = median diameter (m)
σ_s = gradation of sediment ($\sigma_s = \frac{1}{2}\ (d_{84}/d_{50} + d_{50}/d_{16})$)
q_* = dimensionless unit discharge

White, Paris and Bettess' method (1979): the flow resistance equation according to White et al (1979) is described in terms of some dimensionless groups:
- dimensionless particle size D_*

$$D_* = \left[\frac{(s-1)\ g}{\nu^2}\right]^{1/3} d_{35} \qquad \text{(B.23)}$$

- dimensionless particle mobility F_{fg}

$$F_{fg} = \frac{u_*}{\sqrt{g\ d_{35}\ (s-1)}} \qquad \text{(B.24)}$$

- calculation of the mobility parameter related to the effective shear stress

$$F_{gr} = (F_{fg} - A)\left[1.0 - 0.76\left(1 - \frac{1}{\exp\ (\log\ D_*)^{1.7}}\right)\right] + A \qquad \text{(B.25)}$$

- mean velocity:

$$V = \sqrt{32}\ \log\left(\frac{h}{d_{35}}\right)\left[\frac{F_{gr}\ \sqrt{g\ d_{35}\ (s-1)}}{u_*^n}\right]^{\frac{1}{1-n}} \qquad \text{(B.26)}$$

with:

$$n = 1 - 0.56 \log D_* \tag{B.27}$$

$$A = \frac{0.23}{\sqrt{D_*}} + 0.14 \tag{B.28}$$

- compute the Chézy coefficient:

$$C = \frac{g^{0.5}\, V}{u_*} \tag{B.29}$$

where:

D_* = dimensionless particle size
F_{fg} = dimensionless particle mobility
F_{gr} = dimensionless particle mobility related to the effective shear stress
d_{35} = particle size (m)
A = initial motion parameter
n = exponent in the mobility parameter related to the effective shear stress
h = water depth (m)
g = gravity (m/s^2)
u_* = shear velocity (m/s)
V = mean velocity (m/s)
s = relative density
C = Chézy coefficient
ν = kinematic viscosity (m^2/s)

Engelund's method (1966): Engelund proposed that the shear stress due to skin and form resistance can be defined by:

$$\tau = \tau' + \tau'' \tag{B.30}$$

with:

$$\tau = \rho\, g\, h\, S \quad \text{and} \quad \tau' = \rho\, g\, h'\, S \quad \text{and} \quad \tau'' = \rho\, g\, h''\, S \tag{B.31}$$

$$u_* = (g\, h\, S)^{0.5} \quad \text{and} \quad u_*' = (g\, h'\, S)^{0.5} \tag{B.32}$$

with

$$h = h' + h'' \tag{B.33}$$

hence:

$$\left(\frac{u_*'}{u_*}\right)^2 = \frac{h'}{h} \tag{B.34}$$

expressing the shear velocity in terms of the mobility parameter θ equation B.34 becomes:

$$\frac{\theta'}{\theta} = \frac{h'}{h} \tag{B.35}$$

It was found for the lower regime that:

$$\theta' = 0.06 - 0.4\ \theta^2 \tag{B.36}$$

The mean velocity is calculated by:

$$\frac{V}{u_*'} = 6 + 2.5 \ln\left(\frac{h'}{2\ d_{50}}\right) \tag{B.37}$$

combining the equations described above, the Chézy coefficient can be expressed as:

$$C = g^{0.5} \left(\frac{h'}{h}\right)^{0.5} \left[6 + 2.5 \ln\left(\frac{h'}{2.5\ d_{50}}\right) \right] \tag{B.38}$$

where:

h = $h' + h''$ = water depth (m)
τ = $\tau' + \tau''$ = effective shear stress (N/m^2)
g = gravity acceleration (m/s^2)
u_* = shear velocity (m/s)
θ = dimensionless mobility parameter
ρ = density (Kg/m^3)
V = mean velocity (m/s)
s = relative density
C = Chézy coefficient
S = bottom slope

Calculation of the friction factor according to all methods

The friction factor prediction according to all methods is calculated step by step from certain variables given by the flow condition and sediment characteristics. These variables are:

ν = kinematic viscosity (m^2/s)
h = water depth

S_0 = bottom slope
d_{35} = representative particle diameter (m)
d_{50} = representative particle diameter (m)
d_{90} = representative particle size
σ_s = geometric standard deviation
s = relative density

The computation for each friction factor method is carried out as follows:
van Rijn method:
compute the:
- dimensionless grain parameter D_* (eq. 4.2);
- critical mobility parameter θ_{cr} (equations 2.18 to 2.20);
- critical bed shear velocity u_{*cr} and critical shear stress τ_{cr} (eq. 2.14) ;
- Chézy coefficient related to the grains(C') by using $C' = 18 \log (12h/3d_{90})$;
- assume a mean velocity $V = V_1$;
- shear velocity u_* (eq. 2.16);
- effective bed shear velocity u_*' (eq. B.39);

$$u_*' = \frac{g^{0.5}\, V}{C'} \qquad \text{(B.39)}$$

- excess bed shear parameter T (eq. B.40);

$$T = \frac{(u_*')^2 - (u_{*,cr})^2}{(u_{*,cr})^2} \qquad \text{(B.40)}$$

determine the:
- bed form type (table 4.3);
- length and height of the bed form (equations B.9 and B.10 or B.12 and B.13);

compute the:
- equivalent height related to the grains k_s' (eq. B.4) and related to the bed form k_s'' (eq. B.5 or eq. B.6);
- total equivalent height k_s (eq. B.3);
- Chézy coefficient C (equations B.16, B.17 or B.18).
- mean velocity $V = V_2 = C\,(h\,S_0)^{0.5}$

compare V_1 and V_2. Repeat the procedure till V_1 and V_2 are sufficiently accurate

Brownlie method:
compute the:
- dimensionless unit discharge q_* (eq. B.21);
- unit discharge q (eq. B.20);

- Chézy coefficient (eq. B.22).

White, Paris and Bettess method:
compute the:
- dimensionless grain parameter D_* (eq. B.23);
- shear velocity u_* (eq. 2.16);
- n and A factor (equations B.27 and B.28);
- dimensionless particle mobility parameter F_{fg} (eq. B.24);
- dimensionless particle mobility parameter related to the effective shear stress F_{gr} (eq. B.25);
- mean velocity V (eq. B.26);
- Chézy coefficient (eq. B.29).

Engelund and Hansen method:
compute the:
- dimensionless grain parameter D_* (eq. 2.17);
- overall bed shear velocity u_* and the dimensionless mobility parameter θ (eq. 2.16);
- θ' (eq. B.36);
- h' and u_*' (eq. B.35 and B.34);
- mean velocity V (eq. B.37);
- Chézy coefficient (eq. B.38).

APPENDIX C: DATA COLLECTED ON SINGLE AND COMPOSITE ROUGHNESS AT THE HYDRAULICS LABORATORY OF WAGENINGEN AGRICULTURAL UNIVERSITY

Table C.1 Single roughness : smooth side slope - smooth bottom (case 1)

Test No	Q lps	m (-)	B m	h m	Area m^2	P m	R m	V m/s	So 10^{-3}	Sf 10^{-3}	C $m^{1/2}/s$	Froude (-)	u_* m/s	3.3v/u_* m	k_s+3.3v/u m	k_{s1} m	$k_{s1}u_*/v$ (-)	k_{s2} m	k_s m	k_su_*/v (-)
1	14.0	1.53	0.25	0.0881	0.034	0.572	0.059	0.413	1.188	0.653	66.4	0.29	0.020	0.0002	0.0001	(*)	0.0	0.0001	(*)	(*)
2	15.9	1.53	0.25	0.0936	0.037	0.592	0.062	0.432	1.188	0.833	60.0	0.31	0.023	0.0002	0.0003	0.0002	4.0	0.0003	0.0002	4.0
3	17.7	1.53	0.25	0.0959	0.038	0.601	0.063	0.465	1.188	0.986	58.9	0.35	0.025	0.0001	0.0004	0.0003	6.2	0.0004	0.0003	6.2
4	20.2	1.53	0.25	0.1025	0.042	0.625	0.067	0.484	1.188	0.925	61.7	0.36	0.025	0.0001	0.0003	0.0002	3.7	0.0003	0.0002	3.7
5	22.1	1.53	0.25	0.1042	0.043	0.631	0.068	0.518	1.188	1.030	62.1	0.40	0.026	0.0001	0.0003	0.0002	3.8	0.0003	0.0002	3.8
6	23.7	1.53	0.25	0.1090	0.045	0.648	0.070	0.522	1.188	0.992	62.6	0.40	0.026	0.0001	0.0003	0.0001	3.6	0.0003	0.0001	3.6
7	25.7	1.53	0.25	0.1113	0.047	0.657	0.071	0.549	1.188	1.151	60.7	0.43	0.028	0.0001	0.0004	0.0002	6.4	0.0004	0.0002	6.4
8	27.2	1.53	0.25	0.1149	0.049	0.670	0.073	0.556	1.188	1.098	62.1	0.43	0.028	0.0001	0.0003	0.0002	4.9	0.0003	0.0002	4.9
9	29.3	1.53	0.25	0.1168	0.050	0.677	0.074	0.585	1.188	1.194	62.3	0.47	0.029	0.0001	0.0003	0.0002	5.3	0.0003	0.0002	5.3
10	31.4	1.53	0.25	0.1217	0.053	0.695	0.076	0.591	1.188	1.181	62.3	0.47	0.030	0.0001	0.0003	0.0002	5.6	0.0003	0.0002	5.6
11	21.0	1.53	0.25	0.1029	0.042	0.626	0.067	0.501	1.188	0.978	61.9	0.38	0.025	0.0001	0.0003	0.0002	3.7	0.0003	0.0002	3.7
12	26.4	1.53	0.25	0.1696	0.086	0.870	0.099	0.306	1.188	0.252	61.1	0.10	0.016	0.0002	0.0005	0.0003	3.8	0.0005	0.0003	3.8
13	23.8	1.53	0.25	0.1654	0.083	0.855	0.097	0.286	1.188	0.242	58.9	0.09	0.015	0.0002	0.0006	0.0004	5.6	0.0006	0.0004	5.6
14	29.7	1.53	0.25	0.1750	0.091	0.890	0.102	0.328	1.188	0.240	66.4	0.11	0.016	0.0002	0.0003	0.0000	0.4	0.0003	(*)	(*)

(*) Smooth regime

$k_{saver.}$ = 0.0002

$n_{aver.}$ = 0.0101

Table C.2 Single roughness: rough side slope - rough bottom (case 2)

Test No	Q lps	m (-)	B m	h m	Area m^2	P m	R m	V m/s	So 10^{-3}	Sf 10^{-3}	C $m^{1/2}/s$	Froude (-)	u_* m/s	3.3v/u_* m	k_s+3.3v/u m	k_{s1} m	$k_{s1}u_*/v$ (-)	k_{s2} m	k_s m	k_su_*/v (-)
1	9.7	1.59	0.25	0.1340	0.062	0.753	0.082	0.156	2.138	0.314	30.8	0.030	0.016	0.0002	0.0193	0.0191	298.5	0.0193	0.0193	301.8
2	12.5	1.59	0.25	0.1488	0.067	0.809	0.083	0.186	2.138	0.404	32.1	0.042	0.018	0.0002	0.0165	0.0163	290.9	0.0165	0.0165	294.2
3	14.5	1.59	0.25	0.1521	0.070	0.821	0.085	0.208	2.138	0.502	31.8	0.052	0.020	0.0002	0.0175	0.0173	347.5	0.0175	0.0175	350.8
4	16.3	1.59	0.25	0.1551	0.072	0.833	0.086	0.227	2.138	0.586	31.9	0.061	0.022	0.0002	0.0175	0.0174	379.8	0.0175	0.0175	383.1
5	17.9	1.59	0.25	0.1580	0.074	0.844	0.088	0.240	2.138	0.642	31.9	0.067	0.024	0.0001	0.0178	0.0177	408.5	0.0178	0.0178	411.8
6	19.7	1.59	0.25	0.1627	0.078	0.861	0.091	0.252	2.138	0.696	31.7	0.071	0.025	0.0001	0.0188	0.0187	455.7	0.0188	0.0188	459.0
7	21.3	1.59	0.25	0.1656	0.080	0.872	0.092	0.265	2.138	0.751	31.8	0.077	0.026	0.0001	0.0189	0.0188	480.8	0.0189	0.0189	484.1
8	23.3	1.59	0.25	0.1689	0.083	0.884	0.093	0.282	2.138	0.818	32.3	0.087	0.027	0.0001	0.0181	0.0180	482.2	0.0181	0.0181	485.5
9	11.1	1.59	0.25	0.1454	0.066	0.796	0.082	0.169	2.138	0.359	31.1	0.035	0.017	0.0002	0.0185	0.0183	305.3	0.0185	0.0185	308.6
10	7.9	1.59	0.25	0.1378	0.060	0.768	0.078	0.132	2.138	0.227	31.3	0.023	0.013	0.0003	0.0172	0.0169	218.9	0.0172	0.0172	222.2
11	15.8	1.59	0.25	0.1251	0.054	0.720	0.076	0.290	2.138	1.298	29.3	0.113	0.031	0.0001	0.0215	0.0214	651.3	0.0215	0.0215	654.6
12	19.8	1.59	0.25	0.1325	0.059	0.748	0.079	0.335	2.138	1.559	30.1	0.144	0.035	0.0001	0.0201	0.0200	683.7	0.0201	0.0201	687.0
13	25.5	1.59	0.25	0.1423	0.067	0.785	0.085	0.380	2.138	1.842	30.3	0.172	0.039	0.0001	0.0213	0.0212	816.3	0.0213	0.0213	819.6
14	17.9	1.58	0.24	0.1375	0.063	0.754	0.083	0.285	1.163	1.025	30.8	0.099	0.029	0.0001	0.0195	0.0193	527.9	0.0195	0.0195	531.2
15	21.2	1.58	0.24	0.1471	0.066	0.790	0.084	0.320	1.163	1.196	32.0	0.125	0.031	0.0001	0.0168	0.0167	494.6	0.0168	0.0168	497.9
16	24.0	1.58	0.24	0.1514	0.071	0.806	0.088	0.337	1.163	1.330	31.1	0.131	0.034	0.0001	0.0198	0.0197	630.9	0.0198	0.0198	634.2
17	26.2	1.58	0.24	0.1550	0.075	0.820	0.092	0.349	1.163	1.416	30.6	0.135	0.036	0.0001	0.0218	0.0217	731.9	0.0218	0.0218	735.2
18	28.4	1.58	0.24	0.1679	0.082	0.868	0.095	0.345	1.163	1.230	32.0	0.128	0.034	0.0001	0.0190	0.0189	602.2	0.0190	0.0190	605.5
19	30.1	1.58	0.24	0.1706	0.085	0.878	0.097	0.353	1.163	1.274	31.7	0.131	0.035	0.0001	0.0202	0.0201	659.4	0.0202	0.0202	662.7
20	32.9	1.58	0.24	0.1747	0.089	0.893	0.100	0.369	1.163	1.372	31.6	0.140	0.037	0.0001	0.0210	0.0209	723.2	0.0210	0.0210	726.5
21	34.1	1.58	0.24	0.1851	0.095	0.932	0.102	0.359	1.163	1.252	31.8	0.129	0.035	0.0001	0.0211	0.0210	699.9	0.0211	0.0211	703.2
22	8.1	1.58	0.24	0.0872	0.032	0.566	0.057	0.253	1.163	1.196	30.7	0.115	0.026	0.0001	0.0134	0.0133	323.3	0.0134	0.0134	326.6
23	11.4	1.58	0.24	0.0866	0.035	0.564	0.062	0.328	1.163	2.363	27.2	0.179	0.038	0.0001	0.0227	0.0226	805.3	0.0227	0.0227	808.6
24	12.7	1.58	0.24	0.0998	0.040	0.613	0.066	0.315	1.163	1.913	28.0	0.153	0.035	0.0001	0.0219	0.0218	721.3	0.0219	0.0219	724.6
25	14.3	1.58	0.24	0.1084	0.045	0.645	0.070	0.318	1.163	1.775	28.6	0.148	0.035	0.0001	0.0214	0.0213	701.2	0.0214	0.0214	704.5
26	15.6	1.58	0.24	0.1120	0.047	0.659	0.072	0.329	1.163	1.814	28.9	0.154	0.036	0.0001	0.0215	0.0214	722.8	0.0215	0.0215	726.1

$k_{saver.}$ = 0.0194

$n_{saver.}$ = 0.0215

Table C.3 Composite roughness : smooth side slope - rough bottom (Case 3)

Test No	Q lps	m (-)	B m	h m	Area m^2	P m	R m	V m/s	So 10^{-3}	Sf 10^{-3}	C $m^{1/2}/s$	Froude (-)	u_* m/s	$3.3v/u_*$ m	$k_s+3.3v/u_*$ m	k_{s1} m	$k_{s1}u_*/v$ (-)	k_{s2} m	k_s m	k_su_*/v (-)
1	16.0	1.53	0.27	0.1052	0.045	0.655	0.069	0.353	1.150	0.741	49.3	0.183	0.022	0.0002	0.0015	0.0014	30.1	0.0015	0.00137	30.1
2	18.2	1.53	0.27	0.1122	0.047	0.680	0.070	0.383	1.150	0.862	49.4	0.214	0.024	0.0001	0.0015	0.0014	32.7	0.0015	0.00137	32.7
3	19.8	1.53	0.27	0.1162	0.050	0.695	0.072	0.394	1.150	0.805	51.6	0.218	0.024	0.0001	0.0012	0.0010	24.4	0.0012	0.00104	24.4
4	22.3	1.53	0.27	0.1198	0.053	0.708	0.074	0.423	1.150	0.893	52.0	0.246	0.026	0.0001	0.0012	0.0010	25.7	0.0012	0.00103	25.7
5	25.0	1.53	0.27	0.1247	0.056	0.726	0.078	0.444	1.150	0.889	53.5	0.259	0.026	0.0001	0.0010	0.0009	22.1	0.0010	0.00087	22.1
6	26.6	1.53	0.27	0.1271	0.058	0.735	0.079	0.461	1.150	0.978	52.6	0.276	0.027	0.0001	0.0011	0.0010	27.2	0.0011	0.00101	27.2
7	28.7	1.53	0.27	0.1295	0.059	0.743	0.080	0.482	1.150	0.992	54.1	0.296	0.028	0.0001	0.0009	0.0008	22.5	0.0009	0.00082	22.5
8	11.5	1.53	0.27	0.0658	0.027	0.511	0.053	0.427	1.150	1.896	42.7	0.352	0.031	0.0001	0.0027	0.0026	79.2	0.0027	0.00269	82.5
9	21.3	1.53	0.27	0.1382	0.063	0.775	0.082	0.336	1.150	0.467	54.4	0.141	0.019	0.0002	0.0009	0.0008	14.4	0.0009	0.00076	14.4
10	23.0	1.53	0.27	0.1407	0.066	0.784	0.084	0.351	1.150	0.497	54.4	0.150	0.020	0.0002	0.0009	0.0008	15.4	0.0009	0.00078	15.4
11	25.4	1.53	0.27	0.1453	0.068	0.801	0.085	0.371	1.150	0.557	53.8	0.165	0.022	0.0002	0.0011	0.0009	18.9	0.0011	0.00089	18.9
12	27.3	1.53	0.27	0.1479	0.071	0.811	0.087	0.385	1.150	0.597	53.4	0.173	0.023	0.0001	0.0011	0.0010	21.8	0.0011	0.00098	21.8
13	29.3	1.53	0.27	0.1509	0.073	0.822	0.089	0.402	1.150	0.624	54.1	0.186	0.023	0.0001	0.0010	0.0009	20.6	0.0010	0.00090	20.6
14	31.2	1.53	0.27	0.1533	0.075	0.830	0.090	0.418	1.150	0.702	52.7	0.199	0.025	0.0001	0.0013	0.0011	27.8	0.0013	0.00114	27.8
15	32.9	1.53	0.27	0.1559	0.076	0.840	0.091	0.430	1.150	0.706	53.7	0.207	0.025	0.0001	0.0011	0.0010	24.8	0.0011	0.00101	24.8
16	34.9	1.53	0.27	0.1586	0.078	0.850	0.092	0.445	1.150	0.701	55.4	0.219	0.025	0.0001	0.0009	0.0008	19.7	0.0009	0.00080	19.7
17	36.9	1.53	0.27	0.1617	0.081	0.861	0.094	0.457	1.150	0.735	55.0	0.227	0.026	0.0001	0.0010	0.0009	21.9	0.0010	0.00086	21.9
18	38.1	1.53	0.27	0.1627	0.083	0.865	0.095	0.462	1.150	0.749	54.6	0.228	0.026	0.0001	0.0011	0.0009	24.2	0.0011	0.00093	24.2

Table C.4 Composite roughness : rough side slope - smooth bottom (Case 4)

Test No	Q lps	m (-)	B m	h m	Area m^2	P m	R m	V m/s	So 10^{-3}	Sf 10^{-3}	C $m^{1/2}/s$	Froude (-)	u_* m/s	3.3v/u_* m	k_s+3.3v/u m	k_{s1} m	$k_{s1}u_*/v$ (-)	k_{s2} m	k_s m	k_su_*/v (-)
1	19.6	1.56	0.21	0.1674	0.079	0.830	0.095	0.249	1.100	0.347	43.3	0.066	0.018	0.0002	0.0045	0.0043	72.7	0.0045	0.0045	76.0
2	14.7	1.56	0.21	0.1396	0.059	0.727	0.081	0.251	1.100	0.447	41.8	0.080	0.019	0.0002	0.0046	0.0044	78.0	0.0046	0.0046	81.3
3	17.9	1.56	0.21	0.1465	0.063	0.753	0.083	0.286	1.100	0.577	41.2	0.100	0.022	0.0002	0.0051	0.0049	101.3	0.0051	0.0051	104.6
4	22.8	1.56	0.21	0.1568	0.069	0.791	0.088	0.328	1.100	0.763	40.1	0.125	0.026	0.0001	0.0062	0.0061	147.8	0.0062	0.0062	151.1
5	11.2	1.56	0.21	0.0986	0.036	0.575	0.062	0.314	0.775	1.099	38.0	0.161	0.026	0.0001	0.0058	0.0057	138.1	0.0058	0.0058	141.4
6	13.9	1.56	0.21	0.0993	0.037	0.578	0.064	0.379	0.775	1.104	45.2	0.230	0.026	0.0001	0.0023	0.0022	54.6	0.0023	0.0022	54.6
7	15.9	1.56	0.21	0.0996	0.037	0.579	0.064	0.431	0.775	1.098	51.6	0.298	0.026	0.0001	0.0010	0.0009	22.4	0.0010	0.0009	22.4
8	17.7	1.56	0.21	0.1006	0.037	0.583	0.064	0.473	0.775	1.120	55.9	0.356	0.027	0.0001	0.0006	0.0005	11.9	0.0006	0.0005	11.9
9	19.2	1.56	0.21	0.1176	0.047	0.646	0.073	0.405	0.775	1.685	36.5	0.228	0.035	0.0001	0.0083	0.0082	269.7	0.0083	0.0083	273.0
10	19.2	1.56	0.21	0.1458	0.062	0.750	0.083	0.307	0.775	0.798	37.7	0.115	0.026	0.0001	0.0081	0.0079	190.9	0.0081	0.0081	194.2
11	21.3	1.56	0.21	0.1496	0.066	0.764	0.086	0.324	0.775	0.876	37.4	0.125	0.027	0.0001	0.0086	0.0085	217.2	0.0086	0.0086	220.5
12	23.9	1.56	0.21	0.1762	0.083	0.863	0.096	0.287	0.775	0.578	38.5	0.087	0.023	0.0001	0.0085	0.0083	183.2	0.0085	0.0085	186.5
13	26.6	1.56	0.21	0.1806	0.086	0.879	0.098	0.308	0.775	0.649	38.5	0.098	0.025	0.0001	0.0085	0.0084	197.5	0.0085	0.0085	200.8
14	17.2	1.56	0.21	0.1649	0.075	0.821	0.091	0.229	0.775	0.336	41.5	0.059	0.017	0.0002	0.0055	0.0053	85.9	0.0055	0.0055	89.2
15	10.1	1.56	0.21	0.1598	0.073	0.802	0.091	0.138	0.800	0.125	40.7	0.021	0.011	0.0003	0.0060	0.0057	59.2	0.0060	0.0057	59.2
16	13.1	1.56	0.21	0.1146	0.044	0.635	0.070	0.296	0.800	0.844	38.6	0.128	0.024	0.0001	0.0060	0.0059	138.9	0.0060	0.0060	142.2
17	16.5	1.56	0.21	0.1223	0.049	0.663	0.073	0.339	0.800	1.049	38.7	0.160	0.027	0.0001	0.0063	0.0061	165.6	0.0063	0.0063	168.9
18	13.6	1.56	0.21	0.1300	0.052	0.692	0.076	0.260	0.800	0.409	46.8	0.091	0.017	0.0002	0.0023	0.0021	35.3	0.0023	0.0021	35.3
19	16.4	1.56	0.21	0.1434	0.061	0.741	0.083	0.268	0.800	0.604	37.9	0.089	0.022	0.0002	0.0077	0.0076	164.1	0.0077	0.0077	167.4
20	17.3	1.56	0.21	0.1452	0.061	0.748	0.082	0.282	0.800	0.639	39.0	0.099	0.023	0.0001	0.0067	0.0065	145.1	0.0067	0.0067	148.4
21	18.9	1.56	0.21	0.1482	0.064	0.759	0.084	0.295	0.800	0.720	37.9	0.105	0.024	0.0001	0.0080	0.0078	187.7	0.0080	0.0080	191.0
22	21.8	1.56	0.21	0.1528	0.068	0.776	0.087	0.322	0.800	0.822	38.0	0.121	0.027	0.0001	0.0081	0.0080	208.4	0.0081	0.0081	211.7
23	23.6	1.56	0.21	0.1565	0.070	0.790	0.089	0.335	0.800	0.889	37.7	0.129	0.028	0.0001	0.0086	0.0085	232.3	0.0086	0.0086	235.6
24	30.1	1.56	0.21	0.1958	0.099	0.936	0.106	0.303	0.800	0.592	38.2	0.088	0.025	0.0001	0.0096	0.0095	230.8	0.0096	0.0096	234.1
25	28.3	1.56	0.21	0.1932	0.079	0.926	0.085	0.360	0.800	0.579	51.4	0.156	0.022	0.0002	0.0014	0.0013	27.0	0.0014	0.0013	27.0
26	26.5	1.56	0.21	0.1905	0.095	0.916	0.104	0.278	0.800	0.508	38.2	0.076	0.023	0.0001	0.0094	0.0092	206.4	0.0094	0.0094	209.7
27	24.5	1.56	0.21	0.1874	0.093	0.905	0.102	0.264	0.800	0.471	38.1	0.070	0.022	0.0002	0.0094	0.0093	197.6	0.0094	0.0094	200.9
28	23.0	1.56	0.21	0.1849	0.091	0.895	0.101	0.254	0.800	0.434	38.2	0.065	0.021	0.0002	0.0091	0.0090	182.3	0.0091	0.0091	185.6
29	21.2	1.56	0.21	0.1816	0.088	0.883	0.100	0.240	0.800	0.373	39.3	0.059	0.019	0.0002	0.0078	0.0077	143.7	0.0078	0.0078	147.0
30	19.7	1.56	0.21	0.1791	0.086	0.874	0.098	0.229	0.800	0.347	39.1	0.054	0.018	0.0002	0.0079	0.0077	138.6	0.0079	0.0079	141.9
31	18.4	1.56	0.21	0.1767	0.084	0.865	0.097	0.218	0.800	0.322	39.0	0.050	0.018	0.0002	0.0080	0.0078	134.2	0.0080	0.0080	137.5
32	16.1	1.56	0.21	0.1725	0.081	0.849	0.095	0.199	0.800	0.258	40.0	0.042	0.016	0.0002	0.0069	0.0067	101.6	0.0069	0.0069	104.9
33	14.1	1.56	0.21	0.1682	0.077	0.833	0.093	0.182	0.800	0.219	40.5	0.037	0.014	0.0002	0.0062	0.0060	83.1	0.0062	0.0062	86.4

APPENDIX D: DEPTH AVERAGED VELOCITY DISTRIBUTION IN THE CROSS SECTION OF A TRAPEZOIDAL CANAL

The distribution of the velocity in the whole cross section for an open, trapezoidal canal can be estimated by using the 2-D equation of motion expressed in the x- and y-direction. That equation can be described by:

$$\frac{\partial u}{\partial t} + u\frac{\partial u}{\partial t} + v\frac{\partial u}{\partial y} + g\frac{\partial}{\partial x}(h + z) + \frac{1}{\rho\, h}\,\tau_{bx} - \frac{1}{\rho\, h}\left(\frac{\partial}{\partial x}(h\,\tau_{xx}) + \frac{\partial}{\partial y}(h\,\tau_{xy})\right) = 0 \qquad \text{(D.1)}$$

The effective shear stress at the interface between two stream tubes affects the velocity distribution in y-direction. The effective shear stress τ_{xy} in the x-direction perpendicular to the y-direction can be expressed as (Ogink, 1985):

$$\tau_{xy} = \rho\, \nu_t \left(\frac{\partial u}{\partial y} + \frac{\partial v}{\partial x}\right) \qquad \text{(D.2)}$$

The solution of the 2-D equation of motion (eq. D.1) requires an estimate of the effective viscosity coefficient ν_t. This coefficient describes the transfer of momentum in a horizontal direction from one stream tube to another. The coefficient contains the contribution of viscous, turbulence and dispersive effects (Ogink, 1985). Vreugdenhil (1982) mentioned that the effect of the effective viscosity on the two dimensional, depth averaged flow is not well known, but that it is proportional to:

$$\nu_t \sim \Delta y^2 \left| \frac{\partial u}{\partial y} \right| \qquad \text{(D.3)}$$

For simplicity, an averaged value of the effective viscosity ν_t for the total width of the canal will be assumed. For a steady-uniform flow with only velocity in the x-direction, equation D.1 becomes:

$$g\frac{\partial}{\partial x}(h + z) + \frac{1}{\rho\, h}\,\tau_b - \frac{1}{\rho\, h}\left(\frac{\partial}{\partial y}(h\,\tau_{xy})\right) = 0 \qquad \text{(D.4)}$$

replacing equation D.2 in D.4 and rearranging gives:

$$\rho\, h\, g\, \frac{\partial}{\partial x}(h + z) + \tau_b - \frac{\partial}{\partial y}\left(h\,\rho\,\nu_t\,\frac{\partial u}{\partial y}\right) = 0 \qquad \text{(D.5)}$$

doing:

$$\frac{\partial(h + z)}{\partial x} = - S_0 \qquad (D.6)$$

results in:

$$\tau_b = \frac{\partial}{\partial y} (h \rho \nu_t \frac{\partial u}{\partial y}) + \rho g h S_0 \qquad (D.7)$$

using the Chézy formula:

$$Q = C A \sqrt{R S_0} \quad \therefore \quad S_0 = \frac{Q^2}{A^2 C^2 R} \qquad (D.8)$$

the bottom shear stress over the total cross section can be expressed by:

$$\tau_b = \frac{\rho g Q^2}{A^2 C^2} \qquad (D.9)$$

Replacing in equation D.5 and rearranging the terms gives:

$$\nu_t \frac{\partial}{\partial y}(h \frac{\partial u}{\partial y}) = (1 - \frac{h}{R}) \frac{g Q^2}{A^2 C^2} \qquad (D.10)$$

where:

u, v	= depth averaged velocity in x- and y-direction (m/s)
x, y	= length co-ordinates (m)
z	= bottom level (m)
t	= time co-ordinate (s)
h	= water depth (m)
g	= acceleration due to gravity (m/s^2)
ρ	= water density (kg/m^3)
τ_{bx}, τ_{by}	= bottom shear stress in x- and y-direction respectively (N/m^2)
τ_{xy}, τ_{xx}	= effective shear stress (N/m^2)
ν_t	= effective viscosity coefficient (m^2/s)
Q	= discharge (m^3/s)
A	= area of cross section (m^2)
C	= Chézy coefficient ($m^{1/2}/s$)
R	= hydraulic radius (m)
S_0	= bottom slope
Δy	= distance between streamtubes (m)

Numerically equation D.10 can be solved by using the finite difference method, by which the equation can be transformed to:

$$\frac{\partial}{\partial y}(h\,\frac{\partial u}{\partial y}) = \frac{\partial u}{\partial y}\frac{\partial h}{\partial y} + h\frac{\partial^2 u}{\partial y^2} \qquad (D.11)$$

$$\frac{\partial u}{\partial y} = \frac{u_{n+1} - u_{n-1}}{2\,\Delta y} \qquad (D.12)$$

$$\frac{\partial h}{\partial y} = \frac{h_{n+1} - h_{n-1}}{2\,\Delta y} \qquad (D.13)$$

$$\frac{\partial u}{\partial y}\,\frac{\partial h}{\partial y} = \frac{(u_{n+1} - u_{n-1})\,(h_{n+1} - h_{n-1})}{4\,\Delta y^2} \qquad (D.14)$$

$$\frac{\partial^2 u}{\partial y^2} = \frac{u_{n+1} - 2\,u_n + u_{n-1}}{\Delta\, y^2} \qquad (D.15)$$

$$\frac{\partial}{\partial y}(h\,\frac{\partial u}{\partial y}) = \frac{(h_{n-1} + 4\,h_n - h_{n+1})\,u_{n-1} - 8\,h_n\,u_n + (-\,h_{n-1} + 4\,h_n + h_{n+1})\,u_{n+1}}{4\,\Delta y^2} \qquad (D.16)$$

replacing in equation D.10 gives:

$$\frac{\nu_t\,(h_{n-1} + 4\,h_n - h_{n+1})\,u_{n-1} - 8\,h_n\,u_n + (-\,h_{n-1} + 4\,h_n + h_{n+1})\,u_{n+1}}{4\,\Delta y^2} = (1 - \frac{h_n}{R})\,\frac{g\,Q^2}{A^2\,C^2} \qquad (D.17)$$

$$(h_{n-1} + 4\,h_n - h_{n+1})\,u_{n-1} - 8\,h_n\,u_n + (-\,h_{n-1} + 4\,h_n + h_{n+1})\,u_{n+1} = \frac{4\,g}{\nu_t}\,(1 - \frac{h_n}{R})\,(\frac{Q\,\Delta y}{A\,C})^2 \qquad (D.18)$$

equation D.18 can be written as:

$$A_n\,u_{n-1} + B_n\,u_n + C_n\,u_{n+1} = D_n \qquad (D.19)$$

with:

$$A_n = h_{n-1} + 4\,h_n - h_{n+1} \qquad (D.20)$$

$$B_n = -8\ h_n \qquad \text{(D.21)}$$

$$C_n = -h_{n-1} + 4\ h_n + h_{n+1} \qquad \text{(D.22)}$$

$$D_n = \frac{4\ g}{\nu_t}\left(1 - \frac{h_n}{R}\right)\left(\frac{Q\ \Delta y}{A\ C}\right)^2 \qquad \text{(D.23)}$$

equation D.19 is solved by applying two boundary conditions, namely:

$$u_{n=0} = 0 \quad ; \quad u_{n=n} = 0 \qquad \text{(D.24)}$$

For a given trapezoidal cross section (fig. D.1) in a canal with bottom slope S_0, bottom width B and roughness coefficient C, the velocity distribution can be determined by solving numerically equation D.10. Different values of ν_t can be used to solve the equation, giving not only different velocity distributions but also different magnitudes. The calibration of the numerical solution is effected by adjusting the effective viscosity to the following condition:

$$0.99 \le \frac{\sum q_{st}\ \Delta y}{Q} \le 1.01 \qquad \text{(D.25)}$$

where

q_{st} = discharge of each stream tube per unit width (m^3/ms)
Q = discharge given by the Chézy formula in equation D.8 (m^3/s)
Δy = stream tube width (m)

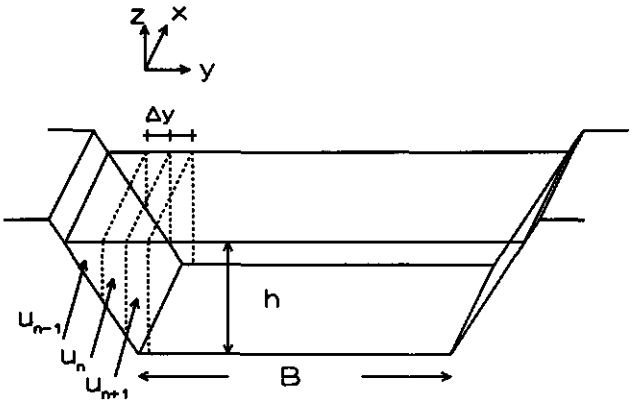

Figure D.1 Schematization of the velocity distribution in the width direction of a trapezoidal cross section

APPENDIX E: DETERMINATION OF THE EXPONENT N IN THE SEDIMENT TRANSPORT PREDICTORS

The sediment transport predictors can be schematized by using a simple relation between q_s and V in the following way:

$$q_s = M\ V^N \tag{E.1}$$

where:

q_s = sediment transport per unit width
V = mean velocity
M, N = parameters depending on water flow and sediment characteristics.

Derivation of the exponent N can be done by:

$$\frac{dq_s}{dV} = M\ N\ V^{N-1} \tag{E.2}$$

and therefore,

$$N = \frac{V}{q_s}\ \frac{dq_s}{dV} \tag{E.3}$$

In this appendix the exponent N will be determined for the following sediment transport predictors: Ackers-White, Brownlie and Engelund-Hansen.

Ackers-White sediment transport predictor: the Ackers-White function to determine the total sediment transport reads as:

$$q_s = G_{gr}\ s\ d\ (\frac{V}{u_*})^n \tag{E.4}$$

with:

$$G_{gr} = c\ (\frac{F_{gr}}{A} - 1)^m \tag{E.5}$$

and:

$$F_{gr} = \frac{u_*^n}{\sqrt{g\ d\ (s-1)}} \left[\frac{V}{\sqrt{32}\ \log\ (\frac{10\ h}{d})} \right]^{1-n} \tag{E.6}$$

$$n = 1.00 - 0.56\ \log\ D_* \tag{E.7}$$

$$A = \frac{0.23}{\sqrt{D_*}} + 0.14 \tag{E.8}$$

$$m = \frac{9.66}{D_*} + 1.334 \tag{E.9}$$

$$\log\ c = 2.86\ \log\ D_* - (\log\ D_*)^2 - 3.53 \tag{E.10}$$

$$D_* = \left[\frac{(s-1)\ g}{\nu^2} \right]^{1/3} d \tag{E.11}$$

and

$$\frac{u_*}{V} = \frac{\sqrt{g}}{C} \tag{E.12}$$

where:

G_{gr} = dimensionless sediment transport parameter;
F_{gr} = dimensionless mobility parameter;
A = value of F_{gr} at the nominal initial movement
c = coefficient in the sediment transport parameter G_{gr}
h = water depth (m)
d = sediment diameter (m)
m, n = exponents in the sediment transport parameter
s = relative density
u_* = shear velocity (m/s)
V = mean velocity (m/s)
q_s = total sediment transport (m^2/s)
C = Chézy coefficient
g = gravity acceleration (m/s^2)

The exponent N is calculated by writing equations E.4 to E.6 in a simple way as:

$$q_s = K' G_{gr} V \tag{E.13}$$

$$G_{gr} = K'' (F_{gr} - A)^m \tag{E.14}$$

and

$$F_{gr} = K''' V \tag{E.15}$$

where K', K'' and K''' are auxiliary variables which contain the rest of independent variables in equations E.4, E.5 and E.6.

Therefore,

$$\frac{dq_s}{dV} = K' K'' [(K''' V - A)^m + K''' V m (k''' V - A)^{m-1}] \tag{E.16}$$

$$\frac{dq_s}{dV} = K' G_{gr} (1 + \frac{m F_{gr}}{F_{gr} - A}) \tag{E.17}$$

replacing in equation E.3:

$$N = K' G_{gr} (1 + \frac{m F_{gr}}{F_{gr} - A}) \frac{V}{K' G_{gr} V} \tag{E.18}$$

results:

$$N = 1 + \frac{m F_{gr}}{F_{gr} - A} \tag{E.19}$$

Brownlie sediment transport predictor (1981): Brownlie (1981) defined a method to compute the sediment transport, which can be expressed as:

$$q_s = \frac{727.6 c_f V h}{s} (F_g - F_{g_{cr}})^{1.978} S^{0.6601} (1000 \frac{h}{d_{50}})^{-0.3301} \tag{E.20}$$

with:

$$F_g = \frac{V}{[(s - 1)\ g\ d_{50}]^{0.5}} \tag{E.21}$$

$$F_{g_{cr}} = 4.596\ \tau_{*_o}^{0.5293}\ S^{-0.1405}\ \sigma_s^{-0.1696} \tag{E.22}$$

$$\tau_{*_o} = 0.22\ Y + 0.06\ (10)^{-7.7\ Y} \tag{E.23}$$

$$Y = (\sqrt{s - 1}\ R_g)^{-0.6} \tag{E.24}$$

$$R_g = \frac{(g\ d_{50}^3)^{0.5}}{31620\ \nu} \tag{E.25}$$

where:

c_f = coefficient for the transport rate ($c_f = 1$ for laboratory conditions and $c_f = 1.268$ for field conditions)
F_g = grain Froude number
F_{gcr} = critical grai n Froude number
τ_{*o} = critical dimensionless shear stress
σ_s = geometric standard deviation
S = bottom slope
d_{50} = median diameter (mm)
s = relative density
R_g = grain Reynolds number
h = water depth (m)
V = mean velocity (m/s)
ν = kinematic viscosity (m^2/s)
q_s = total sediment transport (m^2/s)
g = gravity acceleration (m/s^2)

The exponent N for the Brownlie sediment transport predictor is calculated by writing equations E.19 and E.20 in a simple way as:

$$q_s = K_1\ (F_g - F_{g_{cr}})^{1.978}\ V \tag{E.26}$$

$$F_g = K_2 V \tag{E.27}$$

where K_1 and K_2 are auxiliry variables which contain the independent variables of equations E.20 and E.21.

Therefore,

$$\frac{dq_s}{dV} = K_1 [1.978 K_2 V (K_2 V - F_{g_{cr}})^{0.978} + (K_2 V - F_{g_{cr}})^{1.978}] \tag{E.28}$$

replacing in equation E.3:

$$N = \frac{K_1 [1.978 K_2 V (K_2 V - F_{g_{cr}})^{0.978} + (K_2 V - F_{g_{cr}})^{1.978}] V}{K_1 (K_2 V - F_{g_{cr}})^{1.978} V} \tag{E.29}$$

results:

$$N = 1 + \frac{1.978 F_g}{F_g - F_{g_{cr}}} \tag{E.30}$$

Engelund-Hansen sediment transport predictor (1967): the Engelund-Hansen function for the sediment transport is expressed by:

$$q_s = \frac{0.05 V^5}{(s - 1)^2 g^{0.5} d_{50} C^3} \tag{E.31}$$

where:

q_s = total sediment transport (m^2/s)
V = mean velocity (m/s)
C = Chézy coefficient ($m^{1/2}/s$)
s = relative density
d_{50} = mean diameter (m)

Comparing equation E.31 and equation E.1 shows that the exponent N in the Engelund-Hansen predictor has a constant value for a given cross section and is equal to:

$$N = 5 \tag{E.32}$$

LIST OF SYMBOLS

Symbol	Meaning	Unit	Dimension
a	Height of half roughness	(m)	L
A	Cross section area	(m^2)	L^2
B	Channel bottom width	(m)	L
B_s	Water surface width	(m)	L
B_s	Sediment transport width	(m)	L
c	Sediment concentration	(%, ppm by mass)	-
c_a	Reference concentration at level a from the bottom	(%, ppm by mass)	-
c_b	Bed load concentration	(%, ppm by mass)	-
c_e	Equilibrium concentration	(%, ppm by mass)	-
c_0	Concentration at length x = 0	(%, ppm by mass)	-
c_t	Total sediment concentration	(%, ppm by mass)	-
C	Sediment concentration	(%, ppm by mass)	-
C_t	Total sediment concentration	(%, ppm by mass)	-
C_e	Total equilibrium sediment concentration	(%, ppm by mass)	-
C_0	Total sediment concentration at x=0	(%, ppm by mass)	-
C	Chézy coefficient	($m^{1/2}/s$)	$L^{1/2}T^{-1}$
C_e	Effective Chézy coefficient	($m^{1/2}/s$)	$L^{1/2}T^{-1}$
C_e'	Modified effective Chézy coefficient	($m^{1/2}/s$)	$L^{1/2}T^{-1}$
C'	Chézy coefficient due to skin resistance	($m^{1/2}/s$)	$L^{1/2}T^{-1}$
C''	Chézy coefficient due to form resistance	($m^{1/2}/s$)	$L^{1/2}T^{-1}$
C_c	Contraction coefficient	(-)	-
C_d	Discharge coefficient	(-)	-
C_v	Velocity coefficient	(-)	-
C_D	Drag coefficient	(-)	-
d_{50}	Median particle size	(m)	L
d_i	Diameter i-percent finer than d_i	(m)	L
d_i	Representative particle diameter	(m)	L
d_r	Discrepancy ratio		
D	Diameter	(m)	L
D_*	Dimensionless particle parameter	(-)	-
E	Total energy	(Nm/N)	L
E_s	Specific energy	(Nm/N)	L
f	Friction factor of Darcy-Weisbach equation	(-)	-
f	Lacey's silt factor	(-)	-
f(...)	Function of	(-)	-
F	Shape factor	(-)	-
F_g	Grain Froude number	(-)	-

Symbol	Meaning	Unit	Dimension
F_{gr}	Dimensionless mobility parameter	(-)	-
F_{gcr}	Critical grain Froude number	(-)	-
Fr	Froude number	(-)	-
F_g	Weed factor	(-)	-
g	Acceleration due to gravity	(m/s^2)	LT^{-2}
G_{gr}	Dimensionless mobility parameter	(-)	-
h	Water depth	(m)	L
K	error factor		
k_s	Roughness height of Nikuradse	(m)	L
k_s'	Grain roughness height of Nikuradse	(m)	L
k_s''	Bed form roughness height of Nikuradse	(m)	L
k_{se}	effective equivalent roughness	(m)	L
l, L	Length	(m)	L
L_A	Adaptation length	(M)	T
m	Side slope (1 : m)	(-)	-
M	Momentum function		
n	Manning coefficient	($m^{1/6}$)	$L^{1/6}$
n_e	Equivalent Manning coefficient	($m^{1/6}$)	$L^{1/6}$
P	Wetted perimeter	(m)	L
p	Porosity	(-)	-
Q	Flow discharge	(m^3/s)	L^3T^{-1}
q	Flow discharge per unit width	($m^3/s/m$)	L^2T^{-1}
q_b	Bed load transport rate per unit width	($m^3/s/m$)	L^2T^{-1}
q_e	Equilibrium sediment discharge	($m^3/s/m$)	L^2T^{-1}
q_s	Sediment discharge per unit width	($m^3/s/m$)	L^2T^{-1}
q_{st}	Flow discharge in a stream tube	(m^3/s)	L^3T^{-1}
q_{sus}	Suspended load transport per unit width	($m^3/s/m$)	L^2T^{-1}
q_*	Dimensionless unit discharge	(-)	-
Q_s	Total sediment discharge	(m^3/s)	L^3T^{-1}
Q_{so}	Sediment discharge at upstream point	(m^3/s)	L^3T^{-1}
R	Hydraulic radius	(m)	L
Re	Reynolds number	(-)	-
Re_*	Particle Reynolds number	(-)	-
R_g	Grain Reynolds number	(-)	-
Rv	Velocity ratio	(-)	-
s	Relative density	(-)	-
S_f	Friction slope	(-)	-
S_o	Bed slope	(-)	-
s.f.	Shape factor	(-)	-
t	Time coordinate	(s)	T

Symbol	Meaning	Unit	Dimension
T	Excess bed shear stress parameter	(-)	-
T_A	Adaptation time	(S)	T
u,v,w	Component of velocity X, Y and Z directions	(m/s)	LT^{-1}
u_*	Shear velocity	(m/s)	LT^{-1}
u_{*cr}	Critical shear velocity	(m/s)	LT^{-1}
V	Mean velocity	(m/s)	LT^{-1}
V_{cr}	Critical mean velocity	(m/s)	LT^{-1}
w_s	Fall velocity	(m/s)	LT^{-1}
x,y,z	Cartesian coordinates	(m)	L
y_c	Critical depth	(m)	L
y_n	Normal depth	(m)	L
Z	Suspension number	(-)	-
z	Bed elevation above datum	(m)	L
α	Correction factor	(-)	-
β	Momentum correction factor	(-)	-
δ_b	Saltation height	(m)	-
γ	Specific weight	(N/m^3)	FL^{-3}
γ_d	Form factor	(-)	-
γ_r	Ripple presence	(-)	-
Δ	Bed form height	(m)	L
λ	Bed form length	(m)	L
ϵ	Mixing coefficient	(m^2/s)	L^2T^{-1}
η	Eddy viscosity	(kgs/m^2)	FTL^{-2}
σ_s	Geometric standard deviation	(-)	-
ρ	Water density	(kg/m^3)	FT^2L^{-4}
ρ_s	Sediment density	(kg/m^3)	FT^2L^{-4}
θ	dimensionless mobility parameter	(-)	-
θ_{cr}	Dimensionless critical mobility parameter	(-)	-
κ	Von Karman constant	(-)	-
ϕ	Dimensionless transport rate parameter	(-)	-
ψ	Stratification correction		
ν	Kinematic viscosity	(m^2/s)	L^2T^{-1}
ν_t	Effective viscosity	(m^2/s)	L^2T^{-1}
τ	Shear stress	(N/m^2)	FL^{-2}
τ_{bx}	Bottom shear stress	(N/m^2)	FL^{-2}
τ_{cr}	Critical shear stress	(N/m^2)	FL^{-2}
τ_{cr}'	Critical shear stress for initiation of suspension	(N/m^2)	FL^{-2}
τ'	Grain shear stress	(N/m^2)	FL^{-2}
τ_{xy}	Effective shear stress	(N/m^2)	FL^{-2}
μ	Dynamic viscosity	(kgm/s)	FTL^{-2}

SAMENVATTING

De wereldbevolking neemt snel toe en verwacht wordt dat de bevolking in het jaar 2050 verdubbeld zal zijn tot ongeveer 10 miljard mensen. Om deze groeiende bevolking van voedsel te kunnen blijven voorzien zal de behoefte aan irrigatiewater blijven toenemen. Irrigatie is een van de kritieke voorzieningen om een duurzame en groeiende landbouwproductie te garanderen. Op het terrein van landbouwontwikkeling is het meeste geld in de ontwikkelingswereld naar de irrigatiesector gegaan. Een niet-aflatende ondersteuning van de irrigatie in samenhang met institutionele verbetering op het niveau van waterbeheer is zondermeer noodzakelijk om de voedselvoorziening te kunnen garanderen. Tegelijkertijd zal de behoefte aan water voor andere doeleinden ook toenemen, onder andere voor huishoudelijk gebruik, voor de industrie en voor waterkracht. In verband met deze tegenstrijdige belangen zal het waterverbruik voor irrigatie efficiënter moeten worden. Verbeterde management- en beheersactiviteiten zullen nodig zijn om een dreigende teloorgang van irrigatieprojecten te voorkomen. Daarnaast veroorzaakt het aangevoerde sediment veel problemen in irrigatie-systemen, zoals het blokkeren van inlaatwerken en het verminderen van de aanvoercapaciteit van kanalen. Jaarlijks zijn er grote sommen geld nodig voor beheer, onderhoud en vernieuwing om de bestaande systemen aan hun doelstellingen te kunnen laten voldoen. Plannen voor nieuwe irrigatieprojecten of het verbeteren van bestaande netwerken vereisen een beter begrip van de fysische processen die het sediment transporterend vermogen van irrigatiekanalen bepalen. De toepasbaarheid van de bestaande sedimenttransport theorieën in irrigatiekanalen vereist meer onderzoek en verdieping van kennis om daardoor tot betere en betrouwbare schattingen van sedimenttransport en de daaraan gekoppelde neerslag of opname van sediment te komen.

Dit onderzoek heeft zich met name gericht op sedimenttransport in irrigatiekanalen dat een belangrijke invloed op het beheer en onderhoud van irrigatiesystemen kan hebben. Het ontwerp van een kanaalsysteem zal gebaseerd moeten zijn op het transport van al het in het water aanwezig sediment naar de velden of naar plaatsen in het systeem waar het neergeslagen sediment vervolgens gemakkelijk en tegen de geringste kosten verwijderd kan worden. Het neerslaan van sediment moet zowel in kanalen als bij kunstwerken voorkomen worden omdat het neergeslagen sediment een verantwoord waterbeheer hindert of zelfs in gevaar brengt. In het ontwerp en het beheer van irrigatiekanalen die bijna altijd water met sediment aanvoeren zal rekening moeten worden gehouden met de verschillende eisen die door de irrigatie aan de wateraanvoer en door het sedimenttransport aan het kanaalontwerp gesteld worden. De behoefte om water in variërende hoeveelheden maar op het gewenste peil aan te voeren en tegelijkertijd om een bepaald sedimentaanbod te transporteren zonder dat er aanslibbing of uitschuring optreedt zullen de belangrijkste eisen voor het kanaalontwerp zijn.
Irrigatiekanalen zijn meestal ontworpen met de aanname dat de stroming eenparig en permanent is. Ook wordt verondersteld dat het systeem zich in een evenwichtssituatie bevindt waarbij het sediment dat het kanaalstelsel binnenkomt zonder noemenswaardige aanslibbing of uitschuring doorgevoerd wordt. Echter een eenparige, permanente aanvoer van water wordt in werkelijkheid zelden aangetroffen. Het beheer van de meeste kanaalsystemen wordt gekenmerkt door niet-

permanente stromingsomstandigheden. Omdat het sediment-transport sterk afhankelijk is van de stromingscondities is het duidelijk dat het sediment-transporterend vermogen van de kanalen ook met de tijd varieert.

Onderzoek op het gebied van sedimenttransport in open waterlopen heeft zich voornamelijk gericht op het sedimenttransport in rivieren. Natuurlijk bestaan er bepaalde overeenkomsten tussen kanalen en rivieren, maar toch mogen de voor de rivieren ontwikkelde modellen niet zonder aanpassingen voor irrigatiekanalen gebruikt worden. Een beschrijving en analyse van sedimenttransport voor de karakteristieke omstandigheden in irrigatiekanalen zal bijdragen tot een beter begrip van de specifieke omstandigheden van een kanaalsysteem en tot een juiste beslissing ten aanzien van de toepasbaarheid van transportbeschouwingen voor een bepaalde waterstroming en sedimentaanvoer. Een wiskundig model dat rekening houdt met de bijzondere aspecten en specifieke omstandigheden van sedimenttransport in irrigatiekanalen zal een belangrijk hulpmiddel voor ontwerpers en beheerders van irrigatienetwerken kunnen worden.

Het doel van dit onderzoek is een gedetailleerde analyse van de processen die het sediment transport beheersen, het opstellen van een fysische en wiskundige beschrijving van het sedimentgedrag onder in irrigatiekanalen vaak voorkomende omstandigheden en het ontwikkelen van een model dat het sedimenttransport en het neerslaan of opnemen van het sediment beschrijft voor verschillende stromingsomstandigheden en sedimentaanbod.

Sedimenttransportprocessen

Sedimenttransport en waterstroming zijn van elkaar afhankelijk en kunnen daarom niet gescheiden worden. Deze afhankelijkheid kan wiskundig beschreven worden voor een 1-dimensionale toestand door de volgende vergelijkingen, waarbij geen verandering in de vorm van de dwarsdoorsnede mag optreden:

- *vergelijkingen voor de waterstroming*: continuïteits- en dynamische vergelijking;
- *vergelijkingen voor het sedimenttransport*: stromingsweerstand; een vergelijking voor het sedimenttransport; continuïteitsvergelijking voor het sediment.

Vergelijkingen voor de waterstroming: ondanks het feit dat er in de natuur vrijwel geen 1-dimensionale stromingen aangetroffen worden zal de stroming in irrigatiekanalen als 1-dimensionaal beschouwd worden. De 1-dimensionale stroming kan met de vergelijkingen van de Saint Venant beschreven worden. De hoeveelheid water die gedurende het irrigatieseizoen en in het bijzonder gedurende de gebruiksduur van de irrigatiekanalen door een kanaal stroomt is niet constant. In verband met de tijdsafhankelijke veranderingen van de bodem kan de waterbeweging vereenvoudigd worden tot een quasi-permanente stroming waardoor de tijdsafhankelijke termen in de de Saint Venant vergelijking verwaarloosd mogen worden.

Stromingsweerstand: de stromingsweerstand in open kanalen is afhankelijk van meerdere factoren waaronder de vorming van bedvormen een belangrijke invloed op deze weerstand heeft.

Bepaling van de stromingsweerstand voor een kanaal met een veranderlijke bodem is een ingewikkeld probleem dat kennis van het impliciete proces van waterstroming en bedvorming vereist. Om bedvormen in irrigatiekanalen te kunnen voorspellen zijn de theorieën van Liu, Simons en Richardsons, Bogardi en van Rijn vergeleken met meetgegevens uit het veld en laboratoria. Ook zijn de meest gangbare methoden om de stromingsweerstand te schatten aan de hand van beschikbare veld en laboratoriagegevens met elkaar vergeleken. Dit heeft geleid tot een nieuwe methode die voor vergelijkbare omstandigheden toepasbaar is. De gekozen methoden om de stromingsweerstand te bepalen zijn die van White, Bettess en Paris (1979); Brownlie (1983) en van Rijn (1984).

Vergelijking van de resultaten van de schattingsmethoden voor de bedvorm en voor de wrijvingsweerstand op grond van gemeten veld en laboratoria waarden leidt tot de volgende conclusies:

- de theorieën van van Rijn en van Simons en Richardson geven de beste resultaten wat betreft de schatting van de bedvorm in irrigatiekanalen;
- alle bedvormen die voor het lage regime (ribbels, mega-ribbels en duinen) specifiek zijn kunnen in irrigatiekanalen voorkomen;
- de schatting van de weerstandsfactor volgens de eerder aangegeven methoden brengt alleen de bodemwrijving in rekening;
- de methode van van Rijn om de weerstandsfactor te schatten geeft de beste resultaten vergeleken met de meetgegevens.

Een ander belangrijk aspect van de weerstand in kanalen is de schatting van de wrijvingsweerstand van een kanaal met een samengestelde hydraulische ruwheid. De ontwikkeling van bedvormen, het voorkomen van verschillend materiaal op de bodem en oevers of de aanwezigheid van begroeiing op de oevers zijn typische voorbeelden die resulteren in een samengestelde ruwheid in kanalen. De meeste irrigatiekanalen hebben een trapeziumvormig of rechthoekig dwarsprofiel met een relatief kleine B/h-verhouding. De snelheidsverdeling in deze dwarsprofielen wordt in grote mate beïnvloed door de afnemende waterdiepte boven de oevers en door de randinvloeden die door de oever op de stroming uitgeoefend wordt. Uitgaande van een theoretische snelheidsverdeling is een nieuwe methode ontwikkeld om de samengestelde ruwheidsfactor in deze trapeziumvormige kanalen te kunnen schatten.

Om de samengestelde ruwheid in irrigatiekanalen te kunnen bepalen zijn bestaande methoden voor de schatting van de samengestelde ruwheidfactor vergeleken met laboratoriumgegevens verkregen uit proeven in het Waterloopkundig Laboratorium van de Landbouw Universiteit te Wageningen. Het doel van het onderzoek was de vaststelling van de invloed van verschillende ruwheden langs de oevers en bodem op de totale ruwheid van trapeziumvormige kanaaldoorsneden. Uit het onderzoek blijkt dat de voorgestelde methode betere resultaten geeft dan de bestaande methoden.

Voor rechthoekige dwarsprofielen met samengestelde ruwheid kunnen de bestaande methoden

voor de schatting van de wrijvingsweerstand niet eenduidig worden gebruikt. Daarom wordt voorgesteld om de samengestelde ruwheid in rechthoekige doorsneden volgens dezelfde uitgangspunten te bepalen als gebruikt voor de correctie van de zijwanden. De methode om de samengestelde weerstand in rechthoekige dwarsprofielen te schatten is getoetst aan de hand van gegevens uit het laboratorium onderzoek van Krüger. De voorgestelde methode voorspelt 95% van de gemeten, samengestelde ruwheid binnen een tolerantiegebied van 15 %.

Vergelijkingen voor het sedimenttransport: sedimenttransportformules zijn afhankelijk van de manier waarop het sediment getransporteerd wordt, in evenwichts- of in niet-evenwichtstoestand.

Vergelijkingen voor het sedimenttransport in evenwichtstoestand zijn ontwikkeld voor verschillende omstandigheden en het gebruik van deze formules moet beperkt worden tot die omstandigheden waaronder ze getest zijn. Een vergelijking van de verschillende methoden voor dezelfde stromings- en sedimentomstandigheden beide voorkomend in irrigatiekanalen of gebaseerd op veld- of laboratoriumgegevens zal een doeltreffend middel zijn om de toepasbaarheid van iedere methode voor deze specifieke omstandigheden te bepalen.
In dit onderzoek zijn de vijf, meest gangbare methoden vergeleken namelijk de methoden ontwikkeld door Ackers en White, Brownlie, Engelund en Hansen, van Rijn en Yang. De doelstelling van het onderzoek was het vaststellen van een betrouwbare schattingsmethode voor de sedimenttransportcapaciteit voor die omstandigheden die in irrigatiekanalen gebruikelijk zijn.

Naar aanleiding van deze vergelijking kunnen de volgende opmerkingen gemaakt worden:
- schatting van het sedimenttransport in irrigatiekanalen met een fout-factor die kleiner is dan twee is vrijwel onmogelijk;
- op grond van een algehele beoordeling van alle evaluatie-criteria blijken de methoden van Ackers en White en van Brownlie de beste resultaten wat betreft de voorspelbaarheid van sedimenttransport in irrigatiekanalen te geven.

De meeste sedimenttransporttheorieën zijn ontwikkeld voor zeer brede, open stromen (kanalen). Vele door de mens gemaakte irrigatiekanalen kunnen niet als zeer breed worden beschouwd en de aanbevolen breedte-diepte verhouding (B/h) voor deze kanalen is in veel gevallen kleiner dan acht.

Bestaande methoden om het totale sediment-transporterend vermogen over de gehele doorsnede van een niet-breed kanaal te kunnen schatten houden geen rekening met de snelheidsverdeling in de dwarsdoorsnede. Een nieuwe methode wordt nu voorgesteld om het totale sedimenttransport te berekenen door het transport over de gehele dwarsdoorsnede te integreren. Dit is gebaseerd op de aanname dat de stroming in een kanaal vereenvoudigd kan worden tot een quasi 2-dimensionaal model. Het uitgangspunt is dat rekening wordt gehouden met het effect van de dwarsdoorsnede op de snelheidsverdeling en met het niet-lineaire verband tussen snelheid en sedimenttransport. Om de bestaande schattingsmethoden te kunnen vergelijken met deze nieuwe methode voor de bepaling van het sedimenttransport in niet-brede kanalen zijn alle genoemde

methoden toegepast op een serie geselecteerde laboratoriumgegevens.

Een interessant aspect van het sedimenttransport in kanalen voor niet-evenwichtsomstandigheden is de aanpassing van het werkelijk optredend sedimenttransport aan het sediment transporterend vermogen van een (irrigatie) kanaal. Om het sedimenttransport onder niet-evenwichtsomstandigheden te kunnen simuleren is het over de diepte geïntegreerde model van Gallapatti toegepast om de adaptatielengte van het sediment in suspensie te kunnen bepalen. Tevens is aangenomen dat de adaptatielengte voor het bodemtransport gelijk is aan de adaptatielengte voor het sediment in suspensie. Vervolgens is Gallapatti's methode gebruikt om de aanpassing van het totale sediment-transport aan het sediment transporterend vermogen van een kanaal vast te kunnen stellen.

Mathematisch model voor het sedimenttransport in irrigatiekanalen (SETRIC)
Om het sedimenttransport in irrigatiekanalen te kunnen bepalen is een computerprogramma (SETRIC) ontwikkeld. Het programma kan de waterstroming, het sedimenttransport en de verandering in bodemligging in een kanaalnetwerk bestaande uit een hoofdkanaal en verscheidene secundaire kanalen met tertiaire uitlaten simuleren. Ook kunnen verschillende kunstwerken in het programma worden opgenomen: overstort of opening onder water; verdronken duikers; sifons; goten en bodemvallen.

Het computerprogramma gaat uit van een sub-kritische, quasi permanente, eenparige dan wel niet-eenparige (verhanglijnen) stroming. De stroming kan worden gesimuleerd voor open kanalen met een trapeziumvormig of rechthoekige dwarsdoorsnede met enkelvoudige of samengestelde ruwheid. Alleen wrijvingsverliezen worden in rekening gebracht. Lokale verliezen ten gevolge van plaatselijke veranderingen in bodemligging, bodembreedte of debieten worden niet beschouwd. Veranderingen in bodemligging kunnen op een eenvoudige wijze in het model worden opgenomen.

De eigenschappen van het sediment worden bepaald door de sedimentconcentratie aan het begin van het kanaal en de grootte van het sediment (gemiddelde diameter d_{50}). De spreiding van de diameter is aangenomen als een gelijkmatige namelijk: $0.05 \text{ mm} < d_{50} < 0.5 \text{ mm}$.

De verandering in waterbehoefte gedurende het groeiseizoen kan door het model gesimuleerd worden door het groeiseizoen in maximaal vier perioden te verdelen. Deze perioden zijn gebaseerd op de groeifase van het gewas en de klimatologische omstandigheden. Voor elk van de vier beheersperioden kan de aanvoer in het irrigatiesysteem aangepast worden.

Onderhoudswerkzaamheden kunnen ook gesimuleerd worden. De onderhoudstoestand van een kanaalsectie wordt uitgedrukt door de obstructie ten gevolge van de groei van onkruid op de kanaaloevers en de invloed daarvan op de ruwheidsfactor. Het programma onderscheidt drie soorten onderhoud: ideaal, goed en slecht onderhoud.

Een aantal voorbeelden met het model SETRIC voor het simuleren van sedimenttransport in irrigatiekanalen zijn in deze studie opgenomen. De resultaten van het sedimentgedrag in de voorbeelden zijn specifiek voor de specifieke stromingsomstandigheden en sediment-eigenschappen in elk voorbeeld. De resultaten kunnen daarom niet zondermeer voor algemene beschouwingen gebruikt worden.

De voorbeelden zijn bedoeld om de toepasbaarheid van het model aan te tonen en om het begrip van de processen die zich afspelen bij sedimenttransport in vaak voorkomende situaties in irrigatiekanalen te verbeteren. De hoeveelheid sediment die in een irrigatiekanaal gedurende een bepaalde periode opgenomen wordt of neerslaat wordt voor elk voorbeeld gesimuleerd. Het sedimenttransporterendvermogen van het kanaal is bepaald met de methode van Ackers en White. De aanpassing aan het sedimenttransporterendvermogen vindt plaats volgens het over de diepte geïntegreerde model van Gallapatti. Een sediment-balansbeschouwing voor elke kanaalsectie resulteert vervolgens in de neergeslagen of opgenomen hoeveelheid sediment in die sectie.

Na bestudering van de resultaten van deze voorbeelden kunnen een aantal conclusies getrokken worden:

Verandering van de kanaaldebieten: bij vermindering van de wateraanvoer in het irrigatiekanaal tot 80 % van het oorspronkelijk ontwerpdebiet (evenwichtssituatie) slaat meer dan 40 % van het binnenkomend sediment neer.

Verandering in het binnenkomende sediment (concentratie en grootte): het effect van de veranderingen van het binnenkomend sediment is zowel voor de sedimentconcentratie als de diameter van het sediment nagegaan. Deze effecten zijn zowel gedurende 1 irrigatieseizoen als voor de gehele gebruiksduur van het kanaalnetwerk beschouwd. In het geval dat de sedimentconcentratie 100 % afwijkt van de evenwichtssituatie zal ongeveer 30% van het binnenkomend sediment zich in het kanaal afzetten. Een vergelijkbaar verschijnsel als in het hiervoor beschreven geval doet zich voor indien de gemiddelde diameter van het binnenkomend sediment verandert ten op zichte van de ontwerpwaarde. Bijvoorbeeld, 45 % van het binnenkomend sediment zal neerslaan wanneer de gemiddelde diameter 100% naar boven afwijkt van de ontwerpwaarde (evenwichtssituatie).

Gecontroleerde sedimentneerslag: twee scenario's zijn voorgesteld om het sediment in het begin van het kanaal te laten neerslaan. De scenario's kunnen worden omschreven als verbreding (scenario 1) en verdieping (scenario 2) van het kanaal. Aan deze eenvoudige wijzigingen in de vorm van het dwarsprofiel zijn geen verdere beschouwingen gekoppeld om de vaste en variabele kosten of de optredende sedimentatie te optimaliseren. Voor de gegeven stromingsomstandigheden en sedimenteigenschappen blijkt dat verdieping van het kanaal (scenario 2) tot een 4 maal grotere sedimentneerslag leidt dan het ongewijzigde kanaalprofiel en tot een 1.3 maal grotere neerslag dan het verbrede kanaalprofiel (scenario 1).

Schattingsmethoden voor het transporterend vermogen: voor de verschillende methoden zijn grote verschillen in de sedimentneerslag vastgesteld. Voor de gegeven omstandigheden geeft de methode van Engelund en Hansen een gering transporterend vermogen en de methoden van Brownlie en Ackers en White resulteren in een groter transporterend vermogen. Bij gebruik van de methode van Engelund en Hansen was de sedimentneerslag 2 keer groter dan de neerslag volgens de methode van Brownlie en 3 keer groter dan de neerslag volgens de methode van Ackers en White.

Type kunstwerk: twee hoofdgroepen van kunstwerken voor het regelen van het waterniveau voor variërende debieten zijn beschouwd; namelijk overstorten en kunstwerken met een opening onder water. Het waargenomen sedimentgedrag is voor beide typen kunstwerken vergelijkbaar. Grote verschillen zijn echter waargenomen in de verdeling van de sedimentneerslag in de lengterichting van het kanaal. Deze verschillen treden vooral bovenstrooms van de kunstwerken op.

Mate van onderhoud: onderhoudswerkzaamheden worden uitgevoerd in verband met de sedimentatie en de groei van onkruid; de werkzaamheden zijn geëvalueerd aan de hand van hun invloed op het hydraulisch gedrag van het irrigatiekanaal en vervolgens is de invloed daarvan op het sedimenttransport bestudeerd. Onderhoud is gesimuleerd door gedurende het irrigatieseizoen volledig onderhoud of helemaal geen onderhoud aan te nemen. De directe effecten van onkruid op het sedimenttransport zijn niet in de beschouwingen meegenomen. Uit het onderzoek volgt dat volledig onderhoud tot meer sedimentatie leidt dan helemaal geen onderhoud in kanalen. Omdat gedurende het irrigatieseizoen de waterstand aan het benedenstroomse einde van de kanaalsectie constant gehouden wordt kan de stroming in het geval van volledig onderhoud beschreven worden door een stuwkromme die niet met de tijd verandert. In dit geval is er in het kanaal een continu sedimentatieproces. In het geval waarbij geen onderhoud plaats vindt zal de stromingstoestand na verloop van tijd van een stuwkromme overgaan in een afzuigkromme. Ook nu wordt de waterstand aan het benedenstroomse einde van een kanaalsectie op een constant niveau gehouden. De veranderingen in de hydraulische ruwheid leiden dan tot een verhoging van de bovenstroomse waterstand. Een periode met sedimentneerslag wordt gevolgd door een periode waarbij sediment wordt opgenomen.

Beheerstrategieën: om de effecten van de beheerstrategieën op het sedimentgedrag in het hoofdkanaal te kunnen bepalen zijn vier beheerscenario's gesimuleerd. De vier scenario's zijn: continu wateraanvoer (scenario 1); wateraanvoer met een rotatie op uurbasis (scenario 2); wateraanvoer met een rotatie op dagbasis (scenario 3) en wateraanvoer met een rotatie op weekbasis (scenario 4).
Vergelijking van de vier scenario's leidt tot de volgende conclusies:

- de grootste sedimentneerslag treedt in het gehele kanaal voor scenario 1 op. De neerslag in scenario's 2, 3 en 4 is vergelijkbaar;
- grote verschillen in sedimentneerslag worden in de verschillende secties van het hoofdkanaal aangetroffen.

Een nadere beschouwing van de resultaten van de voorbeelden van het mathematische model SETRIC toont aan dat het model een uitstekend hulpmiddel is om sedimentatie in irrigatiekanalen voor verschillende stromingtoestanden en sedimenteigenschappen te kunnen schatten. Toch zal het mathematisch model verder onderbouwd moeten worden. De met het model verkregen resultaten zullen vergeleken moeten worden met veldmetingen om vast te kunnen stellen of het model de fysische processen goed weergeeft en of er tekortkomingen zijn in de aannamen die voor de beschrijving van deze processen gedaan zijn. Veldmetingen van sedimentatie in irrigatienetwerken zijn vereist om het model voor de specifieke omstandigheden van irrigatiekanalen te kunnen evalueren en om het gedrag van de bodem in tijd en plaats voor bepaalde stromingsomstandigheden en sedimenteigenschappen vast te kunnen stellen. Onderzoek naar de invloeden van het type kunstwerk en de wijze van bediening, de afmetingen van kanaaldwarsprofielen, de stromingsomstandigheden en de eigenschappen van het binnenkomend sediment op de door het model voorspelde sedimentatie zal bijdragen tot een beter begrip van de sedimenttransport processen.

CURRICULUM VITAE

Nestor J. Mendez V. was born in Lagunillas, Edo. Zulia, Venezuela on February 21, 1954. He obtained both his primary and secondary school in Barquisimeto, Venezuela. In 1977 he graduated as Agricultural Engineer at the Universidad Centro Occidental "Lisandro Alvarado" in Barquisimeto, Venezuela.

After graduation he joined the Ministry of Environment and Renewable Natural Resources (MARNR) in Edo. Portuguesa, Venezuela where he worked till 1981. There he was involved in planning, designing and construction of a surface drainage system in the Turen II project in Edos. Portuguesa and Cojedes in Venezuela.

In 1981 he joined as lecturer the Hydraulic department of the Civil Engineering school at the Universidad Centro Occidental "Lisandro Alvarado" in Barquisimeto, Venezuela. Since then he has been lecturing in: Basic Hydraulics, Applied Hydraulics, Groundwater Flow, Land and Water Development and Principles of Irrigation and Drainage. In 1986 he obtained a MSc degree in Land and Water Development in CIDIAT-Merida, Venezuela.

Since 1977 he has attended several postgraduate short courses in water resources development, management of river basins, modelling of groundwater flow.

In 1993 he came to the Netherlands to the International Institute for Infrastructural, Hydraulic and Environmental Engineering (IHE), Delft where he obtained the postgraduate diploma in hydraulic engineering. In 1994 he started with the research on "Sediment transport in irrigation canals". The first stage of that research was focused on suspended sediment transport in irrigation canals and it was used to obtain the MSc degree in Hydraulic Engineering in 1995.